

UCSF

UC San Francisco Electronic Theses and Dissertations

Title

Molecular mechanisms of organic cation and anion transporters

Permalink

<https://escholarship.org/uc/item/3d14t6zs>

Author

Dresser, Mark Jason

Publication Date

2000

Peer reviewed|Thesis/dissertation

Molecular Mechanisms of Organic Cation and Anion Transporters

by

Mark Jason Dresser

DISSERTATION

Submitted in partial satisfaction of the requirements for the degree of

DOCTOR OF PHILOSOPHY

in

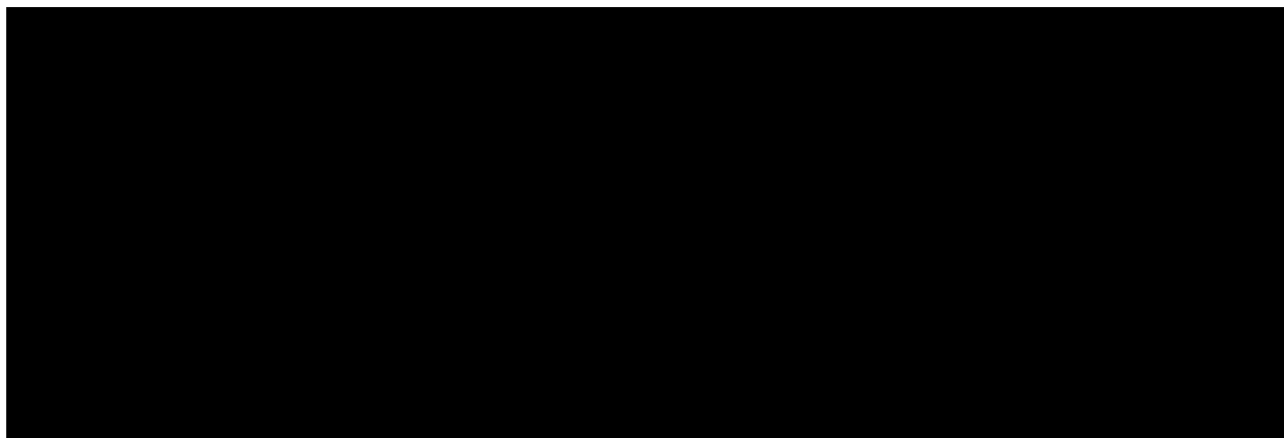
Pharmaceutical Chemistry

in the

GRADUATE DIVISION

of the

UNIVERSITY OF CALIFORNIA SAN FRANCISCO



Date

University Librarian

Degree Conferred:

To my parents

Acknowledgements

First, I would like to thank my advisor, Dr. Kathleen Giacomini, for her support and mentoring during my graduate studies -- one could not hope for a better advisor. I am also grateful to Drs. Leslie Benet and Deanna Kroetz for their willingness to serve on my thesis committee, their suggestions, and their timely reading of the manuscript.

I would also like to thank many members of the Giacomini lab for their support and friendship. First, I need to thank Dr. Marcelo Gutierrez for convincing me to join the Giacomini lab. I thank Dr. Lei Zhang for her outstanding guidance during my rotation project. Thanks to Karin Gerstin, Maya Kaushal Leabman, and Lara Mangravite for reading parts of this thesis. I also gratefully acknowledge Lara Mangravite and Drs. Shieyuki Terashita, Guangqing Xiao, and Bo Feng for assistance with the experiments.

I am indebted to Dr. Andrew Gray for his patience and help with the electrophysiology experiments.

Last but not least, I need to thank my best friend, John-Christopher Thomas, and my strongest supporter, Dr. Claire Brett. Without their advice, friendship, and good humor, I would have never made it this far -- I am eternally grateful to them both.

Mark J. Dresser

December 2000

FCR/mm/nov 00.180
30 November 2000

Mr Mark J Dresser
University of California, San Francisco
School of Pharmacy
Box 0446
San Francisco CA 94143-0446
USA

Dear Mr Dresser

***BIOCHIMICA ET BIOPHYSICA ACTA, Vol 1369, pp 1-6, 1998, Terashira,
"Molecular cloning..."***

As per your letter dated 28th November 2000, we hereby grant you permission to reprint the aforementioned material at no charge in **your thesis** subject to the following conditions:

1. If any part of the material to be used (for example, figures) has appeared in our publication with credit or acknowledgement to another source, permission must also be sought from that source. If such permission is not obtained then that material may not be included in your publication/copies.
2. Suitable acknowledgment to the source must be made as follows:

"Reprinted from Journal title, Volume number, Author(s), Title of article, Pages No., Copyright (Year), with permission from Elsevier Science".
3. Reproduction of this material is confined to the purpose for which permission is hereby given.
4. This permission is granted for non-exclusive world **English** rights only. For other languages please reapply separately for each one required. Permission excludes use in an electronic form. Should you have a specific electronic project in mind please reapply for permission.
5. This includes permission for UMI to supply single copies, on demand, of the complete thesis. Should your thesis be published commercially, please reapply for permission.

Yours sincerely



 Frances Rothwell (Mrs)
Global Rights Manager

**The processing of permission requests for all Elsevier Science (including Pergamon imprint) journals has been centralised in Oxford, UK. Your future requests will be handled more quickly if you write directly to: Subsidiary Rights Department, Elsevier Science, PO Box 800, Oxford OX5 1DX, UK.
Fax: 44-1865 853333; e-mail: permissions@elsevier.co.uk**



Elsevier Science

Global Rights
PO Box 800
Oxford OX5 1DX
England

Tel: +44 (0) 1865 843830
Fax: +44 (0) 1865 853333
E-mail: permissions@elsevier.co.uk
Home Page: www.elsevier.com

Imprints:
Elsevier
Pergamon
North-Holland
Excerpta Medica



ASPET

AMERICAN SOCIETY FOR PHARMACOLOGY
AND EXPERIMENTAL THERAPEUTICS

Council

Sam J. Enna
President
University of Kansas

Marlene L. Cohen
President-Elect
Eli Lilly and Co.

Jerry R. Mitchell
Past President
ClinTrials Research Inc.

David B. Bylund
Secretary-Treasurer
University of Nebraska

Nancy R. Zahnsier
Secretary-Treasurer-Elect
University of Colorado

Lee E. Limbird
Past Secretary-Treasurer
Vanderbilt University

I. Glenn Sipes
Councilor
University of Arizona

Kenneth P. Mianeman
Councilor
Emory University

Joe A. Beavo, Jr.
Councilor
University of Washington

T. Kendall Harden
Board of Publications Trustee
University of North Carolina

Lynn Wecker
Program Committee
University of South Florida

Kenneth E. Moore
Long Range Planning Committee
Michigan State University

Christine K. Carrico
Executive Officer

9650 Rockville Pike
Bethesda, MD 20814-3995

Phone: (301) 530-7060
Fax: (301) 530-7061

info@aspet.org
www.faseb.org/aspet

November 28, 2000

Mark J. Dresser
Department of Biopharmaceutical Sciences
University of California
San Francisco, CA 94143-0446

Fax: 415-476-0688

Dear Mr. Dresser:

This is to grant you permission to include the following article with your doctoral dissertation at the University of California, San Francisco:

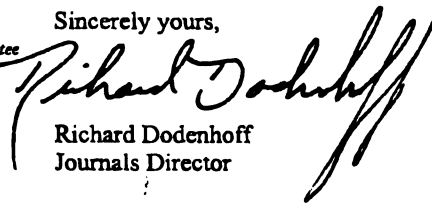
Mark J. Dresser, Andrew T. Gray, and Kathleen M. Giacomini, "Kinetic and Selectivity Differences between Rodent, Rabbit, and Human Organic Cation Transporters (OCT1)", *Journal of Pharmacology and Experimental Therapeutics*, vol. 292, no. 3, pp. 1146-1152, March 2000

On the first page of the article copies, please include the following:

Copied with permission of the American Society for Pharmacology and Experimental Therapeutics. All rights reserved.

Thank you.

Sincerely yours,



Richard Dodenhoff
Journals Director



PERMISSIONS DEPARTMENT
605 Third Avenue
New York, NY 10158-0012

TEL 212.850.6011
FAX 212.850.6008

John Wiley & Sons, Inc.
Publishers Since 1807

December 1, 2000

Mark J Dresser
Dept. of Biopharmaceutical Sciences
School of Pharmacy
Box 0446
University of California-San Francisco
San Francisco, CA 94143-0446
Fax: 415 476 0688

Dear Mark Dresser:

RE: Your 11/28/2000 request for permission to republish your contribution (Manuscript #JS00001) to the forthcoming edition of *Journal of Pharmaceutical Sciences*. This material will appear in your forthcoming dissertation, to be published by University of California in 12/2000.

1. Permission is granted for this use, except that if the material appears in our work with credit to another source, you must also obtain permission from the original source cited in our work.
2. Permitted use is limited to your edition described above, and does not include the right to grant others permission to photocopy or otherwise reproduce this material except for versions made by non-profit organizations for use by visually or physically handicapped persons, and up to five copies of the published thesis may be photocopied by a microfilm company.
3. Appropriate credit to our publication must appear on every copy of your work, either on the first page of the quoted text, in a separate acknowledgment page, or figure legend. The following components must be included: Title, author(s) and /or editor(s), journal title (if applicable), Copyright © (year and owner). "Draft version to be published in the forthcoming *Journal of Pharmaceutical Sciences*." Reprinted by permission of Wiley-Liss, Inc., a subsidiary of John Wiley & Sons, Inc.
4. This permission is for non-exclusive print rights and microfilm storage rights by University of California, for the English language only, throughout the world. For translation rights, please contact our Subsidiary Rights Department.

Sincerely,

Jonathan H Campbell
Permissions Assistant
John Wiley & Sons
212 850 6012
Fax: 850 6008

ABSTRACT

Molecular Mechanisms of Organic Cation and Anion Transporters

Mark Jason Dresser

Organic cation transporters and organic anion transporters in the kidney are important determinants of drug elimination. Based on pharmacokinetic studies and transport studies using renal tissue, these transporters have been shown to interact with and transport structurally and pharmacologically diverse clinical agents. The overall goal of this dissertation was to elucidate the molecular characteristics of renal organic cation and anion transporters. This research contributed to the cloning of these transporters, elucidating their substrate selectivities and intracellular localization, and determining the molecular domains and amino acid residues involved in substrate recognition.

In the first section of this dissertation, I describe the cloning of a rabbit renal organic cation transporter (rOCT1) and the determination of the substrate selectivities of cloned organic cation transporters. rOCT1 was cloned using a PCR-based cloning strategy. Initial studies indicated that rOCT1 interacts with cationic drugs. The cloned transporters were then used to test my hypothesis that intrinsic differences in the functions of OCT1 orthologs may explain observed interspecies differences in the elimination of organic cations. Using tracer uptake, *trans*-stimulation, and voltage-clamp assays, the functional characteristics of four mammalian OCT1 isoforms were studied; significant interspecies differences were found among these isoforms. Similarly, differences in the selectivities of two human organic cation transporters, hOCT1 and hOCT2, were found, although some organic cations were transported by both isoforms. Using a stably transfected cell line expressing GFP-tagged rOCT1, I determined that

rOCT1 is localized to the lateral membrane of polarized epithelial cells. To identify the molecular determinants involved in substrate recognition of organic cation and organic anion transporters, I used a chimera approach and site-directed mutagenesis. These studies revealed that the substrate recognition site resides in the final 7 transmembrane domains of these proteins, and that a conserved charged residue, arginine 454, in rOAT3 acts as an anionic recognition site, but that it is not important for transporting cimetidine. These results suggest that multiple structural domains within transmembrane domains 7 - 12 of rOAT3 are differentially involved in substrate binding and transport.

Harleen M. Giacomini

UCSF LIBRARY

TABLE OF CONTENTS

Acknowledgments	iv
Abstract	viii
Table of Contents	x
List of Tables	xvi
List of Figures	xviii
List of Abbreviations	xxii
Chapter 1	
Introduction	1
Background.....	1
Organic Cation and Organic Anion Renal Transport: Cellular Events	
Involved in Transepithelial Flux in the Kidney.....	6
Expression Cloning of rOCT1 and rOAT1.....	13
Initial Molecular Characterization of rOCT1 and rOAT1.....	16
Summary of Dissertation Studies.....	20
References.....	27
Chapter 2	
Molecular Cloning and Functional Expression of a Rabbit Renal	
Organic Cation Transporter	
Organic Cation Transporter	31
Introduction.....	31
Materials and Methods.....	32
cDNA cloning and analysis.....	32
Expression in <i>Xenopus laevis</i> oocytes and tracer uptake assays.....	34

RT-PCR.....	36
Results and Discussion.....	36
Nucleotide and deduced amino acid sequence of rbOCT1.....	36
Functional expression and characterization of rbOCT1.....	38
Tissue distribution of rbOCT1 mRNA.....	42
References.....	46

Chapter 3

Kinetic and Selectivity Differences Among Rodent, Rabbit, and Human

Organic Cation Transporters (OCT1).....	49
Introduction.....	49
Materials and Methods.....	51
cRNA transcription and <i>Xenopus laevis</i> oocyte expression.....	51
Tracer uptake measurements.....	51
Electrophysiology studies.....	53
Data analysis.....	53
Materials.....	53
Results.....	54
Inhibition of OCT1-mediated uptake by nTAA compounds.....	54
Efflux of nTAAs from oocytes expressing OCT1.....	55
nTAA-dependent currents in voltage clamped oocytes.....	60
Discussion.....	63
References.....	69

Chapter 4

The Interaction and Transport of n-Tetraalkylammonium Compounds and Biguanides with a Human Renal Organic Cation Transporter, hOCT2

hOCT2	74
Introduction.....	74
Materials and Methods.....	76
cRNA transcription and <i>Xenopus laevis</i> oocyte expression.....	76
Tracer uptake measurements.....	76
Electrophysiology studies.....	77
Data analysis.....	78
Materials.....	78
Results.....	78
Inhibition of hOCT2 mediated uptake by nTAA compounds.....	78
Efflux of nTAAs from oocytes expressing hOCT2.....	79
Interactions and transport of biguanides with hOCT2 and hOCT1.....	83
Discussion.....	89
References.....	93

Chapter 5

Stable Expression of a GFP-rOCT1 Fusion Protein in a Polarized

Epithelial Cell Line (MDCK): Intracellular Localization and

Functional Characterization..... 98

Introduction..... 98

Materials and Methods..... 100

DNA constructs..... 100

cRNA transcription and expression in <i>Xenopus laevis</i> oocytes.....	101
Tracer uptake measurements in <i>Xenopus laevis</i> oocytes.....	102
MDCK transfection.....	103
Transport studies using MDCK cell lines.....	104
Confocal microscopy studies.....	105
Chemicals.....	105
Results.....	105
Functional characterization of GFP-tagged rOCT1 expressed in <i>Xenopus laevis</i> oocytes.....	105
Functional localization of GFP-rOCT1 in polarized MDCK.....	106
Localization of GFP-rOCT1 and GFP-rOCT1Δ in stably transfected MDCK cell lines.....	111
Discussion.....	114
References.....	119

Chapter 6

Arginine 454 of the Organic Anion Transporter, rOAT3, is Essential

For <i>para</i>-Aminohippurate Transport.....	125
Introduction.....	125
Materials and Methods.....	127
Construction of chimeric transporters and site-directed mutagenesis..	127
cRNA transcription and expression in <i>Xenopus laevis</i> oocytes.....	128
Tracer uptake measurements.....	128
Partition coefficient determinations.....	129
Data analysis.....	129

UCSF LIBRARY

Materials.....	130
Results.....	130
Substrate specificity of wildtype rOAT3.....	130
Substrate specificity of a rOAT3/rOCT1 chimera.....	131
Functional characteristics of arginine 454 mutants of rOAT3.....	137
Discussion.....	144
References.....	148
Chapter 7	
Summary, Conclusions and Future Directions.....	154
Introduction.....	154
Transporters Involved in the Renal Elimination of Organic Cations.....	155
Background and significance.....	155
OCT1.....	156
OCT2.....	157
OCT3.....	158
OCTN1.....	159
OCTN2.....	160
Summary and conclusions: organic cation transporters.....	163
Transporters Involved in the Renal Elimination of Organic Anions.....	163
Background and significance.....	163
OAT1.....	164
OAT2.....	166
OAT3.....	167
OAT4.....	168

UCSF LIBRARY

UCSF LIBRARY

OAT-K1.....	168
OAT-K2.....	169
OATP1.....	170
OATP2.....	171
OATP3.....	171
Summary and conclusions: organic anion transporters.....	174
Other Transporters Involved in the Renal Elimination of Drugs.....	175
Outlook and Future Directions.....	176
References.....	197

UCSF LIBRARY

UCSF LIBRARY

LIST OF TABLES

Chapter 1

- Table 1. Examples of xenobiotics that are secreted by the renal organic cation transport system..... 3
- Table 2. Examples of xenobiotics that are secreted by the renal organic anion transport system..... 4

Chapter 2

- Table 1. Primers used for PCR cloning of rbOCT1 cDNA..... 35

Chapter 3

- Table 1. Apparent K_i values (μM) of n-tetraalkylammonium (nTAA) compounds..... 58

Chapter 4

- Table 1. Apparent K_i values (μM) of n-tetraalkylammonium (nTAA) compounds in inhibiting $^3\text{H-MPP}^+$ uptake mediated by hOCT2..... 81
- Table 2. Apparent K_i values (μM) of metformin and phenformin in inhibiting $^3\text{H-MPP}^+$ uptake mediated by hOCT2 and hOCT1..... 86

Chapter 7

- Table 1. Organic cation transporter expression in adult kidney, liver, intestine, and brain..... 162
- Table 2. Organic anion transporter expression in adult kidney, liver, intestine and brain..... 173
- Table 3. Intracellular localization of organic anion and organic cation transporters..... 178

Table 4. Compounds that interact with organic anion and organic
cation transporters..... 179

UCSF LIBRARY

UCSF LIBRARY

LIST OF FIGURES

Chapter 1

Figure 1. Chemical structures of model organic cations.....	8
Figure 2. Chemical structures of model organic anions.....	9
Figure 3. Mechanisms of organic cation transport in the kidney	11
Figure 4. Mechanisms of organic anion transport in the kidney.....	12
Figure 5. Flow chart of the steps involved in expression cloning.....	15
Figure 6. Schematic representation of the steps involved in the <i>Xenopus laevis</i> oocyte expression system.....	17
Figure 7. Proposed secondary structures of rOCT1 and rOAT1.....	18

Chapter 2

Figure 1. Nucleotide and deduced amino acid sequence of rbOCT1..	37
Figure 2. ³ H-MPP ⁺ uptake in oocytes injected with rbOCT1 cRNA...	39
Figure 3. Kinetics of ³ H-MPP ⁺ transport in rbOCT1 cRNA-injected oocytes.....	40
Figure 4. Inhibition of ³ H-MPP ⁺ uptake in rbOCT1 cRNA-injected oocytes by model organic cations.....	41
Figure 5. Effect of membrane potential on ³ H-MPP ⁺ uptake in rbOCT1 cRNA-injected oocytes.....	43
Figure 6. RT-PCR analysis of rbOCT1 mRNA transcript expression	44

Chapter 3

Figure 1. Effect of nTAA compounds (50 μM) of increasing chain	
--	--

length on $^3\text{H-MPP}^+$ (1 μM) uptake (1 h) by OCT1- expressing oocytes.....	56
Figure 2. Inhibition of $^3\text{H-MPP}^+$ uptake (1 h) by nTAA compounds in oocytes expressing mOCT1.....	57
Figure 3. Effect of <i>trans</i> nTAA compounds on the influx (10 min) of $^3\text{H-MPP}^+$ in oocytes expressing OCT1.....	59
Figure 4. Representative recordings of nTAA-induced inward currents in OCT1 cRNA- or uninjected oocytes under voltage clamp conditions (-50 mV).....	61
Figure 5. nTAA-induced currents under voltage clamp conditions (- 50 mV) in OCT1 cRNA- and uninjected oocytes.....	62
Figure 6. Multiple sequence alignment of four OCT1 homologs from mouse (mOCT1), rat (rOCT1), rabbit (rbOCT1), and human (hOCT1).....	68

Chapter 4

Figure 1. Effect of nTAA compounds (50 μM) of increasing chain length on $^3\text{H-MPP}^+$ (1 μM) uptake by hOCT2-expressing oocytes.....	80
Figure 2. Effect of <i>trans</i> nTAA compounds on the influx of $^3\text{H-}$ MPP^+ in <i>Xenopus laevis</i> oocytes expressing hOCT2 or hOCT1.....	82
Figure 3. <i>Cis</i> inhibition of $^3\text{H-cimetidine}$ uptake in <i>Xenopus laevis</i> oocytes expressing hOCT2 or hOCT1.....	85
Figure 4. Effect of <i>trans</i> compounds on the influx of $^3\text{H-MPP}^+$ in	

Xenopus laevis oocytes expressing hOCT2 and hOCT1.... 87

Figure 5. Representative recordings of ligand-induced inward currents in hOCT2-expressing oocytes..... 88

Chapter 5

Figure 1. Effect of nTAA compounds (50 μ M) of increasing chain length on 3 H-MPP $^+$ (1 μ M) uptake mediated by wildtype rOCT1 and GFP-rOCT1 expressed in *Xenopus laevis* oocytes..... 108

Figure. 2. Effect of *trans* nTAA compounds on the influx of 3 H-MPP $^+$ in *Xenopus laevis* oocytes expressing wildtype or GFP-tagged rOCT1..... 109

Figure 3. Functional localization of GFP-rOCT1 stably transfected in MDCK..... 110

Figure 4. Vertical optical sections of MDCK cell lines visualized by confocal microscopy..... 112

Figure 5. Cellular localization of GFP-rOCT1 in polarized MDCK cells determined by confocal microscopy..... 113

Chapter 6

Figure 1. Substrate selectivity of wildtype rOAT3..... 133

Figure 2. The inhibitory effect of PAH on rOAT3-mediated cimetidine transport..... 134

Figure 3. Secondary structure of wildtype and chimeric transporters. 135

Figure 4. Substrate selectivity of wildtype and chimeric transporters 136

UCSF LIBRARY

Figure 5. Multiple alignments of transmembrane domain 11 of the OCTs and OATs.....	139
Figure 6. A model of the secondary structure of rOAT3 with arginine 454 in transmembrane domain 11 highlighted.....	140
Figure 7. Substrate selectivity of wildtype rOAT3, and R454D and R454N mutants.....	141
Figure 8. Substrate selectivity of wildtype rOAT3, and R454D and R454N mutants.....	142
Figure 9A. Inhibition of rOAT3 mediated ³ H-cimetidine (1 μM) uptake by various compounds.....	143
Figure 9B. Inhibition of R454D mediated ³ H-cimetidine (1 μM) uptake by various compounds.....	143

UCSF LIBRARY

LIST OF ABBREVIATIONS

araC	cytosine arabinoside
BBM	brush border membrane
BLM	basolateral membrane
BSP	sulfobromophthalein
CIAdo	2-chlorodeoxyadenosine
DHEA-s	dehydroepiandrosterone sulfate
DMA	dimethylamiloride
dTub	2'-deoxytubercidin
GSH	reduced glutathione
MDCK	Madin-Darby canine kidney
MPTP	1-methyl-4-phenyl-1,2,3,6-tetrahydropyridine
MPP ⁺	1-methyl-4-phenylpyridinium
MRP	multidrug resistance-associated protein
NMN	N ¹ -methylnicotinamide
NSAID	nonsteroidal anti-inflammatory drug
P-gp	P-glycoprotein
oatp	organic anion-transporting polypeptide
OAT	organic anion transporter
OCT	organic cation transporter
OCTN	novel organic cation transporter
ORF	open reading frame
PAH	para-aminohippurate
PCG	penicillin G

UCSF LIBRARY

PGE ₂	prostaglandin E2
PMEDAP	9-[2-phosphonylmethoxyethyl]diaminopurine
PMEG	9-[2-phosphonylmethoxyethyl]guanine
RPA	RNase protection assay
TBA	tetrabutylammonium
TBuMA	tributylmethylammonium
TCA	taurocholate
TEA	tetraethylammonium
THA	tetrahexylammonium
TMA	tetramethylammonium
TMD	transmembrane domain
TPeA	tetrapentylammonium
TPrA	tetrapropylammonium

UCSF LIBRARY

CHAPTER 1

INTRODUCTION

Background

Renal excretion is a major pathway of elimination from the systemic circulation for numerous xenobiotics, including clinically used agents and environmental toxins. Hence, renal excretion can greatly affect the pharmacokinetics and toxicokinetics of many drugs. The plasma levels of many drugs are determined by one or more of the processes of renal excretion: glomerular filtration, passive or active reabsorption, and active secretion [1]. Glomerular filtration is a passive unidirectional process by which unbound small molecules are filtered from the plasma. Reabsorption is either a passive or active process. Passive reabsorption occurs for many drugs, whereas active carrier-mediated reabsorption is particularly important for maintaining the homeostasis of essential nutrients, such as glucose and vitamins. However, some drugs also undergo active reabsorption in the kidney. Finally, the kidney has the ability to actively secrete many different types of compounds, including clinically used drugs, via tubular transport systems. Two of the major xenobiotic transport systems in the kidney are the organic cation transport system and the organic anion transport system [2, 3]. Many organic

UCSF LIBRARY

UCSF LIBRARY

cations and organic anions have been shown to undergo net secretion in the kidney (Tables 1 & 2) [1, 4, 5].

Organic cations are a structurally and pharmacologically diverse group of molecules that contain one or more positively charged moieties at physiological pH. Organic cations are estimated to account for approximately fifty percent of clinically used drugs including antiarrhythmics (e.g. quinidine, procainamide, disopyramide, lidocaine), antihistamines (e.g. promethazine, diphenhydramine), opioid analgesics (e.g. morphine, codeine, methadone), β -adrenergic blocking agents (e.g. propranolol, timolol, pindolol, acebutolol) and skeletal muscle relaxants (e.g. tubocurarine, pancuronium, vecuronium). In addition, many organic cations are currently at various stages of drug development (e.g. ropinirole, pramipexole, cabergoline) [6]. Many toxic substances {e.g. paraquat and 1-methyl-4-phenylpyridinium (MPP⁺)} as well as endogenous substances {e.g. dopamine, serotonin, noradrenaline, histamine, acetylcholine, choline and N¹-methylnicotinamide (NMN)} are organic cations, too. Due to their positive charge, organic cations diffuse poorly across biological membranes and instead rely upon membrane transporters to attain movement across membranes [7, 8].

Organic anions are molecules that contain one or more negatively charged moieties. Examples of organic anions include diuretics (furosemide and bumetanide), antibiotics (penicillin G, cephaloridine, and cefazolin), anti-inflammatory agents

**Table 1. Examples of xenobiotics that are secreted by
the renal organic cation transport system.**

Amiloride
Amantadine
Cimetidine
Isoproterenol
Mepiperphenidol
Metformin
Pindolol
Procainamide
Tetraethylammonium

**Table 2. Examples of xenobiotics that are secreted by
the renal organic anion transport system.**

Carbenecillin
Cephaloridine
Ethacrynic acid
Furosemide
Indomethacin
Methotrexate
p-Aminohippurate (PAH)
Penicillin
Phenol red
Phenylbutazone
Probenecid

UCSF LIBRARY

(indomethacin and naproxen), and the anticancer agent methotrexate. All of these compounds are substrates of the renal organic anion transport system [1, 4, 5].

Renal secretion is the major pathway of elimination for many clinically used organic cations and anions, and therefore has important clinical implications. It can greatly influence drug plasma levels, affecting half-life, dosing frequency, therapeutic efficacy, and toxicity. As a carrier-mediated process, tubular secretion is susceptible to both saturation and competition. Although a rare clinical occurrence, saturable tubular secretion can result in nonlinear kinetics. For example, dicloxacillin undergoes substantial tubular secretion; its renal clearance is 2600 mL/min, compared to 120 mL/min for GFR [9]. High dicloxacillin doses saturate its secretory transporter(s), resulting in concentration-dependent renal elimination [9]. Drug-drug interactions due to competition for tubular secretion have also been reported [1, 10]. In some instances, such interactions are beneficial -- the coadministration of a transporter inhibitor allows for a lower dose, and hence a cost savings, of transporter substrate. For example, probenecid has been used to reduce the rapid tubular secretion of antibiotics, allowing for lower doses of antibiotics to be administered [11]. However, most drug-drug interactions due to competition between substrates for tubular secretion are unpredictable and undesirable [1, 10]. For example, toxicities associated with elevated methotrexate levels have been reported when coadministered drugs blocked the renal secretion of methotrexate;

examples of such drugs include naproxen, indomethacin, probenecid, and penicillins [12-14]. Hence, an understanding of the mechanisms and characteristics of renal organic cation and organic anion transport systems should ultimately lead to the development of therapeutic agents with optimized pharmacokinetic properties and lower incidences of toxicities.

Organic Cation and Organic Anion Renal Transport: Cellular Events Involved in Transepithelial Flux in the Kidney

During the past five decades, a variety of *in vivo* and *in vitro* methodologies have been developed to investigate the renal transport of organic cations and organic anions. These methodologies include renal clearance methods, the Sperber chicken preparation, renal cortical slices, stop flow, micropuncture techniques, isolated perfused and nonperfused tubules, isolated brush border and basolateral membrane vesicles, renal cell culture, and, more recently, molecular methodologies such as cloning [15]. Each of these methods allows for the investigation of one or more aspects of renal drug transport. For example, renal clearance methods and the Sperber technique can be used to determine whether a compound undergoes net secretion -- drugs that have renal clearances greater than $fu \cdot GFR$ estimates are actively secreted. Stop flow and micropuncture techniques can be used to determine the site of transport along the nephron. Renal cortical slices and

UCSF LIBRARY

nonperfused tubules allow one to examine transport processes in the basolateral membrane, whereas with perfused tubules, both the basolateral and brush border membranes are functional, allowing for the determination of both secretion and reabsorption. Isolated brush border and basolateral membrane vesicles have been and continue to be used to investigate the mechanisms of transport (i.e. driving forces, kinetic properties, and substrate selectivities). Finally, renal cell culture has also been used to investigate the transport processes in the basolateral and brush border membranes of continuous renal epithelial cell lines, such as MDCK and LLC-PK₁.

The mechanisms and characteristics of the organic cation and organic anion transport systems have been largely defined using prototypical model compounds, which are commercially available in radiolabeled form. The most frequently used model compounds that are employed to study the renal organic cation transport system include tetraethylammonium (TEA), 1-methyl-4-phenylpyridinium (MPP⁺), N¹-methylnicotinamide (NMN), and guanidine (Fig. 1). The most common model compounds used to investigate the renal organic anion transport system include p-aminohippuric acid (PAH), probenecid, and sulfobromophthalein (BPS) (Fig. 2).

Using these methodologies and prototypical model substrates, significant progress has been made in the characterization of the renal organic cation and organic anion transport systems. It has been found that the tubular secretion of organic cations involves

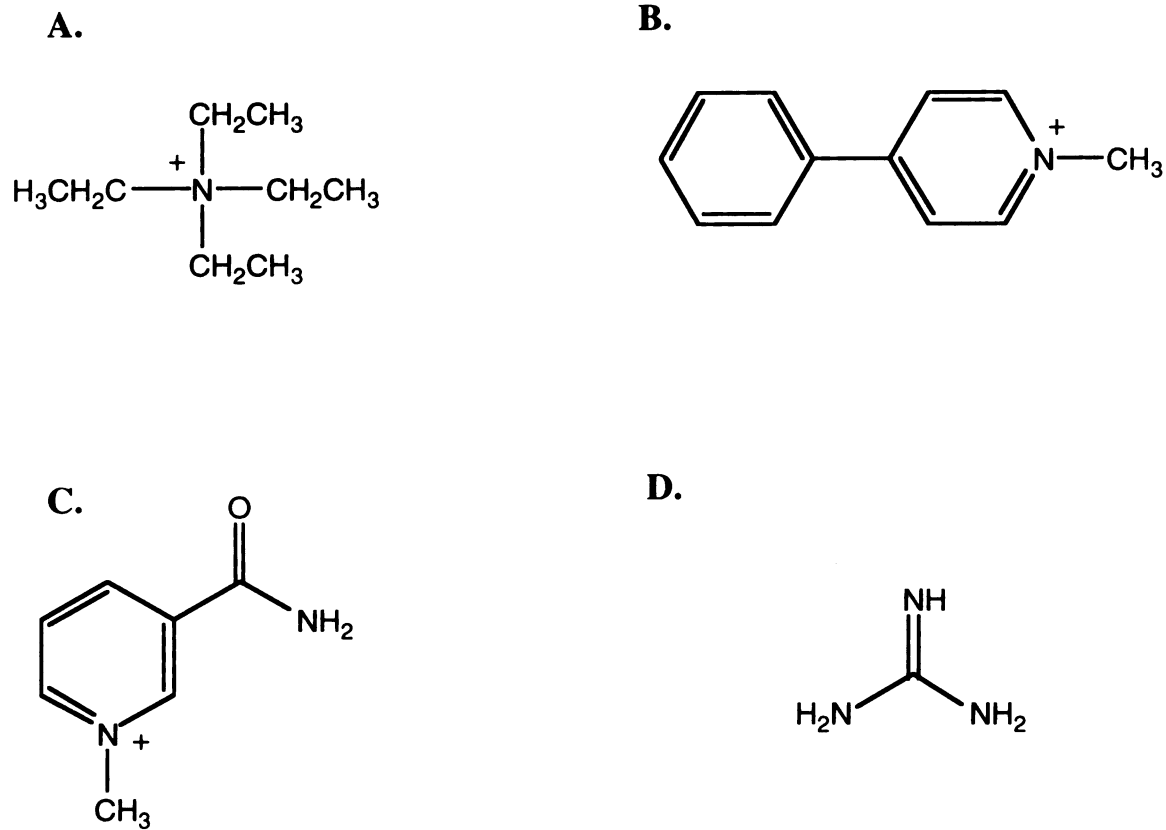
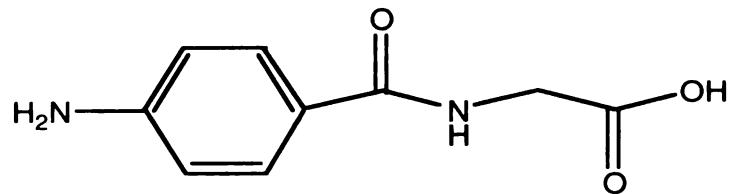
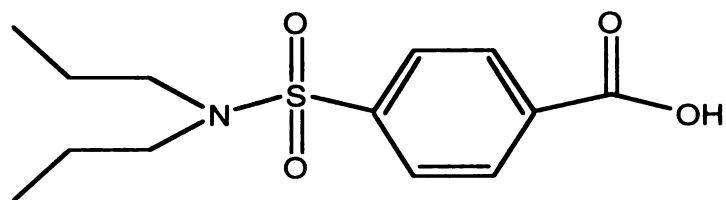


Figure 1. Chemical structures of model organic cations: (A) tetraethylammonium (TEA), (B) 1-methyl-4-phenylpyridinium (MPP⁺), (C) N¹-methylnicotinamide (NMN), (D) guanidine.

A.



B.



C.

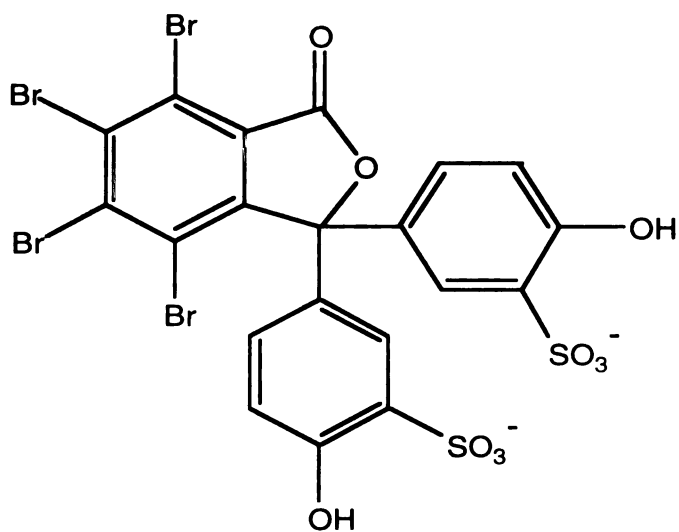


Figure 2. Chemical structures of model organic anions: (A) p-aminohippuric acid (PAH), (B) probenecid, (C) sulfobromophthalein (BPS).

at least two distinct steps (Fig. 3) [2]. In the first step, organic cations move from the blood into the intracellular space via a potential sensitive or an electroneutral exchange mechanism in the basolateral membrane. In the second step, organic cations are transported across the apical membrane and into the tubule lumen by an electroneutral organic cation-proton exchange mechanism(s) (Fig. 3). Collectively, results from many studies suggest that multiple organic cation transporters are present in both membranes of the renal proximal tubule [3]. For example, there is evidence that TEA and NMN are transported across the basolateral membrane by distinct transporters. In nonperfused tubules the relative accumulation of TEA is equal in all three proximal tubule segments, termed S1, S2, and S3 [16], whereas the relative accumulation of NMN is highest in S2 and S3 segments and much lower in the S1 segment [17, 18]. Both an electroneutral organic cation-organic cation exchange mechanism and a potential sensitive organic cation transport mechanism have been characterized in rabbit renal basolateral membrane vesicles. It has been hypothesized that these two transport mechanisms are the result of a single transporter operating in two modes [19].

As with the organic cation transport system in the kidney, renal organic anion secretion involves at least two transporter-mediated events: transport across the basolateral membrane, followed by transport from the tubule cell across the brush border membrane (Fig. 4) [2]. The renal organic anion transport systems have been investigated,

Basolateral

Apical

**Extracellular
fluid**

**Tubule
fluid**

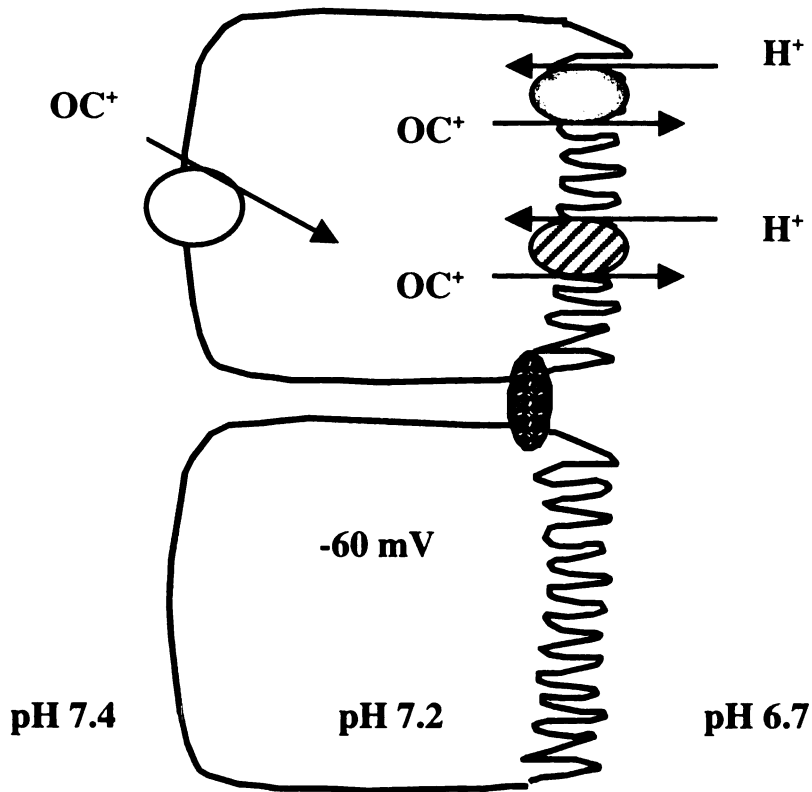


Figure 3. Mechanisms of organic cation transport in the kidney. Organic cations are transported across the BLM down the electrochemical gradient by potential-sensitive transport system(s). At the BBM, intracellular organic cations are exchanged for a luminal proton by one or more transport systems.

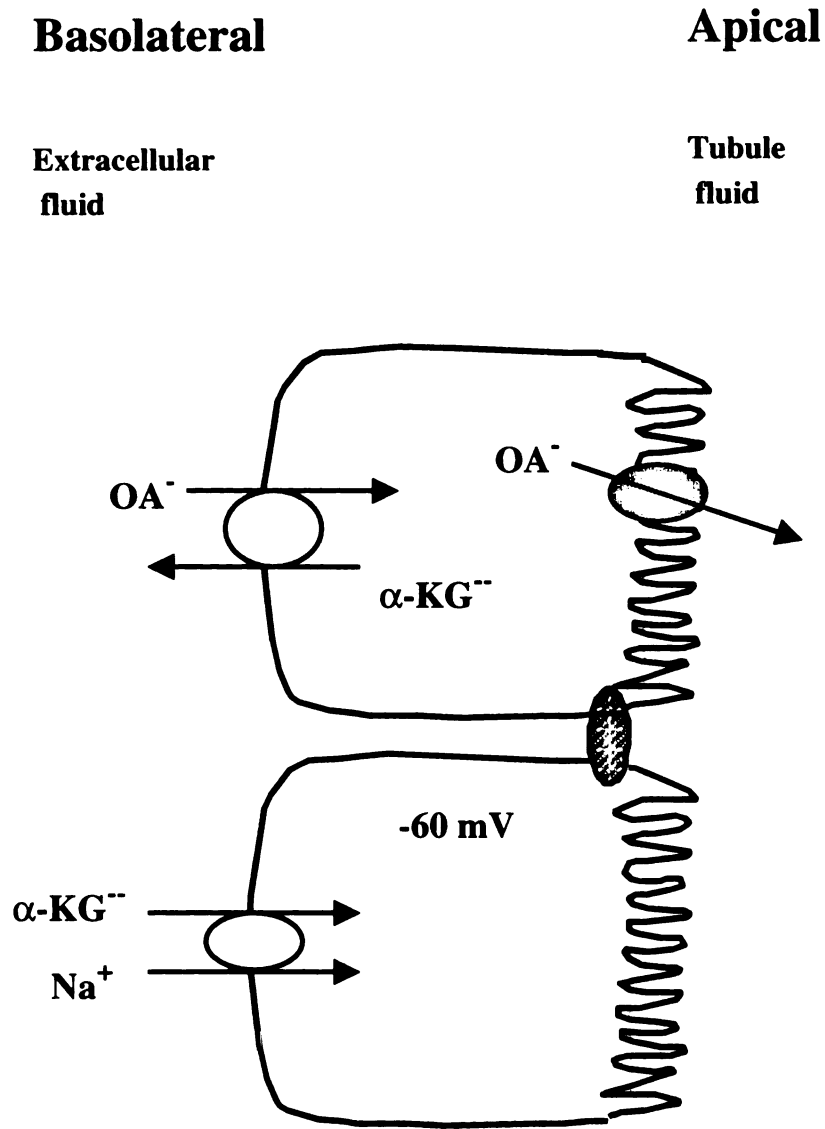
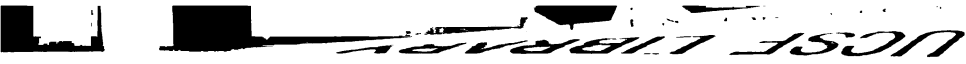


Figure 4. Mechanisms of organic anion transport in the kidney. Organic anions are transported across the BLM in exchange for α -ketoglutarate (α -KG), a divalent endogenous organic anion. The BBM transport mechanisms of organic anions are not well understood - it has been suggested that organic anions are transported across the BBM by facilitated diffusion.



for the most part, using PAH as a model substrate. It has been reported that PAH is transported across the BLM indirectly coupled to the sodium gradient by a tertiary active organic anion-dicarboxylate exchanger [2, 3, 20]. Additional, less well defined transport systems in the BLM of the kidney are also reported [3, 21]. In the BBM, several putative transport systems have been described, but their driving forces and substrate specificities are poorly understood [3, 21]. As with the renal organic cation transport system, multiple overlapping transporters for organic anions are thought to reside in both the basolateral and brush border membranes of renal tubule cells.

Expression Cloning of rOCT1 and rOAT1

To fully characterize these overlapping and multiple transport mechanisms for organic cations and organic anions, it is critical to clone and study the individual transporters in isolation. In this way, the individual components may be characterized and then related back to the system as a whole. During the 1980s, a powerful expression cloning system was developed to clone membrane protein cDNAs -- the *Xenopus laevis* oocyte expression system [22, 23].

The *Xenopus laevis* expression cloning technique has facilitated the cloning of numerous transporters cDNAs and has greatly impacted the transporter field [24-26]. Due to the difficulties in isolating membrane proteins such as transporters, primary

peptide sequence for DNA probe design has not been available for conventional cloning strategies. The *Xenopus laevis* expression system has provided a novel approach for screening a cDNA library by a transport activity assay (Fig. 5). It has been used extensively and successfully as a functional assay to isolate the cDNAs encoding transporters. Moreover, it remains the cloning method of choice for transporter cDNAs when little or no sequence or homology information is available.

The *Xenopus laevis* oocyte expression strategy was used successfully to clone the first organic cation transporter, rOCT1, in 1994 and the first organic anion transporter, rOAT1, in 1997 [27-29]. The cloning of these transporters represents a major milestone in the drug transport field, paving the way to an enhanced understanding of the multiple mechanisms involved in the transport of organic cations and organic anions. With the availability of the cloned transporters, it is now possible to delineate the functional roles of these transporters. More importantly, using the sequence information of the clones, it is now possible to isolate related genes using homology-based cloning methods. From these studies, a more complete understanding of the mechanisms of organic cation and organic anion transport in the body can be established.

Expression Cloning Strategy

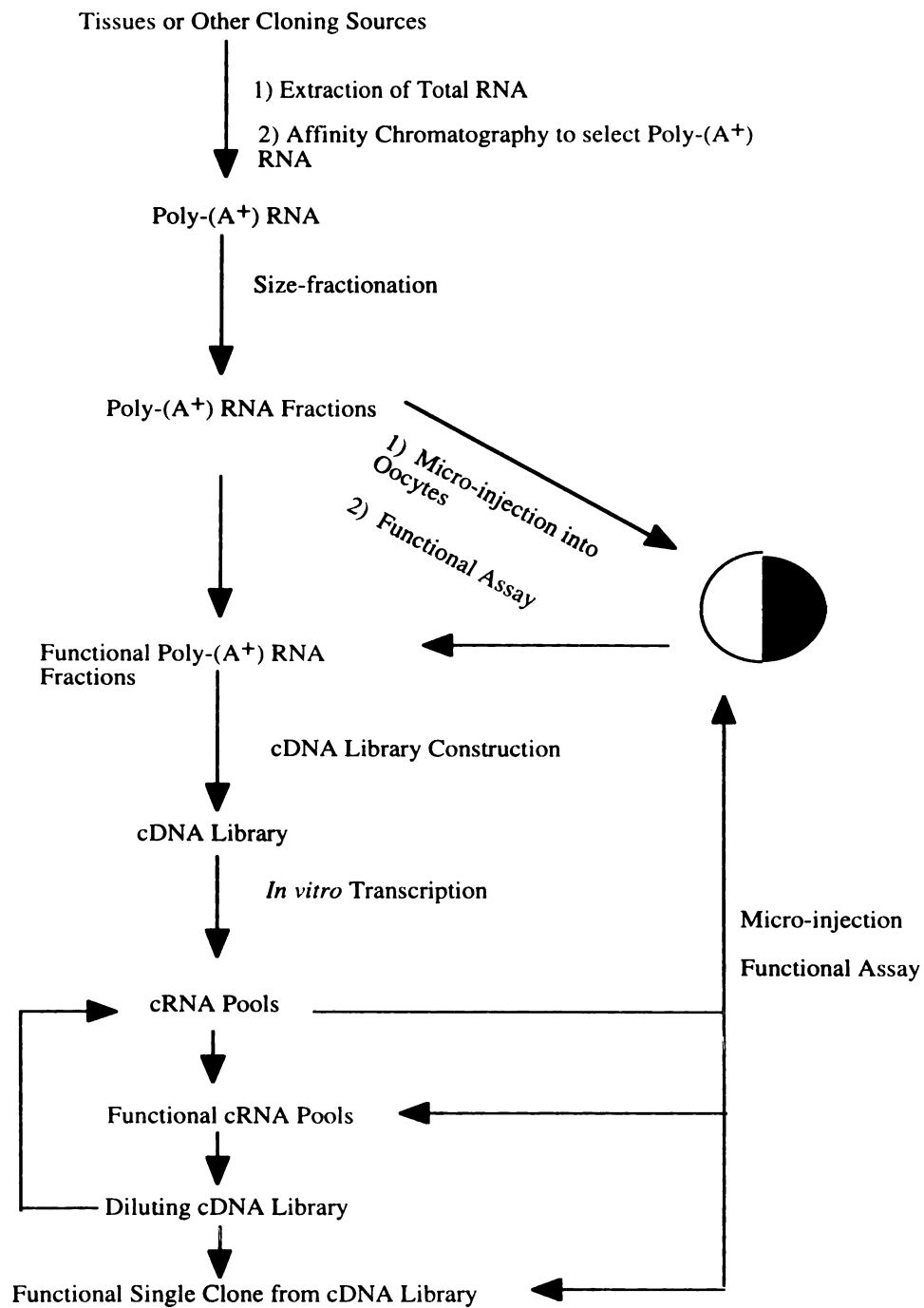
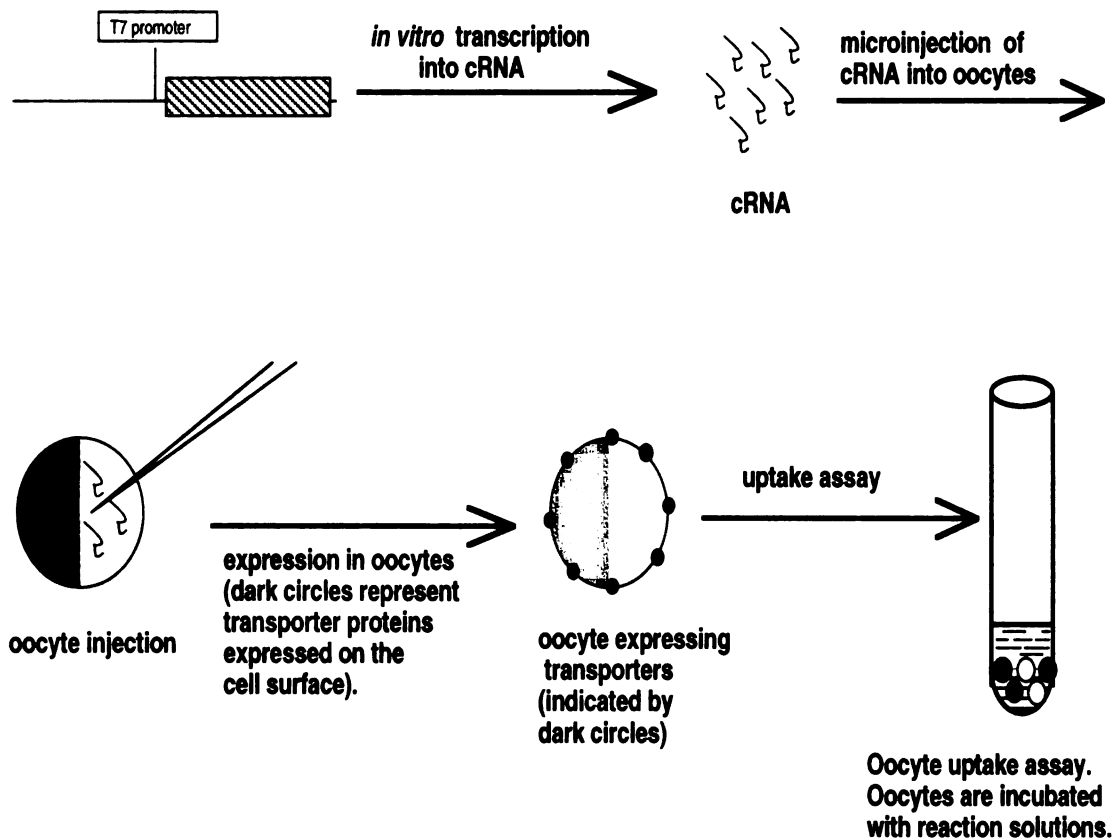


Figure 5. Flow chart of the steps involved in expression cloning.

Initial Molecular Characterization of rOCT1 and rOAT1

Along with the cloning of rOCT1 and rOAT1, initial characterization studies of the transporters were carried out, providing clues to their roles in the renal elimination of drugs [27-29]. Using Northern blot analysis, the tissue distribution of the transporters was determined. In addition, the functional properties of rOCT1 and rOAT1 were examined using the *Xenopus laevis* oocyte expression system. The major steps involved in utilizing this system are shown in Fig. 6. Detailed reviews regarding the *Xenopus laevis* expression system are available [24-26].

rOCT1 was cloned by Grundemann and co-workers in 1994 from a rat kidney cDNA library [27]. rOCT1 is 554 amino acids in length and is predicted to have 12 TMDs (Fig. 7). Northern blot analysis and *in situ* hybridization studies demonstrated that mRNA transcripts of rOCT1 are primarily expressed in the liver (hepatocytes) and kidney (in the proximal tubules) and are expressed at lower levels in the small intestine (enterocytes) [27]. The expression of rOCT1 in the proximal tubules is consistent with the previous intra-nephron localization results from stop flow and micropuncture studies. Although the membrane localization of rOCT1 was not determined in the original cloning study, rOCT1 function was influenced by membrane potential, the hallmark characteristic of a basolateral membrane organic cation transporter. rOCT1 accepts the model organic cation, TEA, as a substrate with an estimated K_m value of 95 μM , which is similar to the



UCST LIBRARY

Figure 6. Schematic representation of the steps involved in the *Xenopus laevis* oocyte expression system.

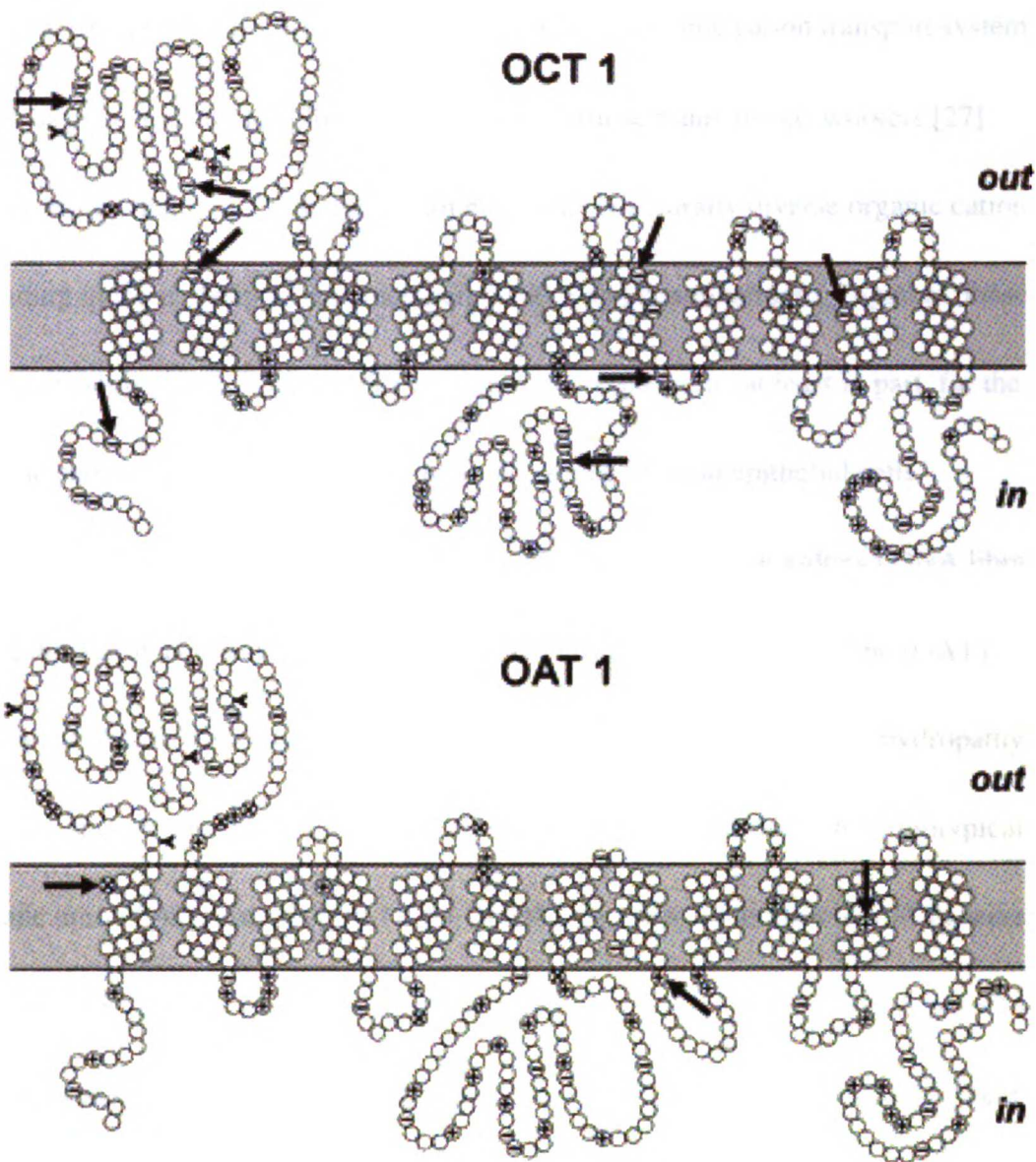


Figure 7. Proposed secondary structures of rOCT1 and rOAT1. The transporters share a common structure of twelve transmembrane domains, but differ in their charged amino acid residues. Arrows indicate negatively charged amino acid residues in rOCT1 and positively charged residues in rOAT1. Adapted from G. Burckhardt *et al.* [31].

UCSF LIBRARY

value of 160 μM found for the basolateral membrane organic cation transport system in rat renal proximal tubules [30]. In their report, Grundemann and co-workers [27] demonstrated that rOCT1 interacts with numerous structurally diverse organic cations, including quinine, desipramine, mepiperphenidol and procainamide. Together, these results strongly suggest that rOCT1 is the protein responsible, at least in part, for the organic cation transport in the basolateral membrane of renal epithelial cells.

rOAT1 was cloned independently by two groups from rat kidney cDNA libraries using the *Xenopus laevis* oocyte expression cloning strategy [28, 29]. The rOAT1 cDNAs are predicted to encode proteins of 551-amino acid residues, and hydropathy analyses suggest that rOAT1 has 12 TMDs (Fig. 7). rOAT1 accepts the prototypical organic anion PAH as a substrate ($K_m = 14 \mu\text{M}$). Specific antibodies to rOAT1 were not available for localization studies when the transporter was originally cloned, but rOAT1 activity was shown to be stimulated by an outwardly directed dicarboxylate gradient [28, 29]. This characteristic suggests that rOAT1 is the tertiary active PAH:dicarboxylate exchange system present in the basolateral membrane of the kidney [2, 3]. Northern blot analyses and *in situ* hybridization studies demonstrated that rOAT1 was expressed only in the kidney, and its expression was restricted to the proximal tubule. Proximal tubule expression of rOAT1 is consistent with early studies on the PAH:dicarboxylate exchanger using tissue and tubule preparations [2, 3]. In addition to PAH, rOAT1

WEST LIBRARY

mediated the uptake of other compounds including methotrexate, cAMP, cGMP, PGE₂, urate, and α -ketoglutarate [28]. Furthermore, numerous structurally diverse compounds, such as cephaloridine, furosemide, ethacrynic acid, indomethacin, and probenecid potently inhibited rOAT1 activity [28]. Together, these results suggest that rOAT1 is a basolateral membrane organic anion transporter. The broad substrate and inhibitor specificities of rOAT1 suggest that this transporter interacts with numerous compounds and could be a major determinant of the renal secretion of clinically used organic anions. Since the cloning of rOCT1 and rOAT1, twelve new members of the organic cation and organic anion transporter family have been cloned; a comprehensive review of the molecular characteristics and function of these transporters is provided in the final chapter of this dissertation.

Summary of Dissertation Studies

The cloning and initial molecular characterization of rOCT1 and rOAT1 represent major advancements, which set the stage for a complete understanding of the molecular functions and *in vivo* roles of organic cation and anion transporters. However, many questions remain to be addressed regarding the molecular characteristics of these cloned transporters and the importance of other transporters to the organic cation and anion renal transport systems. The overall goal of this dissertation was to clone additional organic

WEST LIBRARY
MAY 17 1997

cation transporters from other species and to characterize renal organic cation transporters and organic anion transporters. In particular, a major focus of this work was to elucidate the substrate selectivities of the cloned transporters, in order to gain a better understanding of the types of compounds that the transporters interact with. A secondary goal of this work was to determine the molecular domains and critical amino acid residues responsible for the substrate selectivity of organic cation and organic anion transporters.

Chapter 2. Molecular Cloning and Functional Expression of a Rabbit Renal Organic Cation Transporter

The goal of this study was to clone organic cation transporters from rabbit kidney using a homology-based cloning strategy. A full-length cDNA encoding an organic cation transporter (rbOCT1) was isolated from rabbit kidney. The cDNA is 2732 bp and contains a 55 bp 5'-untranslated region (UTR), a 1665 bp open reading frame (ORF), and a 1012 bp 3'UTR. The 1665 bp ORF is predicted to encode a 554-amino acid protein. Based upon Kyte-Doolittle hydropathy analysis, the protein is predicted to have 12 transmembrane domains. Furthermore, rbOCT1 shares high sequence identity with other mammalian organic cation transporters. When expressed in *Xenopus laevis* oocytes, rbOCT1 mediated ^3H -1-methyl-4-phenylpyridinium (^3H -MPP $^+$) transport was saturable

WEST LIBRARY

(K_m value of $23 \pm 6 \mu\text{M}$), sensitive to membrane potential, and inhibited by various organic cations. rbOCT1 mRNA transcripts are expressed in the kidney, liver, and intestine.

Chapter 3. Kinetic and Selectivity Differences Among Rodent, Rabbit and Human Organic Cation Transporters (OCT1)

Organic cation transporters play an important role in the absorption, distribution, and elimination of clinical agents, toxic substances, and endogenous compounds. In kidney preparations, significant differences in functional characteristics of organic cation transport among various species have been reported. However, the underlying molecular mechanisms responsible for these interspecies differences are not known. The goal of this study was to determine the kinetics and substrate selectivities of organic cation transporter (OCT1) homologs from mouse, rat, rabbit and human, which may contribute to interspecies differences in the renal and hepatic handling of organic cations. Using a series of n-tetraalkylammonium compounds (nTAAs), a correlation between increasing alkyl chain length and affinity for the four OCT1 homologs was observed. However, the apparent affinity constants (K_i) differed among the species homologs. For the mouse homolog, mOCT1, apparent K_i values ranged from $7 \mu\text{M}$ for tetrabutylammonium (TBA) to $2000 \mu\text{M}$ for tetramethylammonium (TMA). In contrast, hOCT1 exhibited weaker

WEST LIBRARY
1997

interactions with the nTAA compounds. *Trans*-stimulation studies and current measurements in voltage-clamped oocytes demonstrated that larger nTAA compounds were transported at greater rates in oocytes expressing hOCT1, whereas smaller nTAAs were transported at greater rates in oocytes expressing mOCT1 or rOCT1. The rabbit homolog, rbOCT1, exhibited intermediate properties in its interactions with nTAAs compared to its rodent and human counterparts. This chapter demonstrates that the human OCT1 homolog has functional properties distinct from those of the rodent and rabbit OCT1 homologs. The study underscores potential difficulties in extrapolating data from pre-clinical studies in animal models to humans.

Chapter 4. The Interaction and Transport of n-Tetraalkylammonium Compounds and Biguanides with a Human Renal Organic Cation Transporter, hOCT2

The goal of this study was to compare the substrate and inhibition profiles of hOCT2 and hOCT1 to determine whether these transporters are functionally distinct. hOCT1 and hOCT2 share 70% sequence identity and their predicted secondary structures, based on hydropathy analysis, are similar. This might suggest that hOCT1 and hOCT2 have similar functional characteristics and are functionally redundant. However, recent chimeric and mutagenesis studies of transporters have shown that even single

amino acid changes in a transporter can dramatically alter its substrate selectivity. Therefore, it is also reasonable to propose that hOCT1 and hOCT2 serve different functions *in vivo*. We examined the interactions of n-tetraalkylammonium (nTAA) compounds and biguanides with hOCT2, an organic cation transporter cloned from the kidney, and compared our results for hOCT1 (Chapter 3). Substantial differences between hOCT2 and hOCT1 in their interactions with nTAAs were found. We then compared the interactions of biguanides with hOCT1 and hOCT2. In contrast to the nTAA compounds, the biguanides appear to interact in a similar manner with hOCT1 and hOCT2. Based on the data reported in this chapter and other recent reports in the literature, it appears that substantial differences, but also similarities, exist in the specificities of hOCT1 and hOCT2.

Chapter 5. Stable Expression of a GFP-rOCT1 Fusion Protein in a Polarized Epithelial Cell Line (MDCK): Intracellular Localization and Functional Characterization

The primary goal of this study was to develop a cell culture model of rOCT1 for use in investigations of its intracellular localization, sorting, and post-transcriptional regulation. rOCT1 is one of the major organic cation transporters in liver and kidney cells, and thus functions as a first step in the elimination pathway of a number of

structurally diverse organic cations. In this study, a polarized epithelial cell line stably transfected with a green fluorescent protein (GFP)-rOCT1 fusion protein was established, and the localization of the fusion protein was investigated via confocal microscopy and functional studies. A secondary goal of this study was to begin to determine structural domains involved in signaling the BLM-sorting of rOCT1. In particular, we determined whether a BLM-sorting signal found in the rOCT1 carboxyl-terminus is required for the basolateral targeting of this transporter. Results from these studies suggest that GFP-rOCT1 is localized to the lateral membrane of polarized MDCK cells, and that amino acids 545 to 556 are not included in the basolateral sorting of rOCT1.

Chapter 6. Arginine 454 of the Organic Anion Transporter, rOAT3, is Essential for *para*-Aminohippurate Transport

Organic anion transporters (OATs) and organic cation transporters (OCTs) mediate the transmembrane flux of numerous xenobiotics across the plasma membrane of epithelial cells. These two gene families differ markedly in their functional characteristics. Substrates of OATs generally carry negative charge(s), whereas substrates of OCTs are cations. In addition to transporting organic anions such as *para*-aminohippurate (PAH), rOAT3 also transports the weak base cimetidine. The goals of this study were to determine the structural domains and amino acid residues essential for

recognition and translocation of PAH by rOAT3. A rOAT3/rOCT1 chimera that encoded a transporter containing transmembrane domains (TMDs) 1-5 of rOAT3 and 6-12 of rOCT1 retained the specificity of rOCT1, suggesting that the critical residues involved in substrate recognition reside within the carboxyl-terminal half of these transporters.

Mutagenesis of arginine 454, a conserved amino acid in TMD 11 of rOAT3, revealed that this amino acid is required for organic anion transport (e.g. PAH, estrone sulfate and ochratoxin A) but not for cimetidine transport. Furthermore, inhibition studies demonstrated that arginine 454 is also not required for inhibition of rOAT3-mediated cimetidine transport by hydrophobic anions and cations, such as indomethacin and quinidine. These studies provide the first insights of molecular determinants in the OAT family that are critical for recognition and translocation of organic anions.

References

1. van Ginneken CA and Russel FG, Saturable pharmacokinetics in the renal excretion of drugs. *Clin Pharmacokinet* **16**(1): 38-54, 1989.
2. Pritchard JB and Miller DS, Mechanisms mediating renal secretion of organic anions and cations. *Physiol Rev* **73**(4): 765-796, 1993.
3. Pritchard JB and Miller DS, Renal secretion of organic anions and cations. *Kidney Int* **49**(6): 1649-1654, 1996.
4. Besseghir K and Roch-Ramel F, Renal excretion of drugs and other xenobiotics. *Ren Physiol* **10**(5): 221-241, 1987.
5. Bendayan R, Renal drug transport: a review. *Pharmacotherapy* **16**(6): 971-985, 1996.
6. LeWitt PA, New drugs for the treatment of Parkinson's disease. *Pharmacotherapy* **20**(1 Pt 2): 26S-32S, 2000.
7. Zhang L, Brett CM and Giacomini KM, Role of organic cation transporters in drug absorption and elimination. *Annu Rev Pharmacol Toxicol* **38**: 431-460, 1998.
8. Koepsell H, Gorboulev V and Arndt P, Molecular pharmacology of organic cation transporters in kidney. *J Membr Biol* **167**(2): 103-117, 1999.
9. Nauta EH and Mattie H, Dicloxacillin and cloxacillin: pharmacokinetics in healthy and hemodialysis subjects. *Clin Pharmacol Ther* **20**(1): 98-108, 1976.

10. Bonate PL, Reith K and Weir S, Drug interactions at the renal level. Implications for drug development. *Clin Pharmacokinet* **34**(5): 375-404, 1998.
11. Brown GR, Cephalosporin-probenecid drug interactions. *Clin Pharmacokinet* **24**(4): 289-300, 1993.
12. Brouwers JR and de Smet PA, Pharmacokinetic-pharmacodynamic drug interactions with nonsteroidal anti-inflammatory drugs. *Clin Pharmacokinet* **27**(6): 462-485, 1994.
13. Davies NM and Anderson KE, Clinical pharmacokinetics of naproxen. *Clin Pharmacokinet* **32**(4): 268-293, 1997.
14. McLeod HL, Clinically relevant drug-drug interactions in oncology. *Br J Clin Pharmacol* **45**(6): 539-544, 1998.
15. Giacomini KM, Hsyu PH and Gisclon LG, Renal transport of drugs: an overview of methodology with application to cimetidine. *Pharm Res* **5**(8): 465-471, 1988.
16. Jacobson HR, Functional segmentation of the mammalian nephron. *Am J Physiol* **241**(3): F203-218, 1981.
17. Besseghir K, Mosig D and Roch-Ramel F, Transport of the organic cation N¹-methylnicotinamide by the rabbit proximal tubule. I. Accumulation in the isolated nonperfused tubule. *J Pharmacol Exp Ther* **253**(2): 444-451, 1990.

WEST LIBRARY

18. Schali C, Schild L, Overney J and Roch-Ramel F, Secretion of tetraethylammonium by proximal tubules of rabbit kidneys. *Am J Physiol* **245**(2): F238-246, 1983.
19. Sokol PP and McKinney TD, Mechanism of organic cation transport in rabbit renal basolateral membrane vesicles. *Am J Physiol* **258**(6 Pt 2): F1599-1607, 1990.
20. Ullrich KJ, Renal transporters for organic anions and organic cations. Structural requirements for substrates. *J Membr Biol* **158**(2): 95-107, 1997.
21. Masereeuw R, Russel FG and Miller DS, Multiple pathways of organic anion secretion in renal proximal tubule revealed by confocal microscopy. *Am J Physiol* **271**(6 Pt 2): F1173-1182, 1996.
22. Sigel E, Use of *Xenopus* oocytes for the functional expression of plasma membrane proteins. *J Membr Biol* **117**(3): 201-221, 1990.
23. Wang HC, Beer B, Sassano D, Blume AJ and Ziai MR, Gene expression in *Xenopus* oocytes. *Int J Biochem* **23**(3): 271-276, 1991.
24. Miller AJ and Zhou JJ, *Xenopus* oocytes as an expression system for plant transporters. *Biochim Biophys Acta* **1465**(1-2): 343-358, 2000.
25. Theodoulou FL and Miller AJ, *Xenopus* oocytes as a heterologous expression system for plant proteins. *Mol Biotechnol* **3**(2): 101-115, 1995.

26. Miller AJ, Smith SJ and Theodoulou FL, The heterologous expression of H(+)-coupled transporters in *Xenopus* oocytes. *Symp Soc Exp Biol* **48**: 167-177, 1994.
27. Grundemann D, Gorboulev V, Gambaryan S, Veyhl M and Koepsell H, Drug excretion mediated by a new prototype of polyspecific transporter. *Nature* **372**(6506): 549-552, 1994.
28. Sekine T, Watanabe N, Hosoyamada M, Kanai Y and Endou H, Expression cloning and characterization of a novel multispecific organic anion transporter. *J Biol Chem* **272**(30): 18526-18529, 1997.
29. Sweet DH, Wolff NA and Pritchard JB, Expression cloning and characterization of ROAT1. The basolateral organic anion transporter in rat kidney. *J Biol Chem* **272**(48): 30088-30095, 1997.
30. Ullrich KJ, Papavassiliou F, David C, Rumrich G and Fritsch G, Contraluminal transport of organic cations in the proximal tubule of the rat kidney. I. Kinetics of N¹-methylnicotinamide and tetraethylammonium, influence of K⁺, HCO₃⁻, pH; inhibition by aliphatic primary, secondary and tertiary amines and mono- and bisquaternary compounds. *Pflugers Arch* **419**(1): 84-92, 1991.
31. Burckhardt G and Wolff NA, Structure of renal organic anion and cation transporters. *Am J Physiol Renal Physiol* **278**(6): F853-866, 2000.

UNIVERSITÄT
DUISBURG
ESSEN



LIBRARY

STAMP

0

0

LIBRARY

STAMP

0

0

0

0

0

0

0

0

0

0

0

0

0

0

0

CHAPTER 2

MOLECULAR CLONING AND FUNCTIONAL EXPRESSION OF A RABBIT RENAL ORGANIC CATION TRANSPORTER*

Introduction

Active secretion in the renal proximal tubule is a major route of elimination of many organic cations from the systemic circulation. Tubule secretion of organic cations in the rabbit involves at least two distinct steps [1]. In the first step, organic cations move from the blood into the intracellular space via a potential sensitive or an electroneutral exchange mechanism in the basolateral membrane. In the second step, organic cations are transported across the apical membrane and into the tubule lumen by an electroneutral organic cation-proton exchange mechanism(s).

The mechanisms of renal organic cation transport have been studied extensively in various experimental preparations from rabbit kidney including perfused [2, 3] and nonperfused [3-7] tubules, apical [8-10] and basolateral [6, 11] membrane vesicles, and isolated tissue slices [12]. Collectively, results from many studies suggest that multiple organic cation transporters are present in both membranes of the renal proximal tubule. For example, there is evidence that tetraethylammonium (TEA) and N¹-methylnicotinamide (NMN) are transported across the basolateral membrane by distinct transporters. Namely, in nonperfused tubules, the relative accumulation of TEA is equal in all three proximal tubule segments whereas the relative accumulation of NMN is highest in S2 and S3 segments and is much lower in the S1 segment [3, 5]. Both an electroneutral organic

*This work was published in *Biochimica et Biophysica Acta* 1369: 1-6, 1998. Permission from the publisher is included in the "Acknowledgments".

cation-organic cation exchange mechanism and a potential sensitive organic cation transport mechanism have been characterized in rabbit renal basolateral membrane vesicles. It has been hypothesized that these two transport mechanisms are the result of a single transporter operating in two modes [11].

The first organic cation transporter was cloned from a rat kidney cDNA library by expression cloning [13]. Subsequently other organic cation transporters have been cloned from rat [14], human [15], and pig [16]. The overall two-step model of renal organic cation transport appears to be conserved among various species based on reports in the literature [1]. However, notable interspecies differences have been reported at the mechanistic and molecular level [4, 15]. For example, a recent study showed a significant species difference between rat and rabbit in the interaction of n-tetraalkylammonium compounds with renal organic cation transport systems [4].

To understand the multiple transport mechanisms present in the rabbit kidney and to investigate the underlying cause(s) of the observed interspecies differences in organic cation transport the molecular cloning of rabbit renal organic cation transporters is essential. Here we report the cloning and functional expression of the first organic cation transporter from rabbit kidney.

Materials and Methods

cDNA Cloning and Analysis. Homology based PCR and Rapid Amplification of cDNA Ends (RACE) PCR methods were used to obtain a full-length cDNA from rabbit kidney. Total RNA was extracted from tissues of adult male New Zealand White rabbits using TriZOL reagent (GIBCO BRL, Rockville, MD). Poly(A)⁺ RNA was purified by oligo(dT) cellulose affinity column chromatography. The cDNA template for PCR was synthesized from isolated kidney mRNA with the oligo (dT) primer using the SuperScript™ Preamplification System (GIBCO BRL, Rockville, MD). Primers 1 and 2 (Table 1) were designed from conserved regions of other mammalian organic cation

WASH STATE LIBRARY



LIB

317

317

317

317

317

317

317

317

317

317

317

317

317

317

317

317

317

317

317

317

317

317

317

317

317

317

317

317

317

317

317

transporters. The PCR was performed in a thermal cycler (PE Applied Biosystems, Foster City, CA) according to the following program: 94°C for 1 min, 48°C for 1 min 50 sec, and 72°C for 3 min for 40 cycles followed by a final 15 min incubation at 72°C. PCR products were subcloned and analyzed by restriction enzyme analysis and/or sequencing. To obtain the remaining 5' - portion of rabbit kidney OCT1 cDNA, a PCR -based method, 5' RACE, was utilized. Three gene specific antisense primers (GSP), designated 5' - GSP - 1, 5' -GSP - 2 and 5' - GSP -3 (Table 1), were designed from the partial rbOCT1 sequence. First - strand cDNA synthesis for 5' -RACE was primed with 5' -GSP - 1 (Table 1) using the 5' RACE System (GIBCO BRL, Rockville, MD) from isolated rabbit kidney total RNA. Homopolymeric tails were added to the 3' - ends of the cDNA which was then amplified by PCR using the anchor primer 1 (Table 1) and nested 5' -GSP -2 primer (Table 1) for 40 cycles according to the following program: 94°C for 1 min, 55°C for 2 min, 72°C for 2 min. A nested PCR was performed with the anchor primer 2 (Table 1) and nested 5' - GSP - 3 primer (Table 1) with a different annealing temperature (50°C) to assess the specificity of the PCR product. 3' - RACE was used to obtain the remaining 3' - portion of rabbit kidney OCT1 cDNA. Two gene specific sense primers, designated 3' - GSP - 1 and 3' - GSP - 2 (Table 1), were designed from the partial rabbit kidney OCT1 sequence (the sequenced PCR fragment). First strand cDNA synthesis was initiated at the poly (A)⁺ tail of isolated rabbit kidney mRNA using the adapter primer (Table 1) in the 3'-RACE kit (GIBCO BRL, Rockville, MD). PCR was performed on this first - strand cDNA using the 3' - GSP - 1 primer (Table 1) and the nested amplification primer (Table 1) with an annealing temperature of 50°C. The resulting amplified products from the nested PCR using the 3' - GSP -2 primer and the amplification primer (Table 1) under the same conditions were then subcloned as described above. The entire rabbit kidney OCT1 cDNA coding region was obtained with the 5' - End primer and 3' - End primer (Table 1) which were designed from the beginning and the end regions of the open reading frame according

to the following PCR protocol: 94°C for 1 min, 55°C for 2 min, 72°C for 2 min for 35 cycles followed by a final 30 minute incubation at 72°C. rbOCT1 cDNA was subcloned into a pGEM-T vector (Promega, Madison, WI) and was then transformed into DH5alpha competent cells.

cDNAs isolated from multiple reverse-transcription and PCR reactions were sequenced by the Biochemical Resource Center DNA Sequence Facility at the University of California, San Francisco with an automated sequencer (Applied Biosystems, Model 373A). Gap and Bestfit programs in the Genetics Computer Group (Wisconsin Package, Version 8) software package as well as the SeqVu program (Version 1.0.1, James Gardner, The Garvan Institute of Medical Research, Australia) were used for multiple sequence alignments. To determine potential protein kinase C phosphorylation and N-glycosylation sites, the Motifs program in the Genetics Computer Group (GCG) package was used. The transmembrane domains of rbOCT1 were predicted based on hydropathy analysis using the Kyte-Doolittle algorithm [17], using a window of 11, in the GCG's Pepplot program.

Expression in Xenopus laevis oocytes and tracer uptake assays. rbOCT1 was expressed in *Xenopus laevis* oocytes for functional characterization as described previously [15]. Stage V and VI oocytes were injected with 25 ng of capped cRNA transcribed in vitro with T7 RNA polymerase (mCAP RNA Capping Kit; Strategene) from linearized plasmid DNA. The injected oocytes were maintained in modified Barth's solution at 18°C until use. The uptake of $^3\text{H-MPP}^+$ (79.9 Ci/mmol, DuPont-New England Nuclear, Boston, MA) in oocytes was measured as described previously [15]. Briefly, groups of six to nine oocytes were incubated in uptake buffer containing MPP⁺ (0.2 μM $^3\text{H-MPP}^+$ and 0.8 μM unlabeled MPP⁺) at 25°C. The incubation time for uptake measurements was 90 minutes; $^3\text{H-MPP}^+$ uptake was linear up to 120 minutes (data not shown). Unlabeled compounds were added to the reaction mixture for inhibition studies. For the Michaelis-Menten study,

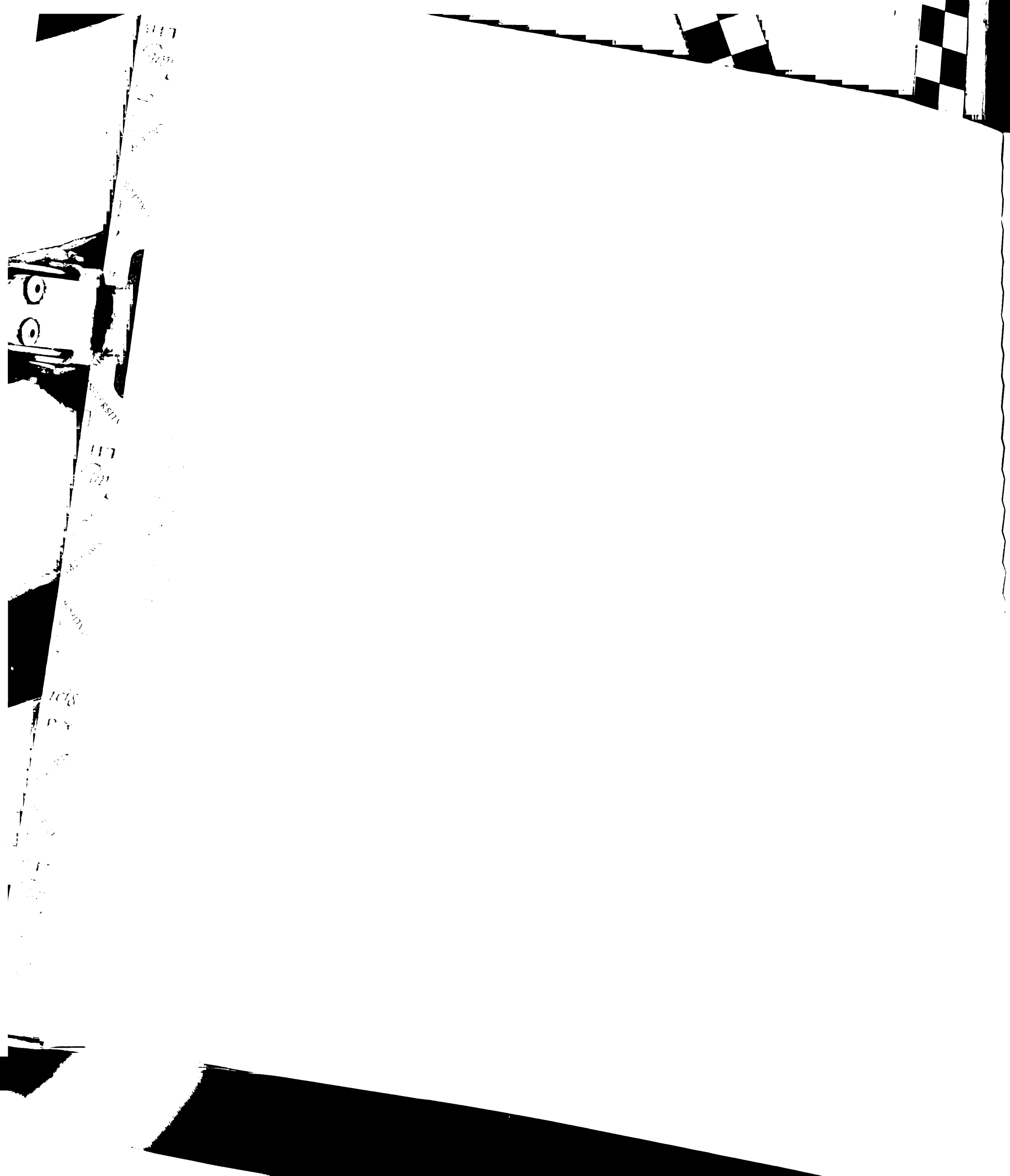


Table 1. Primers used for PCR cloning of rbOCT1 cDNA.

Primer designation	Primer sequence
Primer 1	5'-AGCCATGCCCACCGTGGATGATGATGTC-3'
Primer 2	5'-GAATTCCACCAGAGAAGAATAAAAGAAGTCC-3'
5'-GSP-1	5'-AGCCGGGCGTGTGCATACACCCA-3'
5'-GSP-2	5'-AGCGGCAGGTGGCTCCTGTTGG-3'
5'-GSP-3	5'-CACTGTATAGTTCAGCTCCTCC-3'
Anchor primer 1 ^a (5'-RACE)	5'-CUACUACUACUAGGCCACGCGTCGACTAGTAC GGGIIGGGIIGGGIIG-3'
Anchor Primer 2 ^a (5'-RACE)	5'-CUACUACUACUAGGCCACGCGTCGACTAGTAC-3'
3'-GSP-1	5'-TACTACTGGTGTGTGCCGGAG-3'
3'-GSP-2	5'-TCGCTGGCAGACCTGTTCCG-3'
Adapter primer ^b (3'-RACE)	5'-AGATGAATTCAAGCTTAGGTACCAGTTTTTTTTTTTTTTT TTTT-3'
Amplification primer ^b (3'-RACE)	5'-AGATGAATTCAAGCTTAGGTACCAGT-3'
5'-End primer	5'-TTAGCCCAGAGCAGGCCGGCCGAG-3'
3'-End primer	5'-AAGCGCCGTGTTCCAAAAAAGTTCCT-3'

^a These primers were provided with the 5'- and 3'- RACE system (GIBCO BRL).

^b These primers were modified from Ref. [18].



11
12



11
12

11
12

11
12

$^3\text{H-MPP}^+$ (0.15 μM) with various amounts of unlabeled MPP^+ were included in the reaction mixture. The resting membrane potentials of water and cRNA injected oocytes in depolarizing and physiologic buffers were determined as described previously [15].

RT-PCR. RT-PCR with total RNA isolated from various tissues of adult male New Zealand White rabbits was used to assess tissue distribution of the mRNA transcript of *rbOCT1*. Briefly, total RNA was isolated from the tissues and subjected to RT-PCR with the 5'-End primer and 3'-End primer (Table 1) as described above. The PCR products were electrophoresed through a 1% agarose gel.

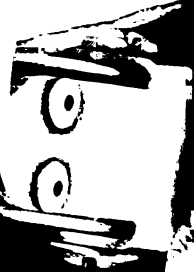
Results and Discussion

Nucleotide and deduced amino acid sequence of rbOCT1. An amplification product of about 1.2 kb in length was obtained when the PCR was performed with Primers 1 and 2 and with rabbit kidney first - strand cDNA as the template. DNA sequencing revealed that the PCR product was 1165 bp in length and was 91% identical to *roCT1* cDNA suggesting that a partial cDNA encoding a rabbit organic cation transporter had been obtained. To clone the full - length cDNA a PCR - based cloning strategy involving 5' - and 3' - RACE protocols was pursued. The resulting 5'-(~300 bp) and 3' - (~1700 bp) RACE products showed overlap with the 1165 bp cDNA isolated above as indicated by sequence analysis. The full - length cDNA was obtained by RT - PCR using primers flanking the 5' - and 3' - ends and rabbit kidney mRNA as the initial template and designated *rbOCT1*.

The full length cDNA is 2732 bp and contains a 55 bp 5'-untranslated region (UTR), a 1665 bp open reading frame (ORF), and a 1012 bp 3'UTR (Fig. 1). The 1665 bp ORF is predicted to encode a 554 amino acid protein, whose initiation codon is in a Kozak consensus sequence, A/GXXAUG [19]. Based upon Kyte-Doolittle hydropathy analysis [17], 12 transmembrane domains are predicted. The protein sequence contains three potential N-linked glycosylation sites (N-X-T/S) at positions 71, 96, and 112. In addition,



117
118
119
120
121
122
123
124
125
126
127
128
129
130
131
132
133
134
135
136
137
138
139
140
141
142
143
144
145
146
147
148
149
150
151
152
153
154
155
156
157
158
159
160
161
162
163
164
165
166
167
168
169
170
171
172
173
174
175
176
177
178
179
180
181
182
183
184
185
186
187
188
189
190
191
192
193
194
195
196
197
198
199
200



117
118
119
120
121
122
123
124
125
126
127
128
129
130
131
132
133
134
135
136
137
138
139
140
141
142
143
144
145
146
147
148
149
150
151
152
153
154
155
156
157
158
159
160
161
162
163
164
165
166
167
168
169
170
171
172
173
174
175
176
177
178
179
180
181
182
183
184
185
186
187
188
189
190
191
192
193
194
195
196
197
198
199
200

117
118
119
120
121
122
123
124
125
126
127
128
129
130
131
132
133
134
135
136
137
138
139
140
141
142
143
144
145
146
147
148
149
150
151
152
153
154
155
156
157
158
159
160
161
162
163
164
165
166
167
168
169
170
171
172
173
174
175
176
177
178
179
180
181
182
183
184
185
186
187
188
189
190
191
192
193
194
195
196
197
198
199
200

117
118
119
120
121
122
123
124
125
126
127
128
129
130
131
132
133
134
135
136
137
138
139
140
141
142
143
144
145
146
147
148
149
150
151
152
153
154
155
156
157
158
159
160
161
162
163
164
165
166
167
168
169
170
171
172
173
174
175
176
177
178
179
180
181
182
183
184
185
186
187
188
189
190
191
192
193
194
195
196
197
198
199
200

117
118
119
120
121
122
123
124
125
126
127
128
129
130
131
132
133
134
135
136
137
138
139
140
141
142
143
144
145
146
147
148
149
150
151
152
153
154
155
156
157
158
159
160
161
162
163
164
165
166
167
168
169
170
171
172
173
174
175
176
177
178
179
180
181
182
183
184
185
186
187
188
189
190
191
192
193
194
195
196
197
198
199
200

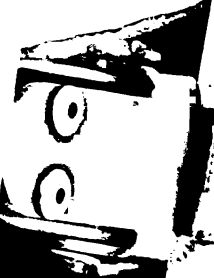
117
118
119
120
121
122
123
124
125
126
127
128
129
130
131
132
133
134
135
136
137
138
139
140
141
142
143
144
145
146
147
148
149
150
151
152
153
154
155
156
157
158
159
160
161
162
163
164
165
166
167
168
169
170
171
172
173
174
175
176
177
178
179
180
181
182
183
184
185
186
187
188
189
190
191
192
193
194
195
196
197
198
199
200


```

1  CCACTGCAGCCCAGACAGGCCGCCGCCAGGGCCGCCAGGTGCACGGGCCGCCACATGCCACCCTGGACGATGTTCTGGAGCAGGTGGGGAGTTCGGC
1  M P T V D D V L E Q V G E F G
101 TGGTTCAGAAAGCAACTTCCTCTTCATGTCTGATCTCGGCCATCTAGCCCCATCTACCTGGGCATCGTCTTCCTGGGCTCACCCCTGACCACC
16 W F Q K R T F L F L C L I S A I L A P I Y L G I V F L G F T P D H R
201 GCTGCCGGAGCCCTGGCGTGGACGAGCTGAGCCAGCGCTGTGGCTGGAGCCCCGAGGAGGAGTGAAGTACACGGTCCCGGGCCTGGGGCCACTGACGG
50 C R S P G V D E L S Q R C G W S P E E E L N Y T V P G L G A T D G
301 GGCTTCGCTCCGCGAGTGCATGCGCTACGAGGTGGACTGGAACAGAGCTCCCTGGGGTGTGTGGACCCCGTGGCCAGCTGGCCCCAAGAGGAGCCAC
83 A F V R Q C M R Y E V D W N Q S S L G C V D P L A S L A P N R S H
401 CTGCCGCTGGGCCCTGTACAGCAGCGGTGGTGTATGACACGGCCCGCTCCATCGTACCGAGTTC AACCTGGTGTGCGCTGACGCCCTGGAAAGGTGG
116 L P L G P C Q H G W V Y D T P G S S I V T E F N L V C A D A W K V D
501 ACCTGTTCAGTCTCGTGAACCTGGGGTTCCTTCCTGGGCTCCCTGGGTGTGCGCTACATCGCAGACAGGTTGGCCGCAAGCTGTGCTGCTGCTGAC
150 L F Q S C V N L G F F L G S L G V G Y I A D R F G R K L C L L L L T
601 CACCCTGATCAACGCGGTTCGGGGTGTCTACGGCCGTGGCCGCCGACTACACGTCCATGCTGCTCTTCGCGCTGTGACGAGGCTGGTTCAGCAAGGGC
183 T L I N A V S G V L T A V A P D Y T S M L L F R L L Q G L V S K G
701 AGCTGGATGTCGGCTACACCCCTGATCAGAGTTCGTGGGCTCAGGCTACAGGAGGACGGTGGCCATCTGTTACAGGTGGCTTCTCTGTGGGGGCTGG
216 S W M S G Y T L I T E F V G S G Y R R T V A I L Y Q V A F S V G L V
801 TGGCCCTCTCGGGCGTCGCCCTACGCCATCCCAGAACTGGCGCTGGCTGCAGCTCACTGTGCTCCCTGGCCACCTTCCTCTGCGCTCTCTACTACTGGTGTGT
250 A L S G V A Y A I P N W R W L Q L T V S L P T F L C L F Y Y W C V
901 GCCCGAGTCCCCTCGATGGCTGTGTCGAGAGAGAAGAACCGGACCGCGTTAAGATCAGGCAACATCGCTCAGAAGAATGGGAAGCTGCCTCCCGCT
283 P E S P R W L L S Q K R N T D A V K I M D N I A Q K N G K L P P A
1001 GACCTCAAGATGCTCTCCCTCGACGAGGAGCTCACGGAGAAGCTGAGCCCATCGCTGGCAGACTGTTCCGGCAGGCCAACCTCAGGAAGCACACCTTCA
316 D L K M L S L D E D V T E K L S P S L A D L F R T P N L R K H T F I
1101 TCCTCATGTTCTATGGTTCACCTGCTCCGTGCTTACCAAGGCTCATCTTGCACATGGGGGCCACTGGCCGGAACTGTACTGGAATTTCTTACTCTC
350 L M F L W F T C S V L Y Q G L I L H M G A T G G N V Y L D F F Y S
1201 CTCTCTGGTGAATTCGCCGACGCTTCGTATCCCTGGTACCATCGACCGCGTGGCCGCTCTATCCCATGGCCGCTCCAATCGGCCGGGGGGGGTGG
383 S L V E F P A A F V I L V T I D R V G R I Y P M A A S N L A A G V
1301 GCCTCCGTCTACCTGATCTTCGTCGCCCAAGACCTGCAGTGGTGCACCTGCTCCTGCTGCTGCGTCGGCCGATGGGGGCCACCATTTGCTCGAGATGA
416 A S V I L I F V P Q D L H W L T I V L S C V G R M G A T I V L Q M I
1401 TCTGCCTGGTGAACGCTGAAGTGTACCCACGTTCCGTCAGGAACCTGGGGTGTGGTGTGTTCTGCGCTATGCGAGCTCGCCGCGCATCACCCCCTT
450 C L V N A E L Y P T F V R N L G V M V C S A L C D V G G I I T P F
1501 CATGGTCTTCGGCTGATGAGGTCTGGCAGCCTTTACCGCTCATGTTTTCGGAGTGTGGGGCTGTTGCGGGGGAATGACCCCTGCTGCTCCAGAG
483 M V F R L M E V W Q P L P L I V F G V L G L L A G G M T L L L P E
1601 ACCAAGGGCGTGGCGTGC CGGAGACCATCGAGGACGCGGAGAACCTCCGGAGGAAAGCAAAGCCCAAGAAAGCAAGATTACCTCCAGGTGCAAACGT
516 T K G V A L P E T I E D A E N L R R K A K P K E S K I Y L Q V Q T S
1701 CGGAAGCTCAAAGGCCCTTAGACAGCAGAGAGAAGAGAGAAGAACCCCGGAGCTGTGCGCTGGGGAAGTGGGGCTCCCTTTCTGCTCCTCCGCGCTC
550 E L K G P
1801 ACCTGCCCCACATTCAGCAAACTCTACGGCATTCTCTCTCTCTTTCTTTCTTTTCTTTTCTTTTCTTTTCTTTTCTTTTCTTTTGGTGGGGGCTTGGC
1901 CTTATTTTGGTTTTATTTTGGCTCAAGTCTCCAGCGTGTGGCTGTCTTTGATCTGCTTCTGTTCCAGTGGGACTGTGGCGTGCAGTTACCCAGGTTTC
2001 TGAAGACACAGTGAACCTACCCTGGCCTCTGTGAGCTGGTTTTCTGGAACGATGATTTATTCACCTACTGGGCAAAACGCTCTTACGACTGGAGGC
2101 ACCTGTGTGGCAAAAGCGTCCACCGTGGAGATTCCTGGGTTTTAAAGACGCGGCTGTGTGACGGGATGGCCCTCCAGCTCATGTTCAAAATATGAGT
2201 CAAGTGGCAGGAAAAGATGTGCTCTTTCCGAAAGCCCAAGGCACCGTGC CGCTTTAGACAAGA AACTTTCGCTGCTGTGTCCCGGGCACCCTCTCT

```

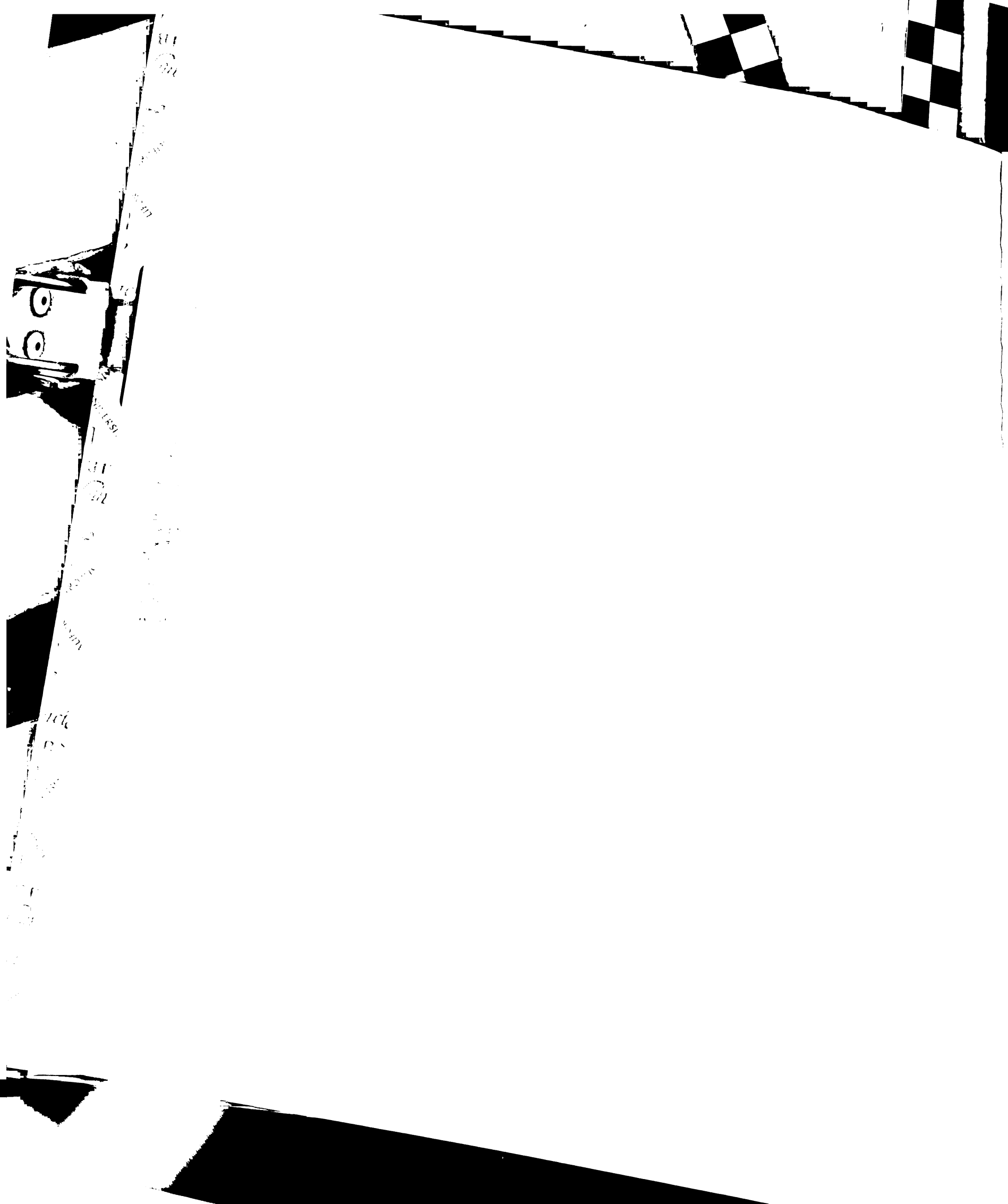
Figure 1. Nucleotide and deduced amino acid sequence of rbOCT1. The start (ATG) and stop (TAA) codons are indicated in bold. The 12 putative transmembrane domains are underlined. Potential N-glycosylation sites of the type N-X-T/S are indicated with asterisks, and potential protein kinase C phosphorylation sites are indicated with points. The sequence was submitted to Genbank with the accession number AF015958.



1
18
19
20
21
22
23
24
25
26
27
28
29
30
31
32
33
34
35
36
37
38
39
40
41
42
43
44
45
46
47
48
49
50
51
52
53
54
55
56
57
58
59
60
61
62
63
64
65
66
67
68
69
70
71
72
73
74
75
76
77
78
79
80
81
82
83
84
85
86
87
88
89
90
91
92
93
94
95
96
97
98
99
100

three potential protein kinase C (PKC) phosphorylation sites were identified at residues 285, 291, and 327, which may be important in the regulation of rbOCT1. There has been one report in the literature which suggests that protein kinase C plays a role in the regulation of organic cation transporter(s) in the S2 segment of the rabbit nephron [20]. With the cloning of rbOCT1, the role of PKC in the regulation of this transporter can now be ascertained. Multiple sequence alignment of the rbOCT1 protein with other members of the gene family showed that the overall positions of secondary structure elements (e.g. transmembrane domains and loops) are well conserved; however, differences in N-linked glycosylation and protein kinase C sites were observed. BLAST searches of the protein and gene databases indicated that the rbOCT1 protein belongs to a growing number of related transporters found in mammals and other organisms. rbOCT1 is most homologous to other mammalian organic cation transporters: rOCT1 [13] (91% similarity and 81% identity), Lx1 [21] (the putative murine homolog of rOCT1) (85% similarity and 81% identity), hOCT1 [15] (83% similarity and 80% identity), rOCT2 [14] (72% similarity and 65% identity), and OCT2p [16] (75% similarity and 69% identity). In addition, it shares significant homology with recently cloned genes from the nematode *C. elegans* (42% similarity and 32% identity; GenBank accession number Z83228) and from the fruit fly *Drosophila* (46% similarity and 36% identity; GenBank accession number Y12400).

Functional expression and characterization of rbOCT1. In *Xenopus laevis* oocytes injected with the cRNA of rbOCT1, the uptake of the model organic cation, $^3\text{H-MPP}^+$, was enhanced 25-fold over that in water-injected oocytes four days post injection (Fig. 2). The rate of MPP^+ uptake was saturable (Fig. 3) with a K_M value of $23 \pm 6 \mu\text{M}$ and a V_{max} of $9.25 \pm 0.66 \text{ pmol/oocyte/90min}$. The organic cations, cimetidine, TEA, and NMN, significantly inhibited the uptake of $^3\text{H-MPP}^+$ (Fig. 4). However, TEA appears to be a more potent inhibitor than NMN. Uptake in cRNA-injected oocytes was dramatically influenced by the membrane potential of the oocytes. In depolarizing buffer (2 mM NaCl,



100

101

102

103

104

105

106

107

108

109

110

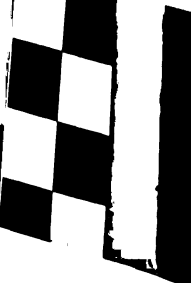
111

112

113

114

115



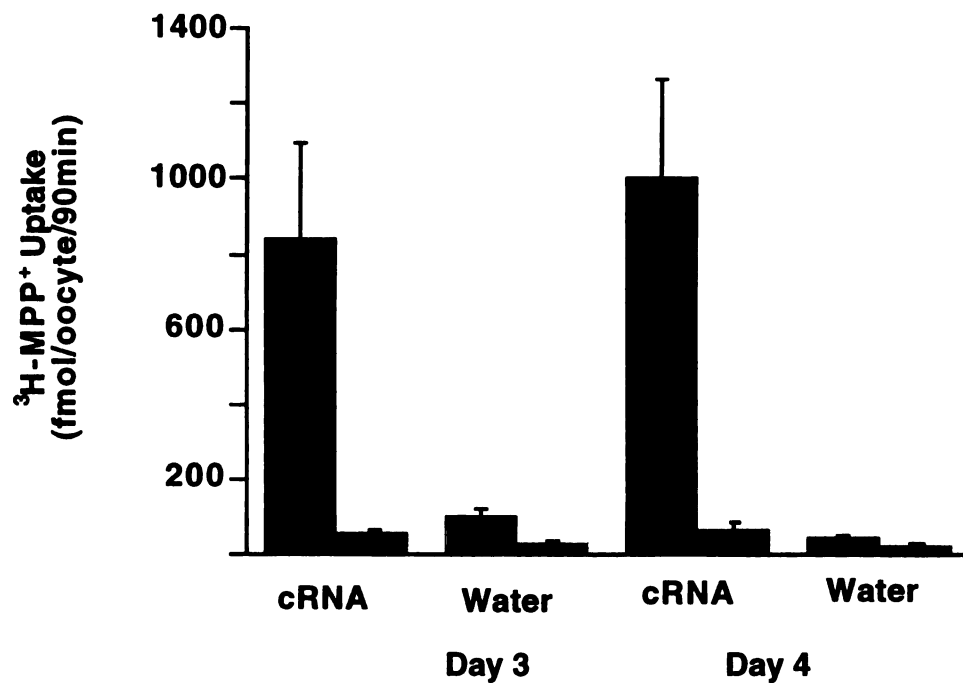
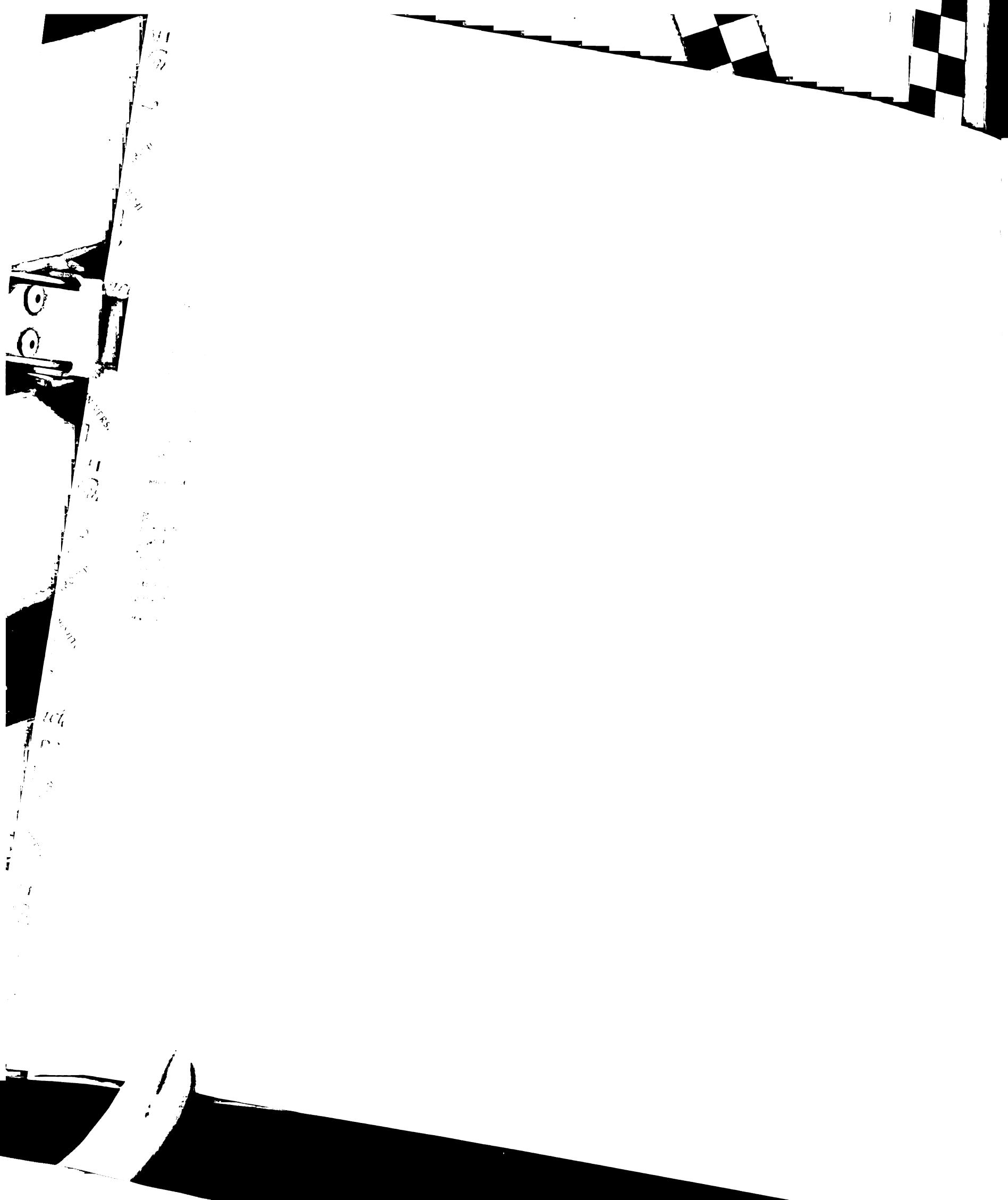


Figure 2. $^3\text{H-MPP}^+$ uptake in oocytes injected with rboOCT1 cRNA. Uptake of $^3\text{H-MPP}^+$ (1 μM) was measured in cRNA and water-injected oocytes in the presence (gray bars) or absence (dark bars) of 5 mM cimetidine three and four days post injection. Data are mean values \pm S.D. from 7 – 9 oocytes.



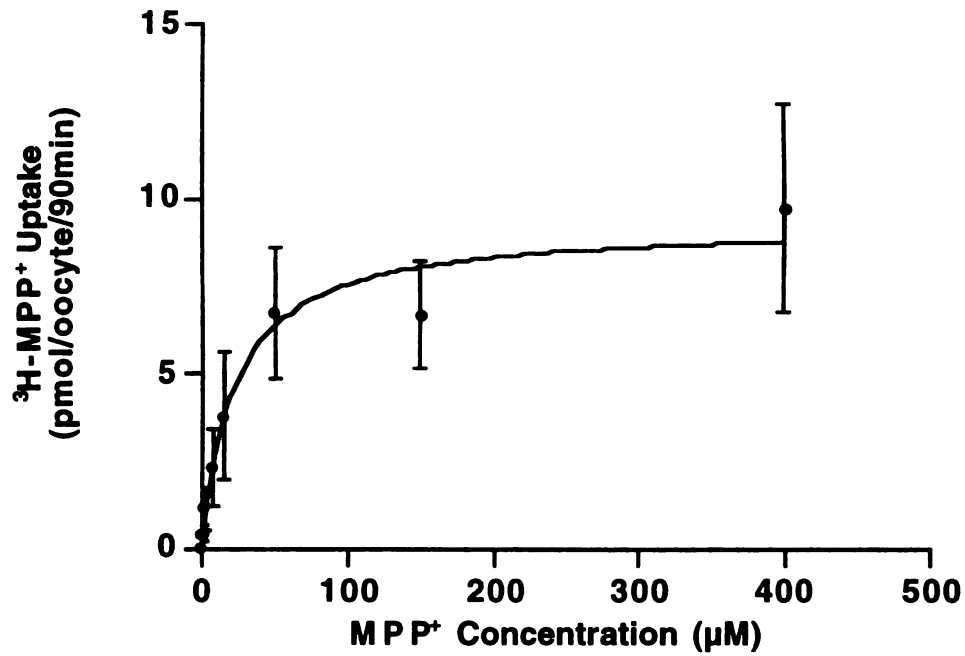


Figure 3. Kinetics of $^3\text{H-MPP}^+$ transport in rbOCT1 cRNA-injected oocytes. Each point represents the mean \pm S.D. from 7 – 9 oocytes. Apparent K_m ($23 \pm 6 \mu\text{M}$) and V_{max} ($9.25 \pm 0.66 \text{ pmol/oocyte/90 min}$) values were determined by fitting to the Michaelis-Menten equation by non-linear regression analysis (Kaleidgraph, Abelbeck Software).

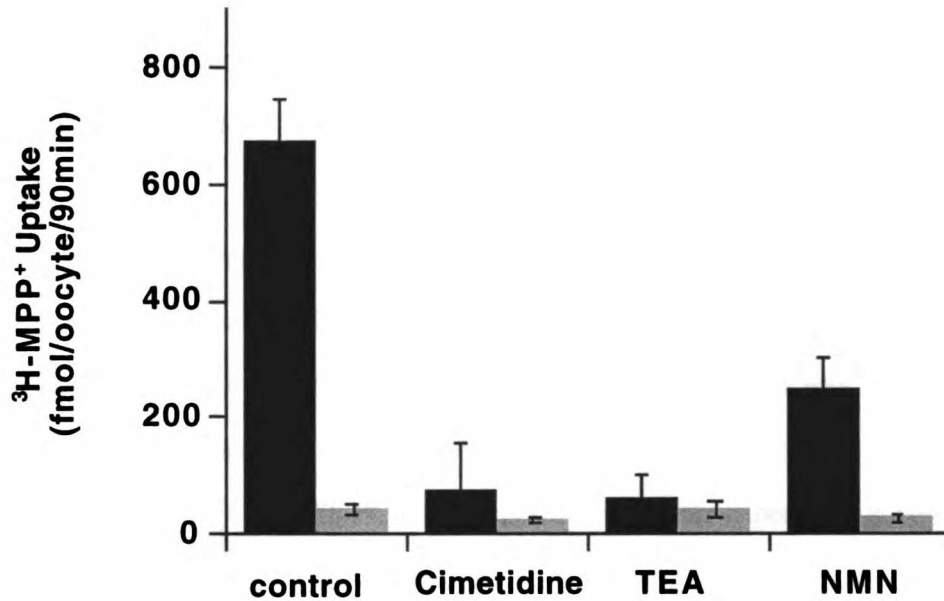


Figure 4. Inhibition of $^3\text{H-MPP}^+$ uptake in rbOCT1 cRNA injected oocytes by model organic cations. Uptake of $^3\text{H-MPP}^+$ ($1\ \mu\text{M}$) was measured in cRNA- (dark bars) and water-injected (gray bars) oocytes in the presence or absence (control) of the indicated organic cations ($5\ \text{mM}$). Data are mean values \pm S.D. from 7 - 9 oocytes

100 mM KCl, 1 mM CaCl₂, 1 mM MgCl₂, 10 mM HEPES/Tris, pH 7.4), in which the membrane potential was -6.4 ± 0.6 mV, the uptake of ³H-MPP⁺ in cRNA-injected oocytes was 60 % lower compared to uptake in oocytes in a physiologic buffer (100 mM NaCl, 2 mM KCl, 1 mM CaCl₂, 1 mM MgCl₂, 10 mM HEPES/Tris, pH 7.4), in which the membrane potential was -38.7 ± 2.2 mV (Fig. 5). This result suggests that rbOCT1 may be localized to the basolateral membrane. As stated earlier, potential sensitive organic cation transport occurs at the basolateral membrane of the rabbit proximal tubule.

Tissue distribution of rbOCT1 mRNA . RT-PCR and Northern blot analysis were used to determine the tissue distribution of rbOCT1 mRNA transcripts. rbOCT1 was cloned from rabbit kidney, and RT-PCR analysis showed that its expression is confined to the cortex in the kidney (Fig. 6). In addition, rbOCT1 transcripts were detected in the liver and intestine (Fig. 6). Based on band intensities, it appears that rbOCT1 is expressed at highest levels in the liver and to a lesser extent in the kidney cortex and intestine. Northern analysis of mRNA derived from various rabbit tissues (including brain, heart, lung, kidney cortex, kidney medulla, intestine, and liver) with a full-length rbOCT1 antisense cRNA probe only detected transcripts in the liver. Two transcripts produced signals of equal intensities at ~2.7-kb and ~4.4-kb (data not shown). Hence, the results of Northern analysis are consistent with the RT-PCR analysis, namely, that rbOCT1 transcripts are expressed most abundantly in the liver and at lower levels in other tissues. The low level of rbOCT1 expression in the kidney is somewhat surprising. This may indicate that other transporters play a greater role in organic cation transport in the rabbit kidney. Alternatively, rbOCT1 may be expressed in only a specific segment of the nephron where it would mediate site specific transport of organic cations. It should be noted that other renal transporters (e.g. the human PEPT2) have been reported to be expressed at low levels and were also undetectable by Northern blot analysis [22].

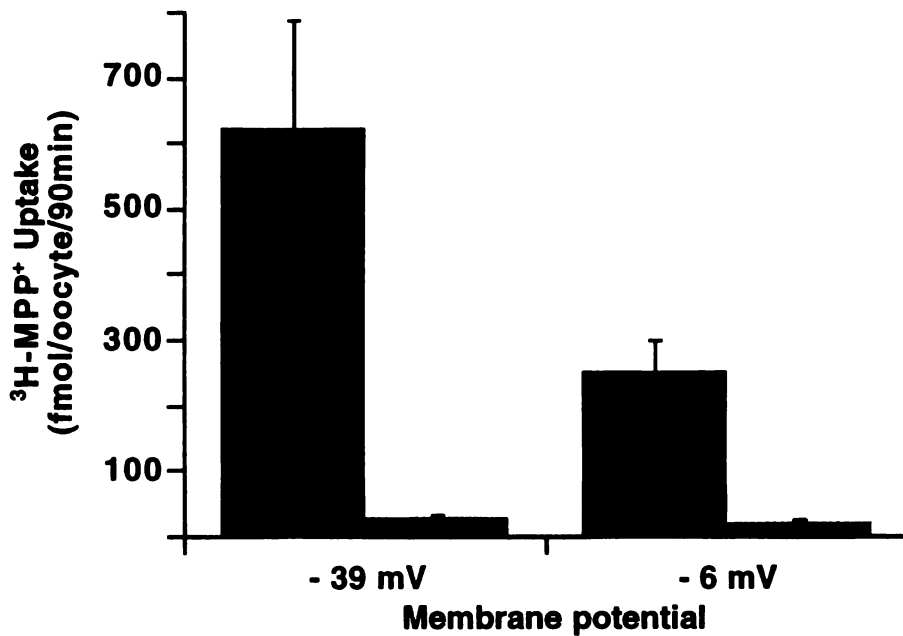


Figure 5. Effect of membrane potential on $^3\text{H-MPP}^+$ uptake in rbOCT1 cRNA-injected oocytes. Uptake of $^3\text{H-MPP}^+$ ($1 \mu\text{M}$) was measured in cRNA- (dark bars) and water-injected (gray bars) oocytes in either sodium uptake buffer ($V_m = -39 \text{ mV}$) or potassium uptake buffer ($V_m = -6 \text{ mV}$). Data are mean values \pm S.D. from 7 – 9 oocytes.

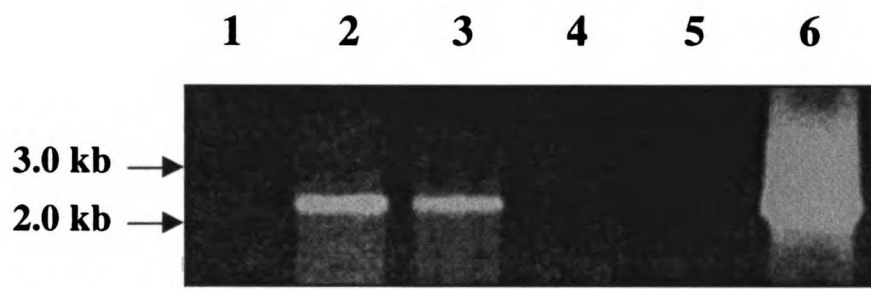


Figure 6. RT-PCR analysis of rbOCT1 mRNA transcript expression. Total RNA from rabbit kidney medulla (lane 1), kidney cortex (lane 2), small intestine (lane 3), heart (lane 4), lung (lane 5), and liver (lane 6) was subjected to RT-PCR using primers 5'-End primer and 3'-End primer (Table 1). The RT-PCR products were analyzed by agarose gel electrophoresis. A molecular weight standard was used to determine the band size.

In summary, we have cloned and functionally expressed the first organic cation transporter from rabbit kidney (rbOCT1). Because much of our understanding of the mechanisms of renal organic cation transport is based primarily upon studies performed in rabbit kidney, the cloning of rbOCT1 represents an essential step in elucidating the mechanisms of organic cation transport in the kidney at a molecular level. In addition, notable interspecies differences in the interaction of bulkier organic cations with the respective transporters in rat and rabbit kidney have been observed [4]. With the availability of rbOCT1 and rOCT1, we can now carry out detailed kinetic studies to elucidate possible interspecies differences in the function of the two transporters.

References

1. Pritchard JB and Miller DS, Mechanisms mediating renal secretion of organic anions and cations. *Physiol Rev* **73**(4): 765-796, 1993.
2. McKinney TD, Heterogeneity of organic base secretion by proximal tubules. *Am J Physiol* **243**(4): F404-407, 1982.
3. Schali C, Schild L, Overney J and Roch-Ramel F, Secretion of tetraethylammonium by proximal tubules of rabbit kidneys. *Am J Physiol* **245**(2): F238-246, 1983.
4. Groves CE, Evans KK, Dantzler WH and Wright SH, Peritubular organic cation transport in isolated rabbit proximal tubules. *Am J Physiol* **266**(3 Pt 2): F450-458, 1994.
5. Besseghir K, Mosig D and Roch-Ramel F, Transport of the organic cation N1-methylnicotinamide by the rabbit proximal tubule. I. Accumulation in the isolated nonperfused tubule. *J Pharmacol Exp Ther* **253**(2): 444-451, 1990.
6. Dantzler WH, Wright SH, Chatsudthipong V and Brokl OH, Basolateral tetraethylammonium transport in intact tubules: specificity and trans-stimulation. *Am J Physiol* **261**(3 Pt 2): F386-392, 1991.
7. Schali C and Roch-Ramel F, Transport and metabolism of [3H]morphine in isolated, nonperfused proximal tubular segments of the rabbit kidney. *J Pharmacol Exp Ther* **223**(3): 811-815, 1982.
8. Gisclon L, Wong FM and Giacomini KM, Cimetidine transport in isolated luminal membrane vesicles from rabbit kidney. *Am J Physiol* **253**(1 Pt 2): F141-150, 1987.
9. Miyamoto Y, Tirupathi C, Ganapathy V and Leibach FH, Multiple transport systems for organic cations in renal brush-border membrane vesicles. *Am J Physiol* **256**(4 Pt 2): F540-548, 1989.
10. Wright SH and Wunz TM, Mechanism of cis- and trans-substrate interactions at the tetraethylammonium/H⁺ exchanger of rabbit renal brush-border membrane vesicles. *J Biol Chem* **263**(36): 19494-19497, 1988.

11. Sokol PP and McKinney TD, Mechanism of organic cation transport in rabbit renal basolateral membrane vesicles. *Am J Physiol* **258**(6 Pt 2): F1599-1607, 1990.
12. Kim YK, Kim YH, Jung JS and Lee SH, Effect of renal ischemia on organic anion and cation transport in rabbit proximal tubule. *Kidney Blood Press Res* **19**(6): 332-339, 1996.
13. Grundemann D, Gorboulev V, Gambaryan S, Veyhl M and Koepsell H, Drug excretion mediated by a new prototype of polyspecific transporter. *Nature* **372**(6506): 549-552, 1994.
14. Okuda M, Saito H, Urakami Y, Takano M and Inui K, cDNA cloning and functional expression of a novel rat kidney organic cation transporter, OCT2. *Biochem Biophys Res Commun* **224**(2): 500-507, 1996.
15. Zhang L, Dresser MJ, Gray AT, Yost SC, Terashita S and Giacomini KM, Cloning and functional expression of a human liver organic cation transporter. *Mol Pharmacol* **51**(6): 913-921, 1997.
16. Grundemann D, Babin-Ebell J, Martel F, Ording N, Schmidt A and Schomig E, Primary structure and functional expression of the apical organic cation transporter from kidney epithelial LLC-PK1 cells. *J Biol Chem* **272**(16): 10408-10413, 1997.
17. Kyte J and Doolittle RF, A simple method for displaying the hydropathic character of a protein. *J Mol Biol* **157**(1): 105-132, 1982.
18. Schaefer BC, Revolutions in rapid amplification of cDNA ends: new strategies for polymerase chain reaction cloning of full-length cDNA ends. *Anal Biochem* **227**(2): 255-273, 1995.
19. Kozak M, The scanning model for translation: an update. *J Cell Biol* **108**(2): 229-241, 1989.
20. Hohage H, Morth DM, Querl IU and Greven J, Regulation by protein kinase C of the contraluminal transport system for organic cations in rabbit kidney S2 proximal tubules. *J Pharmacol Exp Ther* **268**(2): 897-901, 1994.

21. Schweifer N and Barlow DP, The Lx1 gene maps to mouse chromosome 17 and codes for a protein that is homologous to glucose and polyspecific transmembrane transporters. *Mamm Genome* 7(10): 735-740, 1996.

22. Liu W, Liang R, Ramamoorthy S, Fei YJ, Ganapathy ME, Hediger MA, Ganapathy V and Leibach FH, Molecular cloning of PEPT 2, a new member of the H⁺/peptide cotransporter family, from human kidney. *Biochim Biophys Acta* 1235(2): 461-466, 1995.

CHAPTER 3

KINETIC AND SELECTIVITY DIFFERENCES AMONG RODENT, RABBIT AND HUMAN ORGANIC CATION TRANSPORTERS (OCT1)*

Introduction

Renal and hepatic secretion of organic cations is a major pathway of xenobiotic elimination from the systemic circulation. It is now known that numerous clinically used drugs as well as toxic and endogenous compounds are substrates for secretory transporters in the kidney and liver [1, 2]. These transport mechanisms have been studied in detail over the past two decades in a variety of tissue and membrane preparations and in cell culture models as well [3-6]. Electrogenic transport systems have been characterized in kidney and liver basolateral membranes (BLM), which move organic cations down the electrochemical gradient from the blood into tubular cells and hepatocytes.

*This work was published in *The Journal of Pharmacology and Experimental Therapeutics* 292: 1146-1152, 2000. Permission from the publisher is included in the "Acknowledgments".

In contrast, in kidney and liver brush border membranes (BBM) several organic cation/proton exchange mechanisms have been described which are distinct from the BLM transport systems [1, 7-10]. Together the BLM and the BBM transporters are responsible for the transcellular flux of organic cations from the blood to the tubule fluid or bile and hence play an important role in removing many compounds from the systemic circulation.

Although this two step model of transcellular flux of organic cations is similar among species, several interspecies variations in the characteristics of renal organic cation transport have been reported. For example, recent studies of the effects of n-tetraalkylammonium (nTAA) compounds on organic cation transport in the rabbit and rat kidney suggest a marked interspecies variation in the renal handling of organic cations [11, 12].

The goal of the current study was to compare the functional characteristics of the OCT1 transporters from mouse, rat, rabbit and human. Using a series of nTAA compounds with varying alkyl chain lengths, we found a correlation between increasing alkyl chain length and affinity for OCT1 regardless of the species. However, notable differences in the nTAA affinities and turnover rates were found among species. In particular, the rodent transporters had a higher affinity for the nTAAs compared to the human transporter and the human transporter had comparatively higher turnover rates for

larger nTAAs than the rodent homologues. This is the first report of kinetic and selectivity differences among organic cation transporter homologues. Such differences may have important consequences for species comparisons of *in vivo* disposition of organic cations.

Materials and Methods

cRNA transcription and Xenopus oocyte expression. Oocytes were harvested from oocyte positive *Xenopus laevis* (Nasco, Fort Atkinson, WI) and were dissected and treated with collagenase D (Boehringer-Mannheim Biochemicals, Indianapolis, IN) in a calcium-free ORII solution as previously described [13]. Oocytes were maintained at 18°C in modified Barth's medium. Healthy stage V and VI oocytes were injected with capped cRNA (1 µg/µl). Capped cRNA was transcribed *in vitro* with T7 polymerase (mCAP RNA Capping kit; Stratagene) from *Spe* I linearized plasmids containing mouse (mOCT1), rat (rOCT1), rabbit (rbOCT1) or human (hOCT1) transporter cDNAs [13-16].

Tracer uptake measurements. Transport of ³H-MPP⁺ (82 Ci/mmol, Dupont-New England Nuclear, Boston, MA) in oocytes was measured 2 – 7 days after injection as described previously [13, 16]. MPP⁺ uptakes were carried out as follows: groups of seven to nine oocytes were incubated in Na⁺ buffer (100 mM NaCl, 2 mM KCl, 1 mM CaCl₂, 1 mM MgCl₂, 10 mM HEPES/Tris, pH 7.2) containing ³H-MPP⁺ (1 µM: 0.1 µM

$^3\text{H-MPP}^+$ and $0.9\ \mu\text{M}$ unlabeled MPP^+) for 1 h. Uptake was stopped by washing the oocytes 5 times with 3 ml of ice-cold Na^+ buffer. The radioactivity associated with each oocyte was then determined by scintillation counting. For inhibition studies, unlabeled nTAA compounds were added to the reaction solutions as needed.

In *trans*-stimulation studies, groups of 5 – 7 OCT1 cRNA- or uninjected oocytes were washed three times with K^+ buffer (2 mM NaCl, 100 mM KCl, 1 mM CaCl_2 , 1 mM MgCl_2 , 10 mM HEPES/Tris, pH 7.2). The oocytes were then rapidly injected with 50 nl of a K^+ solution containing an unlabeled nTAA compound. The nTAA concentrations (TMA: 100 mM; TEA: 20 mM; TPrA: 10 mM; TBA: 5 mM; TPeA: 2 mM) and injection volume (50 nl) were chosen based upon an average oocyte intracellular volume of 500 nl to produce intracellular nTAA concentrations (shown in Fig. 3) that would be at saturating levels (i.e. ≥ 10 -fold the K_m or K_i value). Oocytes injected with 50 nl of K^+ buffer were used for controls in the *trans*-stimulation studies. After injections, the oocytes were quickly transferred to a small disposable borosilicate glass culture tube; any remaining K^+ was aspirated off, and 85 μl of MPP^+ (1 μM : 0.1 μM $^3\text{H-MPP}^+$ and 0.9 μM unlabeled MPP^+) in K^+ buffer was added. MPP^+ uptake was stopped after 10 min by washing the oocytes 5 times with 3 ml of ice-cold K^+ buffer. The radioactivity associated with each oocyte was then determined by scintillation counting.

Electrophysiology studies. Electrophysiology experiments were performed at room temperature (21 – 23°C) 5 -10 d post injection. Steady-state ligand-induced currents were measured with a two-electrode voltage clamp. Oocytes were voltage clamped at –50 mV and superfused with Na⁺ buffer 2 min before and after 30 s ligand superfusions. Recordings were obtained in a 25 µl recording chamber at flow rates of ~ 3 ml/min. The nTAA-induced current was the difference between the values measured in the presence of nTAA and the average of values recorded in Na⁺ buffer alone before and after nTAA superfusion. Uninjected oocytes were used as controls. In addition, the nontransported inhibitor, quinidine (100 µM), was used as a negative control to ensure that the observed inwardly directed currents were not due to inhibition of cation efflux from the oocyte [17].

Data analysis. Values are expressed as mean ± standard error (S.E.) or mean ± standard deviation (S.D.) as indicated in the legends. Six to nine oocytes were used to generate a data point in each experiment. All experiments were repeated at least once using different batches of oocytes, unless indicated otherwise in the legends. Apparent K_i values were determined as described previously [18, 19].

Materials. The nTAA compounds were purchased from Sigma (St. Louis, MO): tetramethylammonium (5 M solution) (TMA), tetraethylammonium (TEA), tetrapropylammonium (TPrA), tetrabutylammonium (TBA) and tetrapentylammonium

(TPeA). All other reagents were purchased from either Sigma (St. Louis, MO) or Fisher (Pittsburgh, PA) or as indicated. $^3\text{H-MPP}^+$ (82 Ci/mmol) was purchased from Dupont-New England Nuclear (Boston, MA).

Results

Inhibition of OCT1 mediated uptake by nTAA compounds. Inhibition studies with nTAA compounds of increasing chain length were carried out in order to determine the relationship between alkyl chain length and inhibition potency. The inhibition potency of the nTAA compounds (50 μM) for the OCT1 transporters from mouse, rat, rabbit, and human increased with alkyl chain length (Fig. 1). The concentration dependence of the nTAA compounds in inhibiting $^3\text{H-MPP}^+$ (1 μM) uptake was determined. The data were fit as described previously to determine the apparent K_i values [18, 19]. Representative inhibition curves for TMA, TEA, TPrA and TBA are shown in Fig. 2 for mOCT1. The apparent K_i values decreased with increasing chain length from $>2000 \mu\text{M}$ for TMA to $\sim 7 \mu\text{M}$ for TBA (Table 1). Similar trends between increasing chain length and inhibition potency were found for all species. However, notable potency differences were found among species (Table 1). Most apparent were potency differences between the human and rodent transporters. The rabbit OCT1 homologue exhibited intermediate sensitivity to the nTAA compounds. One interesting and notable

exception was TEA; TEA appeared to have a similar affinity for all four OCT1 homologues.

Efflux of nTAAs from oocytes expressing OCT1. *Trans*-stimulation studies are often used to test whether a compound is an actual substrate (permeant) for a transporter [19-22]. *Trans*-stimulation studies were carried out under depolarized conditions (i.e. in K⁺ containing buffer) to minimize the effects of membrane potential on ³H-MPP⁺ (1 μM) uptake. In oocytes expressing hOCT1, ³H-MPP⁺ influx was *trans*-stimulated the most by TEA and TPrA. TMA, TBA or TPeA neither *trans*-inhibited nor -stimulated hOCT1 mediated ³H-MPP⁺ influx (Fig. 3). In marked contrast, in oocytes expressing mOCT1 or rOCT1, the smaller nTAA compounds, TMA and TEA, *trans*-stimulated ³H-MPP⁺ influx, whereas the larger nTAA compounds *trans*-inhibited ³H-MPP⁺ influx (Fig. 3). The rabbit homologue appeared to have a somewhat intermediate function between its rodent and human counterparts. The influx of ³H-MPP⁺ was *trans*-stimulated the most by TEA, weakly by TPrA, but not by TMA in oocytes expressing rbOCT1. The larger nTAA compounds TBA and TPeA weakly *trans*-inhibited ³H-MPP⁺ influx (Fig. 3). It is possible that apparent *trans*-inhibition may result from *cis*-inhibition due to rapid efflux of compounds from the oocytes. This possibility may not be excluded; however, it is unlikely because of the large volume into which the compounds would efflux (i.e., 100 μl), which would substantially reduce their concentrations on the *cis* side.

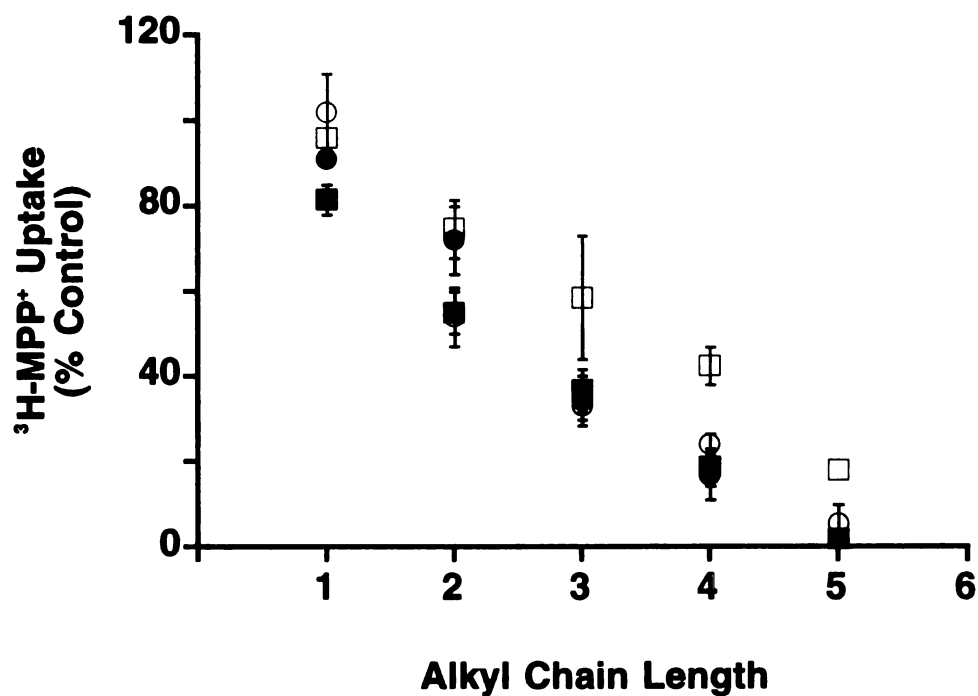


Figure 1. Effect of nTAA compounds (50 μM) of increasing chain length on $^3\text{H-MPP}^+$ (1 μM) uptake (1 h) by OCT1-expressing oocytes. The uptake of $^3\text{H-MPP}^+$ (1 h incubation) in Na^+ uptake buffer was measured in oocytes expressing mOCT1 (●), rOCT1 (■), rbOCT1 (○) or hOCT1 (□). Each data point represents the mean rate of uptake as percent of control in which no inhibitor was present. Data represent mean \pm S.E. (n = 6-9) obtained from two to four experiments in separate batches of oocytes.

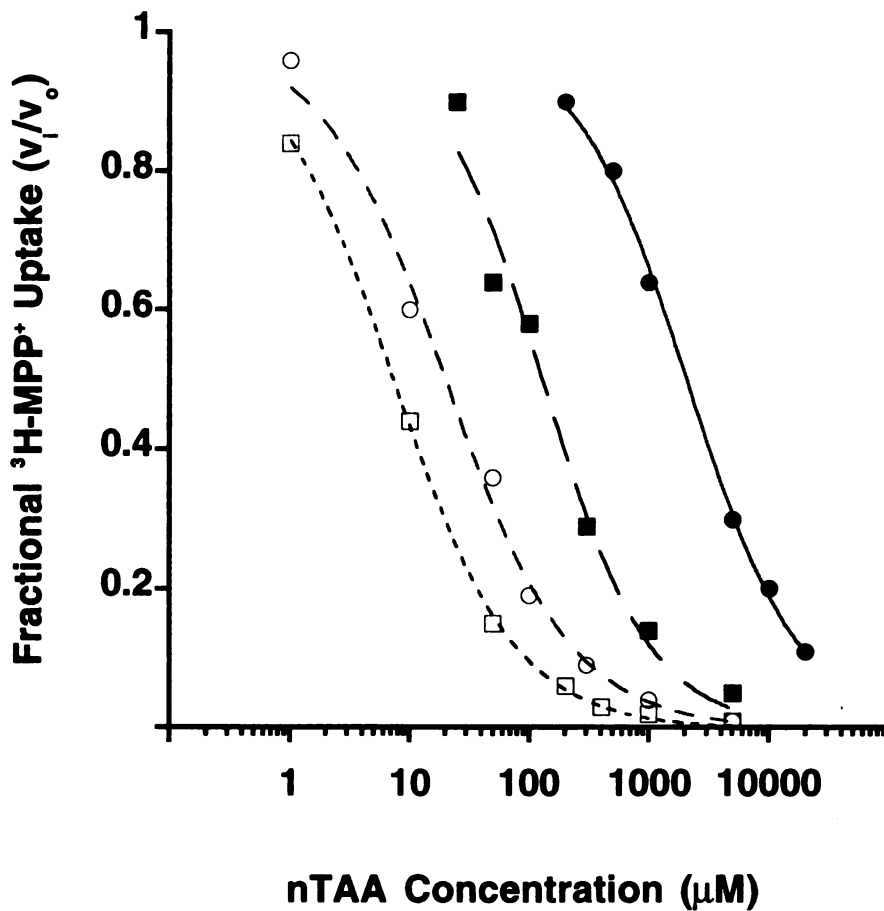


Figure 2. Inhibition of $^3\text{H-MPP}^+$ uptake (1 h) by nTAA compounds in oocytes expressing mOCT1. Mean values of the uptake relative to control (no inhibitor present) are shown. Data normalized to control (no inhibitor) represent mean values from 7 – 9 oocytes in a representative experiment and were fit by non-linear regression as described previously [19]. The K_i values for TMA (●), TEA (■), TPrA (○), TBA (□) are listed in Table 1.

Table 1. Apparent K_i values (μM) of n-tetraalkylammonium (nTAA) compounds.

The inhibition of $^3\text{H-MPP}^+$ ($1 \mu\text{M}$) uptake by increasing concentrations of nTAA compounds was carried out in OCT1 expressing oocytes. The apparent K_i values were determined by fitting representative data from single inhibition studies using nonlinear regression analysis as described in the Methods section. Studies were repeated in at least two batches of oocytes except for TMA (rbOCT1) and TBA (rOCT1), where only one batch of oocytes was used.

Compound	mOCT1	rOCT1	rbOCT1	hOCT1
TMA	2075 ± 75	905 ± 63	5780 ± 1070	12400 ± 1280
TEA	128 ± 17.1	100 ± 10.7	93.6 ± 6.0	158 ± 40.5
TPrA	19.8 ± 2.1	21.0 ± 7.8	35.5 ± 6.0	102 ± 13.0
TBA	7.3 ± 0.2	16.9 ± 6.0	25.1 ± 7.3	29.6 ± 3.6

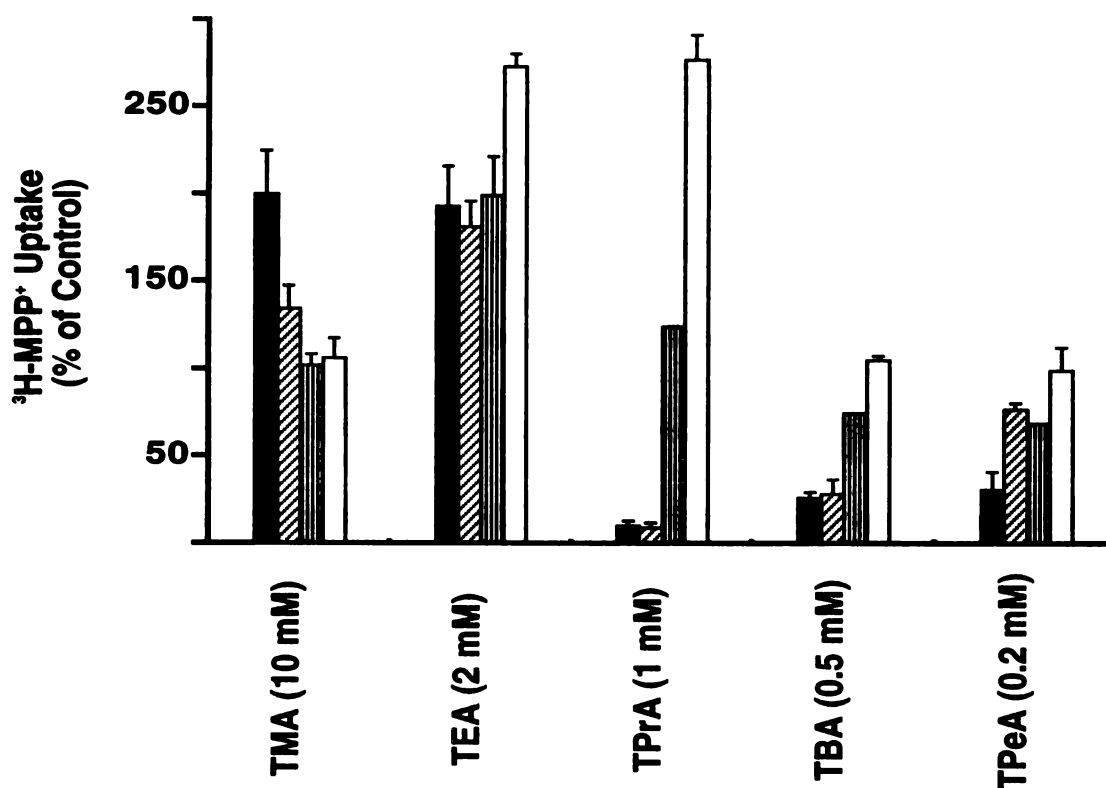


Figure 3. Effect of *trans* nTAA compounds on the influx (10 min) of $^3\text{H-MPP}^+$ in oocytes expressing OCT1. Groups of depolarized oocytes in K^+ uptake buffer (containing 100 mM K^+ and 2 mM Na^+) were injected with 50 nl of an unlabeled nTAA in K^+ buffer (control oocytes were injected with 50 nl of K^+ buffer). The 10-min uptake of $^3\text{H-MPP}^+$ (1 μM) in K^+ buffer was then measured. The mean control uptake (*trans*-zero) was taken as 100%. Data represent mean \pm S.E. from three to seven separate experiments; 5–9 oocytes were used per compound per experiment. The bars represent the different OCT1 clones as follows: mOCT1 (dark bars), rOCT1 (diagonal-striped bars), rbOCT1 (vertical-striped bars), hOCT1 (open bars).

nTAA-dependent currents in voltage clamped oocytes. The translocation of the nTAA compounds was further studied by measuring nTAA-dependent currents under voltage clamped conditions in oocytes expressing OCT1. Fig. 4 shows representative current traces in oocytes superfused with saturating concentrations of nTAA compounds for 30 s (gray bars at the top). Saturating concentrations were used to achieve maximal uptake rates (i.e. maximal currents). Fig. 5 shows the nTAA-dependent currents normalized with the currents from 1 mM TEA superfusion. TEA was chosen because it has a similar affinity for the four OCT1 homologues. In oocytes expressing hOCT1, TEA and TPrA induced the largest currents, followed by the larger nTAA compound TBA, and then the smallest nTAA compound TMA. In rbOCT1 cRNA-injected oocytes TEA induced the largest currents followed by TMA, TPrA, and finally TBA. In contrast, in the rodent OCT1-expressing oocytes, the small nTAA compounds TMA and TEA induced the largest currents and the larger nTAA compounds induced very small currents.

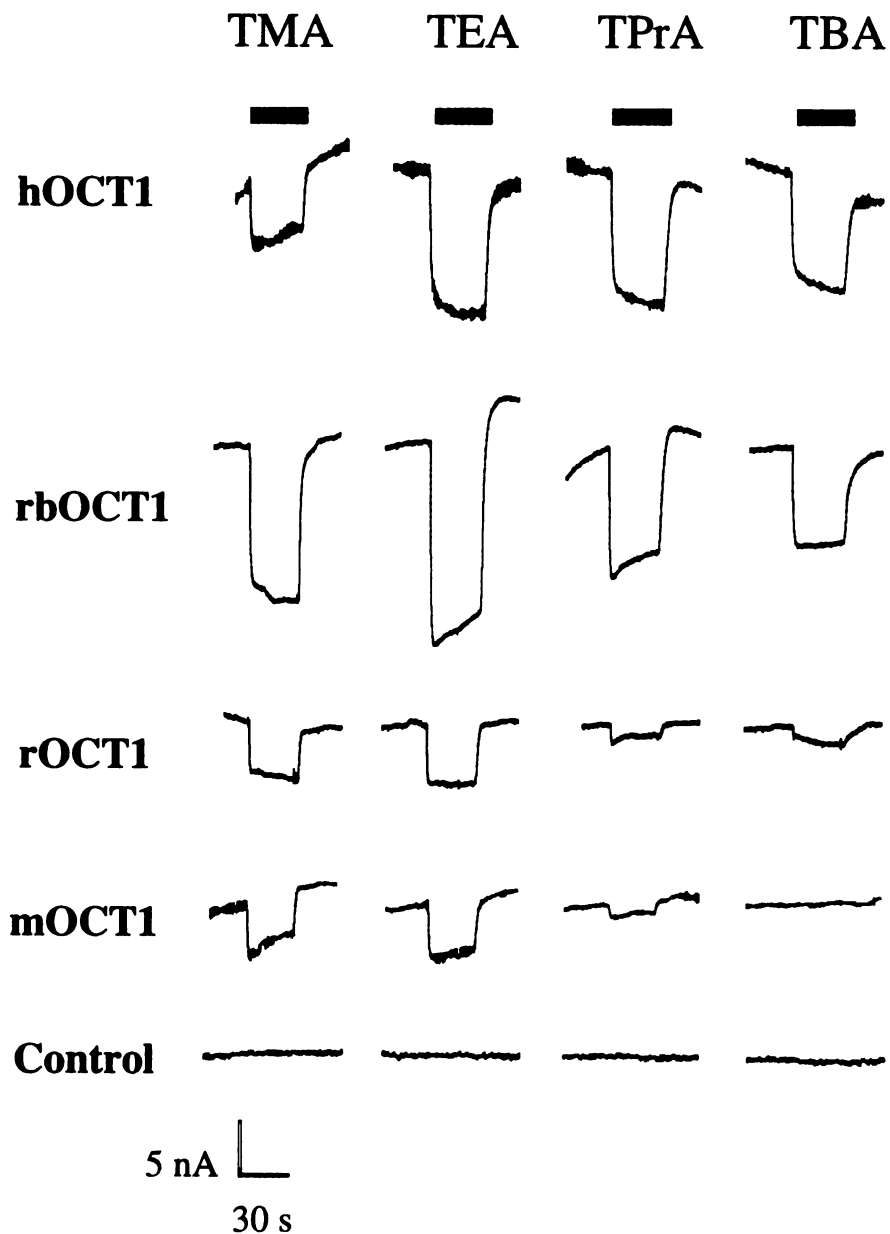


Figure 4. Representative recordings of nTAA-induced inward currents in OCT1 cRNA- or uninjected oocytes under voltage clamp conditions (-50 mV). The oocytes were superfused with nTAA compounds (TMA (5 mM), TEA (1 mM), TPrA (0.5 mM), TBA (0.5 mM)) for 30 s followed by a 2 min Na^+ buffer washout before the application of another ligand. The gray bars at the top indicate the time of nTAA application.

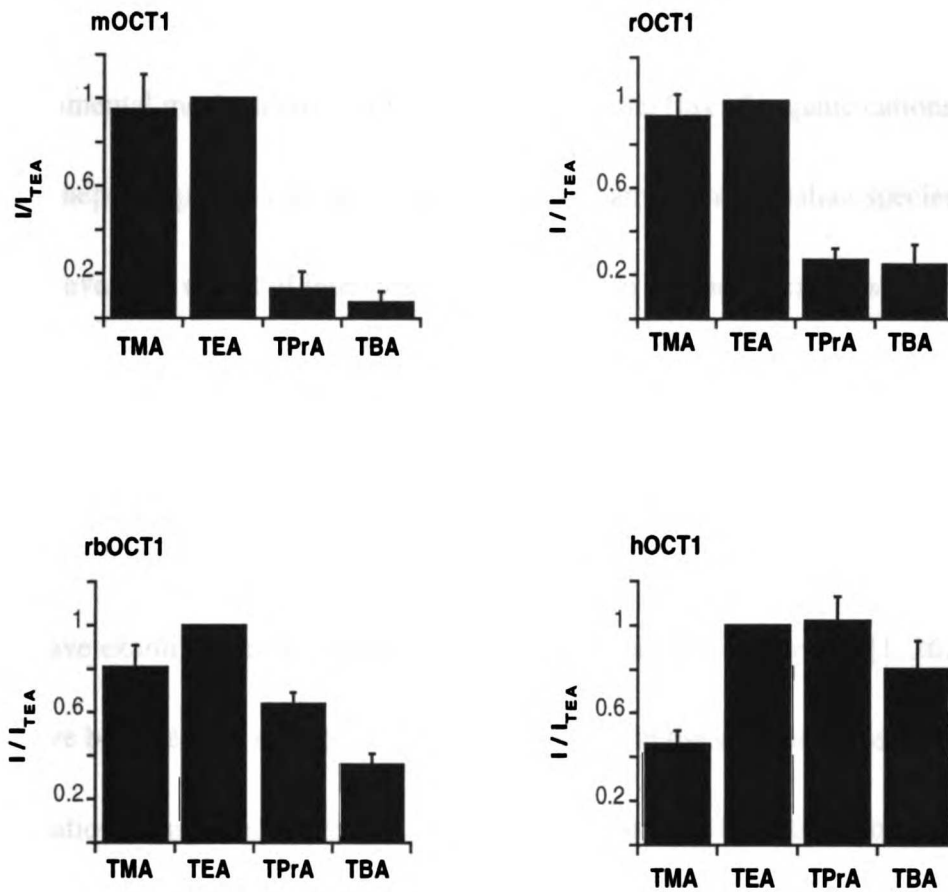


Figure 5. nTAA-induced currents under voltage clamp conditions (-50 mV) in OCT1 cRNA- and uninjected oocytes. The currents (like the ones shown in Fig. 4.) were individually normalized to the TEA-induced currents within one set of recordings. Data represent mean \pm S.D. (n = 5-6).

Discussion

Organic cation transporters in the kidney and liver play an important role in the removal of potentially toxic drugs and their metabolites from the systemic circulation [2]. The fundamental mechanisms involved in the sequential flux of organic cations across renal and hepatic epithelia are reported to be similar among mammalian species [2, 9, 10]. However, the extent of interspecies differences in kinetic characteristics and selectivities of organic cation transporters is not well understood. Our understanding of organic cation transport mechanisms is largely based on studies performed using tissue preparations from the rabbit kidney and rat liver [3, 8, 20, 21, 23-25]. Relatively few studies have examined renal or hepatic transport mechanisms in humans [1, 26, 27]. There have been several reports of species differences in the substrate selectivity of renal organic cation transport systems [11, 12]. This suggests that there could be kinetic and selectivity differences in organic cation transporters among species, which could result in substantial differences in the *in vivo* handling of drugs and toxins.

Marked species differences in the substrate selectivity of the renal organic cation transport system were found when studying the interactions of nTAA compounds with the BLM organic cation transport system in rabbit and rat kidneys [11, 12]. A correlation between alkyl chain length (from methyl to pentyl) and increasing affinity for the rabbit renal OC transport systems in the basolateral membrane was found [12]. In contrast

increasing the alkyl chain length beyond two (ethyl) did not improve the affinity for the BLM transport system in the rat [11]. These data can be rationalized in several ways.

For example, it is possible that different OCT isoforms with different affinities for nTAA compounds are expressed in the rabbit and rat kidney. In fact, marked differences in the tissue distribution of OCT mRNA isoforms have been reported [13, 16, 28].

Alternatively, the same OCT isoform could be expressed in rat and rabbit kidney, but the rat and rabbit isoforms might differ in their kinetic properties and selectivities.

The goal of this study was to compare the kinetics and selectivities of nTAA compounds with the OCT1 transporter isoforms from mouse, rat, rabbit, and human.

OCT1 is expressed in the livers and kidneys of these species. Therefore, intrinsic functional differences between OCT1 species homologues may explain the observed interspecies differences in the transport of nTAA compounds across the basolateral membrane of the nephron.

Cis-inhibition of $^3\text{H-MPP}^+$ (1 μM) uptake in OCT1-expressing oocytes by nTAAs (at 50 μM) demonstrated a correlation between increasing alkyl chain length and increasing affinity for OCT1 regardless of the species. The finding that the nTAAs did not alter current in water injected oocytes (Fig. 4) suggests that the nTAAs were not affecting MPP^+ uptake via indirect effects on membrane potential; rather, these compounds were directly inhibiting MPP^+ transport. This relationship was found in

studies of organic cation transport in isolated rabbit renal tissue preparations and previously for the cloned human transporter, hOCT1, expressed in HeLa cells [4, 19]. This result does not explain the previous finding that the inhibitory potency of nTAAs decreased with increasing alkyl chain length in rat kidney for nTAA compounds with side chains greater than ethyl [11]. It is possible that another transporter, such as rOCT2, plays a greater role in the BLM transport of organic cations in the rat kidney [29]. The inhibition potencies of the nTAA compounds with the OCT1 transporters from mouse, rat, rabbit, and human differed considerably. In general, the nTAA compounds interacted less potently with the human transporter compared with its rodent and rabbit counterparts (Table 1).

The substrate selectivities of the transporters were investigated using both *trans*-stimulation studies and ligand-induced current measurements in voltage clamped oocytes. The findings generally support the following conclusions: (1) The smallest nTAA, TMA, is transported by mOCT1 and rOCT1, but to a lesser extent by rbOCT1 and hOCT1. (2) TEA is transported well (is a substrate) by all four species homologues. (3) TPrA exhibits striking interspecies differences in its transport characteristics. That is, TPrA *trans*-stimulated hOCT1 $^3\text{H-MPP}^+$ influx greatly and rbOCT1 weakly, whereas it potently *trans*-inhibited mOCT1 and rOCT1 $^3\text{H-MPP}^+$ influx. In fact, of the nTAA compounds tested, TPrA was the most potent *trans*-inhibitor of the rodent transporters. Voltage

clamp studies showed that the rodent transporters were able to translocate TPrA, albeit at much slower rates than TMA and TEA. In contrast, hOCT1 and to a lesser extent rbOCT1 took up TPrA at comparatively faster rates relative to TEA. (4) hOCT1 and rbOCT1 transported TBA at a slightly slower rate than TPrA. As saturating concentrations of TPrA and TBA were used in these experiments, the marked interspecies differences in transport are most likely a result of differences in the turnover rates.

The molecular mechanism responsible for the observed interspecies differences in OCT1 function is unknown. It is possible that the permeability pathway in the mouse and rat OCT1 transporters has a smaller diameter and hence is more restrictive in the size of the substrates. Another explanation is that the rodent transporters have a more hydrophobic binding pocket, making subsequent debinding steps slower. At the present time very little is known about the OCT1 molecular structure involved in substrate binding and translocation. Sequence analysis suggests that the OCT1 homologues share a very similar secondary structure consisting of twelve membrane spanning helices. However, as hOCT1 is 80%, 78%, and 81% identical to the mouse, rat, and rabbit homologues respectively there have been numerous amino acid changes during the evolution of the OCT1 transporter (Fig. 6). Changes in tertiary structure of the permeation pathway due to amino acid residue(s) changes must account for the functional

differences described in this study. 109 amino acid differences are found between the human and rodent OCT1 proteins. Of those, 68 are unique to hOCT1 (i.e. only found in hOCT1). Many of these residues (57%) have different chemical properties from corresponding residues of the other OCT1s (e.g., polar versus nonpolar), which could potentially have dramatic effects on function. Recently, it has been shown that even a single amino acid change in a transporter protein can lead to substantial changes in the transporter's function [30]. Chimera and mutation studies could provide insight into the amino acids involved in substrate binding and translocation of OCT1.

In summary, our results show that the human OCT1 is functionally distinct from other mammalian OCT1 homologues. In general, hOCT1 interacts with nTAA compounds with a lower affinity compared to the rodent and rabbit homologues. hOCT1 is also able to translocate larger nTAAs at comparatively greater rates. Based on these results, it is reasonable to expect that kinetic and selectivity differences exist among the OCT1 species homologues in their interactions with drugs and toxins. Currently, assays to study organic cation and other xenobiotic transporters are being developed to screen for drug-drug interactions. These assays can potentially be used to estimate pharmacokinetic parameters based on *in vitro* data. The results reported in this study underscore the importance of using the human clones for pre-clinical drug evaluation.

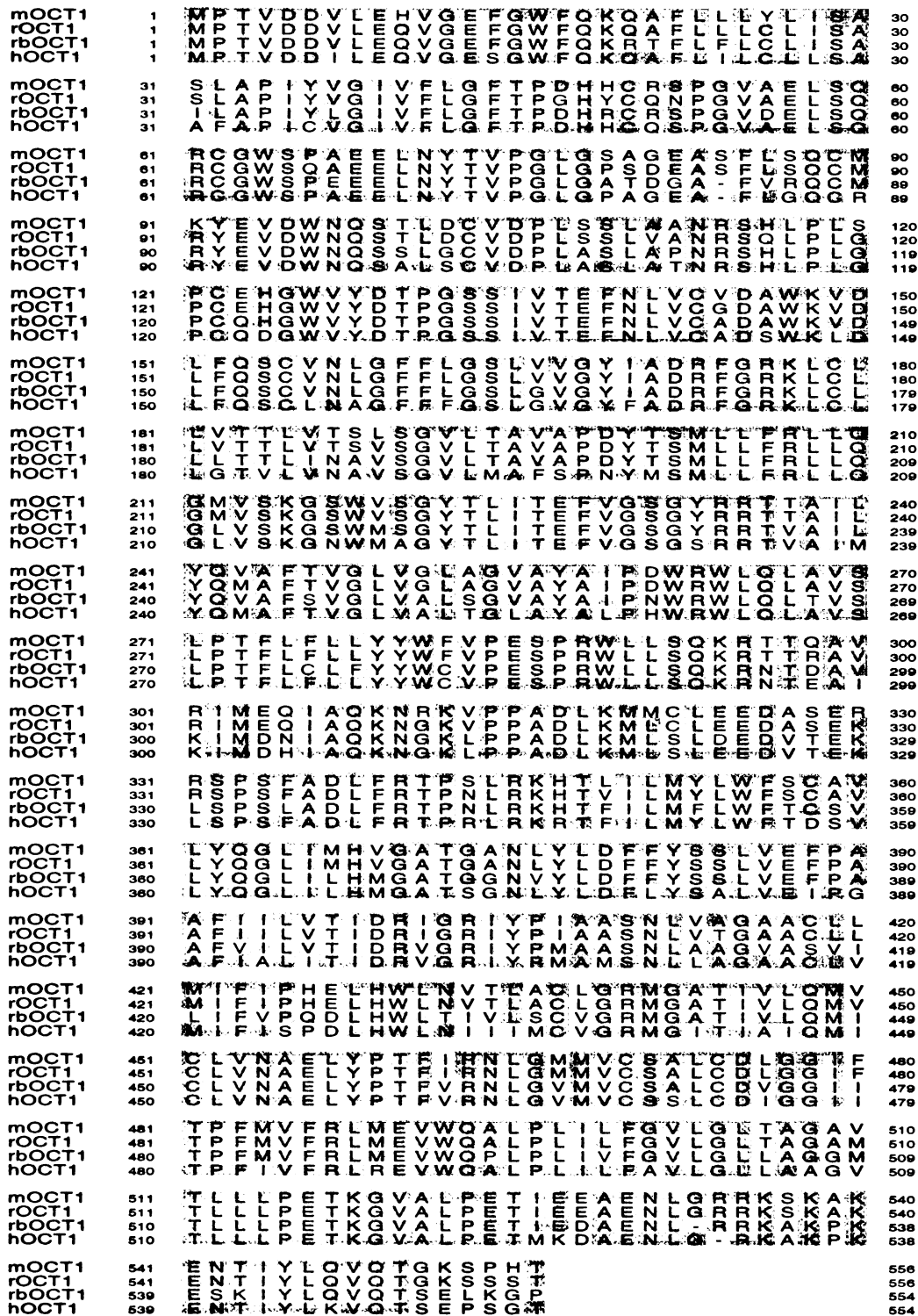


Figure 6. Multiple sequence alignment of four OCT1 homologues from mouse (mOCT1), rat (rOCT1), rabbit (rbOCT1), and human (hOCT1). The alignment was generated with the PILEUP program in the GCG software package. Amino acids conserved in at least three of the four transporters are shaded. 109 amino acid differences are found between the human and rodent transporters. Of these, 68 residues are only found in hOCT1. These amino acid residue differences are distributed throughout the sequence and are not clustered in any obvious regions.

References

1. Muller M and Jansen PL, Molecular aspects of hepatobiliary transport. *Am J Physiol* **272**(6 Pt 1): G1285-1303, 1997.
2. Zhang L, Brett CM and Giacomini KM, Role of organic cation transporters in drug absorption and elimination. *Annu Rev Pharmacol Toxicol* **38**: 431-460, 1998.
3. Gisclon L, Wong FM and Giacomini KM, Cimetidine transport in isolated luminal membrane vesicles from rabbit kidney. *Am J Physiol* **253**(1 Pt 2): F141-150, 1987.
4. Wright SH and Wunz TM, Mechanism of cis- and trans-substrate interactions at the tetraethylammonium/H⁺ exchanger of rabbit renal brush-border membrane vesicles. *J Biol Chem* **263**(36): 19494-19497, 1988.
5. Sokol PP and McKinney TD, Mechanism of organic cation transport in rabbit renal basolateral membrane vesicles. *Am J Physiol* **258**(6 Pt 2): F1599-1607, 1990.
6. Wright SH and Wunz TM, Paraquat²⁺/H⁺ exchange in isolated renal brush-border membrane vesicles. *Biochim Biophys Acta* **1240**(1): 18-24, 1995.
7. Moseley RH, Morrissette J and Johnson TR, Transport of N1-methylnicotinamide by organic cation-proton exchange in rat liver membrane vesicles. *Am J Physiol* **259**(6 Pt 1): G973-982, 1990.

8. Moseley RH, Zuger LJ and Van Dyke RW, The neurotoxin 1-methyl-4-phenylpyridinium is a substrate for the canalicular organic cation/H⁺ exchanger. *J Pharmacol Exp Ther* **281**(1): 34-40, 1997.
9. Pritchard JB and Miller DS, Mechanisms mediating renal secretion of organic anions and cations. *Physiol Rev* **73**(4): 765-796, 1993.
10. Pritchard JB and Miller DS, Renal secretion of organic anions and cations. *Kidney Int* **49**(6): 1649-1654, 1996.
11. Ullrich KJ, Papavassiliou F, David C, Rumrich G and Fritzsich G, Contraluminal transport of organic cations in the proximal tubule of the rat kidney. I. Kinetics of N¹-methylnicotinamide and tetraethylammonium, influence of K⁺, HCO₃⁻, pH; inhibition by aliphatic primary, secondary and tertiary amines and mono- and bisquaternary compounds. *Pflugers Arch* **419**(1): 84-92, 1991.
12. Groves CE, Evans KK, Dantzler WH and Wright SH, Peritubular organic cation transport in isolated rabbit proximal tubules. *Am J Physiol* **266**(3 Pt 2): F450-458, 1994.
13. Zhang L, Dresser MJ, Gray AT, Yost SC, Terashita S and Giacomini KM, Cloning and functional expression of a human liver organic cation transporter. *Mol Pharmacol* **51**(6): 913-921, 1997.

14. Grundemann D, Gorboulev V, Gambaryan S, Veyhl M and Koepsell H, Drug excretion mediated by a new prototype of polyspecific transporter. *Nature* **372**(6506): 549-552, 1994.
15. Schweifer N and Barlow DP, The Lx1 gene maps to mouse chromosome 17 and codes for a protein that is homologous to glucose and polyspecific transmembrane transporters. *Mamm Genome* **7**(10): 735-740, 1996.
16. Terashita S, Dresser MJ, Zhang L, Gray AT, Yost SC and Giacomini KM, Molecular cloning and functional expression of a rabbit renal organic cation transporter. *Biochim Biophys Acta* **1369**(1): 1-6, 1998.
17. Nagel G, Volk C, Friedrich T, Ulzheimer JC, Bamberg E and Koepsell H, A reevaluation of substrate specificity of the rat cation transporter rOCT1. *J Biol Chem* **272**(51): 31953-31956, 1997.
18. Zhang L, Schaner ME and Giacomini KM, Functional characterization of an organic cation transporter (hOCT1) in a transiently transfected human cell line (HeLa). *J Pharmacol Exp Ther* **286**(1): 354-361, 1998.
19. Zhang L, Gorset W, Dresser MJ and Giacomini KM, The interaction of n-tetraalkylammonium compounds with a human organic cation transporter, hOCT1. *J Pharmacol Exp Ther* **288**(3): 1192-1198, 1999.

20. Dantzler WH, Wright SH, Chatsudthipong V and Brokl OH, Basolateral tetraethylammonium transport in intact tubules: specificity and trans-stimulation. *Am J Physiol* **261**(3 Pt 2): F386-392, 1991.
21. Moseley RH, Takeda H and Zugger LJ, Choline transport in rat liver basolateral plasma membrane vesicles. *Hepatology* **24**(1): 192-197, 1996.
22. Wright SH and Wunz TM, Influence of substrate structure on substrate binding to the renal organic cation/H⁺ exchanger. *Pflugers Arch* **437**(4): 603-610, 1999.
23. Wright SH, Transport of N1-methylnicotinamide across brush border membrane vesicles from rabbit kidney. *Am J Physiol* **249**(6 Pt 2): F903-911, 1985.
24. Moseley RH, Jarose SM and Permoad P, Organic cation transport by rat liver plasma membrane vesicles: studies with tetraethylammonium. *Am J Physiol* **263**(5 Pt 1): G775-785, 1992.
25. Martel F, Vetter T, Russ H, Grundemann D, Azevedo I, Koepsell H and Schomig E, Transport of small organic cations in the rat liver. The role of the organic cation transporter OCT1. *Naunyn Schmiedebergs Arch Pharmacol* **354**(3): 320-326, 1996.
26. Ott RJ, Hui AC, Yuan G and Giacomini KM, Organic cation transport in human renal brush-border membrane vesicles. *Am J Physiol* **261**(3 Pt 2): F443-451, 1991.

27. Chun JK, Zhang L, Piquette-Miller M, Lau E, Tong LQ and Giacomini KM, Characterization of guanidine transport in human renal brush border membranes. *Pharm Res* **14**(7): 936-941, 1997.
28. Gorboulev V, Ulzheimer JC, Akhoundova A, Ulzheimer-Teuber I, Karbach U, Quester S, Baumann C, Lang F, Busch AE and Koepsell H, Cloning and characterization of two human polyspecific organic cation transporters. *DNA Cell Biol* **16**(7): 871-881, 1997.
29. Okuda M, Saito H, Urakami Y, Takano M and Inui K, cDNA cloning and functional expression of a novel rat kidney organic cation transporter, OCT2. *Biochem Biophys Res Commun* **224**(2): 500-507, 1996.
30. Wang J and Giacomini KM, Serine 318 is essential for the pyrimidine selectivity of the N2 Na⁺-nucleoside transporter. *J Biol Chem* **274**(4): 2298-2302, 1999.

CHAPTER 4

THE INTERACTION AND TRANSPORT OF n-TETRAALKYLAMMONIUM COMPOUNDS AND BIGUANIDES WITH A HUMAN RENAL ORGANIC CATION TRANSPORTER, hOCT2

Introduction

Many clinically used drugs are actively secreted by the kidney in humans [1-3].

Of the transport systems present in the kidney, the organic cation transport system appears to be one of the major systems involved in the renal secretion of drugs. To date, five organic cation transporters have been cloned and all are expressed to some degree in the human kidney [4, 5]. With the availability of the cloned transporters, it is now possible to begin to investigate their roles in renal drug elimination.

There are two families of organic cation transporters: the OCT gene family (OCT1, OCT2, OCT3) and the OCTN gene family (OCTN1, OCTN2). There is considerable sequence and secondary structure similarity among members of the same family [4, 5]. For example, hOCT1 and hOCT2 share 70% sequence identity and their predicted secondary structures, based on hydropathy analysis, are essentially the same. This might suggest that paralogous organic cation transporters such as hOCT1 and

hOCT2 have similar functional characteristics and are functionally redundant. However, recent chimeric and mutagenesis studies of transporters have shown that even single amino acid changes in a transporter can dramatically alter its substrate selectivity [6]. Therefore, it is reasonable to propose that the five different organic cation transporters serve different functions *in vivo*.

The goal of this study was to compare the substrate and inhibition profiles of hOCT2 and hOCT1 to determine whether these transporters are functionally distinct. We examined the interactions of n-tetraalkylammonium (nTAA) compounds and biguanides with hOCT2, an organic cation transporter cloned from kidney, and compared our results with our previous results for hOCT1 [7, 8, Chapter 3]. nTAA compounds have been used extensively to study the functional characteristics of organic cation transporters in tissue preparations such as vesicles and isolated tubules [9-13]. Substantial differences between hOCT2 and hOCT1 in their interactions with nTAAs were found. We then compared the interactions of biguanides with hOCT1 and hOCT2. Based on its high renal clearance, metformin, a biguanide, is suspected to be a substrate of renal organic cation transporters [14, 15]. In this study, we found that both hOCT1 and hOCT2 interact with the biguanides, indicating that they might be involved in the elimination of these compounds. In contrast to the nTAA compounds, the biguanides appear to interact in a similar fashion with hOCT1 and hOCT2. Based on the data reported in this study and other recent

reports in the literature, it appears that there are substantial differences in the specificities of hOCT1 and hOCT2.

Materials and Methods

cRNA transcription and Xenopus oocyte expression. Oocytes were harvested from oocyte positive *Xenopus laevis* (Nasco, Fort Atkinson, WI) and were dissected and treated with collagenase D (Boehringer-Mannheim Biochemicals, Indianapolis, IN) in a calcium-free ORII solution as previously described [16]. Oocytes were maintained at 18°C in modified Barth's medium. Healthy stage V and VI oocytes were injected with capped cRNA (1 µg/µl). Capped cRNA was transcribed *in vitro* with T3 polymerase using the mCAP RNA Capping kit (Stratagene, La Jolla, CA) from *Not I* linearized plasmids (pOX) containing hOCT2 or hOCT1 transporter cDNAs.

Tracer uptake measurements. Transport of ³H-1-methyl-4-phenylpyridinium (MPP⁺) (82 Ci/mmol, Dupont-New England Nuclear, Boston, MA) or ³H-cimetidine (15 Ci/mmol, Amersham Life Sciences, Arlington Heights, IL) in oocytes was measured 2 – 7 days after injection as described previously [16, 17]. Tracer uptakes were carried out as follows: groups of seven to nine oocytes were incubated in Na⁺ buffer (100 mM NaCl, 2 mM KCl, 1 mM CaCl₂, 1 mM MgCl₂, 10 mM HEPES/Tris, pH 7.2) containing ³H-MPP⁺ (1 µM: 0.1 µM ³H-MPP⁺ and 0.9 µM unlabeled MPP⁺) or ³H-cimetidine (1 µM) for 1 h.

For inhibition and kinetic studies, unlabeled compounds were added to the reaction solutions as needed. To stop the uptake experiments, oocytes were washed 5 times with 3 ml of ice-cold Na⁺ buffer. The radioactivity associated with each oocyte was then determined by scintillation counting.

In *trans*-stimulation studies, groups of 5 – 7 hOCT2-expressing or uninjected oocytes were washed three times with K⁺ buffer (2 mM NaCl, 100 mM KCl, 1 mM CaCl₂, 1 mM MgCl₂, 10 mM HEPES/Tris, pH 7.2). The oocytes were then rapidly injected with 50 nl of a K⁺ solution containing an unlabeled compound. Oocytes injected with 50 nl of K⁺ buffer without compound were used for controls. After injections, the oocytes were quickly transferred to a small disposable borosilicate glass culture tube; any remaining K⁺ was aspirated off, and 85 µl of MPP⁺ (1 µM: 0.1 µM ³H-MPP⁺ and 0.9 µM unlabeled MPP⁺) in K⁺ buffer was added. ³H-MPP⁺ uptake was arrested after 10 min by washing the oocytes 5 times with 3 ml of ice-cold K⁺ buffer. The radioactivity associated with each oocyte was then determined by scintillation counting.

Electrophysiology studies. Electrophysiology experiments were performed at room temperature (21 – 23°C) 5 -10 d post injection. Steady-state ligand-induced currents were measured with a two-electrode voltage clamp. Oocytes were voltage clamped at –50 mV and superfused with Na⁺ buffer 2 min before and after 30 s ligand superfusions. Recordings were obtained in a 25 µl recording chamber at flow rates of ~ 3

ml/min. Uninjected oocytes were used as controls, undergoing the same treatments as hOCT2-expressing oocytes.

Data analysis. Values are expressed as mean \pm standard error (S.E.) or mean \pm standard deviation (S.D.) as indicated in the legends. Six to nine oocytes were used to generate a data point in each experiment. All experiments were repeated at least once using different batches of oocytes, unless indicated otherwise in the legends. Apparent K_m values were determined as described previously [7, 18]. The unpaired *t* test was used to test for statistically significant differences between hOCT1 and hOCT2 data where $P < 0.05$ was considered significant. Other data, involving multiple comparisons, were analyzed by analysis of variance where $P < 0.05$ was considered significant.

Materials. The nTAA compounds and biguanides were purchased from Sigma (St. Louis, MO). All other reagents were purchased from either Sigma (St. Louis, MO) or Fisher (Pittsburgh, PA) or as indicated. $^3\text{H-MPP}^+$ (82 Ci/mmol) was purchased from Dupont-New England Nuclear (Boston, MA), and $^3\text{H-cimetidine}$ (15 Ci/mmol) was purchased from Amersham Life Sciences (Arlington Heights, IL)

Results

Inhibition of hOCT2 mediated uptake by nTAA compounds. Inhibition studies with nTAA compounds of increasing chain length were carried out in order to determine

the relationship between alkyl chain length and inhibition potency for hOCT2. The inhibition potency of the nTAA compounds (50 μ M) for hOCT2 appeared highest for tetrapentylammonium (TPeA) and lowest for tetramethylammonium (TMA) (Fig. 1). However, the apparent K_i values of the four nTAA compounds, TMA, tetraethylammonium (TEA), tetrapropylammonium (TPrA), and tetrabutylammonium (TBA), for hOCT2 were not statistically different from one another, suggesting that these compounds have essentially the same affinity for hOCT2 (Table 1). There were notable differences between hOCT1 and hOCT2 in their affinities for several nTAAs: TMA, the smallest nTAA compound, had a 82-fold higher affinity for hOCT2 compared to hOCT1, and TBA, the largest nTAA, had a 4-fold higher affinity for hOCT1 compared to hOCT2 (Table 1). TEA and TPrA had essentially the same affinities for hOCT1 and hOCT2.

Efflux of nTAAs from oocytes expressing hOCT2. *Trans*-stimulation studies, also known as counterflux studies, are often used to test whether a compound is a *bona fide* substrate of a transporter [7, 13, 19, 20]. If the test compound *trans*-stimulates the uptake of a tracer ligand, the test compound is most likely a substrate of the transporter. *Trans*-stimulation studies were carried out under depolarized conditions (i.e. in K^+ containing buffer) to minimize the effects of membrane potential on 3H -MPP $^+$ (1 μ M) uptake. Marked differences in the function of hOCT2 and hOCT1 were revealed by these studies (Fig. 2). In oocytes expressing hOCT2, 3H -MPP $^+$ influx was *trans*-stimulated only by

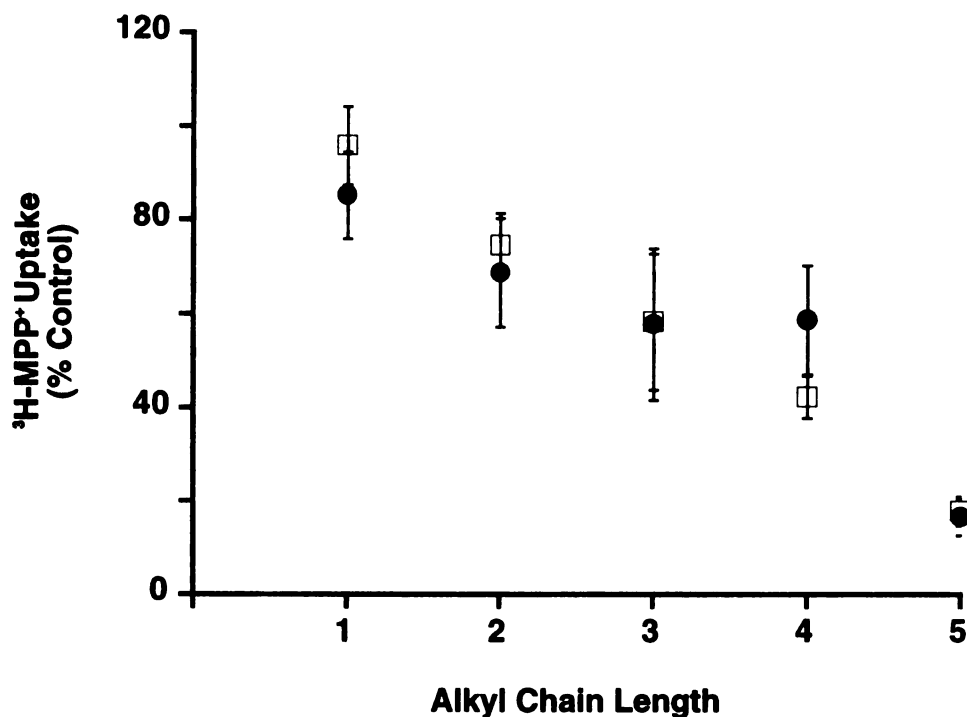


Figure 1. Effect of nTAA compounds (50 μM) of increasing chain length on $^3\text{H-MPP}^+$ (1 μM) uptake by hOCT2-expressing oocytes. The uptake of $^3\text{H-MPP}^+$ (1 h) in Na^+ uptake buffer was measured in oocytes expressing hOCT2 (●) or hOCT1 (□). Each data point represents the mean rate of uptake as percent of control in which no inhibitor was present. Data represent mean of two to four determinations \pm S.E. using separate batches of oocytes. 7 – 9 oocytes were used per compound per experiment. Data for hOCT1 from our laboratory has been previously published [8, Chapter 3].

Table 1. Apparent K_i values (μM) of n-tetraalkylammonium (nTAA) compounds in inhibiting $^3\text{H-MPP}^+$ uptake mediated by hOCT2. The inhibition of $^3\text{H-MPP}^+$ ($1 \mu\text{M}$) uptake by increasing concentrations of nTAA compounds was carried out in hOCT2 expressing oocytes. The apparent K_i values were determined by fitting representative data from single inhibition studies using nonlinear regression. Data represent mean \pm S.E. values of two determinations. * $P < 0.05$ versus hOCT1 (unpaired t test). The apparent K_i values of the nTAA compounds for hOCT2 were not statistically different (analysis of variance).

Compound	hOCT2	hOCT1 ^a
TMA	150 \pm 37*	12400 \pm 1280
TEA	156 \pm 78	158 \pm 40.5
TPrA	128 \pm 32	102 \pm 13.0
TBA	120 \pm 52*	29.6 \pm 3.6

^aData previously published from our laboratory [8, Chapter 3] .

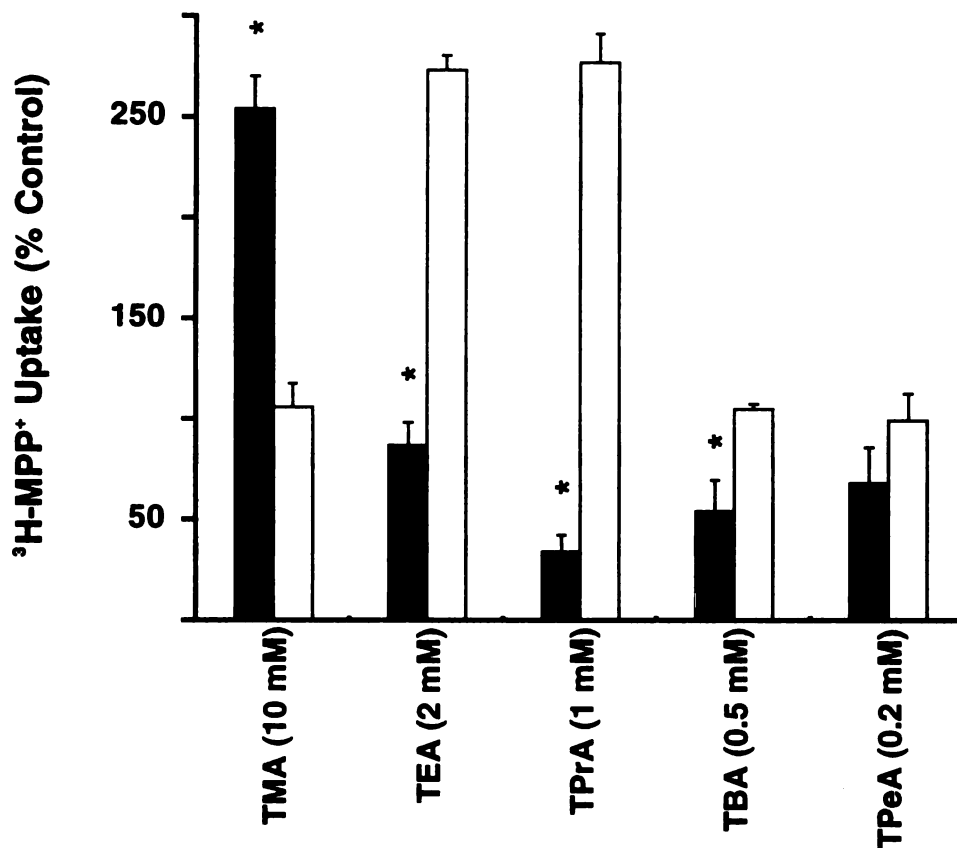


Figure 2. Effect of *trans* nTAA compounds on the influx of $^3\text{H-MPP}^+$ in *Xenopus laevis* oocytes expressing hOCT2 or hOCT1. Depolarized oocytes, expressing either hOCT2 (dark bars) or hOCT1 (open bars) were injected with 50 nl of an unlabeled nTAA compound dissolved in K^+ buffer to give the final intracellular nTAA concentrations indicated in the figure. The 10-min uptake of $^3\text{H-MPP}^+$ ($1\ \mu\text{M}$) in K^+ buffer was then measured. The mean control uptake (*trans*-zero) was taken as 100% (control oocytes were injected with 50 nl of K^+ buffer). Data represent mean \pm S.E. from three separate experiments; 5 – 9 oocytes were used per compound per experiment. * $P < 0.05$ versus hOCT1 (unpaired *t* test). hOCT1 data are were previously published [8, Chapter 3].

TMA, a compound that neither *trans*-stimulated nor *trans*-inhibited hOCT1-mediated ^3H -MPP $^+$ influx (Fig. 2). TEA had essentially no effect on hOCT2 activity, but it greatly stimulated hOCT1 activity. Furthermore, whereas TPrA potently *trans*-inhibited hOCT2, it *trans*-stimulated hOCT1-mediated ^3H -MPP $^+$ influx. Finally, TBA and tetrapentylammonium (TPeA) *trans*-inhibited hOCT2, and had little effect on hOCT1 activity.

Interactions and transport of biguanides with hOCT2 and hOCT1. *Cis*-inhibition studies were carried out in order to determine whether hOCT2 and hOCT1 interact with the biguanides metformin and phenformin. Metformin and phenformin were found to inhibit ^3H -cimetidine transport mediated by hOCT1 and hOCT2 (Fig. 3). TEA, a known substrate of both transporters was used as a positive control. Both of the biguanides interact with hOCT2 and hOCT1 with similar potencies: the apparent K_i values of metformin are $1700 \pm 960 \mu\text{M}$ (hOCT2) and $2010 \pm 220 \mu\text{M}$ (hOCT1), and the values of phenformin are $65 \pm 11 \mu\text{M}$ (hOCT2) and $10 \pm 7 \mu\text{M}$ (hOCT1) (Table 2).

To determine whether metformin and phenformin are substrates of the transporters, *trans*-stimulation studies were carried out. Both of these compounds *trans*-stimulated ^3H -MPP $^+$ influx mediated by hOCT1 and hOCT2, suggesting that they are substrates of these transporters (Fig. 4). For this assay, TMA was used as a positive control for hOCT2, and TEA was used as a positive control for hOCT1.

Electrophysiological-based studies have recently been used to study the substrate selectivities of organic cation transporters. Using this assay, we found that TEA (1 mM) and metformin (0.5 mM) induced significant currents in hOCT2-expressing oocytes (Fig. 5). In contrast, quinidine (200 μ M), a potent inhibitor of organic cation transporters, did not induce a current. These results provide further evidence that metformin is a substrate of hOCT2.

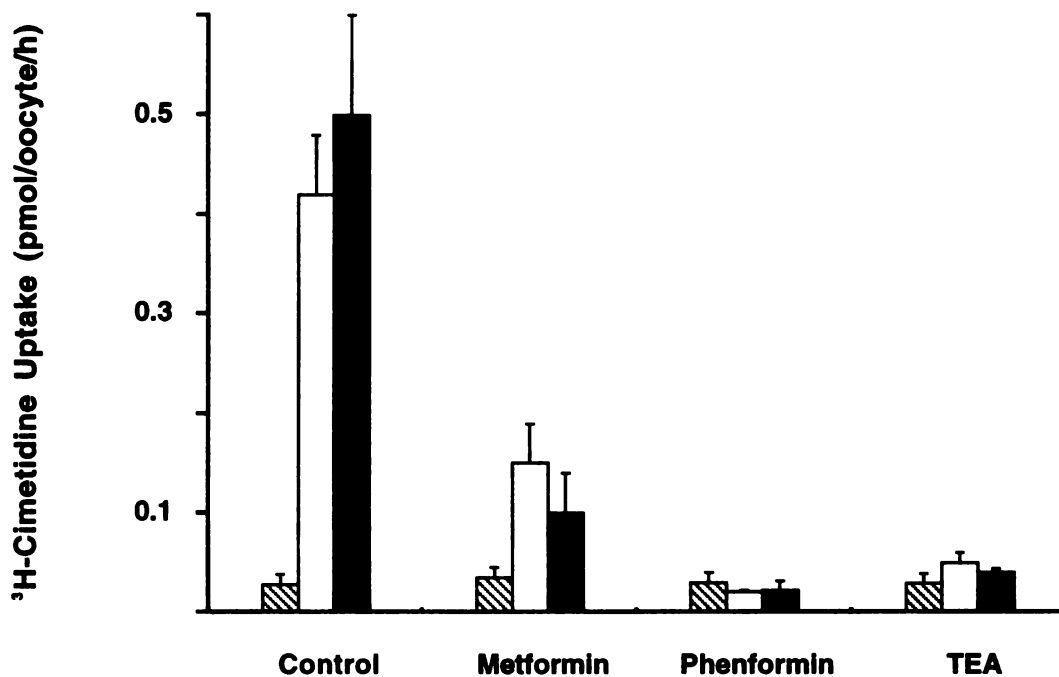


Figure 3. *Cis* inhibition of ^3H -cimetidine uptake in *Xenopus laevis* oocytes expressing hOCT2 or hOCT1. The 60 min uptake of ^3H -cimetidine was determined in the absence (control) or presence of the indicated compounds (2.5 mM) in oocytes injected with hOCT2 cRNA (dark bars) or hOCT1 cRNA (open bars) or uninjected oocytes (striped bars). Data represent mean \pm S.D. from a single representative experiment; 5 – 9 oocytes were used for each experimental condition. Replica experiments using oocytes from different donor frogs gave qualitatively similar results to those shown.

Table 2. Apparent K_i values (μM) of metformin and phenformin in inhibiting ^3H -MPP $^+$ uptake mediated by hOCT2 and hOCT1. The inhibition of ^3H -MPP $^+$ ($1 \mu\text{M}$) uptake by increasing concentrations of metformin and phenformin was carried out in hOCT2- and hOCT1-expressing oocytes. The apparent K_i values were determined by fitting representative data from single inhibition studies using nonlinear regression analysis. Data represent mean \pm S.E. values of two determinations. * $P < 0.05$ versus hOCT1 (unpaired t test).

Compound	hOCT2	hOCT1
Metformin	1700 \pm 960	2010 \pm 220
Phenformin	65 \pm 11*	10 \pm 7

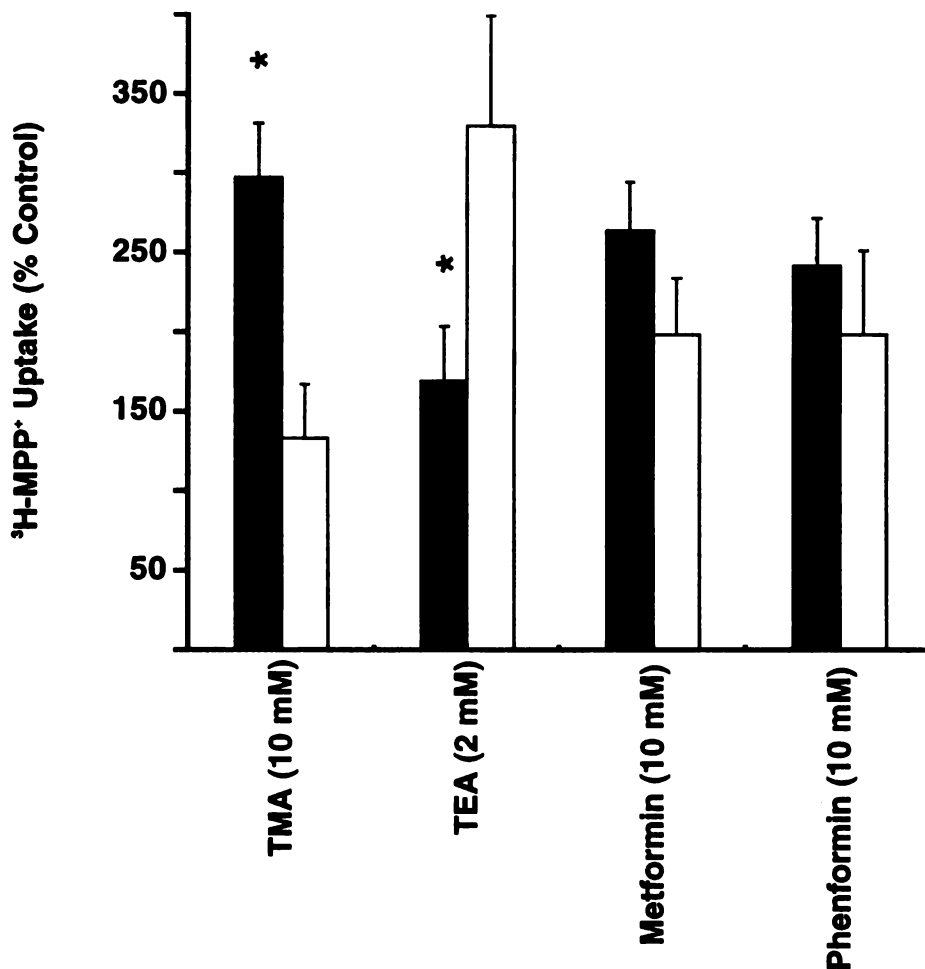


Figure 4. Effect of *trans* compounds on the influx of $^3\text{H-MPP}^+$ in *Xenopus laevis* oocytes expressing hOCT2 and hOCT1. Depolarized oocytes, expressing either hOCT2 (dark bars) or hOCT1 (open bars) were injected with 50 nl of an unlabeled nTAA compound dissolved in K^+ buffer to give the final intracellular concentrations indicated in the figure. The 10-min uptake of $^3\text{H-MPP}^+$ ($1 \mu\text{M}$) in K^+ buffer was then measured. The mean control uptake (*trans-zero*) was taken as 100% (control oocytes were injected with 50 nl of K^+ buffer). Data represent mean \pm S.E. from two to three separate experiments; 5 – 9 oocytes were used per compound per experiment. * $P < 0.05$ versus hOCT1 (unpaired *t* test).

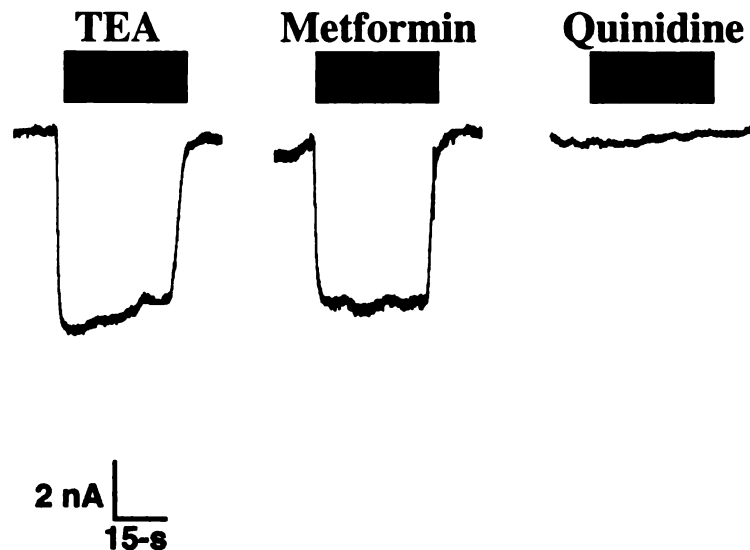


Figure 5. Representative recordings of ligand-induced inward currents in hOCT2-expressing oocytes. An hOCT2-expressing oocyte was voltage-clamped at -50 mV in sodium buffer. The dark bars above the traces indicate 30-s applications of ligands: TEA (1 mM), metformin (0.5 mM), and quinidine (100 μ M). Between applications, the ligands were removed by washing in sodium buffer; the original baseline current was restored before applying a different ligand. Similar results were obtained in other hOCT2-expressing oocytes ($n = 2$). Ligand-induced currents were not observed in control (i.e., uninjected) oocytes ($n = 2$).

Discussion

Organic cation transporters in the kidney, which play critical roles in the secretory transport of numerous drugs, are important determinants of plasma drug concentrations [3, 5, 21]. To date, five organic cation transporters have been cloned, making it possible to design experiments to investigate their roles in renal drug transport. With the availability of *in vitro* assay systems such as *Xenopus laevis* oocytes and transfected cell lines, drug-transporter interactions can be determined. It is still unclear what the differences and similarities are among the cloned organic cation transporters regarding their substrate and inhibitor selectivities. Members of the OCT gene family (OCT1, OCT2, OCT3) share a high degree of sequence identity and are predicted to have very similar secondary structures [22]. It therefore seems reasonable to predict that these transporters will be functionally similar. However, it has been shown that minor alterations in the amino acid sequences of some transporters can affect their function considerably [6]. The question remains unanswered: are paralogous organic cation transporters functionally redundant or distinct?

A number of recent studies have begun to address this question. For example, in two studies, inhibition constants for ten organic cations interacting with rOCT1 and rOCT2 were determined [23, 24]. Only one compound, procainamide, showed a notable preference for one transporter over the other – its inhibition constant was ~ 6-fold greater

for rOCT2 compared to rOCT1. In another study, significant differences in the substrate selectivities of rOCT1 and rOCT2 were reported; rOCT1 was shown to transport several nucleosides whereas rOCT2 did not [25]. Finally, a fourth study also reported differences in the substrate selectivities of rOCT1, rOCT2, and hOCT3 [26]. Together, these studies suggest that there are similarities as well as differences in the specificities of paralogous OCTs.

The goal of this study was to compare the substrate selectivities of hOCT2 and hOCT1 using nTAA compounds and biguanides. nTAA compounds, a class of organic cations, have been used extensively to study the functional characteristics of organic cation transporters, first in tissue and membrane preparations, and recently with the cloned OCT1 [7-13]. The interactions of the biguanides metformin and phenformin with hOCT1 and hOCT2 were also determined. Metformin is secreted by the kidney in humans, suggesting that a transporter(s) is involved in its elimination, but so far this transporter(s) has not been identified [14, 15].

In this study, we observed that the larger nTAA compounds (50 μ M) inhibited hOCT2 more than the smaller nTAA compounds (Fig. 1), similar to what had been observed previously for hOCT1 [7, 8, Chapter 3]. However, kinetic studies revealed substantial differences in their potencies of interaction with the two organic cation transporters. For example, the smallest nTAA, TMA, inhibited hOCT2 80-fold more

potently than hOCT1. Interestingly, TBA, a larger compound, was a 4-fold more potent inhibitor of hOCT1 compared to hOCT2. These differences in inhibition constants suggest that there are significant differences in the binding sites of these transporters. The *trans*-stimulation profiles for hOCT1 and hOCT2 differ considerably (Fig. 2), further suggesting that the binding sites for the two transporter isoforms differ. The rank order of *trans*-inhibition by TPrA, TBA, and TPeA for hOCT2 was strikingly similar to what we previously found for the mouse and rat OCT1 isoforms [8, Chapter 3]. Hence, it is possible that the elements involved in the binding or translocation of these compounds at the *trans*-side of the transporters might be conserved among hOCT2, mOCT1, and rOCT1, but not hOCT1.

Metformin, a biguanide used in the treatment of non-insulin-dependent diabetes mellitus (NIDDM), is eliminated by active secretion in the kidney, and it is likely that one or more of the organic cation transporters are involved in this process [14, 15, 27-29]. We observed that both metformin and phenformin interact with hOCT1 and hOCT2 (Figs. 3 & 4), but that both transporters had a much higher affinity for phenformin compared to metformin. *Cis*-inhibition studies revealed that metformin and phenformin inhibited the ³H-cimetidine uptake mediated by hOCT1 and hOCT2, suggesting that hOCT1 and hOCT2 may be the molecular site of the previously characterized metformin-cimetidine drug-drug interaction [29]. The data demonstrating that both metformin and

phenformin *trans*-stimulated $^3\text{H-MPP}^+$ influx mediated by the transporters suggest that the compounds are substrates of both hOCT1 and hOCT2. Furthermore, metformin induced a current in voltage-clamped oocytes expressing hOCT2, providing more evidence that metformin is a substrate of hOCT2. Although the apparent K_i value of metformin seems large relative to its estimated therapeutic concentrations ($\sim 2 - 8 \mu\text{M}$) [27, 28], hOCT2 may act as a low affinity, high capacity transporter for metformin. There are a number of transporters that function in this manner [30, 31].

In summary, the substrate specificities of hOCT1 and hOCT2 were studied using nTAA compounds and biguanides. The biguanides have similar affinities for hOCT1 and hOCT2 (Table 2), whereas significant differences were found between hOCT1 and hOCT2 in their interaction with nTAA compounds. These results suggest that there are significant differences in the binding sites of these paralogous transporters. Studies ascertaining the critical domains and amino acid residues required for substrate recognition and translocation will shed light on the molecular mechanisms responsible for the distinct substrate selectivities of the hOCT isoforms.

References

1. Bendayan R, Renal drug transport: a review. *Pharmacotherapy* **16**(6): 971-985, 1996.
2. Besseghir K and Roch-Ramel F, Renal excretion of drugs and other xenobiotics. *Ren Physiol* **10**(5): 221-241, 1987.
3. van Ginneken CA and Russel FG, Saturable pharmacokinetics in the renal excretion of drugs. *Clin Pharmacokinet* **16**(1): 38-54, 1989.
4. Burckhardt G and Wolff NA, Structure of renal organic anion and cation transporters. *Am J Physiol Renal Physiol* **278**(6): F853-866, 2000.
5. Koepsell H, Gorboulev V and Arndt P, Molecular pharmacology of organic cation transporters in kidney. *J Membr Biol* **167**(2): 103-117, 1999.
6. Wang J and Giacomini KM, Serine 318 is essential for the pyrimidine selectivity of the N2 Na⁺-nucleoside transporter. *J Biol Chem* **274**(4): 2298-2302, 1999.
7. Zhang L, Gorset W, Dresser MJ and Giacomini KM, The interaction of n-tetraalkylammonium compounds with a human organic cation transporter, hOCT1. *J Pharmacol Exp Ther* **288**(3): 1192-1198, 1999.
8. Dresser MJ, Gray AT and Giacomini KM, Kinetic and selectivity differences between rodent, rabbit, and human organic cation transporters (OCT1). *J Pharmacol Exp Ther* **292**(3): 1146-1152, 2000.

9. Groves CE, Evans KK, Dantzler WH and Wright SH, Peritubular organic cation transport in isolated rabbit proximal tubules. *Am J Physiol* **266**(3 Pt 2): F450-458, 1994.
10. Groves CE and Wright SH, Tetrapentylammonium (TPeA): slowly dissociating inhibitor of the renal peritubular organic cation transporter. *Biochim Biophys Acta* **1234**(1): 37-42, 1995.
11. Kim YK and Dantzler WH, Specificity of basolateral organic cation transport in snake renal proximal tubules. *Am J Physiol* **270**(5 Pt 2): R1025-1030, 1996.
12. Wright SH and Wunz TM, Influence of substrate structure on turnover of the organic cation/H⁺ exchanger of the renal luminal membrane. *Pflugers Arch* **436**(3): 469-477, 1998.
13. Wright SH and Wunz TM, Influence of substrate structure on substrate binding to the renal organic cation/H⁺ exchanger. *Pflugers Arch* **437**(4): 603-610, 1999.
14. Pentikainen PJ, Neuvonen PJ and Penttila A, Pharmacokinetics of metformin after intravenous and oral administration to man. *Eur J Clin Pharmacol* **16**(3): 195-202, 1979.
15. Sirtori CR, Franceschini G, Galli-Kienle M, Cighetti G, Galli G, Bondioli A and Conti F, Disposition of metformin (N,N-dimethylbiguanide) in man. *Clin Pharmacol Ther* **24**(6): 683-693, 1978.

1. *Staphylococcus aureus*

2. *Streptococcus pneumoniae*

3. *Escherichia coli*

4. *Salmonella enteritidis*

5. *Shigella flexneri*

6. *Yersinia enterocolitica*

7. *Legionella pneumophila*

8. *Campylobacter jejuni*

9. *Listeria monocytogenes*

10. *Haemophilus influenzae*

11. *Neisseria meningitidis*

12. *Streptococcus pyogenes*

13. *Streptococcus agalactiae*

14. *Streptococcus pneumoniae*

15. *Streptococcus pneumoniae*

16. Zhang L, Dresser MJ, Gray AT, Yost SC, Terashita S and Giacomini KM, Cloning and functional expression of a human liver organic cation transporter. *Mol Pharmacol* **51**(6): 913-921, 1997.
17. Terashita S, Dresser MJ, Zhang L, Gray AT, Yost SC and Giacomini KM, Molecular cloning and functional expression of a rabbit renal organic cation transporter. *Biochim Biophys Acta* **1369**(1): 1-6, 1998.
18. Zhang L, Schaner ME and Giacomini KM, Functional characterization of an organic cation transporter (hOCT1) in a transiently transfected human cell line (HeLa). *J Pharmacol Exp Ther* **286**(1): 354-361, 1998.
19. Dantzler WH, Wright SH, Chatsudthipong V and Brokl OH, Basolateral tetraethylammonium transport in intact tubules: specificity and trans-stimulation. *Am J Physiol* **261**(3 Pt 2): F386-392, 1991.
20. Moseley RH, Takeda H and Zuger LJ, Choline transport in rat liver basolateral plasma membrane vesicles. *Hepatology* **24**(1): 192-197, 1996.
21. Zhang L, Brett CM and Giacomini KM, Role of organic cation transporters in drug absorption and elimination. *Annu Rev Pharmacol Toxicol* **38**: 431-460, 1998.
22. Burckhardt BC, Wolff NA and Burckhardt G, Electrophysiologic characterization of an organic anion transporter cloned from winter flounder kidney (fROAT). *J Am Soc Nephrol* **11**(1): 9-17, 2000.

23. Okuda M, Urakami Y, Saito H and Inui K, Molecular mechanisms of organic cation transport in OCT2-expressing *Xenopus* oocytes. *Biochim Biophys Acta* **1417**(2): 224-231, 1999.
24. Urakami Y, Okuda M, Masuda S, Saito H and Inui KI, Functional characteristics and membrane localization of rat multispecific organic cation transporters, OCT1 and OCT2, mediating tubular secretion of cationic drugs. *J Pharmacol Exp Ther* **287**(2): 800-805, 1998.
25. Chen R and Nelson JA, Role of organic cation transporters in the renal secretion of nucleosides. *Biochem Pharmacol* **60**(2): 215-219, 2000.
26. Grundemann D, Liebich G, Kiefer N, Koster S and Schomig E, Selective substrates for non-neuronal monoamine transporters. *Mol Pharmacol* **56**(1): 1-10, 1999.
27. Bailey CJ, Biguanides and NIDDM. *Diabetes Care* **15**(6): 755-772, 1992.
28. Scheen AJ, Clinical pharmacokinetics of metformin. *Clin Pharmacokinet* **30**(5): 359-371, 1996.
29. Somogyi A, Stockley C, Keal J, Rolan P and Bochner F, Reduction of metformin renal tubular secretion by cimetidine in man. *Br J Clin Pharmacol* **23**(5): 545-551, 1987.
30. Pajor AM, Hirayama BA and Wright EM, Molecular evidence for two renal Na⁺/glucose cotransporters. *Biochim Biophys Acta* **1106**(1): 216-220, 1992.

1. The first part of the document is a list of names and addresses of the members of the committee.

2. The second part of the document is a list of names and addresses of the members of the committee.

3. The third part of the document is a list of names and addresses of the members of the committee.

4. The fourth part of the document is a list of names and addresses of the members of the committee.

5. The fifth part of the document is a list of names and addresses of the members of the committee.

6. The sixth part of the document is a list of names and addresses of the members of the committee.

7. The seventh part of the document is a list of names and addresses of the members of the committee.

8. The eighth part of the document is a list of names and addresses of the members of the committee.

31. Smith DE, Pavlova A, Berger UV, Hediger MA, Yang T, Huang YG and Schnermann JB, Tubular localization and tissue distribution of peptide transporters in rat kidney. *Pharm Res* **15**(8): 1244-1249, 1998.

CHAPTER 5

STABLE EXPRESSION OF A GFP-rOCT1 FUSION PROTEIN IN A POLARIZED EPITHELIAL CELL LINE (MDCK): INTRACELLULAR LOCALIZATION AND FUNCTIONAL CHARACTERIZATION

Introduction

Organic cations, in general, undergo net secretion in the kidney. To ensure that the net transport of organic cations occurs in the secretory direction, renal organic cation transporters are asymmetrically distributed within the tubule epithelium to the appropriate plasma membrane. Renal epithelial cells have two distinct types of plasma membranes: the basolateral membrane (BLM) and the brush border membrane (BBM). The BLM is attached to a basement membrane and is in contact with the blood, whereas the BBM faces the tubule lumen. These two membranes, separated by tight junctions, differ in their protein contents as well as their physiological functions.

Using a number of kidney tissue preparations such as membrane vesicles and kidney slices, as well as renal cell lines, distinct transport systems for organic cations have been identified in the BLM and BBM [1-4]. In the BLM, organic cations are transported from the blood into the epithelial cells down the electrochemical gradient by

1. The first part of the document discusses the importance of maintaining accurate records of all transactions and activities. It emphasizes that this is crucial for ensuring transparency and accountability in the organization's operations.

2. The second part of the document outlines the specific procedures and protocols that must be followed to ensure that all records are properly maintained and updated. It details the roles and responsibilities of various staff members in this process.

several potential sensitive organic cation transporters. Organic cation transport across the BBM is mediated by organic cation:proton antiporters, which exchange an intracellular organic cation for a luminal proton.

To date, five organic cation transporters have been cloned and functionally characterized [1, 4]. With the availability of the cloned transporters it is now possible to develop transfected polarized cell lines to address questions related to the *in vivo* roles of membrane transporters in drug elimination. Such transfected cell lines can be used to (a) determine and confirm the intracellular localization of membrane transporters; (b) study the functional characteristics of the transporters; (c) investigate the sorting pathways involved in membrane targeting; and (d) study the post-transcriptional regulation of transporters.

The primary goal of this study was to develop a cell culture model of rOCT1, to use in investigations of its intracellular localization, sorting, and post-transcriptional regulation. rOCT1 appears to be one of the major organic cation transporters in liver and kidney cells, and thus functions as a first step in the elimination pathway of a number of structurally diverse organic cations. In this study, a polarized epithelial cell line stably transfected with a green fluorescent protein (GFP)-rOCT1 fusion protein was established, and the localization of the fusion protein was investigated via confocal microscopy and functional studies. Recently, similar strategies have been successfully used in studies of

1. *...*

2. *...*

3. *...*

4. *...*

5. *...*

6. *...*

7. *...*

8. *...*

9. *...*

10. *...*

11. *...*

12. *...*

13. *...*

14. *...*

15. *...*

16. *...*

17. *...*

18. *...*

19. *...*

20. *...*

21. *...*

22. *...*

23. *...*

24. *...*

25. *...*

26. *...*

27. *...*

28. *...*

29. *...*

30. *...*

other transporters [5-8]. A secondary goal of this study was to begin to determine structural domains involved in signaling the BLM-sorting of rOCT1. In particular, we determined if a BLM-sorting signal found in the rOCT1 carboxy-terminus is required for the basolateral targeting of this transporter.

Materials and Methods

DNA constructs. cDNAs of full-length rOCT1 and a truncated rOCT1, termed rOCT1 Δ , in which part of the carboxyl-terminus – amino acids 545 to 556 - was truncated, were amplified by PCR using an rOCT1 containing plasmid as the template. Restriction enzyme sites required for subcloning into the pEGFP-C1 vector (Clontech, Palo Alto, CA) were incorporated into the cDNAs during PCR amplification. The sense primer used in the PCR for both the full-length rOCT1 and rOCT1 Δ was 5'-AGATCTATGCCACCGTGGACGATGTTCTGGAG-3'; the flanking *Bgl* II site needed for subcloning is underlined. The antisense primers used in the PCRs for full-length rOCT1 and rOCT1 Δ contained a flanking *Bam*H I site (underlined). The antisense primer sequence used to amplify full-length rOCT1 was 5'GGATCCTCAGGTAC-TTGAGGACTTGCCTGTTTGGAC-3, and the antisense primer used to amplify rOCT1 Δ was 5'-GGATCCTCACGTGTTTTCTTTGGCCTTTGATTCCT-3'. PCR was performed in a thermal cycler (PE Applied Biosystems, Foster City, CA) according to the

1. The first part of the document is a list of names and titles.

2. The second part of the document is a list of names and titles.

3. The third part of the document is a list of names and titles.

4. The fourth part of the document is a list of names and titles.

5. The fifth part of the document is a list of names and titles.

6. The sixth part of the document is a list of names and titles.

7. The seventh part of the document is a list of names and titles.

8. The eighth part of the document is a list of names and titles.

following program: 5 min 94°C incubation; 94°C for 1 min, 55°C for 1.5 min, and 72°C for 2 min (25 cycles); 15 min 72°C incubation. PCR products were initially subcloned into the pGEM-T vector (Promega, Madison, WI). pGEM-T plasmids containing full-length rOCT1 and rOCT1Δ were digested with *Bgl* II and *Bam*H I (GIBCO BRL, Rockville, MD). The digested rOCT1 and rOCT1Δ inserts were then subcloned into pEGFP-C1 vector, which had also been digested with *Bgl* II and *Bam*H I to give the plasmids rOCT1-pEGFP and rOCT1Δ-pEGFP. The plasmids were analyzed by restriction enzyme analyses to confirm the orientation and integrity of the inserts. For transporter expression in *Xenopus laevis* oocytes, the GFP-rOCT1 insert was amplified by PCR from the rOCT1-pEGFP plasmid using the same antisense primer listed above and the sense primer: 5'-AAGCTTGCTACCGGTCGCCACCATGGTGAGC-3'. This new sense primer incorporated a *Hind* III site (underlined) at the 5'-end of the PCR products. The GFP-rOCT1 DNA was subcloned into pGEM-T, digested with *Hind* III and *Bam*H I, and then subcloned into pOX, a *Xenopus laevis* oocyte expression vector [9].

cRNA transcription and expression in Xenopus laevis oocytes. Oocytes were harvested from oocyte positive *Xenopus laevis* (Nasco, Fort Atkinson, WI) and were dissected and treated with 2 mg/ml collagenase D (Boehringer-Mannheim Biochemicals, Indianapolis, IN) in a calcium-free ORII solution as previously described [10]. Oocytes

1. The first part of the document is a list of names and titles, including "The Hon. Mr. Justice G. D. C. O'Connell, Chief Justice of the Supreme Court of the State of New South Wales" and "The Hon. Mr. Justice G. D. C. O'Connell, Chief Justice of the Supreme Court of the State of New South Wales".

2. The second part of the document is a list of names and titles, including "The Hon. Mr. Justice G. D. C. O'Connell, Chief Justice of the Supreme Court of the State of New South Wales" and "The Hon. Mr. Justice G. D. C. O'Connell, Chief Justice of the Supreme Court of the State of New South Wales".

were maintained at 18°C in modified Barth's medium. Healthy stage V and VI oocytes were injected with capped cRNA (1 µg/µl) that was transcribed *in vitro* with T3 polymerase (mCAP RNA Capping kit; Stratagene, La Jolla, CA) from *Not I* linearized plasmids containing transporter cDNA inserts.

Tracer uptake measurements in Xenopus laevis oocytes. Transport of MPP⁺ in oocytes was measured 3 – 4 days after cRNA injection as described previously [10]. Uptake experiments were carried out as follows: groups of seven to nine oocytes were incubated in 100 µl Na⁺ buffer (100 mM NaCl, 2 mM KCl, 1 mM CaCl₂, 1 mM MgCl₂, 10 mM HEPES/Tris, pH 7.2) containing MPP⁺ (1 µM: 0.1 µM ³H-MPP⁺ (82 Ci/mmol) and 0.9 µM unlabeled MPP⁺) at 25°C for 1 h. The uptake experiment was stopped by washing the oocytes 5 times with 3 ml of ice-cold Na⁺ buffer. Then the oocytes were lysed with 100 µl 10% sodium dodecyl sulfate (SDS) individually, and the amount of radiolabeled substrates associated with each oocyte was determined by liquid scintillation counting. For inhibition studies, unlabeled nTAA compounds (50 µM) were added to the reaction solutions.

In *trans*-stimulation studies, groups of 5 – 7 GFP-rOCT1 cRNA-injected or uninjected oocytes were washed three times with K⁺ buffer (2 mM NaCl, 100 mM KCl, 1 mM CaCl₂, 1 mM MgCl₂, 10 mM HEPES/Tris, pH 7.2). The oocytes were then rapidly injected with 50 nl of a K⁺ solution containing an unlabeled nTAA compound. The

7
1
2
3
4
5
6
7
8
9
10
11
12
13
14
15
16
17
18
19
20
21
22
23
24
25
26
27
28
29
30
31
32
33
34
35
36
37
38
39
40
41
42
43
44
45
46
47
48
49
50
51
52
53
54
55
56
57
58
59
60
61
62
63
64
65
66
67
68
69
70
71
72
73
74
75
76
77
78
79
80
81
82
83
84
85
86
87
88
89
90
91
92
93
94
95
96
97
98
99
100

101
102
103
104
105
106
107
108
109
110
111
112
113
114
115
116
117
118
119
120
121
122
123
124
125
126
127
128
129
130
131
132
133
134
135
136
137
138
139
140
141
142
143
144
145
146
147
148
149
150
151
152
153
154
155
156
157
158
159
160
161
162
163
164
165
166
167
168
169
170
171
172
173
174
175
176
177
178
179
180
181
182
183
184
185
186
187
188
189
190
191
192
193
194
195
196
197
198
199
200

concentration and injection volume were chosen based upon an average oocyte intracellular volume of 500 nl to produce intracellular nTAA concentrations that would be at saturating levels (i.e. ≥ 10 -fold the K_m or K_i value). Oocytes injected with 50 nl of K^+ buffer were used for controls in the *trans*-stimulation studies. After injections, the oocytes were quickly transferred to a small disposable borosilicate glass culture tube; any remaining K^+ was aspirated off, and 85 μ l of MPP⁺ (1 μ M: 0.1 μ M ³H-MPP⁺ and 0.9 μ M unlabeled MPP⁺) in K^+ buffer was added. MPP⁺ uptake was stopped after 10 min by washing the oocytes 5 times with 3 ml of ice-cold K^+ buffer. The radioactivity associated with each oocyte was then determined by scintillation counting.

Statistical analysis of the inhibition and *trans*-stimulation data was carried out by unpaired *t* test where $P < 0.05$ was considered significant.

MDCK transfection. The EMBL MDCK II strain was a generous gift from Dr. Karl Matlin. The cells were maintained at 37°C in a 95% air-5% CO₂ atmosphere in 10 cm dishes and fed with MEM Eagle's Media with Earle's BSS containing glucose (1.0 g/L) supplemented with 5% heat inactivated FBS, 100 units/ml penicillin, and 100 μ g/ml streptomycin. Cells were transfected with pEGFPC1-rOCT1, pEGFPC1-rOCT1 Δ , or pEGFPC1 by the calcium phosphate method as described previously [11]. Briefly, subconfluent cells were exposed to a DNA-Ca⁺⁺ solution for 6 – 8 hours prior to glycerol shock. Cells were then allowed to recover in media at 37°C for three days. Then stable

1
2
3
4
5
6
7
8
9
10
11
12
13
14
15
16
17
18
19
20
21
22
23
24
25
26
27
28
29
30
31
32
33
34
35
36
37
38
39
40
41
42
43
44
45
46
47
48
49
50
51
52
53
54
55
56
57
58
59
60
61
62
63
64
65
66
67
68
69
70
71
72
73
74
75
76
77
78
79
80
81
82
83
84
85
86
87
88
89
90
91
92
93
94
95
96
97
98
99
100

101
102
103
104
105
106
107
108
109
110
111
112
113
114
115
116
117
118
119
120
121
122
123
124
125
126
127
128
129
130
131
132
133
134
135
136
137
138
139
140
141
142
143
144
145
146
147
148
149
150
151
152
153
154
155
156
157
158
159
160
161
162
163
164
165
166
167
168
169
170
171
172
173
174
175
176
177
178
179
180
181
182
183
184
185
186
187
188
189
190
191
192
193
194
195
196
197
198
199
200

clones were selected in media containing 0.7 mg/ml G418 (Calbiochem, La Jolla, CA). After 10 – 14 days, individual stable clones were isolated and positive clones further selected by immunohistochemistry and functional assays. A single clone was selected and used for all subsequent experiments.

Transport studies using MDCK cell lines. For transport studies, MDCK cells were polarized by growth on Transwell® filters (Costar, Cambridge, MA) with a 0.4 µm pore size at a confluent density for 7 days with regular media changes. Immediately before the transport experiments, cells were washed once with PBS (room temperature) on both the apical and basolateral sides. The transport experiment, carried out at room temperature, was commenced by adding ¹⁴C-TEA (50 µM) in the presence or absence of 200 µM quinidine, an organic cation transporter inhibitor, to either the basolateral (0.5 ml) or apical (0.2 ml) compartments; substrate-free PBS was left on the opposite side. Uptake was stopped at 10 min by aspirating off the uptake solution and washing the wells three times in ice-cold PBS buffer. The filters were then allowed to dry at room temperature, after which they were carefully cut from the plastic supports, and placed in scintillation vials. Three ml of scintillation fluid (EcoLite(+)TM, ICN Biochemicals, Inc., Aurora, OH) was added to each vial and the radioactivity associated with each filter was determined by liquid scintillation counting on a Beckman counter. To determine protein levels, the cells were solubilized in 0.5 ml of 1 M NaOH for 2 h, neutralized by the

1. The first part of the document is a list of names and addresses of the members of the committee. The names are listed in alphabetical order, and the addresses are given in full. The list includes the names of the members of the committee, the names of the members of the sub-committee, and the names of the members of the advisory committee. The addresses are given in full, including the street name, the city, and the state.

2. The second part of the document is a list of the names and addresses of the members of the committee. The names are listed in alphabetical order, and the addresses are given in full. The list includes the names of the members of the committee, the names of the members of the sub-committee, and the names of the members of the advisory committee. The addresses are given in full, including the street name, the city, and the state.

addition of 0.5 ml 1 M HCl, and protein levels determined using the Bio-Rad DC Protein Assay (BioRad, Hercules, CA) with a BSA standard (Pierce, Rockford, IL). Statistical analysis was carried out by unpaired *t* test where $P < 0.05$ was considered significant.

Confocal microscopy studies. For microscopy studies, cells were polarized by growth on filters for 7 days as described above. Polarized cells were fixed with 4% paraformaldehyde, permeablized with 0.025% (w/v) saponin in PBS, stained with Texas-red conjugated phalloidin (Molecular Probes, Eugene, OR) to visualize actin and mounted on slides in Vectashield mounting medium (Vector Laboratories, Inc., Burlingame, CA). Samples were analyzed using a Bio-Rad MRC-1024 confocal microscope. Images were processed with Adobe Photoshop 5.0.

Chemicals. ^{14}C -TEA (55mCi/mmol) was obtained from American Radiolabeled Chemicals Inc. (St. Louis, MO). Cell culture media, serum, and antibiotics were purchased from the UCSF Cell Culture Facility. All other unlabeled compounds and buffer components were purchased from Sigma (St. Louis, MO). All plastic cell culture supplies were from Corning Costar Corp (Corning, NY).

Results

Functional characterization of GFP-tagged rOCT1 expressed in Xenopus laevis oocytes. To determine whether the N-terminal GFP tag altered the function of rOCT1,

1. The first part of the document is a list of names and titles, including "The Hon. Mr. Justice" and "The Hon. Mr. Justice".

2. The second part of the document is a list of names and titles, including "The Hon. Mr. Justice" and "The Hon. Mr. Justice".

functional studies of GFP-rOCT1 were carried out in *Xenopus laevis* oocytes. Two types of functional studies using nTAA compounds were carried out: *cis*-inhibition and *trans*-stimulation. The *cis*-inhibition studies were performed to determine whether the GFP tag affected the binding of inhibitors to rOCT1. In the *cis*-inhibition studies, the potencies of the nTAA compounds (50 μ M) for both GFP-rOCT1 and rOCT1 increased with alkyl chain length, and were not statistically different from each other for the two transporters ($P < 0.05$) (Fig. 1). *Trans*-stimulation studies were undertaken to determine if the GFP tag altered the countertransport function of rOCT1. These studies were carried out under depolarized conditions (i.e. in high potassium buffer) to minimize the effects of membrane potential on $^3\text{H-MPP}^+$ influx or efflux of the unlabeled nTAA compounds. Comparable to rOCT1, $^3\text{H-MPP}^+$ influx in oocytes expressing GFP-rOCT1 was *trans*-stimulated by TEA and *trans*-inhibited by TPrA, TBA, and TPeA (Fig. 2). TMA, the smallest nTAA compound, *trans*-stimulated both the tagged and untagged transporters; however, the degree of TMA *trans*-stimulation was significantly different for GFP-rOCT1 ($P < 0.05$), suggesting that the GFP tag might alter the countertransport function of rOCT1 for TMA (Fig. 2).

Functional localization of GFP-rOCT1 in polarized MDCK. The intracellular localization of GFP-rOCT1 was first determined functionally by measuring $^{14}\text{C-TEA}$ uptake from the basolateral or apical membrane compartments of MDCK cells stably

1. The first part of the document discusses the importance of maintaining accurate records of all transactions and activities. It emphasizes that this is crucial for ensuring transparency and accountability in the organization's operations.

2. The second part of the document outlines the various methods and tools used to collect and analyze data. It highlights the need for consistent and reliable data collection processes to support effective decision-making.

expressing GFP-rOCT1. Membrane-specific uptake of ^{14}C -TEA should reflect the intracellular localization of GFP-rOCT1. ^{14}C -TEA uptake at the basolateral membrane of rOCT1-pEGFP-C1 transfected cells was significantly enhanced over empty vector transfected cells ($P < 0.05$) (Fig. 3). Enhanced uptake of ^{14}C -TEA across the apical membrane was also significantly greater in GFP-rOCT1 cells compared to GFP expressing cells ($P < 0.05$) (Fig. 3). But relative to the enhancement of ^{14}C -TEA uptake in the BLM, the enhanced uptake in the apical membrane was minor. Empty vector transfected cells did not exhibit significant differences in ^{14}C -TEA uptake compared to untransfected controls (Fig. 3). In addition, ^{14}C -TEA uptake mediated by GFP-rOCT1 was blocked by 200 μM quinidine, a potent organic cation transporter inhibitor. Both the parental MDCK cell line and the cell line stably transfected with GFP apparently express an endogenous organic cation transporter in the BLM, as quinidine significantly reduced the basolateral uptake of ^{14}C -TEA in these cell lines (Fig. 3).

1. The first part of the document is a list of names and addresses of the members of the committee. The names are listed in alphabetical order, and the addresses are given in full. The list includes the names of the members of the committee, the names of the members of the sub-committee, and the names of the members of the advisory committee. The addresses are given in full, including the street name, the city, and the state.

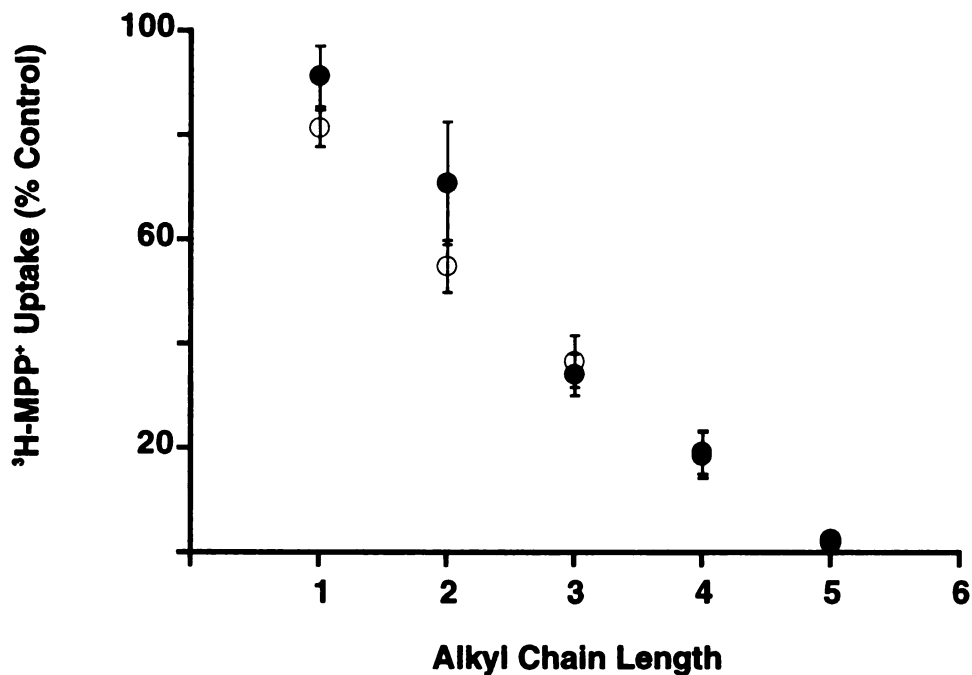


Figure 1. Effect of nTAA compounds (50 μM) of increasing chain length on $^3\text{H-MPP}^+$ (1 μM) uptake mediated by wildtype rOCT1 and GFP-rOCT1 expressed in *Xenopus laevis* oocytes. The uptake of $^3\text{H-MPP}^+$ (1 h) in Na^+ uptake buffer was measured in oocytes expressing wildtype rOCT1 (○) or GFP-rOCT1 (●). Each data point represents the mean rate of uptake as percent of control in which no inhibitor was present. Data represent mean values \pm SE of three experiments in separate batches of oocytes. Six to nine oocytes were used for each uptake experiment. Wildtype rOCT1 data has been previously published by our laboratory [12, Chapter 3].

1. The first part of the document discusses the importance of maintaining accurate records of all transactions and activities. It emphasizes that this is crucial for ensuring transparency and accountability in the organization's operations.

2. The second part of the document outlines the specific procedures and protocols that must be followed to ensure the accuracy and integrity of the records. This includes detailed instructions on how to collect, store, and retrieve data.

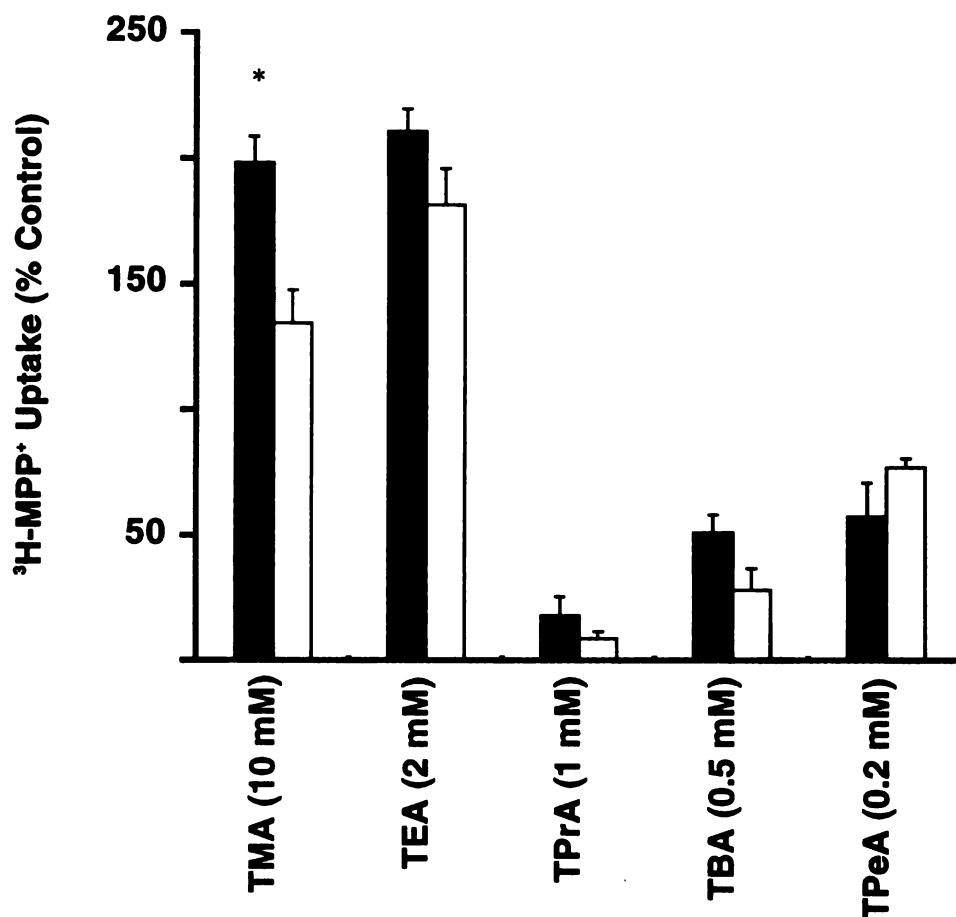


Figure. 2. Effect of *trans* nTAA compounds on the influx of $^3\text{H-MPP}^+$ in *Xenopus laevis* oocytes expressing wildtype or GFP-tagged rOCT1. Oocytes, depolarized using K^+ uptake buffer (100 mM K^+ and 2 mM Na^+), expressing either wildtype rOCT1 (open bars) or GFP-rOCT1 (dark bars) were injected with 50 nl of an unlabeled nTAA compound dissolved in K^+ buffer to give the final intracellular nTAA concentrations indicated in the figure (control oocytes were injected with 50 nl of K^+ buffer). The 10-min uptake of $^3\text{H-MPP}^+$ (1 μM) in K^+ buffer was then measured. The mean control uptake (*trans*-zero) was taken as 100%. Data represent mean \pm S.E. from three separate experiments; 5–9 oocytes were used per compound per experiment. (* significantly different from the untagged transporter, $P < 0.05$).

1. The first part of the document is a list of names and addresses of the members of the committee. The names are listed in alphabetical order, and the addresses are given in full, including the street name, number, and city.

2. The second part of the document is a list of the names and addresses of the members of the committee who have been elected to the office of chairman. The names are listed in alphabetical order, and the addresses are given in full, including the street name, number, and city.

3. The third part of the document is a list of the names and addresses of the members of the committee who have been elected to the office of secretary. The names are listed in alphabetical order, and the addresses are given in full, including the street name, number, and city.

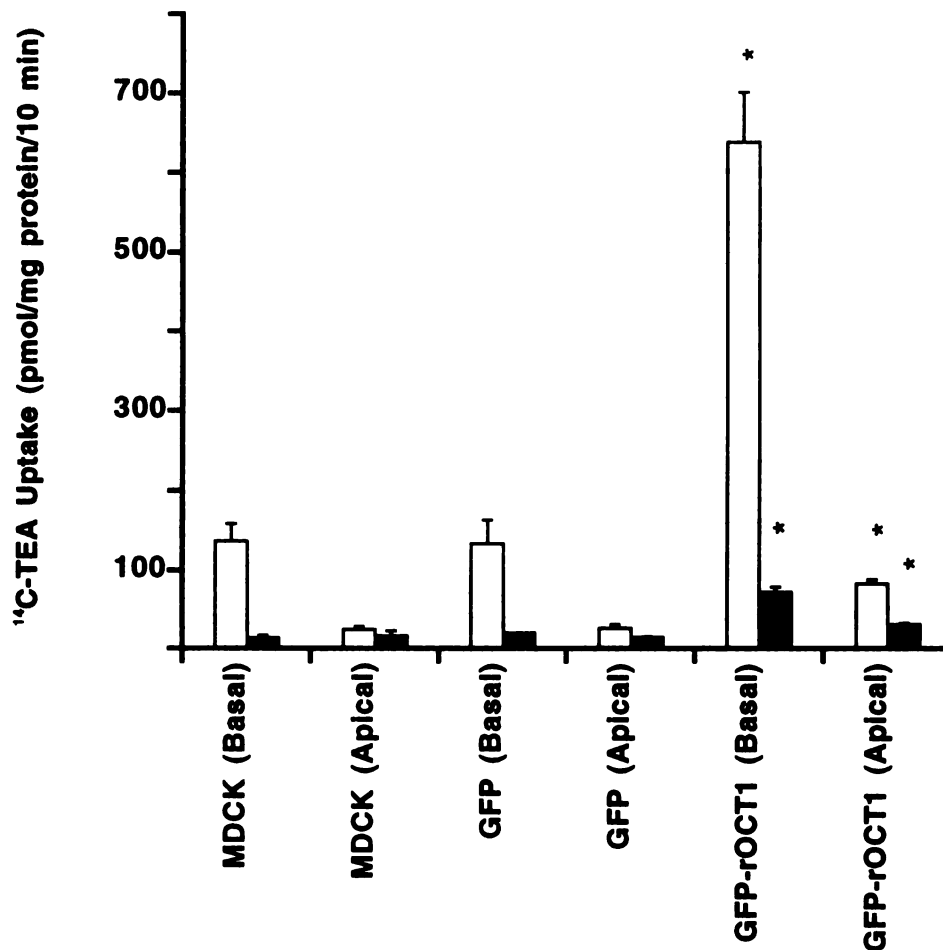


Figure 3. Functional localization of GFP-rOCT1 stably transfected in MDCK. Antibiotic (G418)-resistant MDCK cell clones stably transfected with the parent vector, pEGFP (GFP), or the rOCT1-containing vector, rOCT1-pEGFP (GFP-rOCT1), were isolated. Cells were polarized by growth on 0.4 μ m filters (Costar) for seven days. Uptake of 14 C-TEA (50 μ M) at either the apical or basolateral membrane was examined in the absence (open bar) or presence (dark bars) of 200 μ M quinidine, a potent OCT-inhibitor. Data are mean values \pm S.E. for 4 to 6 filters from two separate experiments. (* significantly different from pEGFP (empty vector) transfected cells, $P < 0.05$).

1
2
3
4
5
6
7
8
9
10
11
12
13
14
15
16
17
18
19
20
21
22
23
24
25
26
27
28
29
30
31
32
33
34
35
36
37
38
39
40
41
42
43
44
45
46
47
48
49
50
51
52
53
54
55
56
57
58
59
60
61
62
63
64
65
66
67
68
69
70
71
72
73
74
75
76
77
78
79
80
81
82
83
84
85
86
87
88
89
90
91
92
93
94
95
96
97
98
99
100

101
102
103
104
105
106
107
108
109
110
111
112
113
114
115
116
117
118
119
120
121
122
123
124
125
126
127
128
129
130
131
132
133
134
135
136
137
138
139
140
141
142
143
144
145
146
147
148
149
150
151
152
153
154
155
156
157
158
159
160
161
162
163
164
165
166
167
168
169
170
171
172
173
174
175
176
177
178
179
180
181
182
183
184
185
186
187
188
189
190
191
192
193
194
195
196
197
198
199
200

Localization of GFP-rOCT1 and GFP-rOCT1Δ in stably transfected MDCK cell

lines. GFP-rOCT1 and GFP-rOCT1Δ transfected MDCK cells were grown as polarized monolayers on permeable supports and examined by confocal microscopy to examine intracellular localization. Vertical optical sections of both clones at 488 nm show basolateral membrane staining patterns (Figs. 4 and 5). In contrast, empty vector transfected cells, containing GFP, display diffuse cytosolic staining and untransfected cells display no GFP staining (Fig. 4). These results suggest that both GFP-rOCT1 and GFP-rOCT1Δ are localized to the lateral membrane of polarized MDCK cells.

1
2
3
4
5
6
7
8
9
10
11
12
13
14
15
16
17
18
19
20
21
22
23
24
25
26
27
28
29
30
31
32
33
34
35
36
37
38
39
40
41
42
43
44
45
46
47
48
49
50
51
52
53
54
55
56
57
58
59
60
61
62
63
64
65
66
67
68
69
70
71
72
73
74
75
76
77
78
79
80
81
82
83
84
85
86
87
88
89
90
91
92
93
94
95
96
97
98
99
100

101
102
103
104
105
106
107
108
109
110
111
112
113
114
115
116
117
118
119
120
121
122
123
124
125
126
127
128
129
130
131
132
133
134
135
136
137
138
139
140
141
142
143
144
145
146
147
148
149
150

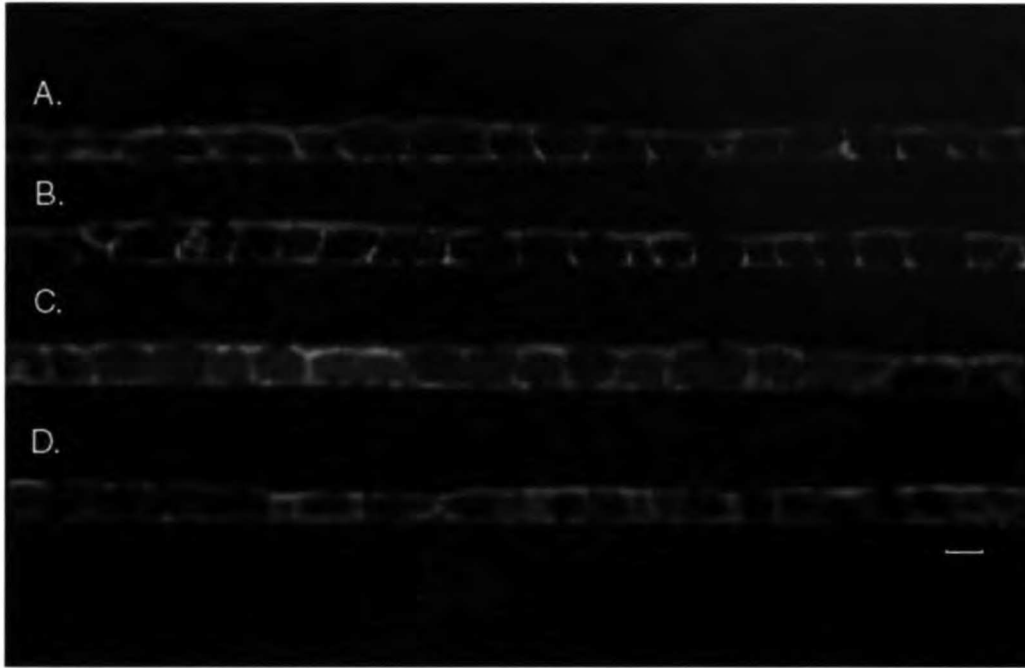


Figure 4. Vertical optical sections of MDCK cell lines visualized by confocal microscopy. MDCK cell lines stably transfected with GFP-rOCT1 (A), GFP-rOCT1 Δ (B), GFP (C), or untransfected MDCK cells (D) were polarized by growth on filters for 7 days. Cells were fixed, permeabilized, and stained for actin with Texas red conjugated-X phalloidin (red). GFP fluorescence (green) is present only in the lateral membranes in the cell lines expressing GFP-rOCT1 (A) and GFP-rOCT1 Δ (B). In contrast, the signal is evenly distributed throughout the cytoplasm of cells expressing GFP (C) and is not present in untransfected cells (D). Sections are shown with apical membrane on top. Bar, 10 μ m

17
The first part of the document
describes the general situation
of the country and the
state of the economy.
It also mentions the
main problems that
the government is facing
at the moment.

The second part of the document
describes the measures
that the government
is taking to solve
these problems.
It also mentions the
results of these
measures so far.

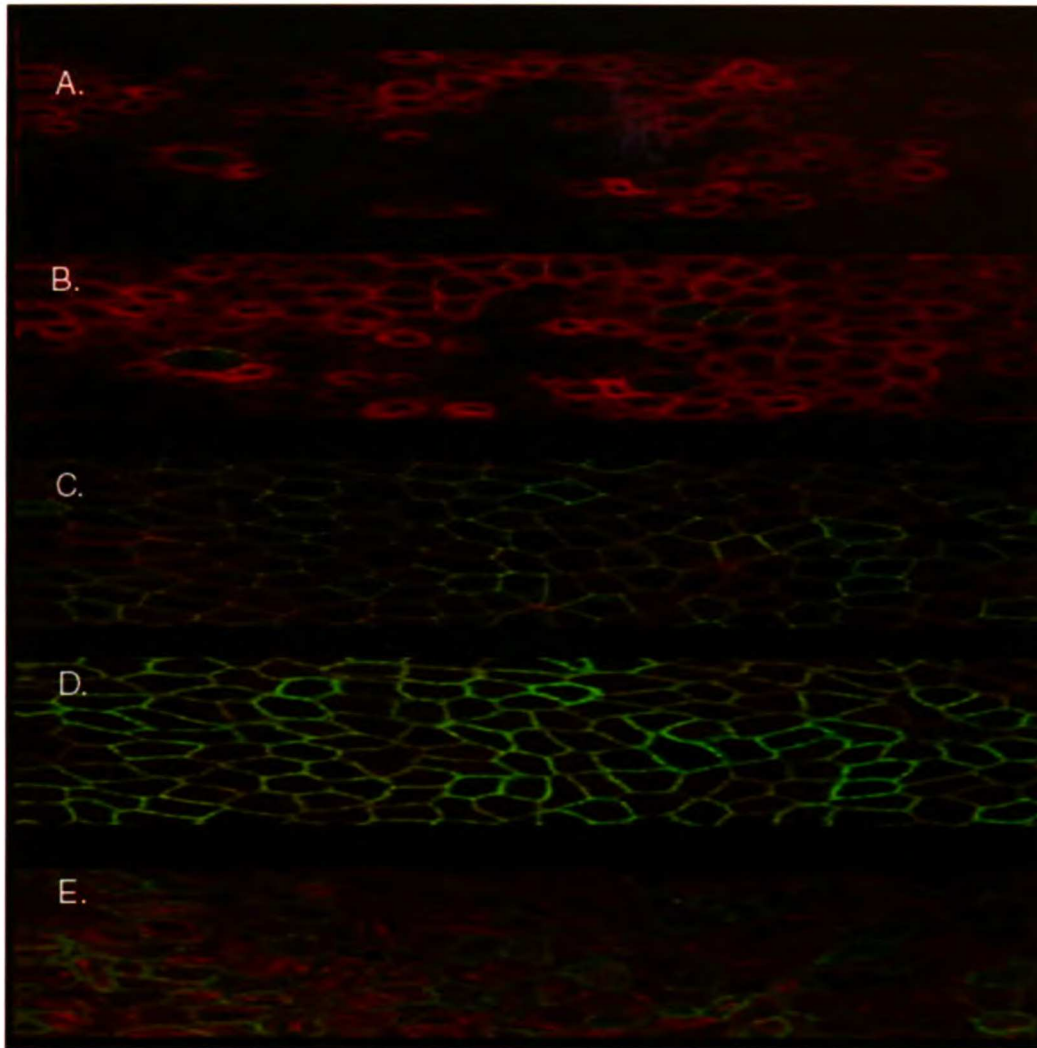


Figure 5. Cellular localization of GFP-rOCT1 in polarized MDCK cells determined by confocal microscopy. Successive images from the apical to the basolateral membrane are shown in the five *en face* images (A – E): A and B correspond to the apical membrane, and C - E correspond to the lateral membrane. Texas red conjugated-X phalloidin was used to stain actin (red). GFP fluorescence is present only in the lateral membranes.

1. The first part of the document is a list of names and addresses of the members of the committee. The names are listed in alphabetical order, and the addresses are listed below each name. The list includes names such as Mr. J. H. Smith, Mr. W. J. Brown, and Mr. C. D. Green, among others.

2. The second part of the document is a list of names and addresses of the members of the committee. The names are listed in alphabetical order, and the addresses are listed below each name. The list includes names such as Mr. J. H. Smith, Mr. W. J. Brown, and Mr. C. D. Green, among others.

Discussion

During the past decade, five organic cation transporter isoforms have been cloned and functionally characterized. To better understand their physiological roles in renal transport, their cell biology and function need to be investigated. In particular, studies of the intracellular localization patterns, sorting and regulation mechanisms of these transporters should lead to a better understanding of their roles in renal organic cation transport. Model systems, such as stably transfected polarized cell lines, are powerful systems to study these aspects of transporter biology and function. In addition, it is possible to use GFP-tagged transporters in such model systems, which expands the experimental possibilities to include visualizing GFP-tagged transporters dynamically within living cells.

The primary goal of this study was to establish a polarized cell culture model of OCT1 that could be used to study the cell biology and function of this transporter. To this end, we stably transfected a GFP-tagged rOCT1 construct in MDCK cells. This model system was used to determine the intracellular localization of rOCT1 in polarized cells. A secondary goal of this study was to determine whether a BLM-sorting sequence found in rOCT1 is required for its membrane targeting.

Originally established from distal tubules of adult female cocker spaniel, the MDCK cell line has several properties that make it a good model of a polarized epithelial

1. The first part of the document discusses the importance of maintaining accurate records of all transactions and activities. It emphasizes that proper record-keeping is essential for ensuring transparency and accountability in financial reporting.

2. The second part of the document outlines the various methods and techniques used to collect and analyze data. It highlights the need for rigorous data collection procedures and the use of appropriate statistical tools to interpret the results.

cell for use in studying protein trafficking and function. First, it forms tight junctions, which definitively segregate the basolateral and apical membranes. Second, the MDCK cell line fully polarizes by growth on permeable support. Third, its protein trafficking patterns appear to mimic those of native tissue for membrane proteins [13-15]. In order to visualize rOCT1 within MDCK, stable transfections of GFP-tagged rOCT1 fusion proteins were generated. GFP is a 27 kDa autofluorescent protein originally derived from the jelly fish, *Aequorea victoria*, which has been applied to investigate diverse problems in biology [16-19]. In the membrane protein fields, GFP-tagged transporters, channels, and receptors have been used to study the intracellular targeting, sorting mechanisms and pathways, and regulation of these proteins [5-8, 20-26].

One potential drawback of using GFP-transporter chimeras for these types of studies is that the GFP tag may affect the function of the protein being studied. In order to determine whether the GFP-tag altered the function of rOCT1, we expressed GFP-rOCT1 in *Xenopus laevis* oocytes and carried out *cis*-inhibition and *trans*-stimulation studies. Our data indicate that the GFP tag does not alter the function of rOCT1 (Figs. 1 & 2).

Our results clearly demonstrate that GFP-rOCT1 is localized within the lateral membranes of polarized MDCK cells (Figs. 4 & 5). Our results are in agreement with two recent studies in intact tissue demonstrating that rOCT1 is localized to the BLM [27,

1. The first part of the document is a list of names and addresses of the members of the committee who have been appointed to investigate the matter.

2. The second part of the document is a list of the names and addresses of the members of the committee who have been appointed to investigate the matter.

28]. rOCT1 has been shown previously to function as a potential sensitive organic cation transporter; it transports organic cations down the electrochemical gradient, which is also consistent with a BLM organic cation transporter [29]. These two pieces of information – lateral localization and potential sensitive transport – provide compelling evidence that rOCT1 functions in the secretory transport of drugs, transporting organic cations from the blood, across the BLM, and into tubule cells. As the basolateral membrane is generally considered to be a homogeneous membrane, it is interesting that GFP-rOCT1 appears to be localized only to the lateral membrane. The significance of this result is currently unclear; however, similar localization patterns have been found for other membrane transporters including MRP6 [30]. Although it is possible that GFP altered the localization of rOCT1, previous studies of GFP-tagged transporters, receptors, and channels, suggest that GFP does not alter localization of membrane proteins [5-7, 20, 31, 32].

Results from the functional studies in stably transfected MDCK cells confirm that GFP-rOCT1 is localized to the basolateral membrane (Fig. 3). ¹⁴C-TEA uptake across the BLM was greatly enhanced in MDCK cells expressing GFP-rOCT1 compared to GFP expressing cells or untransfected cells (Fig. 3). Furthermore, the potent organic cation transporter inhibitor quinidine potently blocked GFP-rOCT1 mediated uptake of ¹⁴C-

1. The first part of the document is a list of names and addresses of the members of the committee. The names are listed in alphabetical order, and the addresses are given in full. The list includes names such as Mr. J. H. Smith, Mr. W. D. Jones, and Mr. R. L. Brown.

2. The second part of the document is a list of the names and addresses of the members of the committee who were present at the meeting. The names are listed in alphabetical order, and the addresses are given in full. The list includes names such as Mr. J. H. Smith, Mr. W. D. Jones, and Mr. R. L. Brown.

TEA. In contrast, the apical uptake rates of ^{14}C -TEA were similar in all three cell lines (Fig. 3).

Tyrosine-based sorting sequences, such as YXXA (where Y is tyrosine, X is any amino acid, and A is any aliphatic amino acid), are thought to play a role in the targeting of membrane proteins to the BLM of polarized epithelial cells [15, 33-35]. rOCT1 has such a sequence, YLQV, in its carboxyl-terminus at amino acids 545 - 548. To investigate whether this sequence is required for the sorting of GFP-rOCT1 to the BLM of MDCK cells, a truncated protein termed GFP-rOCT1 Δ , which lacks amino acids 545 - 556, was stably expressed in MDCK cells. The results of the localization studies of GFP-rOCT1 Δ suggest that the YLQV sequence is not required for the BLM targeting of rOCT1 (Fig. 4B). This raises the interesting possibility that other targeting sequences are responsible for the BLM localization of rOCT1.

In summary, we created a stable transfection in MDCK of GFP-tagged rOCT1 and determined that GFP does not affect the function of rOCT1. GFP-rOCT1 was localized to the BLM of polarized MDCK cells by confocal microscopy and functional studies. A truncated form of GFP-rOCT1, GFP-rOCT1 Δ , which lacks a BLM-sorting sequence, also sorted to the BLM, suggesting that other sorting sequences are responsible for the membrane targeting of rOCT1. The cell culture model established in this study

1. The first part of the document discusses the importance of maintaining accurate records of all transactions and activities. It emphasizes that this is crucial for ensuring transparency and accountability in the organization's operations.

2. The second part of the document outlines the various methods and tools used to collect and analyze data. It highlights the need for consistent and reliable data collection processes to support effective decision-making.

can be further used to investigate the sorting pathways, post-transcriptional regulation, and function of rOCT1.

1. The first part of the document discusses the importance of maintaining accurate records of all transactions and activities. It emphasizes that this is crucial for ensuring transparency and accountability in the organization's operations.

2. The second part of the document outlines the various methods and tools used to collect and analyze data. It highlights the need for consistent data collection procedures and the use of advanced analytical techniques to derive meaningful insights from the data.

3. The third part of the document focuses on the implementation of data-driven decision-making processes. It provides a detailed overview of the steps involved in identifying key performance indicators (KPIs) and using data to inform strategic decisions.

4. The fourth part of the document discusses the challenges and risks associated with data management and analysis. It offers practical advice on how to mitigate these risks and ensure the integrity and security of the data.

5. The fifth part of the document concludes with a summary of the key findings and recommendations. It stresses the importance of ongoing monitoring and evaluation to ensure that the data-driven approach remains effective and relevant over time.

References

1. Zhang L, Brett CM and Giacomini KM, Role of organic cation transporters in drug absorption and elimination. *Annu Rev Pharmacol Toxicol* **38**: 431-460, 1998.
2. Pritchard JB and Miller DS, Mechanisms mediating renal secretion of organic anions and cations. *Physiol Rev* **73**(4): 765-796, 1993.
3. Pritchard JB and Miller DS, Renal secretion of organic anions and cations. *Kidney Int* **49**(6): 1649-1654, 1996.
4. Koepsell H, Gorboulev V and Arndt P, Molecular pharmacology of organic cation transporters in kidney. *J Membr Biol* **167**(2): 103-117, 1999.
5. Sai Y, Nies AT and Arias IM, Bile acid secretion and direct targeting of mdr1-green fluorescent protein from Golgi to the canalicular membrane in polarized WIF-B cells. *J Cell Sci* **112**(Pt 24): 4535-4545, 1999.
6. Tabuchi M, Yoshimori T, Yamaguchi K, Yoshida T and Kishi F, Human NRAMP2/DMT1, which mediates iron transport across endosomal membranes, is localized to late endosomes and lysosomes in HEP-2 cells. *J Biol Chem* **275**(29): 22220-22228, 2000.
7. Petersson J, Pattison J, Kruckeberg AL, Berden JA and Persson BL, Intracellular localization of an active green fluorescent protein-tagged Pho84 phosphate permease in *Saccharomyces cerevisiae*. *FEBS Lett* **462**(1-2): 37-42, 1999.

1. The first part of the document discusses the importance of maintaining accurate records of all transactions. It emphasizes that this is crucial for ensuring the integrity of the financial statements and for providing a clear audit trail.

2. The second part of the document outlines the specific procedures that should be followed when recording transactions. It details the steps from identifying the transaction to posting it to the appropriate ledger account.

8. Oatey PB, Van Weering DH, Dobson SP, Gould GW and Tavare JM, GLUT4 vesicle dynamics in living 3T3 L1 adipocytes visualized with green-fluorescent protein. *Biochem J* **327**(Pt 3): 637-642, 1997.
9. Jegla T and Salkoff L, A novel subunit for shal K⁺ channels radically alters activation and inactivation. *J Neurosci* **17**(1): 32-44, 1997.
10. Zhang L, Dresser MJ, Chun JK, Babbitt PC and Giacomini KM, Cloning and functional characterization of a rat renal organic cation transporter isoform (rOCT1A). *J Biol Chem* **272**(26): 16548-16554, 1997.
11. Mangravite LM, Lipschutz JH, Mostov KE and Giacomini KM, Localization of GFP-tagged concentrative nucleoside transporters, SPNT-GFP and CNT1-GFP, in Renal Polarized Epithelial Cells. *Am J Physiol* (in press).
12. Dresser MJ, Gray AT and Giacomini KM, Kinetic and selectivity differences between rodent, rabbit, and human organic cation transporters (OCT1). *J Pharmacol Exp Ther* **292**(3): 1146-1152, 2000.
13. Ahn J, Mundigl O, Muth TR, Rudnick G and Caplan MJ, Polarized expression of GABA transporters in Madin-Darby canine kidney cells and cultured hippocampal neurons. *J Biol Chem* **271**(12): 6917-6924, 1996.

1. The first part of the document is a list of names and addresses of the members of the committee. The names are listed in alphabetical order, and the addresses are given in full, including street, city, and state.

2. The second part of the document is a list of the names and addresses of the members of the committee who have been elected to the office of chairman. The names are listed in alphabetical order, and the addresses are given in full, including street, city, and state.

14. Gu HH, Ahn J, Caplan MJ, Blakely RD, Levey AI and Rudnick G, Cell-specific sorting of biogenic amine transporters expressed in epithelial cells. *J Biol Chem* **271**(30): 18100-18106, 1996.
15. Roush DL, Gottardi CJ, Naim HY, Roth MG and Caplan MJ, Tyrosine-based membrane protein sorting signals are differentially interpreted by polarized Madin-Darby canine kidney and LLC-PK1 epithelial cells. *J Biol Chem* **273**(41): 26862-26869, 1998.
16. Dickson RM, Cubitt AB, Tsien RY and Moerner WE, On/off blinking and switching behaviour of single molecules of green fluorescent protein. *Nature* **388**(6640): 355-358, 1997.
17. Li CJ, Heim R, Lu P, Pu Y, Tsien RY and Chang DC, Dynamic redistribution of calmodulin in HeLa cells during cell division as revealed by a GFP-calmodulin fusion protein technique. *J Cell Sci* **112**(Pt 10): 1567-1577, 1999.
18. Llopis J, McCaffery JM, Miyawaki A, Farquhar MG and Tsien RY, Measurement of cytosolic, mitochondrial, and Golgi pH in single living cells with green fluorescent proteins. *Proc Natl Acad Sci U S A* **95**(12): 6803-6808, 1998.
19. Miyawaki A, Llopis J, Heim R, McCaffery JM, Adams JA, Ikura M and Tsien RY, Fluorescent indicators for Ca²⁺ based on green fluorescent proteins and calmodulin. *Nature* **388**(6645): 882-887, 1997.

1. The first part of the document is a list of names and addresses of the members of the committee. The names are listed in alphabetical order, and the addresses are given in full, including the street name, city, and state.

2. The second part of the document is a list of the names and addresses of the members of the committee who have been elected to the office of chairman. The names are listed in alphabetical order, and the addresses are given in full, including the street name, city, and state.

20. Kallal L and Benovic JL, Using green fluorescent proteins to study G-protein-coupled receptor localization and trafficking. *Trends Pharmacol Sci* **21**(5): 175-180, 2000.
21. Makhina EN and Nichols CG, Independent trafficking of KATP channel subunits to the plasma membrane. *J Biol Chem* **273**(6): 3369-3374, 1998.
22. Sweet DH, Miller DS and Pritchard JB, Localization of an organic anion transporter-GFP fusion construct (rROAT1-GFP) in intact proximal tubules. *Am J Physiol* **276**(6 Pt 2): F864-873, 1999.
23. Barak LS, Ferguson SS, Zhang J and Caron MG, A beta-arrestin/green fluorescent protein biosensor for detecting G protein-coupled receptor activation. *J Biol Chem* **272**(44): 27497-27500, 1997.
24. Barak LS, Ferguson SS, Zhang J, Martenson C, Meyer T and Caron MG, Internal trafficking and surface mobility of a functionally intact beta2-adrenergic receptor-green fluorescent protein conjugate. *Mol Pharmacol* **51**(2): 177-184, 1997.
25. Grabner M, Dirksen RT and Beam KG, Tagging with green fluorescent protein reveals a distinct subcellular distribution of L-type and non-L-type Ca²⁺ channels expressed in dysgenic myotubes. *Proc Natl Acad Sci U S A* **95**(4): 1903-1908, 1998.



26. Kallal L, Gagnon AW, Penn RB and Benovic JL, Visualization of agonist-induced sequestration and down-regulation of a green fluorescent protein-tagged beta2-adrenergic receptor. *J Biol Chem* **273**(1): 322-328, 1998.
27. Urakami Y, Okuda M, Masuda S, Saito H and Inui KI, Functional characteristics and membrane localization of rat multispecific organic cation transporters, OCT1 and OCT2, mediating tubular secretion of cationic drugs. *J Pharmacol Exp Ther* **287**(2): 800-805, 1998.
28. Meyer-Wentrup F, Karbach U, Gorboulev V, Arndt P and Koepsell H, Membrane localization of the electrogenic cation transporter rOCT1 in rat liver. *Biochem Biophys Res Commun* **248**(3): 673-678, 1998.
29. Grundemann D, Gorboulev V, Gambaryan S, Veyhl M and Koepsell H, Drug excretion mediated by a new prototype of polyspecific transporter. *Nature* **372**(6506): 549-552, 1994.
30. Madon J, Hagenbuch B, Landmann L, Meier PJ and Stieger B, Transport function and hepatocellular localization of mrp6 in rat liver. *Mol Pharmacol* **57**(3): 634-641, 2000.
31. Feng X, Zhang J, Barak LS, Meyer T, Caron MG and Hannun YA, Visualization of dynamic trafficking of a protein kinase C betaII/green fluorescent protein conjugate

1
2
3
4
5
6
7
8
9
10
11
12
13
14
15
16
17
18
19
20
21
22
23
24
25
26
27
28
29
30
31
32
33
34
35
36
37
38
39
40
41
42
43
44
45
46
47
48
49
50
51
52
53
54
55
56
57
58
59
60
61
62
63
64
65
66
67
68
69
70
71
72
73
74
75
76
77
78
79
80
81
82
83
84
85
86
87
88
89
90
91
92
93
94
95
96
97
98
99
100

reveals differences in G protein-coupled receptor activation and desensitization. *J Biol Chem* **273**(17): 10755-10762, 1998.

32. Marshall J, Molloy R, Moss GW, Howe JR and Hughes TE, The jellyfish green fluorescent protein: a new tool for studying ion channel expression and function. *Neuron* **14**(2): 211-215, 1995.

33. Bonifacino JS and Dell'Angelica EC, Molecular bases for the recognition of tyrosine-based sorting signals. *J Cell Biol* **145**(5): 923-926, 1999.

34. Thomas DC, Brewer CB and Roth MG, Vesicular stomatitis virus glycoprotein contains a dominant cytoplasmic basolateral sorting signal critically dependent upon a tyrosine. *J Biol Chem* **268**(5): 3313-3320, 1993.

35. Thomas DC and Roth MG, The basolateral targeting signal in the cytoplasmic domain of glycoprotein G from vesicular stomatitis virus resembles a variety of intracellular targeting motifs related by primary sequence but having diverse targeting activities. *J Biol Chem* **269**(22): 15732-15739, 1994.

1. The first part of the document discusses the importance of maintaining accurate records of all transactions and activities. It emphasizes that proper record-keeping is essential for ensuring transparency and accountability in financial operations.

2. The second part of the document outlines the various methods and tools used to collect and analyze data. It highlights the need for consistent and reliable data sources to support informed decision-making and strategic planning.

3. The third part of the document focuses on the role of technology in modern financial management. It discusses how advanced software solutions can streamline processes, reduce errors, and provide real-time insights into financial performance.

4. The fourth part of the document addresses the challenges and risks associated with financial data management. It identifies common pitfalls such as data loss, security breaches, and compliance issues, and offers strategies to mitigate these risks.

5. The fifth part of the document concludes by summarizing the key findings and recommendations. It stresses the importance of ongoing monitoring and evaluation to ensure that financial management practices remain effective and up-to-date.

6. The sixth part of the document provides a detailed overview of the financial statements and their components. It explains how these statements are prepared and how they are used to assess the financial health and performance of an organization.

7. The seventh part of the document discusses the impact of external factors on financial performance. It examines how market conditions, regulatory changes, and economic trends can influence an organization's financial outcomes and provides strategies to navigate these challenges.

8. The eighth part of the document focuses on the role of financial management in achieving organizational goals. It highlights how sound financial practices can support growth, innovation, and long-term sustainability.

9. The ninth part of the document provides a final summary and key takeaways. It reiterates the importance of financial management and offers practical advice for implementing best practices in the field.

10. The tenth part of the document includes a list of references and sources used in the research. It provides a comprehensive list of books, articles, and other resources that are relevant to the topics discussed in the document.

CHAPTER 6

ARGININE 454 OF THE ORGANIC ANION TRANSPORTER, rOAT3, IS ESSENTIAL FOR *PARA*-AMINOHIPPURATE TRANSPORT

Introduction

Many therapeutic agents and toxic substances carry a net charge under physiological conditions, which hinders their simple diffusion across biological membranes. Organisms have evolved transporter proteins, which are involved in the absorption and disposition of charged organic compounds. Organic cation transporters (OCTs) and organic anion transporters (OATs) are major protein families which appear to have evolved from a common ancestral protein [1], but have different substrate and in particular charge selectivities. In general, OCTs transport positively charged organic molecules whereas OATs transport negatively charged organic ions [2-4]. During the past decade a number of mammalian OCT and OAT isoforms have been cloned and subsequently characterized in heterologous expression systems.

Three OCT isoforms (OCT1-3) [5-15] and four OAT isoforms (OAT1-4) [2, 16-23] have been cloned from several mammalian species. Hydropathy analyses of these transporters suggest that all share a common secondary structure composed of twelve membrane spanning alpha-helices, and all have two large loops: an extracellular loop

1. The first part of the document discusses the importance of maintaining accurate records of all transactions. It emphasizes that proper record-keeping is essential for the integrity of the financial system and for the ability to detect and prevent fraud.

2. The second part of the document outlines the specific procedures for recording transactions. It details the steps involved in the accounting process, from the initial recording of a transaction to the final preparation of financial statements.

between TMD 1 and TMD 2, and an intracellular loop between TMD 6 and TMD 7.

Although evolutionary analyses suggest that OCTs and OATs evolved from the same ancestral protein [1], OCTs share only about 30-40% sequence identity with OATs, and their substrate specificities are distinct. When overexpressed in either *Xenopus laevis* oocytes or mammalian cells, OCTs mediate the uptake of small, hydrophilic organic cations such as 1-methyl-4-phenylpyridinium (MPP⁺), tetraethylammonium (TEA), and guanidine, but do not interact with substrates of organic anion transporters such as *para*-aminohippurate (PAH) [3, 24-26]. Likewise, OATs have been shown to transport several organic anions, but do not, in general, interact with organic cations [2]. One notable exception to this charge specificity is rat organic anion transporter 3, rOAT3, an organic anion transporter cloned from rat brain [21], which transports the weak base cimetidine as well as the organic anions PAH, estrone sulfate, and ochratoxin A.

The goal of this study was to identify structural domains and amino acid residues involved in determining the substrate specificity of rOAT3. Our studies indicate that (a) the substrate recognition site resides in the carboxyl-terminal half of the transporters and that (b) arginine 454 of rOAT3 is an “anionic recognition site” essential for PAH but not for cimetidine transport. This is the first study to delineate molecular determinants involved in substrate and charge specificity of a member of the OAT family.

1. The first part of the document discusses the importance of maintaining accurate records of all transactions and activities. It emphasizes that this is crucial for ensuring transparency and accountability in the organization's operations.

2. The second part of the document outlines the various methods and tools used to collect and analyze data. It highlights the need for consistent data collection procedures and the use of advanced analytical techniques to derive meaningful insights from the data.

3. The third part of the document focuses on the role of technology in data management and analysis. It discusses how modern software solutions can streamline data collection, storage, and analysis processes, thereby improving efficiency and accuracy.

4. The fourth part of the document addresses the challenges associated with data management, such as data quality, security, and privacy. It provides strategies to mitigate these risks and ensure that the data remains reliable and secure throughout its lifecycle.

5. The fifth part of the document concludes by summarizing the key findings and recommendations. It stresses the importance of a data-driven approach in decision-making and the need for continuous monitoring and improvement of data management practices.

Materials and Methods

Construction of chimeric transporters and site-directed mutagenesis. The cDNAs of wildtype rOCT1 and rOAT3 (GenBank™ accession numbers X78855 and AB017446) were amplified by RT-PCR using an oligo (dT) primer (GIBCO BRL, Rockville, MD) with total RNA isolated from rat kidney and rat brain (Clontech, Palo Alto, CA), respectively. The primers for PCR were designed from the published sequences. The pair of primers for rOCT1 were 5'-aagcttcagccatgccaccgtggatgatg-3' (sense), 5'-ggatcctcaggtacttgaggacttgccctgttggac-3' (antisense); the pair of primers for rOAT3 were 5'-gaattcctgcctggtgccatgaccttccg-3' (sense), 5'-ggatccgggtcctatccaccagtcttcagcggg-3' (antisense). The cDNAs were subcloned into a pOX vector [27] under the control of a T3 promoter.

Genetics Computer Group software (Wisconsin Package, version 10.1) was used to align the nucleotides and the deduced amino acid sequences of rOCT1 and rOAT3. Secondary structure models were generated using the TOPO program (Johns, S. J. and Speth, R. C.) based on output from HMMTOP, an automatic server for predicting transmembrane helices and topology of proteins (<http://www.enzim.hu/hmmtop/>) [28]. A rOAT3/rOCT1 chimera consisting of TMD 1 to TMD 5 of rOAT3 and TMD 6 to TMD 12 of rOCT1 was obtained by equivalent exchange at an internal *Hae* II site (position 704 in rOAT3, and position 787 in rOCT1). That is, the fragment between *Hae* II and C-terminal of rOAT3 was switched with the same fragment of rOCT1. The sequence of the

1. The first part of the document discusses the importance of maintaining accurate records of all transactions and activities. It emphasizes that this is crucial for ensuring transparency and accountability in the organization's operations.

2. The second part of the document outlines the specific procedures and protocols that must be followed to ensure that all records are properly maintained and updated. It details the roles and responsibilities of various staff members in this process.

rOAT3/rOCT1 chimera was confirmed by automated DNA sequencing in the Biochemical Resource Center at the University of California at San Francisco.

The Stratagene Quikchange™ site-directed mutagenesis kit (La Jolla, CA) was used to construct mutant cDNA following the manufacturer's protocols. Mutants with single amino acid substitutions R454D (arginine 454 to aspartic acid) and R454N (arginine 454 to asparagine), were prepared using the cDNA of wildtype rOAT3 as the template. The sequences of R454D and R454N mutants were confirmed by directed DNA sequencing.

cRNA transcription and expression in Xenopus laevis oocytes. Oocytes were harvested from oocyte positive *Xenopus laevis* (Nasco, Fort Atkinson, WI) and were dissected and treated with collagenase D (Boehringer-Mannheim Biochemicals, Indianapolis, IN) in a calcium-free ORII solution as previously described [6]. Oocytes were maintained at 18 °C in modified Barth's medium. Healthy stage V and VI oocytes were injected with capped cRNA (1 µg/µl) that was transcribed *in vitro* with T3 polymerase (mCAP RNA Capping kit; Stratagene) from *Not I* linearized plasmids containing transporter cDNA inserts.

Tracer uptake measurements. Transport of radiolabeled compounds in oocytes was measured 3–4 days after cRNA injection as described previously [6]. The compounds were used at the following concentrations: ³H-MPP⁺ (1 µM) (82 Ci/mmol), ³H-cimetidine (1 µM) (15 Ci/mmol), ³H-PAH (10 µM) (4 Ci/mmol), ³H-estrone sulfate

1. The first part of the document is a list of names and addresses of the members of the committee. The names are listed in alphabetical order, and the addresses are given in full. The list includes names such as Mr. J. H. Smith, Mr. J. D. Jones, and Mr. W. E. Brown.

2. The second part of the document is a list of the names and addresses of the members of the committee who were present at the meeting. The names are listed in alphabetical order, and the addresses are given in full. The list includes names such as Mr. J. H. Smith, Mr. J. D. Jones, and Mr. W. E. Brown.

(150 nM) (53 Ci/mmol) and ³H-ochratoxin A (550 nM) (18 Ci/mmol). Uptake experiments were carried out as follows: groups of seven to nine oocytes were incubated in 100 µl Na⁺ buffer (100 mM NaCl, 2 mM KCl, 1 mM CaCl₂, 1 mM MgCl₂, 10 mM HEPES/Tris, pH 7.2) containing a radiolabeled compound at 25 °C for 1 h. Uptake was stopped by washing the oocytes 5 times with 3 ml of ice-cold Na⁺ buffer. Then the oocytes were lysed with 100 µl 10% sodium dodecyl sulfate (SDS) individually, and the amounts of radiolabeled substrates associated with each oocyte were determined by liquid scintillation counting. For inhibition studies, unlabeled compounds (1 mM) were added to the reaction solutions as needed.

Partition coefficient determinations. In order to study the lipophilicity of the organic anion substrates, the partition coefficient (log P) values were determined from an *n*-octanol and water system at pH 7.4 using methods similar to those previously reported [29, 30]. Briefly, 500 µl of radiolabeled PAH, ochratoxin A, and estrone sulfate water solutions were prepared. Then each organic anion aqueous solution was mixed with 500 µl *n*-octanol by vortexing. The aqueous and organic layers were then separated by centrifugation, and the concentrations of the organic anions in the two layers were determined by scintillation counting.

Data analysis. Values are expressed as mean ± standard error (S.E.) or mean ± standard deviation (S.D.) as indicated in the legends. Six to nine oocytes were used to

1. The first part of the document is a list of names and addresses of the members of the committee. The names are listed in alphabetical order, and the addresses are listed below each name. The list includes the names of the members of the committee, their titles, and their addresses.

2. The second part of the document is a list of the names and addresses of the members of the committee. The names are listed in alphabetical order, and the addresses are listed below each name. The list includes the names of the members of the committee, their titles, and their addresses.

generate a data point in each experiment. Due to the intrinsic variability in the expression levels of the transporters between batches of oocytes, the data shown in the figures are generally from a representative experiment performed in the same batch of oocytes. However, replicate experiments performed using oocytes from different donor frogs produced qualitatively similar results. The kinetic parameters (apparent K_m and V_{max}) were determined by nonlinear least squares fits of substrate/velocity profiles to the Michaelis-Menten equation using Kaleidagraph (Version 3.0, Synergy Software).

Materials. All unlabeled compounds (inhibitors) and buffer components were purchased from Sigma (St. Louis, MO). Radiolabeled compounds were from the following suppliers: ^3H -MPP⁺ (82 Ci/mmol) (Dupont-New England Nuclear, Boston, MA), ^3H -cimetidine (15 Ci/mmol) (Amersham Life Sciences, Arlington Heights, IL), ^3H -PAH (4 Ci/mmol), ^3H -estrone sulfate (53 Ci/mmol) and ^3H -ochratoxin A (18 Ci/mmol) (NEN Life Science Products, Boston, MA). Oligonucleotide primers were synthesized by GIBCO BRL (Rockville, MD).

Results

Substrate specificity of wildtype rOAT3. To characterize the substrate selectivity of the wildtype organic anion transporter, rOAT3, we studied the uptake of cimetidine, MPP⁺ and PAH. In oocytes expressing rOAT3, cimetidine and PAH uptakes were ~15-fold and ~10-fold enhanced respectively, over the uninjected oocytes (Fig. 1), similar to

1. The first part of the document discusses the importance of maintaining accurate records of all transactions. It emphasizes that proper record-keeping is essential for the integrity of the financial system and for the ability to detect and prevent fraud.

2. The second part of the document outlines the specific requirements for record-keeping, including the need to maintain original documents and to ensure that all records are properly indexed and filed. It also discusses the importance of regular audits and the need to keep records for a sufficient period of time.

the previous report from Kushihara and co-workers [21]. In contrast, MPP⁺ uptake was only ~2-fold enhanced in oocytes expressing rOAT3. We examined the nature of the interaction between cimetidine and PAH with rOAT3. Preliminary experiments showed that PAH uptake was inhibited by 1 mM cimetidine, and cimetidine uptake was inhibited by 1 mM PAH (data not shown). Further kinetics studies (Fig. 2) showed that PAH (500 μ M) significantly increased the apparent Michaelis-Menten constant (K_m) of cimetidine for rOAT3, from $40 \pm 6 \mu$ M to $289 \pm 92 \mu$ M, whereas the maximum uptake rate (V_{max}) did not change significantly (49 ± 2 pmol/oocyte/h to 63 ± 8 pmol/oocyte/h). A high concentration, 500 μ M, of PAH was used to ensure significant inhibition of cimetidine transport; the K_m value of PAH for rOAT3 is 65 μ M. Cimetidine (250 μ M) also significantly increased the K_m of PAH for rOAT3, from $278 \pm 48 \mu$ M to $1240 \pm 186 \mu$ M, whereas the V_{max} did not change significantly (72 ± 5 pmol/oocyte/h to 78 ± 7 pmol/oocyte/h) (data not shown). These data indicate that PAH inhibits cimetidine uptake by rOAT3 in a competitive manner and vice versa, suggesting that the two compounds share a common recognition site in rOAT3.

Substrate selectivity of a rOAT3/rOCT1 chimera. To determine the domains of rOAT3 and rOCT1 involved in substrate recognition and permeation, chimeric transporters of rOAT3 and rOCT1 were constructed and their substrate and charge selectivities were examined. A chimera rOAT3₁₋₅ : rOCT1₆₋₁₂ corresponding to the TMD

1. The first part of the document discusses the importance of maintaining accurate records of all transactions and activities. It emphasizes that this is crucial for ensuring transparency and accountability in the organization's operations.

2. The second part of the document outlines the various methods and tools used to collect and analyze data. It highlights the need for consistent data collection procedures and the use of advanced analytical techniques to derive meaningful insights from the data.

segments 1-5 of rOAT3 and 6-12 of rOCT1 was constructed from the wildtype transporters (Fig. 3). The splice site between rOAT3 and rOCT1 within the putative extracellular loop between TMD 5 and TMD 6 was selected to minimize the disruption of the TMDs. Functional studies (Fig. 4) indicated that rOAT3₁₋₅ : rOCT1₆₋₁₂ maintained similar functional characteristics as wildtype rOCT1. In particular, this chimera transported MPP⁺, a model organic cation, but not PAH, a model organic anion. These results suggest that the domains responsible for substrate recognition largely reside within the carboxyl-terminal half of the transporter. Chimeras with smaller regions of TMD 6-12 from rOCT1 were nonfunctional (data not shown). Therefore, to further delineate the molecular basis for substrate recognition and translocation by rOAT3, site-directed mutagenesis studies were undertaken.

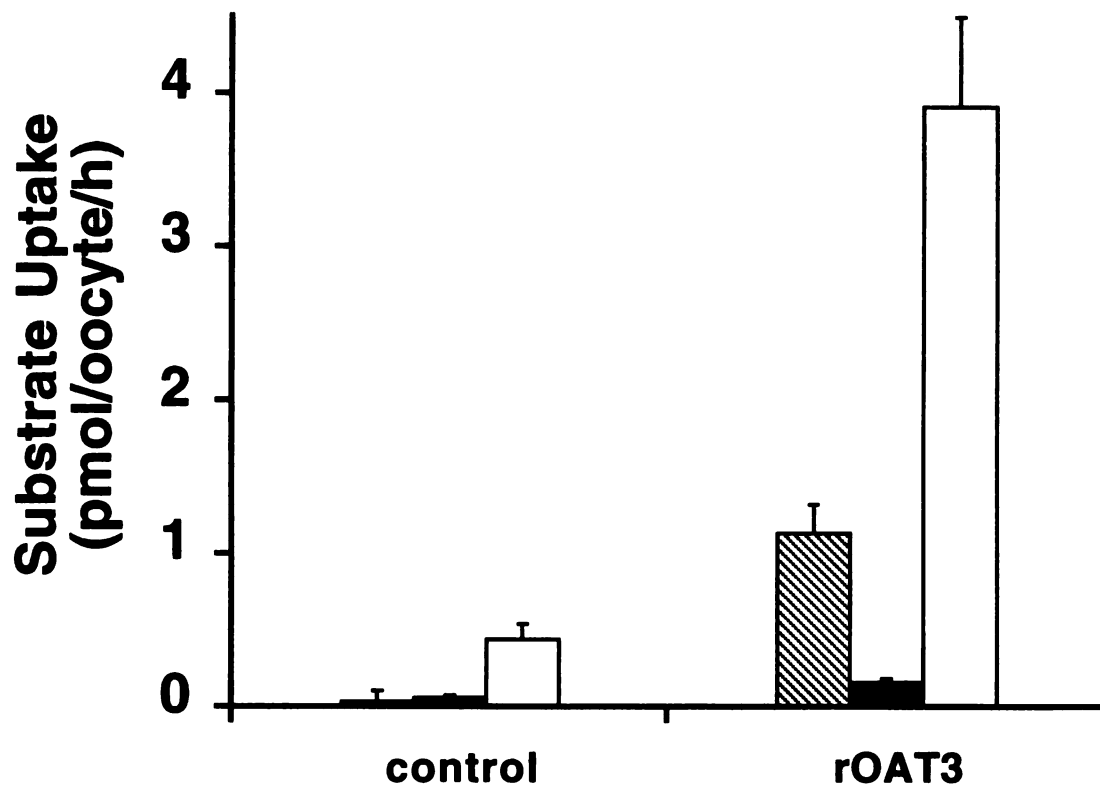


Figure 1. Substrate selectivity of wildtype rOAT3. The uptake of ³H-cimetidine (1 μM) (striped bar), MPP⁺ (1 μM) (dark bar), and PAH (10 μM) (open bar) was measured in uninjected (control) oocytes and in oocytes injected with 50 ng of rOAT3 cRNA. Data are mean values ± S.D. for 7-9 oocytes.

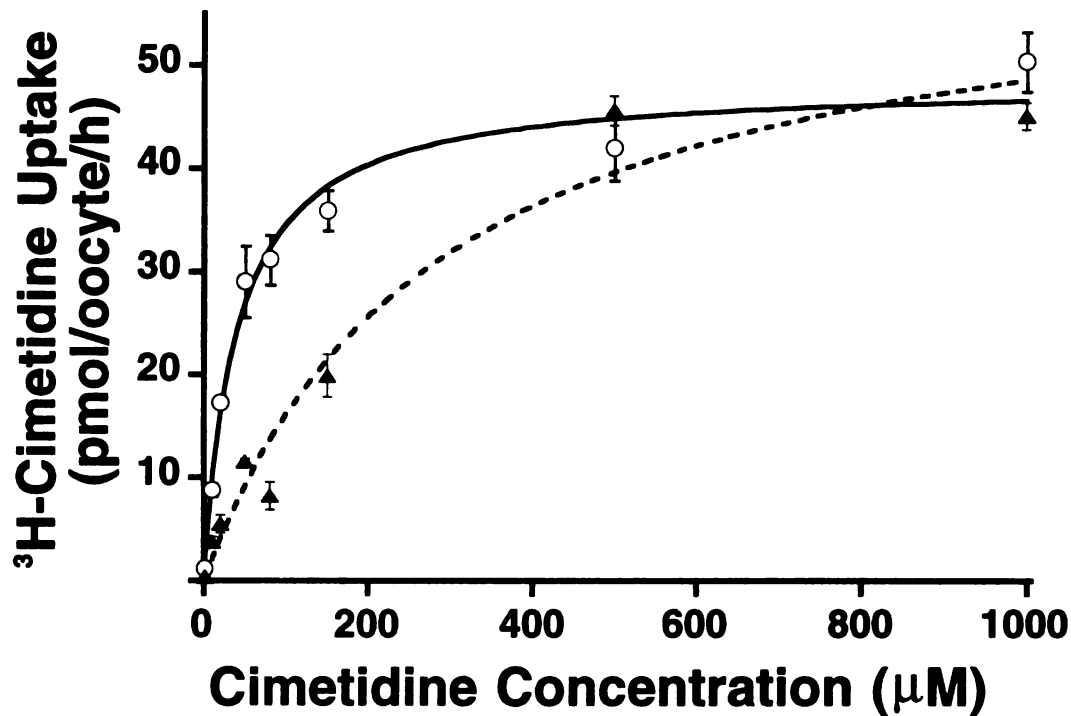


Figure 2. The inhibitory effect of PAH on rOAT3-mediated cimetidine transport. The rate of ^3H -cimetidine uptake at various concentrations was measured without (O) or with (▲) PAH (500 μM). Oocytes were injected with 50 ng of rOAT3 cRNA. In the absence of PAH, the apparent K_m and V_{max} values for cimetidine were $40 \pm 6 \mu\text{M}$ and 49 ± 2 pmol/oocyte/h. In the presence of 500 μM PAH, the apparent K_m and V_{max} values for cimetidine were $289 \pm 92 \mu\text{M}$ and 63 ± 8 pmol/oocyte/h. Kinetic parameters were determined by fitting the data to the Michaelis-Menten equation using a nonlinear least-squares regression-fitting program. rOAT3-mediated transport was obtained by subtracting the transport velocity in uninjected oocytes from that in rOAT3 expressing oocytes. Data are mean \pm S.E. for 6-8 oocytes.

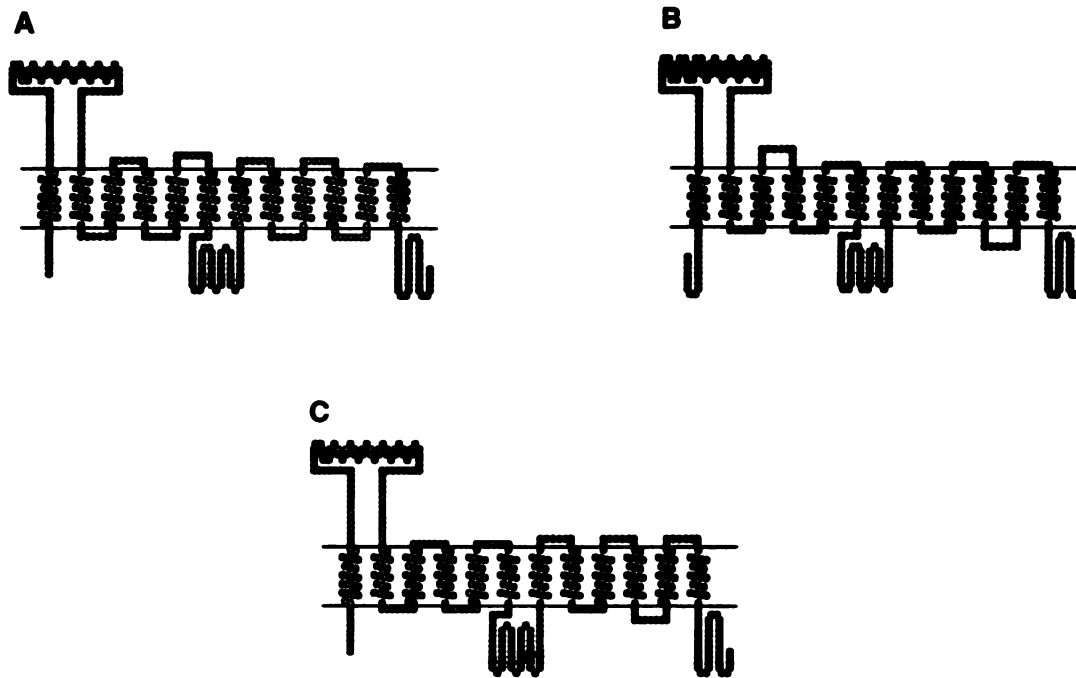


Figure 3. Secondary structure of wildtype and chimeric transporters. Wildtype rOAT3 (A) has 536 amino acids and wildtype rOCT1 (B) has 556 amino acids. Both wildtype transporters are predicted to have twelve transmembrane domains. The chimera (C) contains the first 235 amino acids of rOAT3, which corresponds to the first five transmembrane domains, and amino acids 263-556 of rOCT1, which corresponds to transmembrane domains six through twelve.

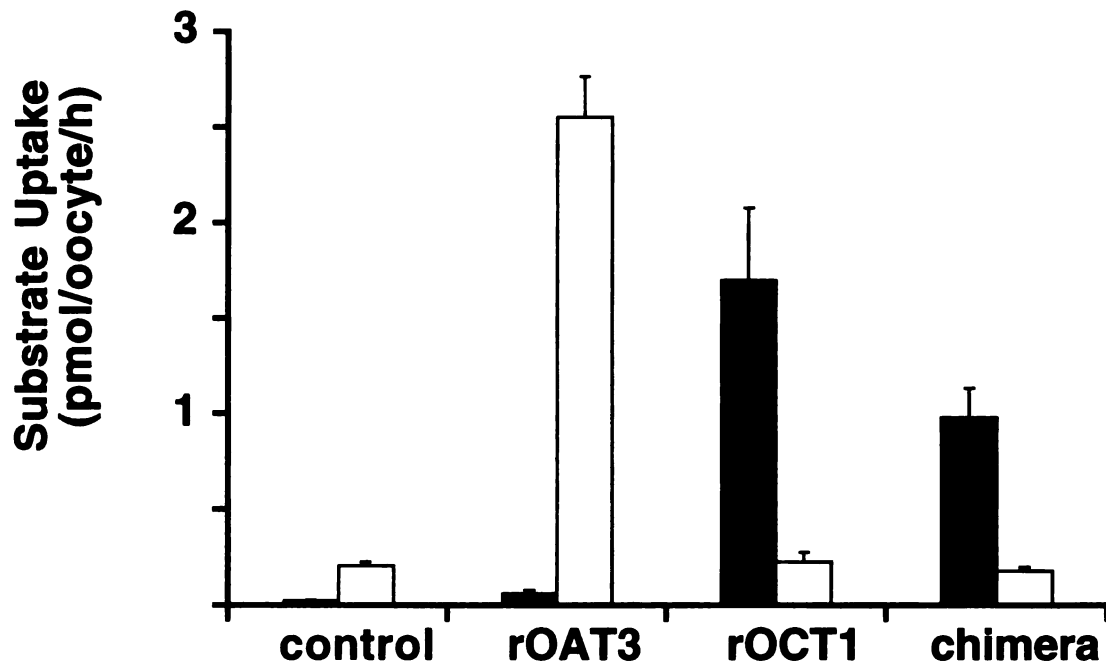


Figure 4. Substrate selectivity of wildtype and chimeric transporters. The uptake of ³H-MPP⁺ (1 μM) (dark bar) and ³H-PAH (10 μM) (open bar) was measured in uninjected (control) oocytes and in oocytes injected with 50 ng of rOAT3, rOCT1, or chimera (rOAT3₁₋₅ : rOCT1₆₋₁₂) cRNA. Data are mean values ± S.D. for 7-9 oocytes.

Functional characteristics of arginine 454 mutants of rOAT3. Alignments of OAT and OCT sequences were performed to identify candidate amino acid residues in TMD segments 6-12 that could be responsible for the substrate selectivity of rOAT3. For anion selectivity, we looked for conserved basic amino acids in OATs in these alignments. Sequence alignments showed that there are three conserved basic amino acids in the OAT family: histidine 34, lysine 370 and arginine 454. We hypothesized that arginine 454 may be critical in substrate discrimination between anions and cations because all OCTs have a conserved negatively charged aspartic acid residue at the corresponding position (Fig. 5). According to the predicted secondary structure of OATs, arginine 454 resides in the middle of TMD 11 of rOAT3 (Fig. 6). In order to investigate the functional significance of this residue, the mutants R454D and R454N, in which the positively charged arginine was replaced by the negatively charged aspartic acid or the uncharged polar amino acid, asparagine, respectively, were constructed. The uptakes of ³H-cimetidine, ³H-MPP⁺ and ³H-PAH in oocytes injected with rOAT3, R454D or R454N cRNA and uninjected (control) oocytes are shown in Fig. 7. ³H-PAH uptake was dramatically reduced in oocytes expressing the R454D and R454N mutants, which suggests arginine 454 is essential for PAH transport by rOAT3. In contrast, both wildtype rOAT3 and the mutants R454D and R454N maintained similar cimetidine uptake activities (more than 10-fold). Further kinetics studies of cimetidine transport demonstrated that the K_m of cimetidine is slightly changed in oocytes expressing R454N

and R454D ($69 \pm 10 \mu\text{M}$ and $103 \pm 12 \mu\text{M}$, respectively) compared to $48 \pm 8 \mu\text{M}$ in oocytes expressing the wildtype transporter. Therefore, arginine 454 appears to be essential for PAH but not for cimetidine transport by rOAT3.

Estrone sulfate and ochratoxin A are also substrates of rOAT3 [21], and our studies showed that arginine 454 is also important in the transport of these two substrates (Fig. 8). The uptakes of estrone sulfate and ochratoxin A were ~48 and ~32-fold enhanced in oocytes expressing wildtype rOAT3, and were only ~6 and ~5-fold enhanced in oocytes expressing R454D. Interestingly, estrone sulfate, ochratoxin A, the hydrophobic organic anions probenecid, indomethacin, and furosemide, as well as the hydrophobic organic cation, quinidine, potently inhibited ^3H -cimetidine uptake mediated by wildtype rOAT3 or R454D mutant (Fig. 9), indicating that for inhibition, these compounds do not require arginine 454. In contrast, the findings that PAH was not able to inhibit cimetidine transport by R454D suggest that arginine 454 is required for both recognition and translocation of PAH as well as its ability to inhibit cimetidine translocation.

```

rOAT3  MGISNVWARRVGSMIAPL-VK
rOAT2  LGLTALMGRLGASLARLAAL
rOAT1  LGMGSTMARVGSIVSPL-VS
mOAT1  LGMGSTMARVGSIVSPL-VS
hOAT1  MGMGSTMARVGSIVSPL-VS
hOAT3  MGVSNLWTRVGSMSVSPK-VK
hOAT4  MGPLILMSRQALPLLPLLY
rOCT1  MMVCSALCRLGGIIFTPFMVF
rOCT2  VLVCSSMCRIGGIITPFLVY
rOCT3  VSLCSGLCRFGGI IAPFLLF
hOCT1  VMVCSSLCRIGGIITPFIVF
hOCT2  VHICSSMCRIGGIITPFLVY
hOCT3  VSLCSGLCRFGGI IAPFLLF
mOCT1  MMVCSALCRLGGIIFTPFMVF
mOCT2  VLVCSSMCRIGGIIVTPFLVY
mOCT3  VSLCSGLCRFGGI IAPFLLF

```

Figure 5. Multiple alignments of transmembrane domain 11 of the OCTs and OATs. The conserved arginine in the OATs and the conserved aspartic acid in the OCTs are highlighted.

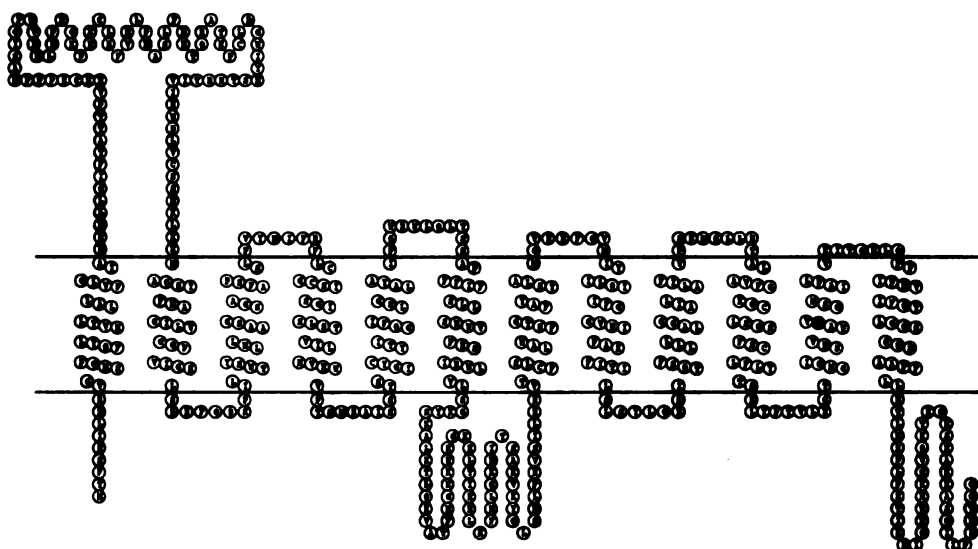


Figure 6. A model of the secondary structure of rOAT3 with arginine 454 in transmembrane domain 11 highlighted.

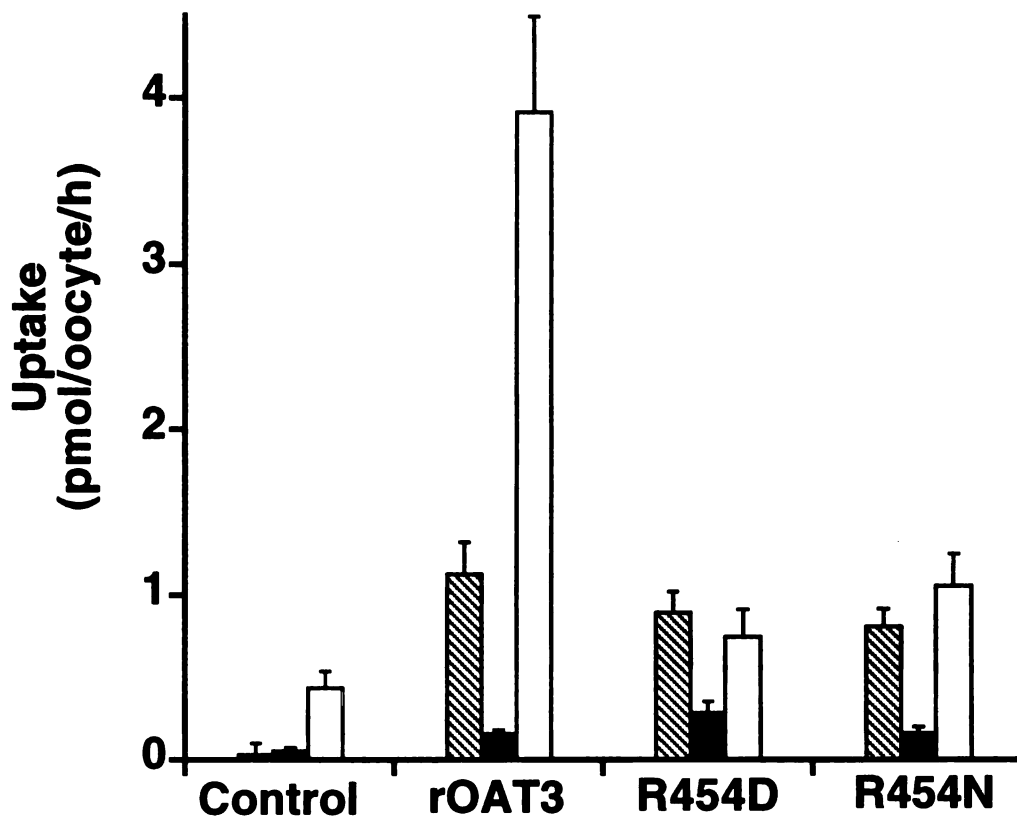


Figure 7. Substrate selectivity of wildtype rOAT3, and R454D and R454N mutants. The uptake of ³H-cimetidine (1 μM) (striped bar), MPP⁺ (1 μM) (dark bar), and PAH (10 μM) (open bar) was measured in uninjected (control) oocytes and in oocytes injected with 50 ng of the cRNA of rOAT3, R454D or R454N.

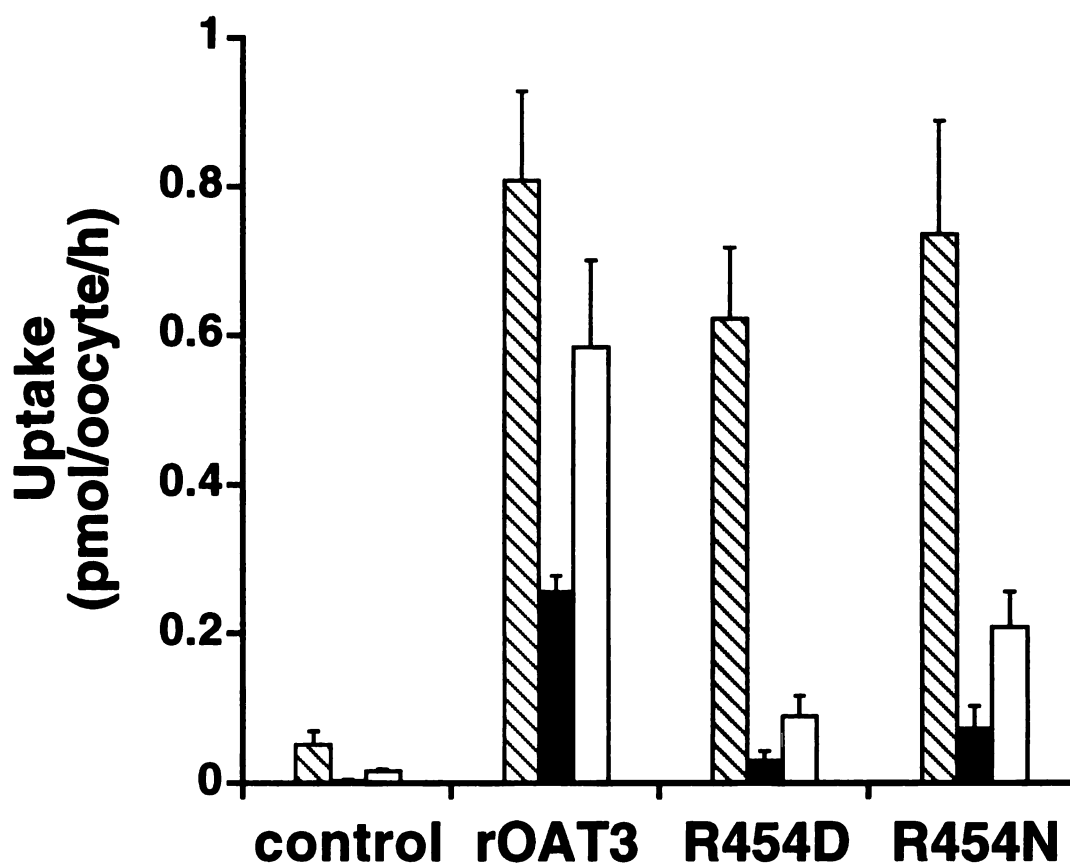


Figure 8. Substrate selectivity of wildtype rOAT3, and R454D and R454N mutants. The uptake of ³H-cimetidine (1 μM) (striped bar), estrone sulfate (150 nM) (dark bar), and ochratoxin A (550 nM) (open bar) was measured in uninjected (control) oocytes and in oocytes injected with 50 ng of the cRNA of rOAT3, R454D, or R454N. Data are mean values ± S.D. for 7-9 oocytes.

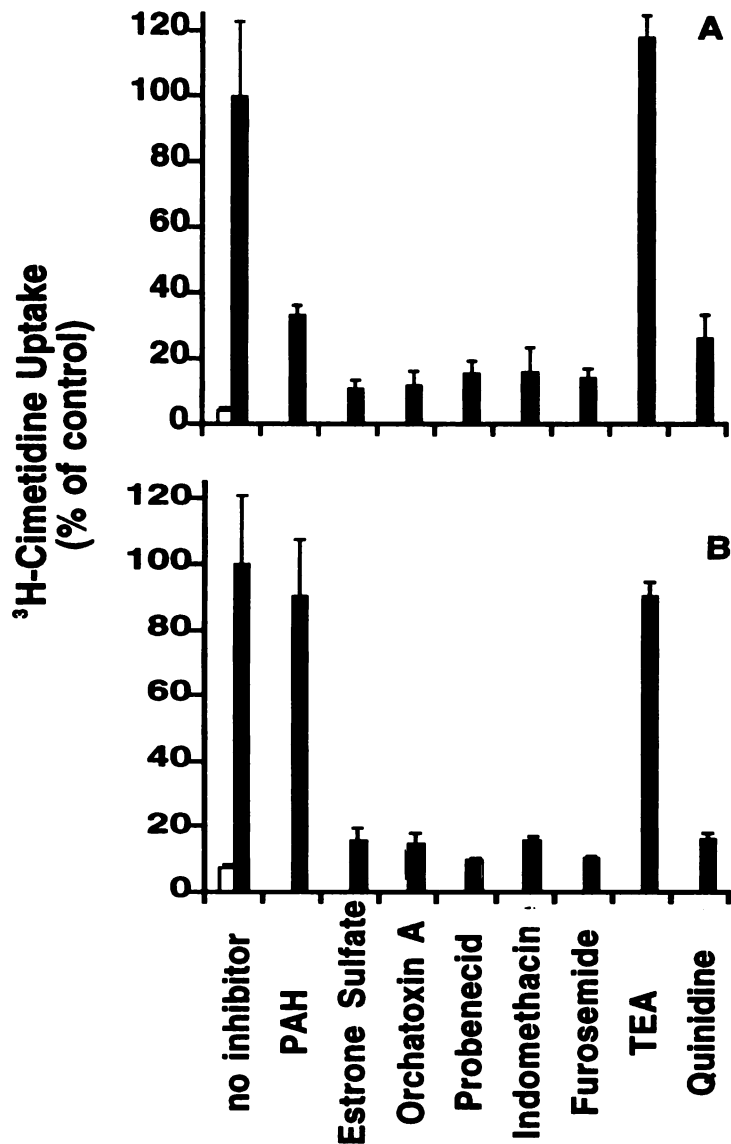


Figure 9. A) Inhibition of rOAT3 mediated ^3H -cimetidine ($1\ \mu\text{M}$) uptake by various compounds or B) R454D mediated ^3H -cimetidine ($1\ \mu\text{M}$) uptake by various compounds. Oocytes were injected with 50 ng of the cRNAs of rOAT3 or R454D. The concentration of inhibitors was 1 mM. The values are expressed as a percentage of rOAT3 or R454D mediated ^3H -labeled cimetidine uptake in the absence of inhibitor. Open bar indicates cimetidine uptake in water-injected control. Data are mean values \pm S.D. for 5-7 oocytes.

Discussion

Although the functional properties of OAT and OCT isoforms have been characterized, very little information regarding the molecular determinants of substrate recognition for these transporters is available [31, 32]. Standard chimera and mutagenesis studies have proven to be difficult when applied to OCTs because there is a considerable overlap in the substrate specificities of OCT isoforms and the same has been found for OAT isoforms. In this study we constructed novel chimeras of rOAT3 and rOCT1 to identify large structural domains of the transporters which are critical in substrate recognition. These studies were followed by site-directed mutagenesis to identify specific residues responsible for substrate recognition in the OAT family.

The first aim of this study was to determine the structural regions involved in substrate recognition by rOAT3 and rOCT1. Since all members of the OAT/OCT gene family share a common secondary structure and appear to have evolved from the same ancestral sequence [1], information regarding the large structural domains responsible for substrate recognition of one isoform might provide insights on the binding domains for other members of this gene family as well. To this end a number of rOAT3/rOCT1 chimeras were constructed and their transport properties assessed. Our results demonstrate that the substrate recognition site for these transporters resides primarily in the TMD 6-12 region (Fig. 4). Our attempts to construct a functional reciprocal chimera with regions containing TM 6-12 of rOAT3 transplanted into rOCT1, and construct

functional OAT/OCT chimeras with smaller OCT domains to identify more specific regions important in substrate recognition were unsuccessful. These chimeras were nonfunctional, possibly because they were not expressed in the plasma membrane due to trafficking or stability problems [33, 34]. Since further chimera studies were unsuccessful, site-directed mutagenesis studies of rOAT3 were performed to determine if conserved, basic amino acids are involved in rOAT3 transport function.

We hypothesized that basic amino acids, such as arginine, lysine, and histidine, which carry a positive charge, in the TMD 6-12 region could be important in rOAT3 transport function. In particular, basic residues may be important for interactions between rOAT3 and charged anionic compounds. Of the three conserved basic residues in the OATs (histidine 34, lysine 370 and arginine 454), only arginine 454 aligned with a conserved negatively charged residue (aspartic acid) at the corresponding position in the OCTs (Fig. 5). Recently, aspartate 475 of rOCT1, which is analogous in position to 454 in rOCT3 (Fig. 5), has been suggested to play a role in the transport function of rOCT1 [35]. Furthermore, arginine 454, located in TMD 11, is in the region (TMD 6-12) we observed to be important in substrate recognition (Fig. 4). Therefore, we hypothesized that this residue may be essential for the transport function of rOAT3.

In this study, we observed that the mutants, R454D and R454N, did not interact with or transport the organic anion PAH. In addition, transport of the organic anion substrates, estrone sulfate and ochratoxin A, was substantially reduced in oocytes

expressing the mutant transporters in comparison to the wildtype rOAT3 (Figs. 7 & 8). In contrast, the mutants retained the ability to transport the weak base, cimetidine (Fig. 7). Hydrophobic organic anions and cations inhibited cimetidine transport by both R454D and wildtype rOAT3, whereas the hydrophilic organic anion PAH, which competitively inhibited cimetidine transport by the wildtype rOAT3, did not inhibit cimetidine transport by the mutant. Collectively, the mutagenesis studies support the following major conclusions. First, arginine 454 plays a critical role in the recognition and translocation of the organic anion substrates, PAH, estrone sulfate and ochratoxin A by rOAT3. Second, arginine 454 is not essential for the transport of cimetidine by rOAT3. Third, arginine 454 is not essential for the inhibitory effects of hydrophobic organic anions and cations on cimetidine transport.

In the absence of three-dimensional information about the structure of organic cation and anion transporters, it is difficult to develop a detailed molecular model explaining these results. However, our data suggest that there is a distinct anion recognition site (i.e., arginine 454) for PAH and other organic anion substrates. When arginine 454 is replaced by aspartic acid, PAH does not interact with the mutant transporter since it requires this site. The transport of estrone sulfate and ochratoxin A by the mutant transporters is also severely impaired since these two anionic substrates require arginine 454 for optimal translocation. In contrast, the basic compound, cimetidine, does not require arginine 454 for interaction with the transporter and its

translocation is not impaired in oocytes expressing the mutant transporters, R454D and R454N. Hydrophobic organic anions and cations such as probenecid, indomethacin, furosemide and quinidine as well as organic anion substrates, estrone sulfate and ochratoxin A, still potently inhibit cimetidine transport by the R454D mutant suggesting that these compounds interact with a site which is distinct from arginine 454. In contrast, PAH does not inhibit cimetidine transport by the mutant transporter. We suggest that this difference may be due to variances in hydrophobicity: PAH is considerably more hydrophilic than estrone sulfate or ochratoxin A ($\log P_{\text{PAH}} = -2.18$; $\log P_{\text{estrone sulfate}} = 0.0389$; $\log P_{\text{ochratoxin A}} = 0.0584$). Our observations thus demonstrate that arginine 454 is essential for the translocation of organic anion substrates of rOAT3 and also indicate the existence of other sites involved in transport of cimetidine and interaction with hydrophobic compounds.

This is the first report of the molecular basis for transporter specificity of an OAT, which along with OCTs, are important determinants of the pharmacokinetic properties of drugs. A better understanding of the binding sites of these transporters may lead to the rational design of therapeutic agents with optimized pharmacokinetic profiles.

References

1. Koepsell H, Gorboulev V and Arndt P, Molecular pharmacology of organic cation transporters in kidney. *J Membr Biol* **167**(2): 103-117, 1999.
2. Sweet DH, Wolff NA and Pritchard JB, Expression cloning and characterization of ROAT1. The basolateral organic anion transporter in rat kidney. *J Biol Chem* **272**(48): 30088-30095, 1997.
3. Okuda M, Urakami Y, Saito H and Inui K, Molecular mechanisms of organic cation transport in OCT2-expressing *Xenopus* oocytes. *Biochim Biophys Acta* **1417**(2): 224-231, 1999.
4. Zhang L, Schaner ME and Giacomini KM, Functional characterization of an organic cation transporter (hOCT1) in a transiently transfected human cell line (HeLa). *J Pharmacol Exp Ther* **286**(1): 354-361, 1998.
5. Schweifer N and Barlow DP, The Lx1 gene maps to mouse chromosome 17 and codes for a protein that is homologous to glucose and polyspecific transmembrane transporters. *Mamm Genome* **7**(10): 735-740, 1996.
6. Zhang L, Dresser MJ, Chun JK, Babbitt PC and Giacomini KM, Cloning and functional characterization of a rat renal organic cation transporter isoform (rOCT1A). *J Biol Chem* **272**(26): 16548-16554, 1997.

7. Zhang L, Dresser MJ, Gray AT, Yost SC, Terashita S and Giacomini KM, Cloning and functional expression of a human liver organic cation transporter. *Mol Pharmacol* **51**(6): 913-921, 1997.
8. Terashita S, Dresser MJ, Zhang L, Gray AT, Yost SC and Giacomini KM, Molecular cloning and functional expression of a rabbit renal organic cation transporter. *Biochim Biophys Acta* **1369**(1): 1-6, 1998.
9. Grundemann D, Babin-Ebell J, Martel F, Ording N, Schmidt A and Schomig E, Primary structure and functional expression of the apical organic cation transporter from kidney epithelial LLC-PK1 cells. *J Biol Chem* **272**(16): 10408-10413, 1997.
10. Verhaagh S, Schweifer N, Barlow DP and Zwart R, Cloning of the mouse and human solute carrier 22a3 (Slc22a3/SLC22A3) identifies a conserved cluster of three organic cation transporters on mouse chromosome 17 and human 6q26-q27. *Genomics* **55**(2): 209-218, 1999.
11. Grundemann D, Gorboulev V, Gambaryan S, Veyhl M and Koepsell H, Drug excretion mediated by a new prototype of polyspecific transporter. *Nature* **372**(6506): 549-552, 1994.
12. Kekuda R, Prasad PD, Wu X, Wang H, Fei YJ, Leibach FH and Ganapathy V, Cloning and functional characterization of a potential-sensitive, polyspecific organic cation transporter (OCT3) most abundantly expressed in placenta. *J Biol Chem* **273**(26): 15971-15979, 1998.

13. Gorboulev V, Ulzheimer JC, Akhoundova A, Ulzheimer-Teuber I, Karbach U, Quester S, Baumann C, Lang F, Busch AE and Koepsell H, Cloning and characterization of two human polyspecific organic cation transporters. *DNA Cell Biol* **16(7)**: 871-881, 1997.
14. Okuda M, Saito H, Urakami Y, Takano M and Inui K, cDNA cloning and functional expression of a novel rat kidney organic cation transporter, OCT2. *Biochem Biophys Res Commun* **224(2)**: 500-507, 1996.
15. Grundemann D, Schechinger B, Rappold GA and Schomig E, Molecular identification of the corticosterone-sensitive extraneuronal catecholamine transporter. *Nat Neurosci* **1(5)**: 349-351, 1998.
16. Lu R, Chan BS and Schuster VL, Cloning of the human kidney PAH transporter: narrow substrate specificity and regulation by protein kinase C. *Am J Physiol* **276(2 Pt 2)**: F295-F303, 1999.
17. Cihlar T, Lin DC, Pritchard JB, Fuller MD, Mendel DB and Sweet DH, The antiviral nucleotide analogs cidofovir and adefovir are novel substrates for human and rat renal organic anion transporter 1. *Mol Pharmacol* **56(3)**: 570-580, 1999.
18. Sekine T, Cha SH, Tsuda M, Apiwattanakul N, Nakajima N, Kanai Y and Endou H, Identification of multispecific organic anion transporter 2 expressed predominantly in the liver. *FEBS Lett* **429(2)**: 179-182, 1998.

19. Sekine T, Watanabe N, Hosoyamada M, Kanai Y and Endou H, Expression cloning and characterization of a novel multispecific organic anion transporter. *J Biol Chem* **272**(30): 18526-18529, 1997.
20. Simonson GD, Vincent AC, Roberg KJ, Huang Y and Iwanij V, Molecular cloning and characterization of a novel liver-specific transport protein. *J Cell Sci* **107**(Pt 4): 1065-1072, 1994.
21. Kusuhara H, Sekine T, Utsunomiya-Tate N, Tsuda M, Kojima R, Cha SH, Sugiyama Y, Kanai Y and Endou H, Molecular cloning and characterization of a new multispecific organic anion transporter from rat brain. *J Biol Chem* **274**(19): 13675-13680, 1999.
22. Race JE, Grassl SM, Williams WJ and Holtzman EJ, Molecular cloning and characterization of two novel human renal organic anion transporters (hOAT1 and hOAT3). *Biochem Biophys Res Commun* **255**(2): 508-514, 1999.
23. Cha SH, Sekine T, Kusuhara H, Yu E, Kim JY, Kim DK, Sugiyama Y, Kanai Y and Endou H, Molecular cloning and characterization of multispecific organic anion transporter 4 expressed in the placenta. *J Biol Chem* **275**(6): 4507-4512, 2000.
24. Zhang L, Brett CM and Giacomini KM, Role of organic cation transporters in drug absorption and elimination. *Annu Rev Pharmacol Toxicol* **38**: 431-460, 1998.

25. Dresser MJ, Gray AT and Giacomini KM, Kinetic and selectivity differences between rodent, rabbit, and human organic cation transporters (OCT1). *J Pharmacol Exp Ther* **292**(3): 1146-1152, 2000.
26. Ullrich KJ, Renal transporters for organic anions and organic cations. Structural requirements for substrates. *J Membr Biol* **158**(2): 95-107, 1997.
27. Jegla T and Salkoff L, A novel subunit for shal K⁺ channels radically alters activation and inactivation. *J Neurosci* **17**(1): 32-44, 1997.
28. Tusnady GE and Simon I, Principles governing amino acid composition of integral membrane proteins: application to topology prediction. *J Mol Biol* **283**(2): 489-506, 1998.
29. Zhang L, Gorset W, Dresser MJ and Giacomini KM, The interaction of n-tetraalkylammonium compounds with a human organic cation transporter, hOCT1. *J Pharmacol Exp Ther* **288**(3): 1192-1198, 1999.
30. Neef C and Meijer DK, Structure-pharmacokinetics relationship of quaternary ammonium compounds. Correlation of physicochemical and pharmacokinetic parameters. *Naunyn Schmiedebergs Arch Pharmacol* **328**(2): 111-118, 1984.
31. Burckhardt G and Wolff NA, Structure of renal organic anion and cation transporters. *Am J Physiol Renal Physiol* **278**(6): F853-866, 2000.
32. Koepsell H, Organic cation transporters in intestine, kidney, liver, and brain. *Annu Rev Physiol* **60**: 243-266, 1998.

33. Buck KJ and Amara SG, Chimeric dopamine-norepinephrine transporters delineate structural domains influencing selectivity for catecholamines and 1-methyl-4-phenylpyridinium. *Proc Natl Acad Sci U S A* **91**(26): 12584-12588, 1994.
34. Zhang X, Collins KI and Greenberger LM, Functional evidence that transmembrane 12 and the loop between transmembrane 11 and 12 form part of the drug-binding domain in P-glycoprotein encoded by MDR1. *J Biol Chem* **270**(10): 5441-5448, 1995.
35. Gorboulev V, Volk C, Arndt P, Akhoundova A and Koepsell H, Selectivity of the polyspecific cation transporter rOCT1 is changed by mutation of aspartate 475 to glutamate. *Mol Pharmacol* **56**(6): 1254-1261, 1999.

CHAPTER 7

SUMMARY, CONCLUSIONS AND FUTURE DIRECTIONS*

Introduction

Renal excretion is one of the major routes of drug elimination in the body. Most drugs are eliminated to some extent by the kidneys and for many drugs the kidney is the primary organ of elimination. As previously reviewed, the importance of renal transport systems in drug elimination has been established for many xenobiotics, including clinically used drugs [1-3]. Organic anion and organic cation transport systems are two of the major drug transport systems in the mammalian kidney. During the past two decades, organic cation and organic anion transport mechanisms have been studied extensively using various tissue and membrane preparations and cell culture models. These studies helped define transport mechanisms and, to a limited degree, substrate specificities [2, 4, 5]. Since I started my dissertation research, many of the transporters underlying these transport systems have been cloned, opening up new and exciting areas of research in the pharmaceutical sciences. To date, more than fourteen distinct renal organic anion transporters and organic cation transporters have been cloned and found to belong to one of the following gene families: OAT, OAT-K/oatp, OCT, or OCTN. Although more work is needed to fully decipher the roles of these transporters in renal

*Draft version to be published in the forthcoming *Journal of Pharmaceutical Sciences*. Reprinted by permission of Wiley-Liss, Inc., a subsidiary of John Wiley & Sons, Inc. Permission from the publisher is included in the "Acknowledgments".

drug elimination, significant progress has been made in the initial molecular and cellular characterization of these transporters. In this conclusion chapter, I summarize and evaluate the progress made in the cloning and characterization of organic anion transporters and organic cation transporters and consider their roles in renal drug elimination. Three critical areas are discussed: transport mechanism, intracellular localization, and drug-transporter interactions. In addition, other topics will be briefly discussed. The reader is referred to other recent reviews for more information on additional aspects of organic cation transporters and organic anion transporters [6-11].

Transporters Involved in the Renal Elimination of Organic Cations

Background and significance. Renal secretion is a major pathway of elimination for many clinically used organic cations. For example, amantadine, cimetidine, pindolol, and quinidine are all secreted by the kidneys [1]. In addition, transport of toxic organic cations (e.g. paraquat) into the kidneys may lead to nephrotoxicity. Over the past several decades, the mechanisms of renal organic cation transport have been investigated using a number of different tissue preparations and cell culture models [2, 4, 6]. From these studies it was determined that multiple organic cation transporters exist in the BLM and BBM of the kidney. These transporters are found primarily in the proximal tubule and, to a lesser degree, in the distal tubule. At the BLM, several potential-sensitive organic cation transport mechanisms have been described [2, 4]. Thus, organic cations are transported across the BLM down the electrochemical gradient. In contrast, at the BBM, organic cation-proton antiport mechanisms have been described [2, 4]. In this case, organic cations are transported from inside the cell into the tubule lumen in exchange for a luminal proton. These two systems working together result in net secretion of organic cations from the blood to the tubule fluid. Recently, a number of the transporters involved in these processes have been cloned.

To date, five distinct organic cation transporter isoforms have been isolated. Based on sequence analysis and functional data, these transporters fall into one of two gene families: OCT or OCTN [6, 8, 9, 11]. The transporter isoforms have been termed OCT1, OCT2, OCT3, OCTN1 and OCTN2. They are all expressed to some degree in the kidney and are likely to play a role in the renal elimination of cationic drugs. In order to understand the role of these transporters in renal drug elimination, their transport mechanisms, membrane localizations, and substrate/inhibitor selectivities need to be determined. Below we summarize this information for each of the organic cation transporter isoforms.

OCT1: *1. Molecular characteristics.* The first organic cation transporter, rOCT1, was cloned by Grundemann and co-workers in 1994 from a rat kidney cDNA library using expression cloning techniques in *Xenopus laevis* oocytes [12]. rOCT1 is 554 amino acids in length and is predicted to have 12 TMDs. Following the cloning of rOCT1, the rabbit, mouse and human orthologs were cloned using homology-based cloning methods [13-16]. These transporters have been termed rbOCT1, mOCT1, and hOCT1. The human and rabbit orthologs are approximately 80% identical to rOCT1, whereas mOCT1 shares higher sequence identity with rOCT1. In addition, a novel splice variant of rOCT1, termed rOCT1A, was later cloned by Zhang and co-workers [17]. This variant is virtually identical to rOCT1 with the exception of a 104 base pair deletion at the 5-prime end of the cDNA. *2. Tissue distribution and localization.* Much work has been done to characterize the tissue expression patterns and membrane localization of OCT1. Northern blot analyses and in situ hybridizations show that mRNA transcripts of rOCT1 are primarily expressed in the liver (hepatocytes) and kidney (in the proximal tubules) and are expressed at lower levels in the small intestine (enterocytes) (Table 1) [12, 18]. In the kidney, rOCT1 has been further localized to the BLM, while in the liver, it has been localized to the sinusoidal membrane of the hepatocyte (Table 3) [19, 20].

Although the rabbit, mouse, and human homologs of OCT1 have not yet been localized to particular membranes, their tissue expression patterns have been determined and are, in general, similar to those of rOCT1 (Table 1). However, the relative amounts of each isoform may vary from one tissue to another. Both rbOCT1 and hOCT1 are expressed most strongly in the liver and have lower levels of expression in other tissues, including the kidney and intestine (as well as the muscle and heart, for hOCT1) [14-16]. Thus, overall, OCT1 has a wide tissue distribution with primary expression in the kidney and liver. *3. Functional characteristics.* All of the OCT1 orthologs have been shown to take up the prototypical organic cations TEA and/or MPP⁺. Furthermore, studies in *X. laevis* oocytes have shown that transport of these organic cations by rOCT1, rbOCT1, and hOCT1 is sensitive to membrane potential, a characteristic of the renal BLM organic cation transporter [6, 12, 14, 15]. In addition, transport of substrates by rOCT1 is significantly inhibited by numerous drugs, including procainamide, desipramine, clonidine, araC, and AZT (Table 4). Many drugs also significantly inhibit hOCT1. A recent study has shown that hydrophobicity is a major determinant of drug interactions with hOCT1 (Table 4) [21, 22]. In general, the K_i values of most organic cations are higher for hOCT1 than for rOCT1, suggesting that hOCT1 may have a lower affinity for organic cations [21, 23, Chapter 3]. In a study comparing the kinetics and substrate selectivities among the cloned OCT1 transporters from mouse, rat, rabbit and human, significant differences were found among these four transporters, which suggests that OCT1 may be responsible, in part, for interspecies differences in the absorption, distribution, and elimination of organic cations [23, Chapter 3].

OCT2: *1. Molecular characteristics.* Soon after the cloning of rOCT1, rOCT2 was cloned from a rat kidney cDNA library [24]. Subsequently, the pig, mouse, and human orthologs were cloned and termed pOCT2, mOCT2, and hOCT2 [16, 25, 26]. The OCT2 cDNAs are predicted to encode proteins of 593, 555, 554 and 555 amino acids in length

for the rat, human, pig and murine homologs, respectively. All of the OCT2 proteins are predicted to consist of 12 TMDs. *2. Tissue distribution and localization.* Unlike OCT1, which has a wide tissue distribution, OCT2 is expressed predominantly in the kidney and to a lesser extent in the brain (Table 1) [16, 24-28]. In situ studies demonstrate rOCT2 expression exclusively in the S3 segment of the proximal tubule [27]. The membrane localization of OCT2 has been extensively studied, but many discordant results are found in the literature (Table 3) [8, 16, 19, 25, 29]. However, detailed mechanistic studies in stably transfected MDCK cells suggest that rOCT2 is a potential sensitive transporter, which is consistent with a renal BLM OCT, and not a BBM organic cation:proton exchanger [29]. *3. Functional characteristics.* TEA is a substrate of rOCT2, hOCT2, and pOCT2. rOCT2, like OCT1, is a potential-sensitive transporter [29]. The OCT2 class of transporters appears to interact with many of the same organic cation drugs as OCT1, including procainamide, desipramine, and cimetidine (Table 4). In fact, inhibition of TEA uptake in stably transfected MDCK cells indicates that rOCT1 and rOCT2 have similar affinities for many organic cations [19]. But more work is needed to determine if the specificities of these two isoforms completely overlap - a recent study has shown that there are differences between rOCT1 and rOCT2 specificities, as least for some compounds [30]. Studies in rOCT2 expressing NIH3T3 cells have shown that the anti-cancer drug cisplatin inhibits TEA uptake with a K_i of 925 μM , but other anti-tumor agents such as daunomycin and vinblastine did not interact with rOCT2 [31].

OCT3: *1. Molecular characteristics.* OCT3 was first cloned from a rat placental cDNA library [32]. Subsequently, the human and mouse orthologs were cloned [33-35]. OCT3 from rat and mouse each have 551 amino acid residues, whereas the human has 556; all three transporters are predicted to consist of 12 TMDs. At the protein level, rOCT3 shares 95% and 83% identity with mOCT3 and hOCT3 (EMT), respectively. The OCT3 proteins share ~ 50% identity with the other two OCT isoforms. *2. Tissue distribution*

and localization. Unlike OCT1 and OCT2, OCT3 is expressed at high levels in the placenta. In addition, Northern blot analysis demonstrates that rOCT3 is also expressed in the kidney, intestine, heart, and brain (Table 1) [32]. Studies using in situ hybridization have further localized rOCT3 to the hippocampus, cerebellum, and cerebral cortex regions of the rat brain and to the cortex of the mouse kidney [18, 35]. While the expression pattern of mOCT3 is similar to that of rOCT3, hOCT3 has a much broader tissue distribution [34]. Northern blot analysis has shown that in addition to the placenta, hOCT3 is highly expressed in the aorta, liver, prostate, salivary glands, adrenal glands, skeletal muscle, and fetal lung [34]. Intracellular localization of OCT3 has not yet been determined in any species. **3. Functional characteristics.** Studies in a transfected human retinal pigment epithelial cell line (HRPE) and *Xenopus laevis* oocytes have demonstrated OCT3-mediated transport of the prototypical organic cations TEA, guanidine, and MPP⁺ [32, 35]. Efflux studies in HeLa cells as well as electrophysiology studies in oocytes have shown that TEA transport via rOCT3 is H⁺-independent and membrane potential dependent - the functional characteristic of a renal BLM organic cation transporter [32]. Studies suggest that rOCT3 interacts with dopamine, the neurotoxins amphetamine and methamphetamine, as well as a variety of steroids (Table 4) [18]. TEA uptake in rOCT3-transfected HRPE cells shows marked inhibition by the steroids beta-estradiol, corticosterone, deoxycorticosterone, papaverine, testosterone, and progesterone. Uptake studies have shown that hOCT3 transports a variety of organic cations, including catecholamines [33, 35].

OCTN1: **1. Molecular characteristics.** The first member of a new subfamily of organic cation transporters (OCTNs), termed hOCTN1, was cloned from human fetal liver by Tamai and co-workers in 1997 [36]. Recently, rOCTN1, the rat ortholog, was cloned from placenta [37]. hOCTN1 and rOCTN1 consist of 551 and 553 amino acids, respectively, and are predicted to have 12 TMDs. These two OCTN1 orthologs share

85% identity at the protein level; in addition, they share ~ 70% identity with OCTN2 and ~ 30% identity with the OCT family. hOCTN1 is unique among the organic cation transporters in that it has a nucleotide binding site sequence motif [36].

2. Tissue distribution and localization. Initial studies suggest that hOCTN1 has a broad tissue distribution. Northern blot analysis shows strong mRNA expression of hOCTN1 in fetal kidney, lung, and liver as well as adult kidney, trachea, and bone marrow (Table 1) [36]. Weak signals are detected in many other tissues. In addition, hOCTN1 mRNA transcripts are detected in several human cancer cell lines. rOCTN1 is also expressed in numerous tissues: intestine, liver, kidney, brain, thymus, lung, heart, spleen, and skin (Table 1) [37]. Intracellular localization studies have not yet been performed for either transporter.

3. Functional characteristics. rOCTN1 and hOCTN1 accept the prototypical organic cation, TEA, as a substrate [36, 37]. However, kinetic studies in transfected cells and *X. laevis* oocytes have shown that their affinity for TEA is lower than that of the OCT family (Table 4) [36, 38]. TEA efflux from transfected HEK 293 cells expressing hOCTN1 is stimulated by acidic pH in the external media, suggesting that transport via hOCTN1 might be driven by a H⁺ gradient, the driving force of the renal BBM transport system [38]. hOCTN1 transports not only TEA, but also other drugs and endogenous compounds including quinidine, verapamil, and carnitine (Table 4) [38]. In addition, hOCTN1 is inhibited by a variety of structurally diverse compounds including cimetidine, procainamide, pyrilamine, quinine, cephaloridine, and verapamil (Table 4) [38]. rOCTN1 interacts with many of these compounds, but some specificity differences between rOCTN1 and hOCTN1 have been reported (Table 4) [37].

OCTN2: **1. Molecular characteristics.** hOCTN2 was originally cloned from a human placental trophoblast cell line using homology screening. Since then the mouse and rat homologs of OCTN2 have also been isolated [39, 40]. The OCTN2 cDNAs are predicted to encode proteins of 557 amino acids and consist of 12 TMDs. The three

OCTN2 orthologs share ~ 83% identity in amino acid sequence. OCTN2 is ~ 88% similar to hOCTN1 and, like OCTN1, contains a nucleotide binding site sequence motif. OCTN2 shares ~ 35% identity with members of the OCT family. *2. Tissue distribution and localization.* Northern blot analysis has shown that hOCTN2 is strongly expressed in fetal as well as adult kidney, skeletal muscle, placenta, heart, prostate, thyroid, and brain (Table 1) [41]. The fetal expression of OCTN2 differs from that of OCTN1 in that hOCTN2 is expressed mainly in the kidney, while hOCTN1 is expressed mainly in the liver. However, both hOCTN1 and hOCTN2 have a fairly wide tissue distribution. In situ hybridization studies demonstrated that rOCTN2 is expressed in the kidney (cortex), heart, placenta, and brain (Table 1) [40]. *3. Functional characteristics.* Studies in transfected HEK293 cells have shown that unlike most organic cation transporters, hOCTN2 does not significantly take up TEA [41]. However, it transports carnitine in a sodium-dependent fashion [40]. Carnitine transport can be inhibited by desipramine and verapamil [40]. In contrast, the rat homolog rOCTN2 takes up TEA to an extent greater than carnitine [40]. Studies in HRPE cells have demonstrated that rOCTN2 TEA uptake is sodium-independent, whereas rOCTN2-mediated carnitine uptake is sodium-dependent [40]. Both hOCTN2 and rOCTN2 transport the acyl esters of carnitine, acetyl-L-ester and propionyl-L-carnitine and exhibit electrogenic transport of carnitine [40]. In addition, both transporters have been shown to interact with numerous drugs; however, comprehensive substrate specificity studies, including kinetic studies, remain to be performed (Table 4) [40, 42]. Recently Wagner and co-workers have shown that carnitine transport via hOCTN2 is electrogenic [43]. In addition, they conducted experiments to determine whether hOCTN2 is also capable of operating as an organic cation-proton antiporter using TEA, choline, and carnitine as model organic cations; the results of these experiments suggest that hOCTN2 does not function in this mode [43].

Table 1. Organic cation transporter expression in adult kidney, liver, intestine, and brain^a.

Transporter	Kidney	Liver	Intestine	Brain	Reference
mOCT1	xxx	xxx	xxx	NF	[13]
rOCT1	s, xxx; xxx; ###	s, xxx; xxx; ###	s, x; x; #	NF, NF, NF	[12, 18, 25]
rOCT1A	r, ###	###	#	NF	[17]
rbOCT1	#	###	#	ND	[14]
hOCT1	x, #	xxx, ***	NF, #	x, #	[15, 16]
mOCT2	***	NF	ND	#	[26]
rOCT2	***, ###, s	NF, NF, ND	NF, NF, ND	NF, ##, ND	[24, 25, 27]
hOCT2	***, s; ND	NF, ND	#, ND	#, x, s	[16, 28]
mOCT3	s	ND	ND	ND	[35]
rOCT3	x, x	NF, NF	xx, xx	x, s; x	[18, 32]
hOCT3	ND, xx, **	###, xxx, xx	ND, ND, NF	#, NF, #	[33-35]
rOCTN1	xx, s	xxx	xxx	x, s	[37]
hOCTN1	xxx	NF	NF	NF	[36]
rOCTN2	s	ND	ND	s	[40]
hOCTN2	xxx, xxx	x, x	xx, ND	x, x	[39, 41]

^a Tissue distribution determined by Northern blot only (x), RT-PCR (#), both Northern blot and RT-PCR (*), in situ hybridization (s), or RPA (r). “?” indicates that conflicting data exist in the literature (see the appropriate section for more information and references). xxx: high expression level; xx: moderate expression level; x: low expression level; NF: not found; ND: not determined.

Summary and conclusions: organic cation transporters. Five organic cation transporter isoforms have been cloned thus far: OCT1, OCT2, OCT3, OCTN1, and OCTN2. Based on their functional characteristics – namely, sensitivity of membrane potential – OCT1, OCT2, and OCT3 are likely to be found within the BLM of epithelial cells in the kidney. Hence, these transporters are most likely involved in the first step in the renal secretion of drugs (i.e. transporting drugs from the blood into tubule cells across the BLM). But so far only rOCT1 has been convincingly localized to the BLM of the kidney, so caution is warranted until definitive localization studies for the other isoforms are reported. In contrast, OCTN1 is thought to transport organic cations in exchange for protons, which is consistent with a renal BBM transporter. However, localization and further mechanistic studies are still needed to confirm these speculations. While OCTN2 transports the small zwitterion carnitine in a sodium-dependent fashion, organic cations are transported in a sodium-independent manner. It is currently not known to which membrane OCTN2 is localized.

All of the organic cation transporter isoforms have been shown to interact with numerous structurally and pharmacologically diverse compounds (Table 4). However, it is not currently clear whether most of these compounds are *bona fide* substrates of the transporters or only inhibitors. The wider use of more robust assays, such as the voltage-clamp assay, should help address this problem [23, 35, 43, 44].

Transporters Involved in the Renal Elimination of Organic Anions

Background and significance. Organic anions are, by definition, organic molecules that possess one or more negatively charged moieties at physiological pH. Many organic anions are removed from the systemic circulation by the kidneys. For example, penicillin is rapidly excreted by the kidneys at rates as high as 2 g/h: 10% of its renal excretion occurs by glomerular filtration, while 90% occurs by tubular secretion (i.e. a transporter-mediated process) [45]. Likewise, tubular secretion is the primary

pathway of methotrexate elimination from the systemic circulation [46]. The mechanisms and specificities of renal organic anion transport systems have been studied over the past two decades using a number of different animal models, tissue preparations (e.g., membrane vesicles and tissue slices), and cultured cells. Renal organic anion transport mechanisms have been examined, for the most part, using PAH as a model substrate. [2, 4, 5]. It has been reported that PAH is transported across the BLM by a tertiary active organic anion-dicarboxylate exchanger, the most extensively studied organic anion transport system in the kidney [2, 4, 5]. There are additional transport systems in the BLM of the kidney, but these are not as well defined [4, 47]. In the BBM, several putative transport systems have been described, but their driving forces and substrate specificities are poorly understood [4, 47].

In the past five years, nine distinct organic anion transporters have been cloned; these transporters belong to one of two gene families: OAT or oatp/OAT-K. Organic anion transporters are expressed primarily in epithelial tissues such as kidney, liver, and intestine, where they play roles in drug absorption, distribution, and elimination. In addition, several isoforms have been detected in the brain, where they may function in drug transport across the blood-brain barrier or the blood-CSF barrier. The molecular characterization of these transporters is under way, and significant progress has been made in some areas, such as inhibitor specificities. Below we summarize the available data for each of the cloned organic anion transporters and consider the role of these transporters in renal drug elimination.

OAT1: *1. Molecular characteristics.* OAT1 was first cloned from a rat kidney cDNA library in 1997 [48, 49]. The orthologs from human (hOAT1, also termed hPAHT), and mouse (mOAT1, also termed NKT) have been identified as well [50-55]. The three OAT1 orthologs share approximately 80% sequence identity. The OAT1 cDNAs are predicted to encode proteins of 546-, 551-, and 550-amino acid residues for the mouse,

rat, and human transporters, respectively. Hydropathy analyses suggest that OAT1 has 7 to 12 TMDs [48-50, 52-54]. Variants of OAT1 have been identified. A variant of hOAT1, termed hOAT1-1, has been isolated; it is identical to the other hOAT1 sequences, except that it has an additional 13 amino acids near the carboxyl-terminus [56]. Two splice variants of hOAT1, hOAT1-3 and hOAT1-4, have also been isolated, but their function remains to be determined [57].

2. Tissue distribution and localization. Northern blot analyses show that OAT1 transcripts are expressed abundantly in the kidney and at lower levels in the brain (Table 2) [48-50, 52, 53, 54]. In situ studies demonstrate that mOAT1 and rOAT1 mRNA transcripts are expressed in renal proximal tubules [48, 54]. Immunohistochemical studies have revealed that rOAT1 and hOAT1-1 are localized to the BLM of renal proximal tubule cells (Table 3) [56, 58].

3. Functional characteristics. The transport of the classical model organic anion, PAH, by OAT1 is saturable and sodium-independent [48-50, 52, 55, 56]. The uptake rate of PAH is increased by an outwardly directed dicarboxylate gradient, the signature characteristic of the PAH transport system in the basolateral membrane of the kidney [2, 4]. OAT1 interacts with numerous clinically used anionic drugs from various classes: beta-lactam antibiotics, diuretics, NSAIDs, antiviral drugs, and antidiabetic, antiepileptic and antineoplastic agents (Table 4) [48, 50, 52, 55, 59-61]. The substrate and inhibitor specificity of rOAT1 has been extensively examined [49, 50, 59-62]. In a detailed study of the interactions of antibiotics with rOAT1, it was found that seventeen beta-lactam antibiotics reduced rOAT1-mediated PAH uptake (Table 4) [59]. In addition, cells expressing rOAT1 accumulated radiolabeled penicillin G and cephaloridine 3- to 4-fold over controls, indicating that rOAT1 transports these compounds. It has also been found that the NSAIDs interact with rOAT1: ibuprofen, indomethacin, salicylate, and naproxen potently inhibited PAH uptake mediated by rOAT1 in a competitive manner ($K_i = 2 - 10 \mu\text{M}$); acetylsalicylate, salicylate, and phenacetin were less potent inhibitors ($K_i = 300 - 400 \mu\text{M}$), while acetaminophen was a weak inhibitor ($K_i = 2 \text{ mM}$) (Table 4) [60]. In

addition, acetylsalicylate, salicylate, and indomethacin were found to be substrates of rOAT1, but their uptake rates were low. The antiviral agents cidofovir and adefovir are actively secreted in the kidneys and accumulate in renal cells. Cihlar and co-workers demonstrated that cidofovir and adefovir are transported by hOAT1 and by rOAT1 [50, 63]. In a recent study, it was shown that antiviral nucleosides, which lack anionic moieties, interact with and in some cases are transported by rOAT1 (Table 4) [62].

OAT2: *1. Molecular characteristics.* rOAT2 was first isolated from a rat cDNA library using a glucagon receptor antibody and was named NLT (novel liver-specific transport protein) [64]. NLT was shown to be expressed within the sinusoidal membrane of hepatocytes, but its substrates were not determined. Subsequently, Sekine and co-workers found that NLT transports organic anions and proposed to rename NLT as rOAT2 [65]. NLT shares 42% sequence identity with OAT1. *2. Tissue distribution and localization.* Northern blot analysis showed that rOAT2 is expressed at high levels in the liver, at low but significant levels in the kidney, and was not detected in any of the other tissues tested (testes, colon, ileum, spleen, brain, eye, placenta, lung) (Table 2) [65]. Although rOAT2 has not been localized in the kidney, it was determined to reside in the sinusoidal membrane of hepatocytes (Table 3) [64]. *3. Functional characteristics.* Organic anion transport mediated by rOAT2 was shown to be sodium-independent and was not driven by an outwardly directed glutarate gradient [65]. Therefore, it appears that transport via rOAT2 may be facilitative or is driven by a yet unidentified mechanism. The substrate and inhibitor selectivity of rOAT2 appears to be similar to that of OAT1, with a limited number of inhibitors tested [65]. rOAT2 was shown to transport radiolabeled PAH, methotrexate, acetylsalicylate, alpha-ketoglutarate and PGE₂. Salicylate uptake mediated by rOAT2 was potently inhibited by a number of clinically used drugs (at 1 mM) such as bumetanide, cefoperazone, and ketoprofen (Table 4). Whether or not these compounds are also substrates of OAT2 remains to be determined.

OAT3: *1. Molecular characteristics.* rOAT3 was cloned from rat brain using a homology-based cloning method [66]. rOAT3 shares sequence identity with other organic anion as well as cation transporters as follows: rOAT1 (49%), rOAT2 (39%), and rOCT1 (36%). In addition, the putative murine ortholog (termed Roct) of rOAT3 was isolated in 1998 from an animal model for osteopetrosis, the oc mouse, in which its expression level was found to be greatly reduced compared to that in wild-type mice [67, 68]. Recently, the putative human ortholog, hOAT3, was cloned from kidney [53]. rOAT3 and hOAT3 have 536 and 568 amino acid residues respectively and are predicted to have 12 TMDs. *2. Tissue distribution and localization.* Northern blot analyses showed that rOAT3 is most abundantly expressed in the liver, followed by the kidney, brain, and eye; hOAT3 transcripts are expressed abundantly in the kidney, and at lower levels in the brain, but were not detected in the liver, placenta or other tissues tested (Table 2) [53, 66]. The subcellular localization of OAT3 is not known. *3. Functional characteristics.* Uptake via rOAT3 was shown to be sodium-independent, but its transport mechanism is not currently known. rOAT3 mediated the uptake of radiolabeled PAH, estrone sulfate, ochratoxin A. In addition, rOAT3 was shown to accept cimetidine, a weak base, as a substrate [66]. Most of the other organic cations tested (TEA, guanidine, etc.) did not interact with rOAT3. A number of compounds inhibited rOAT3-mediated uptake of labeled estrone sulfate. These compounds included probenecid, bumetanide, cefoperazone, piroxicam, furosemide, zidovudine (AZT), penicillin G (PCG), methotrexate and cimetidine (Table 4) [66]. In addition, several compounds did not inhibit the estrone sulfate uptake mediated by rOAT3, including indomethacin, digoxin, TEA, guanidine, and verapamil. While there are many similarities in the substrate and inhibitor profiles of rOAT1, rOAT2 and rOAT3, some interesting differences have been observed among these isoforms. In particular, the isoforms differ in their interactions with indomethacin: rOAT1 is potently inhibited by indomethacin ($K_i = 10 \mu\text{M}$), whereas rOAT3 activity is unaffected by it at 1 mM [60, 66]. This finding

suggests that it may be possible to develop OAT-isoform specific inhibitors, which would be of great value in determining the *in vivo* roles of these transporters (see "Outlook" section). In contrast to rOAT3, hOAT3 has not been successfully expressed. In preliminary studies using *Xenopus laevis* oocytes injected with hOAT3 cRNA, PAH, urate, oxalate, and TEA transport was not enhanced above controls [53].

OAT4: *1. Molecular characteristics.* The 2210 base pair cDNA of hOAT4 was isolated from a human kidney library and is predicted to encode a 550-amino acid protein [69]. As with other OAT isoforms, hOAT4 is predicted to consist of 12 TMDs. It only shares 38 - 44% sequence identity with the other OAT family members. *2. Tissue distribution and localization.* Northern blot analysis revealed that hOAT4 transcripts are abundantly expressed in kidney and placenta, but not in brain, liver, intestine, or other tissues [69]. The intracellular membrane localization of hOAT4 is not known. *3. Functional characteristics.* Unlike other OAT isoforms, hOAT4 does not readily accept PAH as a substrate. It does, however, transport estrone sulfate, DHEA-s, and ochratoxin A. The driving force of OAT4-mediated transport is undetermined. Inhibition studies revealed that hOAT4 interacts with a wide variety of organic anions including probenecid, penicillin G, indomethacin, furosemide, BSP, and others (Table 4).

OAT-K1: *1. Molecular characteristics.* rOAT-K1 was isolated from a rat kidney cDNA library [70]. A clone containing a 2.8-kb insert was isolated; it is predicted to encode for a 669-amino acid protein consisting of 12 TMDs. rOAT-K1 does not share significant sequence identity with the OAT isoforms and therefore appears to belong to a distinct gene family. *2. Tissue distribution and localization.* Data from Northern blot analysis and RT-PCR studies demonstrated that rOAT-K1 is expressed in the kidney, but not in the brain, heart, lung, liver, small intestine or spleen; thus rOAT-K1 appears to be a kidney-specific transporter (Table 2) [70]. rOAT-K1 was originally localized to the

BLM based on functional studies using polarized LLC-PK₁ cells (Table 3) [70]. In contrast, immunolocalization studies in isolated plasma membrane vesicles as well as functional characterization studies of rOAT-K1 in polarized MDCK cells indicate that this transporter is expressed in the BBM (Table 3) [71, 72]. Further studies are needed to resolve these discordant results. *3. Functional characteristics.* rOAT-K1 expressed in LLC-PK₁ cells mediates the BLM uptake of radiolabeled methotrexate, but not taurocholate, PGE₂, or leukotriene C₄ [70]. In addition, rOAT-K1, unlike most OATs, does not transport PAH [70]. Methotrexate transport mediated by rOAT-K1 can occur bidirectionally in a sodium- and chloride-independent manner [72, 73]. A number of NSAIDs interact weakly with rOAT-K1 (Table 4) [74].

OAT-K2: *1. Molecular characteristics.* rOAT-K2 was isolated from a rat kidney cDNA library [75]. The 2.5-kb cDNA was predicted to encode a 498-amino acid protein that shares 91% identity with rOAT-K1 and is proposed to consist of 8 TMDs. *2. Tissue distribution and localization.* rOAT-K2 is expressed in the kidney, but not in the brain, heart, lung, liver, small intestine or spleen as determined by Northern blot and RT-PCR analysis (Table 2) [75]. In stably transfected MDCK cells, rOAT-K2 was localized functionally to the BBM (Table 3). *3. Functional characteristics.* rOAT-K2 mediated the uptake of radiolabeled methotrexate, folate, taurocholate and PGE₂ (Table 4) [75]. This is in contrast to rOAT-K1, which did not mediate folate or TCA uptake. However, the relative uptakes compared to controls were low (i.e. 1-fold to 14-fold). No enhanced uptake of indomethacin, digoxin, or testosterone was observed in rOAT-K2 transfected cells compared to controls [75]. Probenecid, indomethacin, methotrexate, furosemide and benzylpenicillin reduced TCA uptake in rOAT-K2 transfected cells, as did numerous bile acid analogs and steroids (Table 4) [75]. PAH interacts only weakly with rOAT-K2.

OATP1: *1. Molecular characteristics.* roatp1 was first cloned from a rat liver cDNA library using an expression cloning strategy in *Xenopus laevis* oocytes [76]. It shares 72% sequence identity with rOAT-K1, suggesting that roatp1 and OAT-K1 belong to the same gene family. Like OAT-K1, roatp1 does not share significant sequence identity with the OAT isoforms. The human ortholog, termed hOATP1, has been cloned and characterized [77]. The rat and human clones are predicted to encode proteins of 670-amino acids, which are predicted to have 10 to 12 TMDs. The human protein shares 67% identity with roatp1. *2. Tissue distribution and localization.* Northern blot analysis shows that roatp1 is expressed in the liver, kidney, brain, lung, skeletal muscle and proximal colon but not in the heart or distal colon (Table 2) [76]. hOATP1 has a similar tissue distribution (Table 2) [77]. Immunologic analysis of roatp1 expression in the kidney reveals a BBM localization in the S3 segment of the proximal tubule (Table 3) [78]. roatp1 has also been localized to the BBM of choroid plexus epithelial cells, but interestingly is found on the BLM in the liver [78, 79]. Similar tissue-specific differences in membrane targeting have been reported for other transporters as well [80]. *3. Functional characteristics.* Functional studies indicate that roatp1 and hOATP1 mediate the sodium-independent uptake of a number of compounds including BSP, bile acids, and steroid conjugates (Table 4) [76, 77, 81]. PAH does not appear to interact with hOATP1 [77]. The transport mechanism of roatp1 may involve solute/HCO₃⁻ exchange, solute/GSH exchange, or another yet unidentified mechanism [82, 83]. A large number of bile acids, steroid conjugates, neutral steroids as well as a mycotoxin, ochratoxin A, are high affinity substrates (i.e. low micromolar) of OATP1 [77, 81]. In addition, roatp1 has been shown to transport the peptide-based drugs CRC 200 (a thrombin inhibitor) and enalapril (an angiotensin-converting enzyme inhibitor) (Table 4) [81, 84]. Both the human and rat OATP1 homologs can transport the antihistamine fexofenadine (Table 4) [85].

OATP2: *1. Molecular characteristics.* roatp2 was isolated from a rat brain cDNA library [86]. It is predicted to encode a 661 amino acid protein that shares 77% sequence identity with roatp1. Like roatp1, roatp2 is predicted to have 12 TMDs. *2. Tissue distribution and localization.* Initial studies using Northern blot analysis indicated that roatp2 is highly expressed in the brain, liver, and kidney but not in the heart, spleen, lung, skeletal muscle, or testes (Table 2) [86]. However, in a second study in which a more specific oligonucleotide probe was used, roatp2 was not detected in the kidney [87]. roatp2 has been localized to the BLM of choroid plexus epithelial cells and hepatocytes (Table 3) [88-90]. *3. Functional characteristics.* roatp2 was shown to mediate the sodium-independent uptake of a number of bile acids and steroid conjugates including taurocholate, cholate, 17-beta-estradiol-glucuronide, estrone-3-sulfate as well as ouabain (Table 4) [86]. roatp2 has also been shown to transport fexofenadine (Table 4) [85]. Hence, based on the available data, the substrate selectivities of roatp1 and roatp2 appear to overlap. However, unlike roatp1, roatp2 was shown to mediate high-affinity digoxin uptake ($K_m \sim 0.2 \mu\text{M}$) [86]. In addition, roatp2 has been shown to mediate the transport of thyroxine and tri-iodothyronine [87]. Other compounds that were tested as roatp2 substrates included PAH, pyruvate, glutamate, norepinephrine, corticosterone and leukotriene C_4 , but none of these compounds appeared to be transported by roatp2 [86].

OATP3: *1. Molecular characteristics.* roatp3 was isolated from a rat retina cDNA library [87]. roatp3 contains 670-amino acids and is predicted to possess 12 TMDs. It shares 80% amino acid identity with roatp1 and 77% with rOAT-K1. *2. Tissue distribution and localization.* Northern blot analysis shows that roatp3 is expressed most abundantly in the kidney and at lower levels in retina and liver (Table 2) [87]. The intracellular localization of roatp3 is not known. *3. Functional characteristics.* roatp3 mediates the transport of taurocholate, thyroxine, and tri-iodothyronine in a sodium- and chloride-independent fashion (Table 4) [87]. PAH does not interact with roatp3 [87].

The transport mechanism of roatp3 remains to be determined. Further functional characterization and intracellular localization of roatp3 will aid in understanding the role of this transporter in the renal elimination of drugs.

Table 2. Organic anion transporter expression in adult kidney, liver, intestine and brain^a.

Transporter	Kidney	Liver	Intestine	Brain	Reference
mOAT1	s, xxx	NF	NF	x	[54]
rOAT1	xxx, s; xxx	NF, NF	NF, ND	x, NF	[48, 49]
hOAT1	***, xxx,	NF, NF,	NF, NF, NF,	#, NF, x, x	[50, 52, 53, 56]
	xxx, xxx	NF, NF	NF		
rOAT2	x	xxx	NF	NF	[65]
rOAT3	xx	xxx	NF	xx	[66]
hOAT3	xxx	NF	ND	x	[53]
hOAT4	xxx	NF	NF	NF	[69]
rOAT-K1	***	NF	NF	NF	[70]
rOAT-K2	***	NF	NF	NF	[75]
roatp1	xxx, ND	xxx, s	NF, ND	xxx, ND	[76, 90]
hOATP1	xxx	xxx	NF	xxx	[77]
roatp2	?	xxx,	ND, ND,	xxx; xxx, s;	[86, 87, 90]
		xxx, s	ND	ND	
roatp3	xxx	x	ND	NF	[87]

^a Tissue distribution determined by Northern blot only (x), RT-PCR (#), both Northern blot and RT-PCR (*), in situ hybridization (s), or RPA (r). “?” indicates that conflicting data exist in the literature (see the appropriate section for more information and references). xxx: high expression level; xx: moderate expression level; x: low expression level; NF: not found; ND: not determined.

Summary and conclusions: organic anion transporters. Nine organic anion transporter isoforms, which are expressed in the kidney, have been cloned, and more isoforms may be identified in the future. How do the cloned transporters compare to the previously described transport systems found in tissue preparations and cell culture models? Based on the molecular studies available thus far, it is clear that the renal organic anion transport system is much more complicated at the molecular level. Of the nine cloned transporters, only one transporter, OAT1, exhibits characteristics of a previously described transport system – in this case, the classical basolateral membrane, tertiary active PAH:dicarboxylate transport system. Hence, OAT1 is involved in the first step in the renal secretion of drugs – it transports drugs from the blood, across the BLM, and into renal epithelial cells. It has been found that the other organic anion transporters, like OAT1, interact with numerous clinically used anionic drugs, so it is reasonable to presume that these transporters are also involved in the renal handling of organic anions, yet their roles in specific drug elimination have yet to be defined. One complicating issue is the fact that the transport mechanisms utilized by OAT2, OAT3, OAT4, OAT-K1, OAT-K2, oatp1, oatp2, and oatp3 remain, for the most part, to be established. Several of these transporters appear to operate as exchangers or as facilitative transporters, yet without full knowledge of their transport mechanism(s) it is difficult to postulate, with reasonable certainty, the roles of these transporter in renal drug handling (e.g. secretion or absorption). In addition to the transport mechanism, the intracellular localization of the transporters must be established. Thus far this has been determined in kidney only for OAT1, rOAT-K1, and roatp1 (Table 3). Likewise, a detailed profile of drug-transporter interactions needs to be established for each transporter. Thus far, functional studies – substrate inhibition studies or uptake studies with radiolabeled compounds - with the cloned organic anion transporters suggest that they interact with numerous structurally diverse compounds (Table 4). But substrate inhibition studies are limited, because an inhibitor may or may not actually be translocated by a transporter, and uptake studies

with radiolabeled compounds are limited to the availability of labeled compounds. Clearly, more robust and high-throughput assays are needed to study drug-transporter interactions in pharmaceutical laboratories. An example of these is an electrophysiological-based assay, which has been used successfully to differentiate between substrates and inhibitors for the flounder OAT1 ortholog [91]. And recently, a fluorescence-based assay has been developed to screen for hOAT1-drug interactions. This assay appears to have the potential to be used for high-throughput screening [92].

Other Transporters Involved in the Renal Elimination of Drugs

In addition to the transporters discussed above, other transporters are involved in the renal elimination of drugs. Although not the subject of this review, we feel that it is important to mention them and to direct the reader to pertinent references. Based on the data available, it is likely that multidrug resistance-associated proteins (MRPs) play important roles in the renal handling of drugs – all six MRP isoforms have been detected in the kidney and interact with numerous anionic drugs and their metabolites [93-95]. MRP1, MRP3, and MRP5 are localized to the BLM and MRP2 is localized to the BBM. Recently, MRP2 has been shown to mediate the transport of PAH, the classical organic anion used to study renal organic anion transport mechanisms [96, 97]. Hence, MRP2 may be the most relevant MRP isoform in the renal secretion of drugs, but much more work is needed to determine the roles of these transporters in renal drug transport. The multidrug resistance protein P-glycoprotein (P-gp) interacts with numerous drugs, including a variety of organic cations [98-100]. P-gp is expressed in the BBM in renal cells, where it transports drugs from the tubule cells into the tubule lumen [101]. P-gp knockout mice have been generated and have become invaluable in elucidating the role of this transporter in drug absorption, disposition, and elimination [102-104].

Outlook and Future Directions

During the past decade significant progress has been made in the cloning and molecular characterization of renal organic anion and organic cation transporters. Based on the characterization studies of the available cloned organic cation and anion transporters, it is clear that many drugs interact with multiple transporter isoforms. For example, methotrexate is known to interact with five different organic anion transporters (Table 4), as well as MRP1 and MRP2 [105]. What roles do these transporters play in the renal elimination of methotrexate or other drugs? At present, it is extremely difficult to dissect the role of any individual transporter in the renal handling of drugs. To address this problem, at a minimum, the intracellular localization and driving force(s) of the transporters must be established; as discussed in this review, much more work is needed in these areas. Ideally, a knockout animal model or an isoform-specific inhibitor should be used to better assess the *in vivo* roles of each transporter in drug elimination. For example, P-gp knockout mice have been invaluable in elucidating the role of this transporter in drug disposition [102-104]. Currently, neither knockout mice nor isoform-specific inhibitors exist for any organic cation or organic anion transporter. Other animal models, such as the nematode *C. elegans*, may ultimately prove useful in elucidating the roles of these transporters in the whole animal; recently, an organic cation transporter and an organic anion transporter were isolated from *C. elegans* [106, 107]. Finally, there have been very few studies on the genetic variations of organic anion or organic cation transporters in human populations. Such variants could have profound effects on interpatient variability in drug response and pharmacokinetics. Recently, a functional polymorphism of P-gp was discovered [108]. In summary, over fourteen distinct organic anion and organic cation transporter isoforms have been cloned. With the completion of the human, as well as other, genome projects, all of the xenobiotic transporters will soon be identified. Much work remains to be done in order to reach the ultimate goal of understanding the *in vivo* roles of these transporters in drug absorption, disposition, and

elimination. With the likely future development of transporter-knockout mice and the utilization of more sophisticated electrophysiological- and fluorescence-based assays to screen for drug-transporter interactions, this goal could be reached within a decade.

Table 3. Intracellular localization of organic anion and organic cation transporters.

Transporter	Localization	Tissue or cell line	Method^a	Reference
rOAT1	BLM	kidney	I	[58]
hOAT1	BLM	kidney	I	[56]
rOAT2	BLM	liver	I	[64]
rOAT-K1	BLM	LLC-PK ₁	F	[70]
	BBM	kidney	I	[71]
	BBM	MDCK	F	[72]
rOAT-K2	BBM	MDCK	F	[75]
roatp1	BBM	kidney	I	[78]
	BLM	liver	I	[78, 90]
	BBM	choroid plexus	I	[79, 88]
roatp2	BLM	liver	I	[89, 90]
	BLM	choroid plexus	I	[88]
rOCT1	BLM	liver	I	[20]
	BLM	kidney	I	[19]
	BLM	MDCK	F	[19]
rOCT2	BLM	MDCK	F	[19]
	BLM and BBM	MDCK	F	[29]
pOCT2	BBM	LLC-PK ₁	F	[25]
hOCT2	BBM	kidney	I	[16]

^a Localization determined by the following methods: I, immunohistochemistry; F, functional localization in a polarized cell line

Table 4. Compounds that interact with organic anion and organic cation transporters^a.

Compound	Transporter	K_i or (K_m) (μM)	Reference
acebutolol	hOCT1	96	[21]
acetyl-L-carnitine	<u>hOCTN2</u>	(8.5)	[42]
acetylsalicylate	<u>rOAT1</u>	428	[60]
	<u>rOAT2</u>	ND	[65]
acyclovir (ACV)	<u>rOAT1</u>	(242)	[62]
adefovir	<u>rOAT1</u>	(270)	[50]
	<u>hOAT1</u>	(30), (24)	[50, 63]
adrenaline	<u>rOCT2</u>	(1900)	[27]
	<u>hOCT3</u>	ND	[33]
aldosterone	hOCTN2	ND	[42]
amantadine	hOCT1	ND	[21]
	<u>hOCT2</u>	(27)	[28]
aminopterin	rOAT-K1	0.5	[73]
cAMP	<u>rOAT1</u>	ND	[48]
amphetamine	rOCT3	42	[18]
araC	<u>rOCT1</u>	ND	[30]
atorvastatin	roatp1	ND	[109]
AZT (zidovudine)	<u>rOCT1</u>	ND	[30]
	<u>rOAT1</u>	(68)	[62]
	rOAT3	ND	[66]
betaine	<u>hOCTN2</u>	ND	[43]
BSP	rOAT2	ND	[65]

Compound	Transporter	K_i or (K_m) (μM)	Reference
	rOAT3	ND	[66]
	hOAT4	ND	[69]
	rOAT-K1	ND	[70]
	<u>roatp1</u>	(1.5), (3.0)	[76, 81]
	<u>hOATP1</u>	(20), ND	[77, 85]
bumetanide	hOAT1	ND	[53]
	rOAT2	ND	[65]
	rOAT3	ND	[66]
	hOAT4	ND	[69]
captopril	mOAT1	ND	[55]
carbenicillin	rOAT1	500	[59]
L-carnitine	<u>hOCTN1</u>	ND	[38]
	<u>mOCTN2</u>	ND	[40]
	<u>rOCTN2</u>	(15)	[40]
	<u>hOCTN2</u>	ND, (4.3), (4.8)	[40, 42, 43]
D-carnitine	hOCTN1	ND	[38]
	<u>hOCTN2</u>	(11), (98)	[42, 43]
carprofen	mOAT1	ND	[55]
cefazolin	rOAT1	450	[59]
cefepime	rOCTN2	2100	[110]
	hOCTN2	1700	[110]
cefluprenam	rOCTN2	ND	[110]
	hOCTN2	ND	[110]
cefoperazone	rOAT1	ND	[59]
	rOAT2	ND	[65]

Compound	Transporter	K_i or (K_m) (μM)	Reference
	rOAT3	ND	[66]
cefoselis	rOCTN2	6400	[110]
	hOCTN2	6400	[110]
cefsulodin	hOCTN2	ND	[42]
ceftazidime	hOCTN2	ND	[42]
cephalexin	rOAT1	2310	[59]
cephaloridine	<u>rOAT1</u>	2330, ND	[48, 59]
	hOCTN1	ND	[38]
	rOCTN2	790	[110]
	hOCTN2	ND, 230	[42, 110]
cephalothin	rOAT1	290	[59]
chlorpropamide	rOAT1	39.5	[61]
cholate	rOAT3	ND	[66]
	<u>roatp1</u>	ND, (54)	[76, 81]
	<u>hOATP1</u>	(93)	[77]
	<u>roatp2</u>	(46)	[86]
choline	<u>rOCT1</u>	(1100), 400	[111, 112]
	rOAT1A	ND	[17]
	hOCT1	ND	[21]
	rOCT2	159	[112]
	<u>hOCT2</u>	(210)	[16]
	rOCT3	ND	[18, 32]
	rOCTN2	ND	[40]
	<u>hOCTN2</u>	ND	[43]
	cidofovir	<u>rOAT1</u>	(238)

Compound	Transporter	K_i or (K_m) (μM)	Reference
	<u>hOAT1</u>	(46), (58)	[50, 63]
cimetidine	<u>rOCT1</u>	5.7, 329, ND	[19, 112, 113]
	rOCT1A	ND	[17]
	rbOCT1	ND	[14]
	hOCT1	166	[21]
	<u>rOCT2</u>	9.4, 198, 373, (21)	[19, 31, 112, 113]
	mOCT3	ND	[35]
	rOCT3	ND	[18, 32]
	<u>hOCT3</u>	ND	[113]
	rOCTN1	1540	[37]
	hOCTN1	ND	[38]
	rOCTN2	ND	[40]
	hOCTN2	ND	[18, 40, 42]
	<u>rOAT3</u>	ND	[66]
cisplatin	rOCT2	925	[31]
ClAdo	rOCT1	ND	[30]
clonidine	rOCT1	1.4	[114]
	hOCT1	0.55	[21]
	mOCT3	ND	[35]
	rOCT3	ND	[18]
	hOCT3	373	[35]
	rOCTN2	ND	[40]
	hOCTN2	ND	[42]
corticosterone	rOCT1	10, 72	[12, 114]

Compound	Transporter	K_i or (K_m) (μM)	Reference
	hOCT1	7.0	[21]
	pOCT2	0.67	[25]
	rOCT2	4.2, 0.5	[18, 27]
	rOCT3	4.9	[18]
	hOCT3	0.12	[33]
	hOCTN2	ND	[42]
	hOAT4	ND	[69]
creatinine	hOCT1	ND	[21]
	<u>rOCT2</u>	ND	[113]
CRC 220	<u>roatp1</u>	(57)	[81]
cyanine-863	rOCT1	0.13, 0.67	[12, 114]
	pOCT2	0.5	[25]
	hOCT2	0.21	[16]
cysteine	hOCTN2	ND	[43]
decynium-22	rOCT1	0.36, 22, 0.5	[12, 112, 114]
	hOCT1	4.4, 2.7	[15, 21]
	rOCT2	14	[112]
	pOCT2	0.05	[25]
	hOCT2	0.10	[16]
deoxycorticosterone	rOCT2	1.9	[18]
	rOCT3	8.4	[18]
desipramine	rOCT1	2.8	[12]
	hOCT1	5.3	[21]
	hOCT2	16	[16]
	rOCT3	68	[18, 32]

Compound	Transporter	K_i or (K_m) (μM)	Reference
	hOCT3	14	[35]
	rOCTN1	80	[37]
	rOCTN2	ND	[40]
	hOCTN2	ND	[40]
DHEA-s	<u>hOAT4</u>	(0.63)	[69]
	<u>roapt1</u>	(5.0)	[81]
	<u>roatp2</u>	ND	[89]
diclofenac	mOAT1	ND	[55]
	rOAT1	ND	[60]
didanosine	<u>rOAT1</u>	ND	[62]
digoxin	<u>roatp2</u>	(0.24), ND	[86, 89]
	rOAT-K2	ND	[75]
disopyramide	hOCT1	ND	[21]
disprocynium24	rOCT1	0.11	[114]
	rOCT2	0.01	[27]
	hOCT3	0.01	[33]
DMA	mOCT3	ND	[35]
	rOCT3	ND	[18, 32]
	rOCTN1	180	[37]
	rOCTN2	ND	[40]
dTub	<u>rOCT1</u>	(10)	[30]
dopamine	<u>rOCT1</u>	(1100), (51)	[115, 116]
	hOCT1	ND	[21]
	<u>rOCT2</u>	2300, (2100)	[18, 27]
	<u>hOCT2</u>	(390), (330)	[28]

Compound	Transporter	K_i or (K_m) (μM)	Reference
	rOCT3	620	[18]
emetine	hOCTN2	4.2	[43]
enalapril	mOAT1	ND	[55]
	<u>roatp1</u>	(214)	[84]
erythromycin	hOATP1	ND	[85]
beta-estradiol	rOCT2	84.8	[18]
	rOCT3	1.1	[18]
estradiol-17β-glucuronide	<u>roatp1</u>	(4)	[81]
	<u>roatp2</u>	(3), ND	[86, 89]
estrone sulfate	<u>rOAT3</u>	(2.3)	[66]
	<u>hOAT4</u>	(1.0)	[69]
	<u>roatp1</u>	(11)	[81]
	<u>roatp2</u>	ND	[89]
ethacrynic acid	rOAT1	ND	[48]
fexofenadine	<u>roatp1</u>	(32)	[85]
	<u>hOATP1</u>	(6.4)	[85]
	<u>roatp2</u>	(6.0)	[85]
flufenamate	rOAT-K1	ND	[74]
fluorescein	hOAT1	ND	[52]
folic acid	mOAT1	ND	[55]
	rOAT-K1	ND, 14	[70, 73]
	<u>rOAT-K2</u>	ND	[75]
folinic acid	rOAT-K1	8.2	[73]
furosemide	rOAT1	ND	[48]

Compound	Transporter	K_i or (K_m) (μM)	Reference
	hOAT1	ND	[52, 53, 56]
	rOAT3	ND	[66]
	hOAT4	ND	[69]
	rOAT-K1	ND	[70]
	rOAT-K2	ND	[75]
cGMP	<u>rOAT1</u>	ND	[48]
guanidine	rOCT1	724, 4200	[19, 113]
	rOCT1A	ND	[17]
	<u>rOCT2</u>	714, (730)	[19, 113]
	<u>mOCT3</u>	ND	[35]
	<u>rOCT3</u>	ND	[18, 32]
	hOCT3	6200, 13,000	[35, 113]
glibenclamide	rOAT1	1.6	[61]
glutarate	hOAT1	ND	[52]
histamine	rOCT1	1400	[113]
	<u>rOCT2</u>	(540)	[113]
	<u>hOCT2</u>	(1300)	[28]
	<u>hOCT3</u>	(180)	[113]
hippurate	hOAT1	ND	[52]
ibuprofen	rOAT1	3.5	[60]
	hOAT4	ND	[69]
	rOAT-K1	ND	[74]
imipramine	hOCT3	42	[35]
	rOCTN1	ND	[37]
indinavir	hOCT1	62	[117]

Compound	Transporter	K_i or (K_m) (μM)	Reference
	hOATP1	ND	[85]
indomethacin	mOAT1	ND	[55]
	<u>rOAT1</u>	ND, 10	[48, 60]
	hOAT1	ND	[52, 56]
	hOAT4	ND	[69]
	rOAT-K1	1000	[74]
	rOAT-K2	ND	[75]
alpha-ketoglutarate	mOAT1	ND	[55]
	<u>rOAT1</u>	ND	[48, 49]
	hOAT1	ND	[50, 52, 53, 56]
	<u>rOAT2</u>	(18)	[65]
ketoprofen	rOAT1	ND	[60]
	rOAT2	ND	[65]
	rOAT-K1	1900	[74]
lamivudine	<u>rOAT1</u>	ND	[62]
levofloxacin	rOCT2	ND	[112]
	rOAT-K2	ND	[75]
losartan	hOAT1	ND	[53]
lovastatin	roatp1	ND	[109]
	hOATP1	ND	[85]
lysine	<u>hOCTN2</u>	ND	[43]
memantine	<u>hOCT2</u>	(34)	[28]
mepiperphenidol	rOCT1	5.2	[12]
	hOCT2	1.8	[16]

Compound	Transporter	K_i or (K_m) (μM)	Reference
methamphetamine	rOCT3	247	[18]
methionine	<u>hOCTN2</u>	ND	[43]
methotrexate	mOAT1	ND	[55]
	<u>rOAT1</u>	ND	[48]
	<u>rOAT2</u>	ND	[65]
	rOAT3	ND	[66]
	<u>rOAT-K1</u>	(1.0), 1.8	[70, 73]
	<u>rOAT-K2</u>	ND	[75]
	O-methylisoprenaline	rOCT1	43, 25
pOCT2		880	[25]
hOCT2		570	[16]
midazolam	hOCT1	3.7	[21]
MPTP	mOCT3	ND	[35]
	rOCT3	ND	[32]
	rOCTN2	ND	[40]
	hOCTN2	ND	[39, 40]
MPP ⁺	<u>rOCT1</u>	13, 0.8, (10), 64, (13)	[12, 19, 111, 112, 114]
	<u>rbOCT1</u>	(23)	[14]
	<u>hOCT1</u>	(15), 12	[15, 21]
	rOCT2	1.8, 44	[19, 112]
	<u>hOCT2</u>	(19), 2.4; (16)	[16, 28]
	<u>mOCT3</u>	ND	[35]
	<u>rOCT3</u>	(91), 143; ND	[18, 32]
	<u>hOCT3</u>	ND; 54, (47)	[33, 35]

Compound	Transporter	K_i or (K_m) (μM)	Reference
	rOCTN1	ND	[37]
	rOCTN2	ND	[40]
	hOCTN2	ND	[39, 42]
naproxen	rOAT1	2	[60]
nateglinide	rOAT1	9.2	[61]
nelfinavir	hOCT1	22	[117]
	hOATP1	ND	[85]
nicotine	rOCT1	64.3	[19]
	rOCT2	50.5, ND	[19, 112]
	rOCT3	ND	[32]
	hOCT1	ND	[21]
	rOCTN1	ND	[37]
	hOCTN1	ND	[38]
	rOCTN2	ND	[40]
	hOCTN2	ND	[39, 42]
NMN	<u>rOCT1</u>	1000, (340), 2400, 670	[12, 19, 111, 112]
	rOAT1A	ND	[17]
	rbOCT1	ND	[14]
	hOCT1	7700	[21]
	rOCT2	400, 1600	[19, 112]
	<u>hOCT2</u>	(300)	[16]
	mOCT3	ND	[35]
	rOCT3	ND	[18, 32]
noradrenaline	<u>rOCT1</u>	(2800)	[115]

Compound	Transporter	K_i or (K_m) (μM)	Reference
	<u>rOCT2</u>	(4400)	[27]
	<u>hOCT3</u>	(510)	[33]
norepinephrine	rOCT2	11,000	[18]
	<u>hOCT2</u>	(1900)	[28]
	rOCT3	434	[18]
ochratoxin A	<u>rOAT3</u>	(0.74)	[66]
	<u>hOAT4</u>	ND	[69]
	<u>roatp1</u>	(29)	[81]
oxyphenbutazone	rOAT1	32	[60]
ouabain	rOATK-2	ND	[75]
	<u>roatp2</u>	(470)	[86]
PAH	<u>mOAT1</u>	(37)	[55]
	<u>rOAT1</u>	(14), (70)	[48, 49]
	<u>hOAT1</u>	(9), (9.3), (15)	[52, 56, 63]
	<u>rOAT2</u>	ND	[65]
	<u>rOAT3</u>	(65)	[66]
pancuronium	hOCT1	ND	[15]
pantothenic acid	mOAT1	ND	[55]
paracetamol	rOAT1	2099	[60]
penicillin G	<u>rOAT1</u>	1680	[59]
	rOAT3	ND	[66]
	hOAT4	ND	[69]
PGE ₂	<u>rOAT1</u>	ND	[48]
	<u>rOAT2</u>	ND	[65]
	<u>rOAT-K2</u>	ND	[75]

Compound	Transporter	K_i or (K_m) (μM)	Reference
phenacetin	rOAT1	488	[60]
phenol red	hOAT1	ND	[56]
phenylbutazone	rOAT-K1	ND	[74]
piroxicam	rOAT1	52	[60]
	rOAT3	ND	[66]
PMEDAP	<u>rOAT1</u>	ND	[50]
	<u>hOAT1</u>	ND	[50]
PMEG	<u>rOAT1</u>	ND	[50]
	<u>hOAT1</u>	ND	[50]
pravastatin	<u>roatp1</u>	(30)	[109]
	roatp2	38	[118]
probenecid	mOAT1	ND	[55]
	rOAT1	ND	[48, 49]
	hOAT1	ND	[50, 52, 53, 56]
	rOAT3	ND	[66]
	hOAT4	ND	[69]
	rOAT-K2	ND	[75]
	procainamide	rOCT1	13, 44.4
	rOCT1A	ND	[17]
	hOCT1	73.9, 107	[21, 22]
	rOCT2	257	[112]
	hOCT2	50	[16]
	hOCT3	738	[35]
	rOCTN1	860	[37]

Compound	Transporter	K_i or (K_m) (μM)	Reference
	hOCTN1	ND	[38]
	rOCTN2	ND	[40]
	hOCTN2	ND	[39, 42]
progesterone	rOCT2	1.6	[18]
	rOCT3	10.5	[18]
pyrilamine	<u>hOCTN1</u>	ND	[38]
	hOCTN2	ND	[42]
quinidine	rOCT1	14.6, 6.0	[19, 114]
	hOCT1	17.5, 23.4	[21, 22]
	rOCT2	19.1, ND	[19, 112]
	<u>hOCTN1</u>	ND	[38]
	<u>hOCTN2</u>	ND	[42, 43]
	rOAT3	ND	[66]
	hOATP1	ND	[85]
quinine	rOCT1	0.93, 4.3	[12, 114]
	hOCT1	22.9, 22.6	[21, 22]
	hOCT2	3.4	[16]
	pOCT2	5.5	[25]
	hOCTN1	ND	[38]
	hOCTN2	ND	[42]
reserpine	rOCT1	20	[12]
riboflavin	mOAT1	ND	[55]
rifampicin	rOAT2	ND	[65]
ritonavir	hOCT1	5.2	[117]
	hOATP1	ND	[85]

Compound	Transporter	K_i or (K_m) (μM)	Reference
salicylate	<u>rOAT1</u>	341	[60]
	hOAT1	ND	[53]
	<u>rOAT2</u>	(88)	[65]
salicylurate	rOAT1	11	[60]
saquinavir	hOCT1	8.3	[117]
	hOATP1	ND	[85]
semustine	mOAT1	ND	[55]
serotonin	<u>rOCT1</u>	(650)	[115]
	<u>rOCT2</u>	(3600)	[27]
	<u>hOCT2</u>	(80)	[28]
	rOCT3	970, ND	[18, 32]
simvastatin	roatp1	ND	[109]
stavudine	<u>rOAT1</u>	ND	[62]
sulindac	mOAT1	ND	[55]
taurocholate	rOAT3	ND	[66]
	rOAT-K1	ND	[70]
	<u>rOAT-K2</u>	(10)	[75]
	<u>roatp1</u>	(32)	[76, 81, 109]
	<u>hOATP1</u>	(60)	[77]
	<u>roatp2</u>	ND	[89]
	<u>roatp3</u>	(18)	[87]
TBA	<u>mOCT1</u>	7.3	[23]
	<u>rOCT1</u>	17	[23]
	<u>rbOCT1</u>	25	[23]
	<u>hOCT1</u>	52, 30	[22, 23]

Compound	Transporter	K_i or (K_m) (μM)	Reference
TBuMA	<u>hOCT1</u>	66	[22]
TEA	<u>mOCT1</u>	128	[23]
	<u>rOCT1</u>	(95); 47, (36); 100, 167	[12, 19, 23, 112]
	<u>rOAT1A</u>	(42)	[17]
	<u>rbOCT1</u>	ND, 94	[14, 23]
	<u>hOCT1</u>	161, 260, 158	[21-23]
	<u>rOCT2</u>	52, (45); (34), 142	[19, 112]
	<u>pOCT2</u>	(20), 38	[25]
	<u>hOCT2</u>	(76)	[16]
	<u>mOCT3</u>	(1900)	[35]
	<u>rOCT3</u>	(2500)	[32]
	<u>hOCT3</u>	1300	[35]
	<u>rOCTN1</u>	960	[37]
	<u>hOCTN1</u>	(436)	[36]
	<u>mOCTN2</u>	ND	[40]
	<u>rOCTN2</u>	(63)	[40]
	<u>hOCTN2</u>	ND	[39, 40, 42, 43]
testosterone	<u>rOCT3</u>	ND	[18]
THA	<u>hOCT1</u>	3.0	[22]
	<u>rOCTN2</u>	ND	[40]
thyroxine	<u>roatp2</u>	(6.5), ND	[87, 89]
	<u>roatp3</u>	(4.9)	[87]
TMA	<u>mOCT1</u>	2040	[23]

Compound	Transporter	K_i or (K_m) (μM)	Reference
	<u>rOCT1</u>	1000, 905	[12, 23]
	<u>rbOCT1</u>	5800	[23]
	<u>hOCT1</u>	10,000, 12,000	[22, 23]
	hOCT2	180	[16]
	rOCTN2	ND	[40]
tolbutamide	rOAT1	55.5	[61]
TPeA	mOCT1	ND	[23]
	rOCT1	0.43, ND	[12, 23]
	rbOCT1	ND	[23]
	hOCT1	7.4, 8.6, ND	[21-23]
	hOCT2	1.5	[16]
TPrA	<u>mOCT1</u>	20	[23]
	<u>rOCT1</u>	21	[23]
	<u>rbOCT1</u>	36	[23]
	<u>hOCT1</u>	90, 102	[22, 23]
trifluridine	<u>rOAT1</u>	ND	[62]
tri-iodothyronine	<u>roatp2</u>	(5.8)	[87]
	<u>roatp3</u>	(7.3)	[87]
tyramine	<u>hOCT3</u>	ND	[33]
urate	<u>rOAT1</u>	ND	[48]
	hOAT1	ND	[56]
valproic acid	rOAT1	ND	[48]
	hOCTN2	ND	[42]
verapamil	hOCT1	2.9	[21]
	rOCTN1	ND	[37]

Compound	Transporter	K_i or (K_m) (μM)	Reference
	<u>hOCTN1</u>	ND	[38]
	<u>hOCTN2</u>	ND	[40, 42, 43]
	hOATP1	ND	[85]
vecuronium	hOCT1	120, 232, 237	[15, 21, 22]
zalcitabine	<u>rOAT1</u>	ND	[62]

^a Underlining indicates that the compound is a substrate. Otherwise, the compound has only been shown to inhibit the transport of a model compound (i.e. it is not known whether the drug is a substrate or only an inhibitor). Values in parentheses in the K_i/K_m column indicate a K_m value, otherwise it is a K_i value. All of the available kinetic constants are reported from the primary literature. ND: not determined.

References

1. Bendayan R, Renal drug transport: a review. *Pharmacotherapy* **16**(6): 971-985, 1996.
2. Pritchard JB and Miller DS, Mechanisms mediating renal secretion of organic anions and cations. *Physiol Rev* **73**(4): 765-796, 1993.
3. Moller JV and Sheikh MI, Renal organic anion transport system: pharmacological, physiological, and biochemical aspects. *Pharmacol Rev* **34**(4): 315-358, 1982.
4. Pritchard JB and Miller DS, Renal secretion of organic anions and cations. *Kidney Int* **49**(6): 1649-1654, 1996.
5. Ullrich KJ, Renal transporters for organic anions and organic cations. Structural requirements for substrates. *J Membr Biol* **158**(2): 95-107, 1997.
6. Zhang L, Brett CM and Giacomini KM, Role of organic cation transporters in drug absorption and elimination. *Annu Rev Pharmacol Toxicol* **38**: 431-460, 1998.
7. Koepsell H, Organic cation transporters in intestine, kidney, liver, and brain. *Annu Rev Physiol* **60**: 243-266, 1998.
8. Koepsell H, Gorboulev V and Arndt P, Molecular pharmacology of organic cation transporters in kidney. *J Membr Biol* **167**(2): 103-117, 1999.
9. Dresser MJ, Zhang L and Giacomini KM, Molecular and functional characteristics of cloned human organic cation transporters. In: *Membrane Transporters as Drug Targets* (Eds. Amidon G and Sadee W), pp. 441-469. Kluwer Academic/Plenum Publishers, New York, 1999.
10. Sekine T, Cha SH and Endou H, The multispecific organic anion transporter (OAT) family. *Pflugers Arch* **440**(3): 337-350, 2000.
11. Burckhardt G and Wolff NA, Structure of renal organic anion and cation transporters. *Am J Physiol Renal Physiol* **278**(6): F853-866, 2000.

12. Grundemann D, Gorboulev V, Gambaryan S, Veyhl M and Koepsell H, Drug excretion mediated by a new prototype of polyspecific transporter. *Nature* **372**(6506): 549-552, 1994.
13. Schweifer N and Barlow DP, The Lx1 gene maps to mouse chromosome 17 and codes for a protein that is homologous to glucose and polyspecific transmembrane transporters. *Mamm Genome* **7**(10): 735-740, 1996.
14. Terashita S, Dresser MJ, Zhang L, Gray AT, Yost SC and Giacomini KM, Molecular cloning and functional expression of a rabbit renal organic cation transporter. *Biochim Biophys Acta* **1369**(1): 1-6, 1998.
15. Zhang L, Dresser MJ, Gray AT, Yost SC, Terashita S and Giacomini KM, Cloning and functional expression of a human liver organic cation transporter. *Mol Pharmacol* **51**(6): 913-921, 1997.
16. Gorboulev V, Ulzheimer JC, Akhoundova A, Ulzheimer-Teuber I, Karbach U, Quester S, Baumann C, Lang F, Busch AE and Koepsell H, Cloning and characterization of two human polyspecific organic cation transporters. *DNA Cell Biol* **16**(7): 871-881, 1997.
17. Zhang L, Dresser MJ, Chun JK, Babbitt PC and Giacomini KM, Cloning and functional characterization of a rat renal organic cation transporter isoform (rOCT1A). *J Biol Chem* **272**(26): 16548-16554, 1997.
18. Wu X, Kekuda R, Huang W, Fei YJ, Leibach FH, Chen J, Conway SJ and Ganapathy V, Identity of the organic cation transporter OCT3 as the extraneuronal monoamine transporter (uptake2) and evidence for the expression of the transporter in the brain. *J Biol Chem* **273**(49): 32776-32786, 1998.
19. Urakami Y, Okuda M, Masuda S, Saito H and Inui KI, Functional characteristics and membrane localization of rat multispecific organic cation transporters, OCT1 and OCT2, mediating tubular secretion of cationic drugs. *J Pharmacol Exp Ther* **287**(2): 800-805, 1998.

20. Meyer-Wentrup F, Karbach U, Gorboulev V, Arndt P and Koepsell H, Membrane localization of the electrogenic cation transporter rOCT1 in rat liver. *Biochem Biophys Res Commun* **248**(3): 673-678, 1998.
21. Zhang L, Schaner ME and Giacomini KM, Functional characterization of an organic cation transporter (hOCT1) in a transiently transfected human cell line (HeLa). *J Pharmacol Exp Ther* **286**(1): 354-361, 1998.
22. Zhang L, Gorset W, Dresser MJ and Giacomini KM, The interaction of n-tetraalkylammonium compounds with a human organic cation transporter, hOCT1. *J Pharmacol Exp Ther* **288**(3): 1192-1198, 1999.
23. Dresser MJ, Gray AT and Giacomini KM, Kinetic and selectivity differences between rodent, rabbit, and human organic cation transporters (OCT1). *J Pharmacol Exp Ther* **292**(3): 1146-1152, 2000.
24. Okuda M, Saito H, Urakami Y, Takano M and Inui K, cDNA cloning and functional expression of a novel rat kidney organic cation transporter, OCT2. *Biochem Biophys Res Commun* **224**(2): 500-507, 1996.
25. Grundemann D, Babin-Ebell J, Martel F, Ording N, Schmidt A and Schomig E, Primary structure and functional expression of the apical organic cation transporter from kidney epithelial LLC-PK1 cells. *J Biol Chem* **272**(16): 10408-10413, 1997.
26. Mooslehner KA and Allen ND, Cloning of the mouse organic cation transporter 2 gene, Slc22a2, from an enhancer-trap transgene integration locus. *Mamm Genome* **10**(3): 218-224, 1999.
27. Grundemann D, Koster S, Kiefer N, Breidert T, Engelhardt M, Spitzenberger F, Obermuller N and Schomig E, Transport of monoamine transmitters by the organic cation transporter type 2, OCT2. *J Biol Chem* **273**(47): 30915-30920, 1998.
28. Busch AE, Karbach U, Miska D, Gorboulev V, Akhoundova A, Volk C, Arndt P, Ulzheimer JC, Sonders MS, Baumann C, Waldegger S, Lang F and Koepsell H, Human neurons express the polyspecific cation transporter hOCT2, which translocates

- monoamine neurotransmitters, amantadine, and memantine. *Mol Pharmacol* **54**(2): 342-352, 1998.
29. Sweet DH and Pritchard JB, rOCT2 is a basolateral potential-driven carrier, not an organic cation/proton exchanger. *Am J Physiol* **277**(6 Pt 2): F890-F898, 1999.
30. Chen R and Nelson JA, Role of organic cation transporters in the renal secretion of nucleosides. *Biochem Pharmacol* **60**(2): 215-219, 2000.
31. Pan BF, Sweet DH, Pritchard JB, Chen R and Nelson JA, A transfected cell model for the renal toxin transporter, rOCT2. *Toxicol Sci* **47**(2): 181-186, 1999.
32. Kekuda R, Prasad PD, Wu X, Wang H, Fei YJ, Leibach FH and Ganapathy V, Cloning and functional characterization of a potential-sensitive, polyspecific organic cation transporter (OCT3) most abundantly expressed in placenta. *J Biol Chem* **273**(26): 15971-15979, 1998.
33. Grundemann D, Schechinger B, Rappold GA and Schomig E, Molecular identification of the corticosterone-sensitive extraneuronal catecholamine transporter. *Nat Neurosci* **1**(5): 349-351, 1998.
34. Verhaagh S, Schweifer N, Barlow DP and Zwart R, Cloning of the mouse and human solute carrier 22a3 (Slc22a3/SLC22A3) identifies a conserved cluster of three organic cation transporters on mouse chromosome 17 and human 6q26-q27. *Genomics* **55**(2): 209-218, 1999.
35. Wu X, Huang W, Ganapathy ME, Wang H, Kekuda R, Conway SJ, Leibach FH and Ganapathy V, Structure, function, and regional distribution of the organic cation transporter OCT3 in the kidney. *Am J Physiol* **279**(3): F449-F458, 2000.
36. Tamai I, Yabuuchi H, Nezu J, Sai Y, Oku A, Shimane M and Tsuji A, Cloning and characterization of a novel human pH-dependent organic cation transporter, OCTN1. *FEBS Lett* **419**(1): 107-111, 1997.
37. Wu X, George RL, Huang W, Wang H, Conway SJ, Leibach FH and Ganapathy V, Structural and functional characteristics and tissue distribution pattern of rat OCTN1,

an organic cation transporter, cloned from placenta. *Biochim Biophys Acta* **1466**(1-2): 315-327, 2000.

38. Yabuuchi H, Tamai I, Nezu J, Sakamoto K, Oku A, Shimane M, Sai Y and Tsuji A, Novel membrane transporter OCTN1 mediates multispecific, bidirectional, and pH-dependent transport of organic cations. *J Pharmacol Exp Ther* **289**(2): 768-773, 1999.

39. Wu X, Prasad PD, Leibach FH and Ganapathy V, cDNA sequence, transport function, and genomic organization of human OCTN2, a new member of the organic cation transporter family. *Biochem Biophys Res Commun* **246**(3): 589-595, 1998.

40. Wu X, Huang W, Prasad PD, Seth P, Rajan DP, Leibach FH, Chen J, Conway SJ and Ganapathy V, Functional characteristics and tissue distribution pattern of organic cation transporter 2 (OCTN2), an organic cation/carnitine transporter. *J Pharmacol Exp Ther* **290**(3): 1482-1492, 1999.

41. Tamai I, Ohashi R, Nezu J, Yabuuchi H, Oku A, Shimane M, Sai Y and Tsuji A, Molecular and functional identification of sodium ion-dependent, high affinity human carnitine transporter OCTN2. *J Biol Chem* **273**(32): 20378-20382, 1998.

42. Ohashi R, Tamai I, Yabuuchi H, Nezu J, Oku A, Sai Y, Shimane M and Tsuji A, Na(+)-dependent carnitine transport by organic cation transporter (OCTN2): its pharmacological and toxicological relevance. *J Pharmacol Exp Ther* **291**(2): 778-784, 1999.

43. Wagner CA, Lukewille U, Kaltenbach S, Moschen I, Broer A, Risler T, Broer S and Lang F, Functional and pharmacological characterization of human Na(+)-carnitine cotransporter hOCTN2. *Am J Physiol* **279**(3): F584-F591, 2000.

44. Nagel G, Volk C, Friedrich T, Ulzheimer JC, Bamberg E and Koepsell H, A reevaluation of substrate specificity of the rat cation transporter rOCT1. *J Biol Chem* **272**(51): 31953-31956, 1997.

45. Katzung BG, Basic & Clinical Pharmacology. 7th ed. Appleton & Lange, Stamford, 1998.

46. Bourke RS, Chheda G, Bremer A, Watanabe O and Tower DB, Inhibition of renal tubular transport of methotrexate by probenecid. *Cancer Res* **35**(1): 110-116, 1975.
47. Masereeuw R, Russel FG and Miller DS, Multiple pathways of organic anion secretion in renal proximal tubule revealed by confocal microscopy. *Am J Physiol* **271**(6 Pt 2): F1173-1182, 1996.
48. Sekine T, Watanabe N, Hosoyamada M, Kanai Y and Endou H, Expression cloning and characterization of a novel multispecific organic anion transporter. *J Biol Chem* **272**(30): 18526-18529, 1997.
49. Sweet DH, Wolff NA and Pritchard JB, Expression cloning and characterization of ROAT1. The basolateral organic anion transporter in rat kidney. *J Biol Chem* **272**(48): 30088-30095, 1997.
50. Cihlar T, Lin DC, Pritchard JB, Fuller MD, Mendel DB and Sweet DH, The antiviral nucleotide analogs cidofovir and adefovir are novel substrates for human and rat renal organic anion transporter 1. *Mol Pharmacol* **56**(3): 570-580, 1999.
51. Reid G, Wolff NA, Dautzenberg FM and Burckhardt G, Cloning of a human renal p-aminohippurate transporter, hROAT1. *Kidney Blood Press Res* **21**(2-4): 233-237, 1998.
52. Lu R, Chan BS and Schuster VL, Cloning of the human kidney PAH transporter: narrow substrate specificity and regulation by protein kinase C. *Am J Physiol* **276**(2 Pt 2): F295-F303, 1999.
53. Race JE, Grassl SM, Williams WJ and Holtzman EJ, Molecular cloning and characterization of two novel human renal organic anion transporters (hOAT1 and hOAT3). *Biochem Biophys Res Commun* **255**(2): 508-514, 1999.
54. Lopez-Nieto CE, You G, Bush KT, Barros EJ, Beier DR and Nigam SK, Molecular cloning and characterization of NKT, a gene product related to the organic cation transporter family that is almost exclusively expressed in the kidney. *J Biol Chem* **272**(10): 6471-6478, 1997.

55. Kuze K, Graves P, Leahy A, Wilson P, Stuhlmann H and You G, Heterologous expression and functional characterization of a mouse renal organic anion transporter in mammalian cells. *J Biol Chem* **274**(3): 1519-1524, 1999.
56. Hosoyamada M, Sekine T, Kanai Y and Endou H, Molecular cloning and functional expression of a multispecific organic anion transporter from human kidney. *Am J Physiol* **276**(1 Pt 2): F122-F128, 1999.
57. Bahn A, Prawitt D, Buttler D, Reid G, Enklaar T, Wolff NA, Ebbinghaus C, Hillemann A, Schulten HJ, Gunawan B, Fuzesi L, Zabel B and Burckhardt G, Genomic Structure and in Vivo Expression of the Human Organic Anion Transporter 1 (hOAT1) Gene. *Biochem Biophys Res Commun* **275**(2): 623-630, 2000.
58. Tojo A, Sekine T, Nakajima N, Hosoyamada M, Kanai Y, Kimura K and Endou H, Immunohistochemical localization of multispecific renal organic anion transporter 1 in rat kidney. *J Am Soc Nephrol* **10**(3): 464-471, 1999.
59. Jariyawat S, Sekine T, Takeda M, Apiwattanakul N, Kanai Y, Sophasan S and Endou H, The interaction and transport of beta-lactam antibiotics with the cloned rat renal organic anion transporter 1. *J Pharmacol Exp Ther* **290**(2): 672-677, 1999.
60. Apiwattanakul N, Sekine T, Chairoungdua A, Kanai Y, Nakajima N, Sophasan S and Endou H, Transport properties of nonsteroidal anti-inflammatory drugs by organic anion transporter 1 expressed in *Xenopus laevis* oocytes. *Mol Pharmacol* **55**(5): 847-854, 1999.
61. Uwai Y, Saito H, Hashimoto Y and Inui K, Inhibitory effect of anti-diabetic agents on rat organic anion transporter rOAT1. *Eur J Pharmacol* **398**(2): 193-197, 2000.
62. Wada S, Tsuda M, Sekine T, Cha SH, Kimura M, Kanai Y and Endou H, Rat multispecific organic anion transporter 1 (rOAT1) transports zidovudine, acyclovir, and other antiviral nucleoside analogs. *J Pharmacol Exp Ther* **294**(3): 844-849, 2000.

63. Ho ES, Lin DC, Mendel DB and Cihlar T, Cytotoxicity of antiviral nucleotides adefovir and cidofovir is induced by the expression of human renal organic anion transporter 1. *J Am Soc Nephrol* **11**(3): 383-393, 2000.
64. Simonson GD, Vincent AC, Roberg KJ, Huang Y and Iwanij V, Molecular cloning and characterization of a novel liver-specific transport protein. *J Cell Sci* **107**(Pt 4): 1065-1072, 1994.
65. Sekine T, Cha SH, Tsuda M, Apiwattanakul N, Nakajima N, Kanai Y and Endou H, Identification of multispecific organic anion transporter 2 expressed predominantly in the liver. *FEBS Lett* **429**(2): 179-182, 1998.
66. Kusuhara H, Sekine T, Utsunomiya-Tate N, Tsuda M, Kojima R, Cha SH, Sugiyama Y, Kanai Y and Endou H, Molecular cloning and characterization of a new multispecific organic anion transporter from rat brain. *J Biol Chem* **274**(19): 13675-13680, 1999.
67. Brady KP, Dushkin H, Fornzler D, Koike T, Magner F, Her H, Gullans S, Segre GV, Green RM and Beier DR, A novel putative transporter maps to the osteosclerosis (oc) mutation and is not expressed in the oc mutant mouse. *Genomics* **56**(3): 254-261, 1999.
68. Heaney C, Shalev H, Elbedour K, Carmi R, Staack JB, Sheffield VC and Beier DR, Human autosomal recessive osteopetrosis maps to 11q13, a position predicted by comparative mapping of the murine osteosclerosis (oc) mutation. *Hum Mol Genet* **7**(9): 1407-1410, 1998.
69. Cha SH, Sekine T, Kusuhara H, Yu E, Kim JY, Kim DK, Sugiyama Y, Kanai Y and Endou H, Molecular cloning and characterization of multispecific organic anion transporter 4 expressed in the placenta. *J Biol Chem* **275**(6): 4507-4512, 2000.
70. Saito H, Masuda S and Inui K, Cloning and functional characterization of a novel rat organic anion transporter mediating basolateral uptake of methotrexate in the kidney. *J Biol Chem* **271**(34): 20719-20725, 1996.

71. Masuda S, Saito H, Nonoguchi H, Tomita K and Inui K, mRNA distribution and membrane localization of the OAT-K1 organic anion transporter in rat renal tubules. *FEBS Lett* **407**(2): 127-131, 1997.
72. Masuda S, Takeuchi A, Saito H, Hashimoto Y and Inui K, Functional analysis of rat renal organic anion transporter OAT-K1: bidirectional methotrexate transport in apical membrane. *FEBS Lett* **459**(1): 128-132, 1999.
73. Takeuchi A, Masuda S, Saito H, Hashimoto Y and Inui K, Trans-stimulation effects of folic acid derivatives on methotrexate transport by rat renal organic anion transporter, OAT-K1. *J Pharmacol Exp Ther* **293**(3): 1034-1039, 2000.
74. Masuda S, Saito H and Inui KI, Interactions of nonsteroidal anti-inflammatory drugs with rat renal organic anion transporter, OAT-K1. *J Pharmacol Exp Ther* **283**(3): 1039-1042, 1997.
75. Masuda S, Ibaramoto K, Takeuchi A, Saito H, Hashimoto Y and Inui KI, Cloning and functional characterization of a new multispecific organic anion transporter, OAT-K2, in rat kidney. *Mol Pharmacol* **55**(4): 743-752, 1999.
76. Jacquemin E, Hagenbuch B, Stieger B, Wolkoff AW and Meier PJ, Expression cloning of a rat liver Na(+)-independent organic anion transporter. *Proc Natl Acad Sci U S A* **91**(1): 133-137, 1994.
77. Kullak-Ublick GA, Hagenbuch B, Stieger B, Schteingart CD, Hofmann AF, Wolkoff AW and Meier PJ, Molecular and functional characterization of an organic anion transporting polypeptide cloned from human liver. *Gastroenterology* **109**(4): 1274-1282, 1995.
78. Bergwerk AJ, Shi X, Ford AC, Kanai N, Jacquemin E, Burk RD, Bai S, Novikoff PM, Stieger B, Meier PJ, Schuster VL and Wolkoff AW, Immunologic distribution of an organic anion transport protein in rat liver and kidney. *Am J Physiol* **271**(2 Pt 1): G231-G238, 1996.

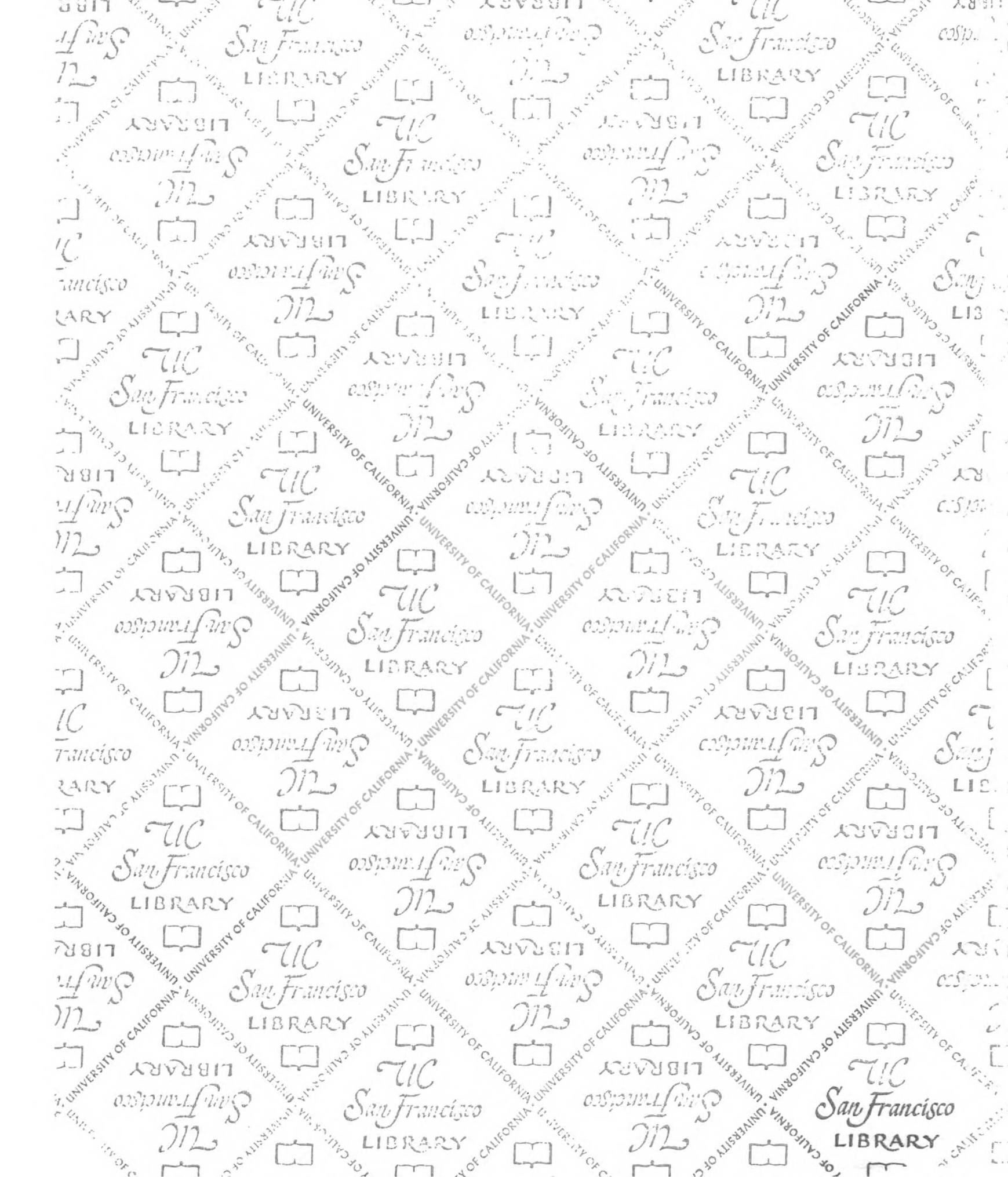
79. Angeletti RH, Novikoff PM, Juvvadi SR, Fritschy JM, Meier PJ and Wolkoff AW, The choroid plexus epithelium is the site of the organic anion transport protein in the brain. *Proc Natl Acad Sci U S A* **94**(1): 283-286, 1997.
80. Karniski LP, Lotscher M, Fucentese M, Hilfiker H, Biber J and Murer H, Immunolocalization of sat-1 sulfate/oxalate/bicarbonate anion exchanger in the rat kidney. *Am J Physiol* **275**(1 Pt 2): F79-87, 1998.
81. Eckhardt U, Schroeder A, Stieger B, Hochli M, Landmann L, Tynes R, Meier PJ and Hagenbuch B, Polyspecific substrate uptake by the hepatic organic anion transporter Oatp1 in stably transfected CHO cells. *Am J Physiol* **276**(4 Pt 1): G1037-G1042, 1999.
82. Satlin LM, Amin V and Wolkoff AW, Organic anion transporting polypeptide mediates organic anion/HCO₃⁻ exchange. *J Biol Chem* **272**(42): 26340-26345, 1997.
83. Li L, Lee TK, Meier PJ and Ballatori N, Identification of glutathione as a driving force and leukotriene C₄ as a substrate for oatp1, the hepatic sinusoidal organic solute transporter. *J Biol Chem* **273**(26): 16184-16191, 1998.
84. Pang KS, Wang PJ, Chung AY and Wolkoff AW, The modified dipeptide, enalapril, an angiotensin-converting enzyme inhibitor, is transported by the rat liver organic anion transport protein. *Hepatology* **28**(5): 1341-1346, 1998.
85. Cvetkovic M, Leake B, Fromm MF, Wilkinson GR and Kim RB, OATP and P-glycoprotein transporters mediate the cellular uptake and excretion of fexofenadine. *Drug Metab Dispos* **27**(8): 866-871, 1999.
86. Noe B, Hagenbuch B, Stieger B and Meier PJ, Isolation of a multispecific organic anion and cardiac glycoside transporter from rat brain. *Proc Natl Acad Sci U S A* **94**(19): 10346-10350, 1997.
87. Abe T, Kakyo M, Sakagami H, Tokui T, Nishio T, Tanemoto M, Nomura H, Hebert SC, Matsuno S, Kondo H and Yawo H, Molecular characterization and tissue distribution of a new organic anion transporter subtype (oatp3) that transports thyroid

- hormones and taurocholate and comparison with oatp2. *J Biol Chem* **273**(35): 22395-22401, 1998.
88. Gao B, Stieger B, Noe B, Fritschy JM and Meier PJ, Localization of the organic anion transporting polypeptide 2 (Oatp2) in capillary endothelium and choroid plexus epithelium of rat brain. *J Histochem Cytochem* **47**(10): 1255-1264, 1999.
89. Kakyo M, Sakagami H, Nishio T, Nakai D, Nakagomi R, Tokui T, Naitoh T, Matsuno S, Abe T and Yawo H, Immunohistochemical distribution and functional characterization of an organic anion transporting polypeptide 2 (oatp2). *FEBS Lett* **445**(2-3): 343-346, 1999.
90. Reichel C, Gao B, Van Montfoort J, Cattori V, Rahner C, Hagenbuch B, Stieger B, Kamisako T and Meier PJ, Localization and function of the organic anion-transporting polypeptide Oatp2 in rat liver. *Gastroenterology* **117**(3): 688-695, 1999.
91. Burckhardt BC, Wolff NA and Burckhardt G, Electrophysiologic characterization of an organic anion transporter cloned from winter flounder kidney (fROAT). *J Am Soc Nephrol* **11**(1): 9-17, 2000.
92. Cihlar T and Ho ES, Fluorescence-based assay for the interaction of small molecules with the human renal organic anion transporter 1. *Anal Biochem* **283**(1): 49-55, 2000.
93. Borst P, Evers R, Kool M and Wijnholds J, The multidrug resistance protein family. *Biochim Biophys Acta* **1461**(1): 347-357, 1999.
94. Borst P, Evers R, Kool M and Wijnholds J, A family of drug transporters: the multidrug resistance-associated proteins. *J Natl Cancer Inst* **92**(16): 1295-1302, 2000.
95. Keppler D, Kamisako T, Leier I, Cui Y, Nies AT, Tsujii H and Konig J, Localization, substrate specificity, and drug resistance conferred by conjugate export pumps of the MRP family. *Adv Enzyme Regul* **40**: 339-349, 2000.

96. Leier I, Hummel-Eisenbeiss J, Cui Y and Keppler D, ATP-dependent para-aminohippurate transport by apical multidrug resistance protein MRP2. *Kidney Int* **57**(4): 1636-1642, 2000.
97. Van Aubel RA, Peters JG, Masereeuw R, Van Os CH and Russel FG, Multidrug resistance protein Mrp2 mediates ATP-dependent transport of classic renal organic anion p-aminohippurate. *Am J Physiol* **279**(4): F713-F717, 2000.
98. Smit JW, Weert B, Schinkel AH and Meijer DK, Heterologous expression of various P-glycoproteins in polarized epithelial cells induces directional transport of small (type 1) and bulky (type 2) cationic drugs. *J Pharmacol Exp Ther* **286**(1): 321-327, 1998.
99. Smit JW, Schinkel AH, Weert B and Meijer DK, Hepatobiliary and intestinal clearance of amphiphilic cationic drugs in mice in which both *mdr1a* and *mdr1b* genes have been disrupted. *Br J Pharmacol* **124**(2): 416-424, 1998.
100. Smit JW, Schinkel AH, Muller M, Weert B and Meijer DK, Contribution of the murine *mdr1a* P-glycoprotein to hepatobiliary and intestinal elimination of cationic drugs as measured in mice with an *mdr1a* gene disruption. *Hepatology* **27**(4): 1056-1063, 1998.
101. Thiebaut F, Tsuruo T, Hamada H, Gottesman MM, Pastan I and Willingham MC, Cellular localization of the multidrug-resistance gene product P-glycoprotein in normal human tissues. *Proc Natl Acad Sci U S A* **84**(21): 7735-7738, 1987.
102. Borst P and Schinkel AH, What have we learnt thus far from mice with disrupted P-glycoprotein genes? *Eur J Cancer* **32A**(6): 985-990, 1996.
103. Sparreboom A, van Asperen J, Mayer U, Schinkel AH, Smit JW, Meijer DK, Borst P, Nooijen WJ, Beijnen JH and van Tellingen O, Limited oral bioavailability and active epithelial excretion of paclitaxel (Taxol) caused by P-glycoprotein in the intestine. *Proc Natl Acad Sci U S A* **94**(5): 2031-2035, 1997.
104. Schinkel AH, Wagenaar E, van Deemter L, Mol CA and Borst P, Absence of the *mdr1a* P-Glycoprotein in mice affects tissue distribution and pharmacokinetics of dexamethasone, digoxin, and cyclosporin A. *J Clin Invest* **96**(4): 1698-1705, 1995.

105. Hooijberg JH, Broxterman HJ, Kool M, Assaraf YG, Peters GJ, Noordhuis P, Scheper RJ, Borst P, Pinedo HM and Jansen G, Antifolate resistance mediated by the multidrug resistance proteins MRP1 and MRP2. *Cancer Res* **59**(11): 2532-2535, 1999.
106. George RL, Wu X, Huang W, Fei YJ, Leibach FH and Ganapathy V, Molecular cloning and functional characterization of a polyspecific organic anion transporter from *Caenorhabditis elegans*. *J Pharmacol Exp Ther* **291**(2): 596-603, 1999.
107. Wu X, Fei YJ, Huang W, Chancy C, Leibach FH and Ganapathy V, Identity of the F52F12.1 gene product in *Caenorhabditis elegans* as an organic cation transporter. *Biochim Biophys Acta* **1418**(1): 239-244, 1999.
108. Hoffmeyer S, Burk O, von Richter O, Arnold HP, Brockmoller J, John A, Cascorbi I, Gerloff T, Roots I, Eichelbaum M and Brinkmann U, Functional polymorphisms of the human multidrug-resistance gene: multiple sequence variations and correlation of one allele with P-glycoprotein expression and activity in vivo. *Proc Natl Acad Sci U S A* **97**(7): 3473-3478, 2000.
109. Hsiang B, Zhu Y, Wang Z, Wu Y, Sasseville V, Yang WP and Kirchgessner TG, A novel human hepatic organic anion transporting polypeptide (OATP2). Identification of a liver-specific human organic anion transporting polypeptide and identification of rat and human hydroxymethylglutaryl-CoA reductase inhibitor transporters. *J Biol Chem* **274**(52): 37161-37168, 1999.
110. Ganapathy ME, Huang W, Rajan DP, Carter AL, Sugawara M, Iseki K, Leibach FH and Ganapathy V, beta-lactam antibiotics as substrates for OCTN2, an organic cation/carnitine transporter. *J Biol Chem* **275**(3): 1699-1707, 2000.
111. Busch AE, Quester S, Ulzheimer JC, Waldegger S, Gorboulev V, Arndt P, Lang F and Koepsell H, Electrogenic properties and substrate specificity of the polyspecific rat cation transporter rOCT1. *J Biol Chem* **271**(51): 32599-32604, 1996.

112. Okuda M, Urakami Y, Saito H and Inui K, Molecular mechanisms of organic cation transport in OCT2-expressing *Xenopus* oocytes. *Biochim Biophys Acta* **1417**(2): 224-231, 1999.
113. Grundemann D, Liebich G, Kiefer N, Koster S and Schomig E, Selective substrates for non-neuronal monoamine transporters. *Mol Pharmacol* **56**(1): 1-10, 1999.
114. Martel F, Vetter T, Russ H, Grundemann D, Azevedo I, Koepsell H and Schomig E, Transport of small organic cations in the rat liver. The role of the organic cation transporter OCT1. *Naunyn Schmiedebergs Arch Pharmacol* **354**(3): 320-326, 1996.
115. Breidert T, Spitzenberger F, Grundemann D and Schomig E, Catecholamine transport by the organic cation transporter type 1 (OCT1). *Br J Pharmacol* **125**(1): 218-224, 1998.
116. Busch AE, Quester S, Ulzheimer JC, Gorboulev V, Akhoundova A, Waldegger S, Lang F and Koepsell H, Monoamine neurotransmitter transport mediated by the polyspecific cation transporter rOCT1. *FEBS Lett* **395**(2-3): 153-156, 1996.
117. Zhang L, Gorset W, Washington CB, Blaschke TF, Kroetz DL and Giacomini KM, Interactions of HIV protease inhibitors with a human organic cation transporter in a mammalian expression system. *Drug Metab Dispos* **28**(3): 329-334, 2000.
118. Tokui T, Nakai D, Nakagomi R, Yawo H, Abe T and Sugiyama Y, Pravastatin, an HMG-CoA reductase inhibitor, is transported by rat organic anion transporting polypeptide, oatp2. *Pharm Res* **16**(6): 904-908, 1999.



For reference

Not to be taken from the room.

San Francisco

628406



3 1378 00628 4064



